INVESTIGATIONS INTO PHOSPHODIESTERASES AS TARGETS FOR ANTIMALARIAL DRUG DISCOVERY

Laura Gabrielle Drought

Thesis submitted in accordance with the requirements for the degree of

Doctor of Philosophy

University of London

September 2014

Department of Pathogen Molecular Biology

Faculty of Infectious and Tropical Diseases

LONDON SCHOOL OF HYGIENE & TROPICAL MEDICINE

Abstract

Phosphodiesterases are key enzymes in cyclic-nucleotide signalling pathways, regulating the levels of cAMP and cGMP in the cell. Cyclic nucleotides play an important role in regulating progression of the complex parasite life cycle. There are four *Plasmodium* PDEs, PDEα-δ. PDEβ has proved refractory to deletion and is predicted to be essential in asexual blood stages. PDEs α, γ and δ have been successfully disrupted in previous studies, which revealed stage-specific roles for PDEγ and PDEδ in the mosquito. PDEβ is a promising drug target due to the proven ability to create specific inhibitors for individual human PDEs (e.g. Viagra inhibits human PDE5), the established safety record of current inhibitors and the predicted essential nature of PDEβ in *P. falciparum* blood stages. The lack of useful reagents; knockout strains, tagged lines and recombinant proteins, has severely limited progress in this field.

Conditional genetic disruption (required to study essential genes) is notoriously difficult in *P. falciparum.* This project has attempted to generate a conditional knock-out using the destabilisation domain system and the novel DiCre system, which involves recombinase-mediated genomic excision of the target DNA upon introduction of a drug. A PDEβ haemagglutanin (HA) tagged line has been successfully generated and used to investigate the cellular biology of PDEβ, including, the subcellular localisation and cyclic nucleotide specificity of PDEβ, which until now has remained speculative.

A small library of PDE inhibitors generated by Pfizer has been evaluated using a parasite growth inhibition assay and a PDE assay, with compounds active at sub-micromolar concentrations against the parasite and the protein. These assays have used wild type parasites and also a PDEα KO line which has no obvious phenotype in blood stage parasites.

Acknowledgements

Contents

List of tables and figures

List of abbreviations

μF	microfarad
μl	microlitre
μM	micromolar
3D7	ild type *P. falciparum*
AC	adenylyl cyclase
AcMNPV	*Autographa californica* multiple nucleopolyhedrosis virus
ACT	artemisinin combination therapy
ADA	adenosine deaminase
AKAP	A-kinase anchoring proteins
AMA1	apical membrane antigen 1
AMP	adenosine monophosphate
APAD	3-acetyl pyridine nicotinamide adenine dinucleotide
ApiAP2	Apicomplexan AP2
BCKDH	branched chain ketoacid dehydrogenase
BiP	heat shock protein 7 type molecular chaperone
bp	basepair
BSA	bovine serum albumin
BSD	blasticidin S deaminase
C1	compound 1
C2	compound 2
Ca^{2+}	calcium ions
$CaCl_2$	calcium chloride
CaM	calmodulins
cAMP	cyclic adenosine monophosphate
CBL	calcineurin B-like
CCPM	combined counts per minute
CD	catalytic domain
CDPKs	calcium-dependent protein kinases
CGG	chicken gamma globulin
cGMP	cyclic guanosine monophosphate
cNMP	cyclic nucleotides
COPD	chronic obstructive pulmonary disorder
cox1	cytochrome c oxidase subunit 1
cox3	cytochrome c oxidase subunit 3
CPM	counts per minute
CRE	cAMP response element
CREB	CRE-binding protein
CRISPR/Cas9	clustered regularly interspaced short palindromic repeat targeting of Cas9
CRT	chloroquine resistance transporter
CSP	circumsporozoite protein
cytb	cytochrome b
DAG	diacylglycerol

DBL	duffy binding like
DD	destabilisation domain
DHFR	dihydrofolate reductase
DHOD	dihydroorotate dehydrogenase
DHPS	dihydropteroate synthetase
DMSO	dimethyl sulphoxide
DNA	deoxyribonucleic acid
dNTPs	deoxynucleotides
EBA	erythrocyte binding antigens
EBL	erythrocyte binding-like
EC50	half maximal effective concentration
EDTA	ethylenediaminetetraacetic acid
EGTA	ethylene glycol tetraacetic acid
EMP1	parasite ligand erythrocyte membrane protein 1
ER	endoplasmic reticulum
FlpL	flippase
FRT	FLP recombinase target
G6PD	glucose-6-phosphate-dehydrogenase
GAP45	glideosome associated protein 45
GAPDH	glyceraldehyde-3-phosphate dehydrogenase
GC	guanylyl cyclase
gDNA	genomic DNA
GEST	gametocyte egress and sporozoite traversal
G_i	inhibitory G proteins
GKIP	PKG interacting partners
GMP	guanosine monophosphate
GOI	gene of interest
GPCR	G-protein coupled receptor
G_s	stimulatory G proteins
h.p.i.	hours post invasion
HA	Haemagglutination
Hda2	histone deacetylase 2
HEPES	4-(2-hydroxyethyl)-1-piperazineethanesulphonic acid
HP1	heterochromatin protein 1
HPPK	hydroxymethylpterin pyrophosphokinase
HSPGs	Heparan sulphate proteoglycans
IC50	half maximal inhibitory concentrations
ICAM1	intracellular adhesion molecule 1
IFA	immunofluorescence assay
IgG	immunoglobulin G
IMAC	immobilised metal affinity chromatography
IMC	inner membrane complex
IP_3	inositol 1,4,5-trisphosphate
IPT	intermittent preventive treatment
iRBC	infected red blood cell

IRS	indoor residual spraying
kb	kilobase
KCl	potassium chloride
kDa	kilodaltons
K_m	Michaelis constant
LB	Luria-Bertani
LDH	lactate dehydrogenase
LLIN	long-lasting insecticide treated nets
mA	milliamps
MACS	magnetic cell separation
mb	megabase
MDR1	multidrug resistance gene 1
Mg^{2+}	magnesium ions
$MgCl_2$	magnesium chloride
Mistic	membrane integrating sequence for translation of integral membrane protein constructs
Mn^{2+}	manganese ions
MOI	multiplicity of infection
MSP	merozoite surface protein
mtRMA	mitochondrial RNA
NaCl	sodium chloride
NAD	nicotinamide adenine dinucleotide
NaOAc	sodium acetate
NBT/PES	nitro blue tetrazolium/phenazine ethosulphate
nCi	nanocurie
NEO	neomycin phosphotransferase II
nM	nanomolar
NO	Nitric oxide
Pb	*Plasmodium berghei*
PBS	phosphate buffered saline
PCR	polymerase chain reaction
PDE	cyclic nucleotide phosphodiesterase
PDH	pyruvate dehydrogenase
Pf	*Plasmodium falciparum*
PFU	particle forming units
PH	pleckstrin homology
PIP_2	phosphatidylinositol 4,5-disphosphate
PI-PLC	phosphoinositide phospholipase C
PKA	cAMP dependent protein kinase A
PKA-C	PKA catalytic domain
PKA-R	PKA regulatory domain
PKG	cGMP dependent protein kinase G
PLP	perforin-like protein
PM	plasma membrane
PMV	plasmepsin V

POI	protein of interest
PV	parasitophorous vacuole
Pv	*Plasmodium vivax*
RAS	rennin-angiotensin system
RBC	red blood cell
Rh	reticulocyte-binding protein homologs
rifin	repetitive interspersed family
RNA	ribonucleic acid
RPKM	reads per kilobase of exon model per million mapped reads
rRNA	ribosomal RNA
SDS	sodium dodecyl sulphate
SDS-PAGE	sodium dodecyl sulphate polyacrylamide gel electrophoresis
SEA-1	schizont egress antigen-1
SEM	standard error of the mean
SERA	serine repeat antigens
SERCA	sarco/endoplasmic reticulum Ca^{2+}-ATPase
Sf	*Spodoptera frugiperda*
SP	sulphadoxin-pyrimethamine
SPA	scintillation proximity assay
stevor	sub-telomeric variable open reading frame
TEA	triethanolamine
Tg	*Toxoplasma gondii*
TK	thymidine kinase
TM	transmembrane
TS	thymidylate synthetase
uRBC	uninfected red blood cell
UV	ultraviolet
V	volts
WHO	World Health Organisation
WT	wild type
XA	xanthurenic acid
ZFN	zinc finger nuclease
Zn^{2+}	zinc ions

Chapter 1: Introduction

Malaria represents a major public health issue across the world and was responsible for an estimated 207 million cases and 627,000 deaths in 2012, predominantly in sub-Saharan Africa, but also throughout the tropics. As of 2013, 97 countries have confirmed malaria transmission with in excess of 3 billion people at risk of contracting this parasitic disease (WHO, 2013). Despite international and domestic funding increases over the last decade, in 2013 the total funds committed to malaria control were an estimated 2.5 billion USD. This figure is less than half the predicted 5.1 billion USD required each year to reach universal coverage of control interventions (WHO, 2013).

In humans the disease can be caused by several species of apicomplexan parasites in the genus *Plasmodium*, *P. falciparum, P. vivax, P. malariae, P. ovale* (*P. ovale curtisi* and *P. ovale wallikeri* (Sutherland et al., 2010)) and *P. knowlesi*. Of these, *P. falciparum* causes the most severe manifestation of malaria. These species differ in morphology, blood stage cycle length, disease severity, geographical distribution, relapse patterns and in their responses to drugs. These protozoan parasites have a complex life cycle, involving two hosts, human and *Anopheles* mosquito, and numerous developmental stages.

1.1 The history of malaria

Malaria is not a newly documented disease and has a history extending into antiquity. It is generally believed that human malaria originated in our primate ancestors and has been co-evolving with us since. In ancient writings from many regions of the globe, recurring fevers, characteristic of malarial infection, have been documented in many early civilisations including in China, the Roman Empire and the Arab world (Reviewed in Cox 2002). The word malaria originated from Medieval Italian for 'bad air' from the association between the disease and marshes. It was long thought malaria was caused by miasmas rising from the swamps. In the 19th century, after the advent of germ theory there was a race to find the causative agent of different infectious diseases. In 1880, Alphonse Laveran, a French army surgeon, was the first to visualise parasites in the blood of infected patients using microscopy. Subsequently in 1897, Ronald Ross, a British army surgeon, discovered that *Anopheles* mosquitoes were responsible for transmitting the disease and that the association with marshes was due to their habitat range. In the same year the mosquito developmental stages were described by the Italian

scientists Giovanni Grassi, Amico Bignami, and Giuseppe Bastianelli. The life cycles of *P. falciparum*, *P. vivax* and *P. malariae* were described a year later. It was not until 1947 that London based Henry Shortt and Cyril Garnham described the liver stages of malaria, thereby explaining why parasites were not observed in the blood until 10 days post infection (Reviewed in Cox 2002). In 1980, Krotoski et al. described a putative latent form of *P. cynomolgi* in rhesus monkey liver cells (Krotoski et al., 1980), later termed hypnozoites and their existence was confirmed in the human malaria *P. vivax* (Krotoski et al., 1982).

1.2 Life cycle of *Plasmodium* species

Malaria parasites are transmitted to humans through the saliva associated with the bite of an infected *Anopheles* mosquito. There are at least 30 documented species of *Anopheles* that are of major importance in malaria spread, with a further 30 capable of transmission (Tuteja, 2007). Of the *Plasmodium* species that infect humans, *P. falciparum* causes the majority of fatalities worldwide and is most associated with drug resistance. It is mostly found in sub-Saharan Africa, but is also prevalent in areas of Southeast Asia and South America. *P. vivax* is the most common and is globally distributed. *P. malariae, P. ovale* and *P. knowlesi* are the least common. Whilst *P. malariae* is also found throughout the globe, *P. ovale* is restricted to West Africa and *P. knowlesi* is restricted to Southeast Asia (Singh et al., 2004).   *P. vivax* and *P. ovale* are able to form dormant liver stages, called hypnozoites, which can lead to relapses in disease from weeks to even years after the initial infection. *P. malariae* can remain in the blood for decades as a low level asymptomatic infection (Tuteja, 2007).

1.2.1 Exo-erythrocytic liver stages

Human infection begins when an infected *Anopheles* mosquito takes a blood meal and injects motile infectious sporozoites into the skin. The parasites are injected into the extracellular matrix of the skin as the mosquitoes probe for a blood vessel (Sidjanski and Vanderberg, 1997; Vanderberg and Frevert, 2004). The sporozoites then invade blood or lymphatic vessels via which they are passively conveyed to the liver. A parasite surface protein, circumsporozoite protein (CSP), binds to highly sulphated glycosamino glycan chains in liver heparan sulphate proteoglycans (HSPGs) on the host cell surface (Pradel et al., 2002) to invade hepatocytes inside a parasitophorous vacuole (PV). Once inside a liver cell, the elongated sporozoite rounds up and undergoes schizogony, generating tens of thousands of liver merozoites. The parasite is able to

control host cell death in such a way that the host cell membrane is preserved (Graewe et al., 2011), forming vesicles called merosomes full of hundreds of merozoites and surrounded by the host cell membrane. The merosomes then detach from the cell and bud off. This is thought to immunologically protect the merozoites from the host's immune system surveillance (Sturm et al., 2006). Merosomes are transported by the blood into the narrow vessels in the lungs where they rupture, releasing merozoites which are able to initiate the blood stage infection (Baer et al., 2007). From the initial bite to a blood stage infection, the entire process takes about 8-30 days for human malaria, depending on the infecting species and only 2 days for rodent malaria (Hollingdale and Leland, 1982). This is termed the prepatent period.

1.2.2 Asexual erythrocytic stages

Invasion of red blood cells (RBCs) by merozoites is a highly complex process that involves; initial recognition and attachment to the RBC membrane, tight junction formation, rhoptry and microneme secretion inducing formation of the PV, host cell invagination to enclose the merozoite and resealing of both the PV and the RBC membranes. As one of the few extracellular life cycle stages, merozoites are attractive vaccine targets. Asexual blood stage replication takes 48 hours for *P. falciparum*, *P. ovale*, and *P. vivax*, 72 hours for *P. malariae* and 24 hours for *P. knowlesi*, as the parasites grow from early trophozoites, called ring-stages due to their distinctive morphology, through trophozoites to schizonts (figure 1.1).
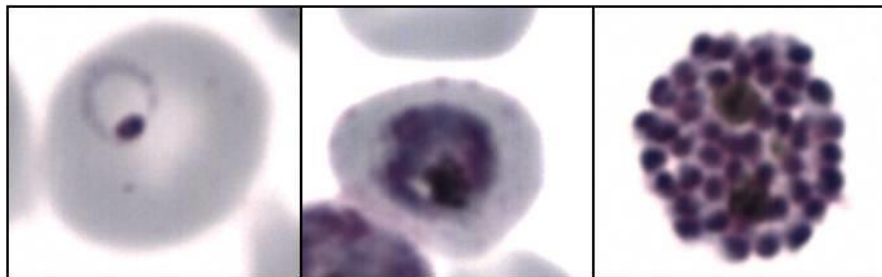
Figure 1.1 Giemsa staining of the major erythrocytic asexual stages of *P. falciparum*
The image on the left shows a ring-stage parasite, the middle image is a trophozoites and a late stage schizont is shown on the right.

The trophozoite phase is highly metabolically active, notably in the glycolysis of imported glucose, RBC cytoplasm ingestion and scavenging of amino acids from haemoglobin (Tuteja, 2007). Free haem is liberated during haemoglobin digestion which is toxic to the parasite via oxidative stress. To combat this, haem is polymerised into crystalline haemozoin (malaria pigment) and stored in the food vacuole (Coronado et al., 2014).

Schizonts are formed as the parasite undergoes DNA replication and multiple rounds of nuclear division with no cytokinesis. The schizonts undergo cytokinesis to form a number of merozoites (around 20, depending on the species), which are liberated on parasite egress, reinvade new RBCs and perpetuate the infection. The molecular process of egress and invasion is discussed in more detail below.

1.2.3 Sexual and mosquito stages

A small percentage of parasites differentiate into sexual stage gametocytes, macro- and microgametocytes (female and male, respectively). Whilst gametocytes are a dead end within the human host, they are essential for onward transmission. Gametocytes are taken up by the *Anopheles* mosquito when they take a blood meal from an infected host. Once inside the insect's midgut, the drop in temperature and the mosquito factor xanthurenic acid (XA) triggers a change in morphology of the gametocytes, from crescent shaped to spherical with an accompanying loss of erythrocyte membrane (Billker et al., 1998). This process is termed rounding up. Whilst the female parasite does not undergo many morphological changes to form a macrogamete, the male parasite rapidly undergoes three rounds of replication, leading to the formation and release of eight highly motile microgametes in a process called exflagellation. The microgamete then penetrates the macrogamete, fusion and fertilisation occurs to form a zygote. Within about 24 hours, the zygote transforms into a motile ookinete that is capable of moving by gliding motility which subsequently penetrates the midgut wall. From there the ookinetes migrate to the basal sub-epithelial space and form replicating oocysts (Sinden, 2002; Vlachou et al., 2004).

As the oocyst develops it becomes spherical, produces a thick cyst wall and proceeds to undergo many rounds of replication leading to the development of several thousand sporozoites within 12-18 days. As the oocyst ruptures, it liberates the motile sporozoites which migrate to the insects salivary glands (Sinden, 2002). Once the sporozoites have reached the salivary glands the mosquito infects new vertebrate hosts upon each blood meal (Tuteja, 2007).
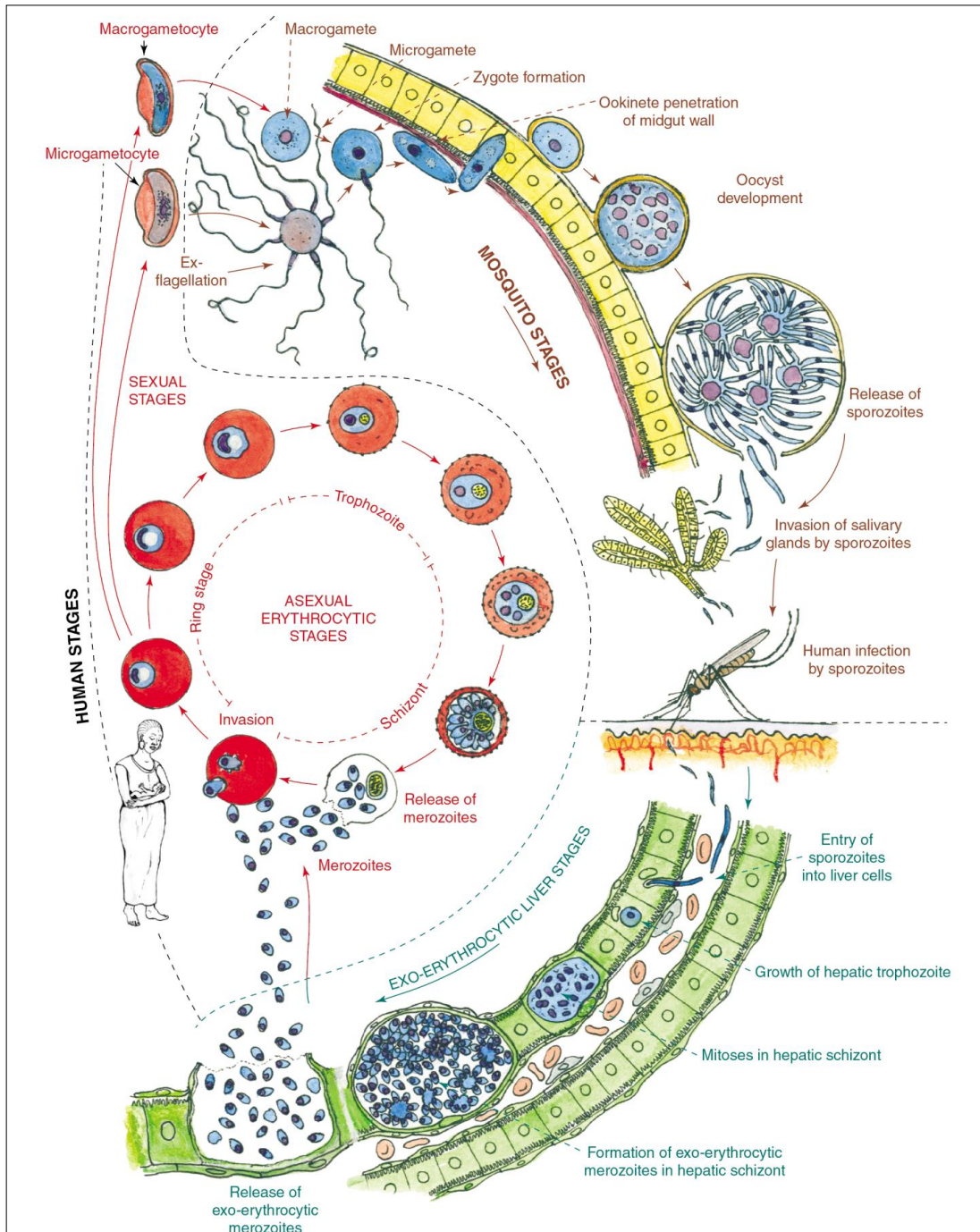
Figure 1.2 Life cycle of *P. falciparum*
The main phases of the life cycle of *Plasmodium falciparum* parasites within the human host and insect vector (Bannister and Mitchell, 2003).

1.3 Pathogenesis

The asexual blood stage replication of the malaria parasite is the cause of pathology within the vertebrate host. Malaria symptoms can appear from around day six after a bite by an infected mosquito, to several months later, depending on the species of *Plasmodium*. Infections can range from asymptomatic to life threatening, with clinical outcome dependent on numerous factors, many of which are currently unknown (Miller et al., 2002). Symptoms of malaria are varying and include; fever, headache, shivering, sweating, cough, joint pain, vomiting, diarrhoea, with severe malaria symptoms of respiratory distress, convulsions, kidney failure, jaundice, coma and anaemia (Miller et al., 2002; Tuteja, 2007). Progression to severe malaria is very poorly understood and involves three overlapping syndromes; severe anaemia, cerebral malaria and metabolic acidosis. With severe malaria there is a mortality rate of up to 20%, and those that recover may still suffer from neurological sequelae after the infection is cleared (Miller et al., 2013).

A major factor in the pathogenesis of *P. falciparum* is the ability of the infected RBCs (iRBCs) to adhere to small blood vessel linings, termed sequestration. In particular, sequestration is a principle feature in cerebral malaria and pregnancy associated malaria with parasites binding to vascular endothelial cells in the brain and placenta, respectively. Sequestration leads to blockage of blood flow and reduced tissue perfusion. *P. falciparum* late trophozoites and schizonts and express the parasite ligand erythrocyte membrane protein 1 (PfEMP1) which is able to bind to various host cell receptors including CD36 and intracellular adhesion molecule 1 (ICAM1) (Franke-Fayard et al., 2010; Roberts et al., 1992; Scherf et al., 2001). Gametocytes are also sequestered in internal organs, however it is though that mechanical rather than adhesion properties regulate this interaction (Tibúrcio et al., 2012).

1.4 Treatment and control

The treatment and control of malaria has a history spanning centuries rather than decades. Prior to the development of germ theory in the mid-19th century, fevers (malarial or otherwise) were often treated with various different and usually ineffective approaches such as blood-letting or consuming large amounts of garlic (Meshnick and Dobson, 2001). However, two herbal remedies utilised for fever treatment for hundreds of years are still greatly important in malaria control today, cinchona bark (quinine) and qinghao (artemisinin). Whilst the story of the 'discovery' of quinine is debated, whether it was a Spanish Countess in Peru who was cured using the bark or observations of a Jesuit missionary in South America, ground cinchona bark was certainly used to treat fever in Europeans by the late 17th Century, and possibly by the indigenous population before this (reviewed in Achan et al. 2011). Quinine remained the principal treatment until the 1930s when synthetic malaria drugs were developed, chiefly chloroquine in 1934 by Hans Andersay, for the German pharmaceutical company Bayer AG. Chloroquine was hugely effective and was used extensively in the WHO Global Eradication Programme of the 1950s and 60s, until drug resistance in P. *falciparum* developed in South East Asia and spread to the majority of the malaria endemic world, rendering it ineffective. However chloroquine is still commonly used to treat *P. vivax* malaria, often in combination with primaquine to target the liver hypnozoites (Thomé et al., 2013). Many other antimalarials were discovered in the period from 1940-1970, including pyrimethamine-sulphadoxine combination, marketed as Fansidar and atovaquone-proguanil, sold as Malarone (Meshnick and Dobson, 2001). Artemisinin, from the qinghao herb (*Artemisia annua,* also called sweet wormwood) was used for thousands of years in Chinese herbal medicine, originally for haemorrhoids. In 1596, a Chinese herbalist wrote about its use as a treatment for fever (Klayman, 1985). In the People's Republic of China, in the late 1960s, qinghaosu (qinghao essence) was found to be extremely effective as an antimalarial (Meshnick and Dobson, 2001), and with the opening up of China in the late 1970s to early 1980s, the artemisinins were soon in clinical trials and they have been the frontline treatment for *P. falciparum* malaria since the 1990s (Miller and Su, 2011).

Antimalarial drugs cover only a few unique classes, with many of the compounds acting on the parasites ability to degrade haemoglobin. Resistance is therefore a major problem and generally develops within a short time from drug introduction. Resistance has developed in *P. falciparum* to every major class of antimalarial so far introduced, with the possible exception of artemisinin combination therapy (ACTs) where delayed clearance times have been recorded, but with no full treatment failure as yet (Noedl et al., 2008).

1.4.1 Amino alcohols

Quinine is an alkaloid, belonging in the aryl amino alcohol group of drugs, with schizonticidal activity against blood stages of all species of human malaria. The mechanism of action remains unknown, although it seems likely to interfere with haem metabolism (Hoppe et al., 2004). Quinine resistance occurs mostly in Southeast Asia, and is associated with amplification of the *pfmdr1* (*Plasmodium falciparum* multidrug resistance gene 1) locus, a transporter in the food vacuole membrane (Schlitzer, 2008). There are significant side effects of quinine, including tinnitus, vomiting and hypoglycaemia. However it remains an important drug in treatment during the first trimester of pregnancy and as a second line treatment for severe malaria (Achan et al., 2011). Other aryl amino alcohols used for antimalarial therapy include mefloquine, lumefantrine and halofantrine.

1.4.2 4-Aminoquinolines

The 4-Aminoquinolines include chloroquine and its derivatives (e.g. amodiaquine, piperaquine) which act on the asexual blood stages of malaria. The mechanism of action has not been conclusively proven, but current consensus is that the drugs prevent polymerisation of toxic haem products into inert haemozoin in the digestive vacuole of the developing parasite, although via a different mechanism to quinine derivatives (Griffin et al., 2012; Hoppe et al., 2004). Chloroquine is known to accumulate in the digestive vacuole and raise the internal pH (Homewood et al., 1972). However, in chloroquine resistant *P. falciparum,* this accumulation is much less in comparison to chloroquine sensitive strains, suggesting an efflux based resistance mechanism. The two genes, *pfcrt* (*Plasmodium falciparum* chloroquine resistance transporter) and *pfmdr1* have been implicated in chloroquine resistance (Krogstad et al., 1987; Peel, 2001). Amodiaquine can be used against chloroquine tolerant, but not highly-resistant *P. falciparum*. However, it has serious adverse effects when used over a prolonged period of time, but is still used in endemic regions (Schlitzer, 2008).

1.4.3 8-Aminoquinolines

 Primaquine and tafenoquine (still in development), among others are examples of 8-aminoquinolines. Primaquine is currently the only drug available that can clear hepatocyte and sexual stages of the parasite. It is used to kill liver stage hypnozoites in *P. vivax* infections (Wells et al., 2010). However, primaquine is contraindicated in people with G6PD (glucose-6-phosphate-dehydrogenase) deficiency, in whom it can cause life-threatening haemolysis of

RBCs. Unfortunately G6PD deficiency is relatively common in much of Africa and parts of Asia (Taylor and White, 2004).

1.4.4 Endoperoxides

The current WHO recommended treatment is artemisinin combination therapy (ACT) (WHO, 2013). The most commonly used artemisinin derivatives are artemether and artesunate. These compounds are hemisynthetic, initially dihydroartemisinin is obtained from the *Artemisia annua* plant and methylated or acylated to the commercial prodrug form. When administered, the compounds are rapidly reverted to dihydroartemisinin which is extremely potent, but has a very short half-life of approximately 40-60 minutes (Haynes, 2001). Artemisinins kill asexual parasites and gametocytes, thereby providing some transmission blocking potential (Abay, 2013). However, they are not effective at killing liver stages of the parasites (Meshnick et al., 1996). The exact mode of action of artemisinins is still under debate, although it appears to rely on the endoperoxide bridge structure. Studies have shown various effects of artemisinins on the parasites including haem alkylation, inhibition of sarcoplasmic/endoplasmic reticulum Ca^{2+} ATPase, interference with transporter proteins, depolarisation of the mitochondrial membrane and increased levels of reactive oxygen species (Golenser et al., 2006; Müller and Hyde, 2010), however no overall consensus has emerged.

Although there has been no clinically relevant resistance reported, delayed parasite clearance times have been described in *P. falciparum* infections at the Thai-Cambodian border (Noedl et al., 2008). Studies have shown that delayed parasite clearance times are associated with reduced susceptibility of ring-stages to artemisinin derivatives. A combination of stage-specific lag time and the short half-life of artemisinins could be a mechanism for developing resistance (Klonis et al., 2013). Until recently there was no obvious candidate for a molecular marker of resistance to artemisinin, however, a recent study has shown that kelch (K13-) propeller polymorphisms are linked to resistance both *in vitro* and *in vivo.* A drug sensitive strain of *P. falciparum* was grown in culture for five years with intermittent exposure to artemisinin, after which the proportion of parasites surviving a treatment increased from 0.01 to over 10%. Whole genome sequencing of this strain and the non-treated control strain was compared to the sequences of Cambodian isolates and this single K13 gene was identified. (Ariey et al., 2014).

1.4.5 Antifolates

Pyrimethamine and proguanil (metabolised to active drug cycloguanil) inhibit parasite dihydrofolate reductase (DHFR) activity of the bifuctional DHFR-thymidylate synthetase (TS)

enzyme. DHFR is found in both the host and the parasite and is essential in almost all organisms to reduce dihydrofolate to tetrahydrofolate to provide folates for many essential one-carbon transfer reactions, including DNA synthesis (Hyde, 2005). DHFR inhibitors must therefore be highly specific to the parasite protein, but not the human DHFR to minimise collateral effects. Sulpha drugs, such as sulphadoxin and sulphonamide, affect dihydropteroate synthetase (DHPS) activity of the hydroxymethylpterin pyrophosphokinase (HPPK)-DHPS protein, which is responsible for *de novo* synthesis of folate coenzymes in the parasite (Müller and Hyde, 2010). If monotherapy is used, then parasites can quickly develop resistance, however combination therapy of DHFR and DHPS inhibitors proves synergistic and is much less prone to resistance. The combination of sulphadoxin-pyrimethamine (SP, Fansidar™), introduced in the 1960s, has been of long-term use (Hyde, 2007). It is most widely used in intermittent preventive treatment (IPT) for pregnant women and children. IPT is a curative dose of SP to all individuals in a cohort (pregnant women or infants) in areas of high transmission, regardless of whether they are infected with malaria or not (Warsame et al., 2010).

1.4.6 Antibiotics

The apicoplast is a prokaryotic derived organelle, biochemically similar to bacteria cells, that is essential to *Plasmodium spp.* ((Goodman and McFadden, 2013) and described further in chapter 1.6). This allows use of some antibiotics, notably doxycyclin and clindamycin, that inhibit proteins present in both organisms (Schlitzer, 2008). Doxycyclin is a member of the tetracycline class of antibiotics, and in prokaryotes it inhibits protein synthesis. In *Plasmodia spp.*, doxycyclin specifically blocks expression of apicoplast genes, with non-functional apicoplasts dispensed into the dividing merozoites (Dahl et al., 2006). Clindamycin is a lincosamide antibiotic, derived from lincomycin, that is also a translation blocker in bacteria. Studies in the related apicomplexan parasite *Toxoplasma gondii* have also identified the apicoplast 70S ribosome as the target of clindamycin (Camps et al., 2002). *In vitro* assays with both doxycyclin and clindamycin have shown that they produce a 'delayed-death phenotype'. Parasites that have been treated with these compounds are able to develop normally, produce daughter merozoites, egress and invade new RBCs, however these daughter cells are unable to maintain growth and die shortly after invasion. This phenomenon is apparent even if the drug is removed prior to egress (Dahl and Rosenthal, 2008). The apicoplast appears morphologically normal for the first replication cycle, but is unable to elongate into the typical branching pattern seen in healthy cells (Dahl et al., 2006).

Due to the slow parasite killing nature of these apicoplast inhibitors, both doxycyclin and clindamycin must be used in combination with faster acting antimalarials such as quinine or artesunate for treatment. Doxycyclin is widely used as prophylaxis especially in areas where, for example, resistance to mefloquine is prevalent (Shanks and Edstein, 2005). Unfortunately, it is contra-indicated in young children and pregnant women as it can be incorporated into developing teeth and bones, in such cases clindamycin can be used. Clindamycin is unsuitable for use as a prophylactic due to its short half-life (Schlitzer, 2008).

1.4.7 Others drugs

Atovaquone is a broad spectrum antiparasitic that is used clinically with proguanil, an antifolate, under the brand name Malarone™, often used as chemoprophylaxis for travellers. Atovaquone inhibits electron transfer in the mitochondria by acting as a structural analogue to coenzyme Q in the respiratory chain, leading to loss of membrane potential and preventing pyrimidine biosynthesis (Srivastava et al., 1997). Specifically, atovaquone stops movement of the iron-sulphur protein subunit from cytochrome *b*, preventing electron transfer from cytochrome *b*-bound ubihydroquinone to cytochrome c_1 of the cytochrome bc_1 complex (Mather et al., 2005). A single nucleotide point mutation in the *cytochrome b* gene can confer complete resistance to atovaquone (Srivastava et al., 1999). Although this should not be a problem clinically as atovaquone is always used as a prophylactic.

The chemical family of spiroindolones are an example of new antimalarial agents that were developed from phenotypic screening by Novartis. The compound NITD609 was generated after lead compound optimisation from a natural product library of 12,000 molecules. NITD609 has strong *in vitro* and *in vivo* potency and is potentially suitable for single-dose cure (Rottmann et al., 2010). The vacuolar proton pump PfATP4 has been identified as the molecular target. PfATP4 regulates sodium homeostasis which is essential to parasite survival (Spillman et al., 2013). NITD609 is currently in Phase II clinical trials (Gamo, 2014).

1.4.8 Vector control

Vector control is currently the most effective form of malaria prevention worldwide, particularly in regions with endemic high transmission. Interventions such as distribution of long-lasting insecticide treated nets (LLINs), indoor residual spraying (IRS) and larval source management, amongst others, have contributed to large reductions in the incidence of malaria cases over the past decade (Hemingway, 2014). Although 12 WHO approved insecticides exist in four different chemical classes (organochlorines, organophosphates, carbamates and pyrethroids), currently pyrethroids are used in all LLINs and the majority of IRS operations (WHO). As with the antimalarial drugs, huge selection pressure has driven the development of insecticide resistant mosquitoes thereby generating a major threat to vector control, particularly in Africa where resistance is widespread (Ranson et al., 2011). Whilst there are several new compounds in various chemical classes in the pipeline, it will be some years before they reach the market (Hemingway, 2014).

1.4.9 Vaccines

Since the demonstration of the protective immunity of attenuated sporozoites inoculated into mice (Nussenzweig et al., 1967) and humans (Clyde et al., 1973) in the late 1960s to early 1970s, the promise of a protective vaccine seemed high. However, despite decades of research, there is still no effective vaccine. The complex life cycle and huge genetic variability of *Plasmodium* parasites has seriously impeded development (Thera and Plowe, 2012).

In endemic moderate to high transmission regions, natural protective immunity to disease develops with repeated exposure to the parasites. Newborns and very young infants are initially protected by maternal antibodies (Hviid and Staalsoe, 2004). The highest at risk population tends to be children who are in the process of developing acquired immunity. Adults are generally semi-immune, whilst they do not acquire sterilising immunity (infection and a detectable parasitaemia can be frequently observed), they are protected from clinical symptoms (Doolan et al., 2009). Another at risk population is women pregnant with their first child as they lack antibodies to placenta-specific cytoadherance antigens (Menendez, 2006).

There are several approaches that are being attempted in order to develop a useful vaccine, pre-erythrocyctic, blood stage and transmission blocking. Pre-erythrocytic vaccines could target the sporozoite or liver stages, and if 100% effective could prevent both clinical disease and transmission. The vaccine candidate RTS,S/AS01,the most advanced vaccine candidate to date for *P. falciparum*, is predicted to give a protective efficacy of around 30-50% (Agnandji et al.,

2011, 2012). A recent study has found that at 18 months post-immunisation, vaccine efficiency against clinical malaria in children after three doses of the vaccine was 46% (2014). The RTS,S vaccine is comprised of a C-terminal section of the *P. falciparum* circumsporozoite protein (CSP), a sporozoite surface protein, conjugated to a hepatitis B virus S antigen, which forms virus-like particles (Riley and Stewart, 2013). As RTS,S is only partially effective, it is not a useful transmission blocking strategy. The use of live attenuated sporozoites has been studied extensively. However huge hurdles exist in using this approach, including intravenous injection, safety, production and storage of live parasites, and not least that protection is often strain specific (Epstein and Richie, 2013).

Blood stage vaccines could be used to prevent clinical disease by targeting merozoites or iRBCs. Whilst it is unlikely sterilising immunity can be achieved, these vaccines could still be useful in preventing morbidity and mortality (Riley and Stewart, 2013). Potential merozoite candidate proteins include merozoite surface protein 1 (MSP-1), merozoite surface protein 2 (MSP-2) and apical membrane antigen 1 (AMA-1), although trials so far have only produced allele specific protection, with no cross reactivity (Genton et al., 2002; Thera et al., 2011). However, since the discovery of the RBC antigen basigin as an essential invasion receptor for *P. falciparum* merozoites, its ligand, reticulocyte-binding protein homolog 5 (PfRh5) has been under the spotlight (Crosnier et al., 2011). PfRh5 has been shown to be highly susceptible to cross-strain neutralizing vaccine-induced antibodies (Douglas et al., 2011)by blocking the tight attachment of merozoites to the RBC surface by inhibiting its interaction with basigin (Douglas et al., 2014).

A recent study has identified *P. falciparum* schizont egress antigen-1 (PfSEA-1) as a parasite antigen expressed on the surface of the iRBC that has potential as a vaccine candidate. *In vitro*, antibodies against PfSEA-1 are able to prevent schizont rupture. Vaccination of mice with recombinant *P. berghei* SEA-1 demonstrated longer survival and reduced parasitaemia when challenged with a lethal dose of *P. berghei* parasites. In addition, in two cohorts of individuals from malaria endemic regions in east Africa, presence of antibodies against PfSEA-1 were associated with protection against parasitaemia and severe disease (Raj et al., 2014). These data suggests that PfSEA-1 might be a good target for vaccine development for erythrocytic stages of the life cycle.

Vaccines specifically preventing transmission are somewhat of a controversial idea, but would have a huge positive impact on global public health. Targeting the sexual stages of the parasite lifecycle would reduce transmission and ultimately prevent disease by providing herd immunity to a population, but would not provide clinical protection to the immunised individuals. This

could make regulation and acceptance of the vaccine more complex (malERA Consultative Group on Vaccines., 2011). Gamete surface proteins are significantly more conserved than erythrocytic and pre-erythrocytic stages, and therefore more likely to give broader immunity than strain specific merozoite surface proteins, for example. Unquestionably, a multistage vaccine to prevent clinical disease and transmission, with no potential for breakthrough would be ideal.

1.5 Overview of *Plasmodium* genomics

Plasmodium parasites are single-celled eukaryotic protozoa of the *Apicomplexa* phylum which also includes the causative agents of, babesiosis (*Babesia sp.*), cryptosporidiosis (*Cryptosporidium parvum*), coccidiosis (*Eimeria sp.*), East Coast fever (*Theileria parva*), tropical theileriosis (*Theileria annulata*) and toxoplasmosis (*T. gondii*).

The first draft of a malaria genome (*P. falciparum*) was published in 2002, using a whole chromosome shotgun sequencing approach (Gardner et al., 2002). Human malaria genomes are haploid with 14 nuclear chromosomes, an approximately 6- kilobase (kb) mitochondrial and a 35-kb apicoplast genome (Gardner et al., 2002). The *P. falciparum* 3D7 genome is currently estimated to contain 23.33 megabase pairs, with 5398 protein coding genes. The *P. vivax* Sal-1 genome is 27.01 megabases with 5530 protein coding genes (genome version: 2013-03-01, http://plasmodb.org/plasmo/). Approximately half of the genome has no sequence homology with other studied model organisms, with many coding regions annotated as hypothetical proteins. At present, the genome of *P. falciparum* remains the most AT-rich discovered at over 80% on average and rising to 95% in intergenic regions and introns (Le Roch et al., 2012). About 31% of the genome is predicted to encode membrane spanning proteins, with a lower percentage of multispanning membrane proteins compared with other eukaryotes (Gardner et al., 2002). Gene regulation in *Plasmodium* species is only beginning to be elucidated. It appears to be complex and with little homology to other known eukaryote systems.

The centromeres of all *P. falciparum* chromosomes have been mapped and generally correspond to a roughly 2 kb, highly repetitive and AT-rich, length of sequence (Kelly et al., 2006). *P. falciparum* chromosomes show considerable variation in length and polymorphism between isolates, presumably due to a combination of frequent chromosome breakage and healing (Scherf et al., 1992) and meiotic recombination in the mosquito (Hinterberg et al., 1994).

Epigenetic regulation by chromosome architecture changes is extremely important in the transcriptional regulation of *Plasmodium* parasites. Throughout the erythrocytic stage of its lifecycle, the parasite's genome is mostly retained as open, unstructured eucharomatin. There are stretches of heterochromatin dispersed throughout the genome, regulating expression of various genes involved in crucial pathogenic processes such as invasion, antigenic variation and environmental stress responses (Duffy et al., 2013). Many of the genes involved in antigenic variation are located in the telomeric and subtelomeric regions of the chromosomes, and are regulated epigenetically. *P. falciparum* contains three highly variable gene families, *stevor*, *rifin* and *var*, coding for proteins known as, sub-telomeric variable open reading frame (stevor), repetitive interspersed family (rifin) and erythrocyte membrane protein 1 (PfEMP1) (Wickstead et al., 2003). In each parasite, only one PfEMP1 variant is active at any time (Scherf et al., 1998). Infrequently, a reversible switch to an alternative antigen will occur, leading to evasion of the adaptive immune response allowing the parasite to persist within the host (Deitsch et al., 2009). The histone modifications H3K36me3 and H3K9me3 are primarily responsible for maintaining heterochromatin mediated silencing around the virulence genes (Duraisingh et al., 2005; Jiang et al., 2013). The ApiAP2 transcription factor PfSIP2 is implicated in this process (Flueck et al., 2010). Two recent studies have highlighted a link between the epigenetic machinery of var gene switching and the commitment to sexual stages. Conditional knockdowns of two components of *P. falciparum* epigenetic machinery, heterochromatin protein 1 (PfHP1) (Brancucci et al., 2014)and histone deacetylase 2 (PfHda2) (Coleman et al., 2014), leads to derepression of var genes and other virulence associated genes. Additionally there is derepression of the AP2-G transcription factor (see next paragraph) leading to a three-fold increase in the gametocyte switching rate (Flueck and Baker, 2014).

When the *P. falciparum* genome was first published in 2002, about 60% of the genes had insufficient similarity to those in other sequenced species to be able to assign a function. In addition, there were comparatively few genes that could be assigned to the categories 'cell organisation and biogenesis', 'transcription factors' and 'cell cycle' proteins (Gardner et al., 2002). Rather than this being a result of fewer genes, it is likely to be a result of substantial evolutionary divergence from other sequenced species. Indeed, apicomplexan AP2 (ApiAP2) transcription factors in *Plasmodium* have recently been identified as major regulators of *Plasmodium* gene expression (Campbell et al., 2010). They are related to plant transcription factors (Jofuku et al., 1994). *P. falciparum* is predicted to contain 27 ApiAP2 factors, containing 1-3 AP2 DNA binding domains (Balaji et al., 2005; Campbell et al., 2010). Expression of the ApiAP2 genes is developmentally regulated, with different genes active at different stages of the

parasite's erythrocytic lifecycle. In addition, they appear to be able to regulate their own expression, forming an interaction network throughout the developmental stages (Campbell et al., 2010). The DNA binding motifs of each ApiAP2 protein have been predicted and the function of each protein is beginning to be elucidated. One such transcription factor, AP2-G (PFL1085w), has recently been found to be essential in the switch from asexual blood stages to gametocyte stages (Kafsack et al., 2014; Sinha et al., 2014).

All of the currently identified transcription factors in *P. falciparum* account for less than 2% of the total genome, which is approximately half the number predicted to be required for a classical transcription factor-mediated model of gene regulation (Coulson et al., 2004; Le Roch et al., 2012). Therefore there are either elusive transcription factors yet to be found or gene regulation in *Plasmodium* is mediated via alternative means (Le Roch et al., 2012).

Studies have indicated that post-transcriptional and post-translational modifications are widespread in *P. falciparum* (Foth et al., 2008). mRNA to protein production analysis shows a substantial delay for some genes, suggesting that post-transcriptional modification may be crucial for parasite development (Hall et al., 2005; Le Roch et al., 2004). One particular example is the repression of female blood stage gametocyte mRNA, which forms a complex with the DDX6-class RNA helicase, DOZI (development of zygote inhibited). These translationally repressed complexes are stored in cytoplasmic bodies for translation post-fertilisation (Mair et al., 2006). Post-translational modifications including proteolytic cleavage, phosphorylation, myristoylation, acetylation, glycosylation and ubiquitination, are prevalent in the regulation of protein activity in *Plasmodium* species (Foth et al., 2008). One major example is the proteolytic cleavage of various merozoite surface antigens, an essential step in RBC invasion (Blackman et al., 1994). This will be discussed in greater detail in chapter 1.8.

1.6 Cellular organisation in erythrocyte stages of *P. falciparum*

During the asexual blood stage of the life cycle, the parasite resides within an erythrocyte. Erythrocytes are terminally differentiated cells, lacking all intracellular organelles, unable to perform protein or lipid synthesis and lacking endocytic machinery (Haldar et al., 2002). In some respects this is an advantage for the parasite, RBCs are unable to present antigens on their plasma membrane due to a lack of MHC molecules, reducing the chance of T-cell recognition by the immune system, and have a ready supply of protein in the form of haemoglobin. However, the parasite needs to invade, survive and prevent splenic clearance of RBCs with altered deformability and antigenicity.

Merozoite stages have been extensively studied for many years. They are the only extracellular blood stage and therefore have been a major target for vaccine development. Merozoites are amongst the smallest known eukaryotic cells at about 1.6 µm long, similar dimensions to a large bacterium, oval shaped with a flat apical projection (Langreth et al., 1978). The apex contains many secretory organelles for invasion (rhoptries, micronemes, and exonemes), and cytoskeletal elements (polar rings). The merozoite is surrounded by three membranes, the outer plasma membrane (PM) and two inner membranes (the inner membrane complex, IMC), forming the pellicle, onto which microtubules are attached. The nucleus is at the basal side and there is a single mitochondrion and an apicoplast plastid (Bannister and Mitchell, 2009) (figure 1.3, image A).

The rhoptries, micronemes, dense granules and exonemes are vesicles that discharge their contents prior to and during invasion to prime the parasite cell and the RBC for entry. There are two rhoptries that contain host cell recognition and invasion proteins, as well as lipids to help establish the parasitophorous vacuole that the parasite will reside in (Kats et al., 2006). Micronemes have overlapping functions with rhoptries, but contain distinct additional adhesins for host cell identification and attachment, as well as proteins involved in gliding and invasion (Dowse and Soldati, 2004). Exonemes have been more recently identified as vesicles involved in RBC egress and invasion, distinct from the previously mentioned dense granules. Exonemes discharge PfSUB1 protease leading to destruction of the parasitophorous vacuole and RBC membrane, in addition to priming merozoite surface proteins for invasion (Janse and Waters, 2007; Yeoh et al., 2007). The precise mechanism of egress and invasion is discussed in chapters 1.7 and 1.8.

Post-invasion, the parasite flattens into a cup-shaped early trophozoite, called a ring-stage due to the ring-like structural appearance visible in Giemsa stained blood smears. The ring-stage is typically formed of a thick outer periphery, containing the majority of the organelles, and a thin central portion. The endoplasmic reticulum is close to the nucleus, with small clusters of rough and smooth ER and a Golgi body (Bannister et al., 2000) (figure 1.3, image B).

The parasite will begin to consume the host cell haemoglobin, with degradation mostly occurring within the digestive vacuole of the parasite. The digestive vacuole is an acidic environment, with a pH of between 5.0-5.4, maintained by a ATPase pump induced proton gradient (Klonis et al., 2007). Haemoglobin is digested not only for a source of amino acids, but also potentially for lysis prevention or to facilitate the increase in parasite cell volume (Ginsburg, 1990). The aspartic proteases plasmepsin I and plasmepsin II, along with a cysteine protease falcipain, have been implicated in haemoglobin degradation (Coronado et al., 2014; Gluzman et al., 1994). How the toxic product of haemoglobin degradation, haem, is converted to the inert haemozoin is, at present, unknown (Coronado et al., 2014).

As the parasite grows, it loses its ring-like structure and begins to take up more of the volume of the host cell, becoming a trophozoite. Haemoglobin degradation is most active during trophozoites stages, forming a large brown vacuole full of haemozoin. The number of ribosomes and size of the ER increases markedly and the mitochondrion and apicoplast lengthen. As the parasite ages, there is increased protein export into the RBC cytosol and surface, often to membranous clefts on the cell plasma membrane (figure 1.3, image C). Some of these proteins are associated with parasite sequestration (Bannister et al., 2000).

Parasites are defined as schizonts after the initiation of nuclear division, roughly 36 hours post invasion. *Plasmodium spp*. divide by schizogony, firstly the nuclei replicate asynchronously in several rounds of mitosis, with the last round synchronous for all nuclei coinciding with assembly of the daughter merozoites (Francia and Striepen, 2014). During schizogony, the amount of ribosomes and rough ER increases greatly, the mitochondria and apicoplast multiply and large lipid vacuoles accumulate (figure 1.3, image D). The merozoites assemble in an ordered manner, beginning with the apical organelles. The cytoskeleton assembles and a single nucleus, mitochondrion and apicoplast move into each merozoite. A constriction ring segregates each merozoite from the schizont residual body. Finally the PV membrane and the RBC membranes rupture and the merozoites are liberated into the blood stream, ready to infect new erythrocytes and perpetuate the infection (Bannister et al., 2000).

A

Mitochondrion
Plastid
Microtubules
Dense granules
Nucleus
Microneme
Polar rings
Apical prominence
Merozoite coat
Plasma membrane
Rhoptry
Ribosomes
Pellicular cisterna

LHBannister

Parasitology Today

B

Rough ER
Golgi complex (?)
Exocytic vesicles
Small pigment vacuoles
Cytostome
Plastid
Plasma membrane
Mitochondrion
Nucleus
Free ribosomes

LHBannister

Parasitology Today

Figure 1.3 The main stages of the asexual blood cycle of *Plasmodium falciparum*.
Drawings depicting the ultrastructure of P. falciparum asexual blood stages. A. Merozoite stage
B. Ring stage trophozoites C. Mid-trophozoite D. Late stage schizont with budding merozoites
(Bannister et al., 2000)

Apicomplexan mitochondria are highly divergent in terms of both the organisation and their genomic content (Vaidya and Mather, 2009). The mtDNA of malaria parasites is just 6 kb in length and encodes only three genes, cytochrome c oxidase subunit 1 (cox1), cytochrome c oxidase subunit 3 (cox3) and cytochrome b (cytb), along with several rRNA subunits (Suplick et al., 1990). However, many nuclear encoded genes are trafficked to the mitochondrion. It was long thought that the mitochondrion in asexual stages was not a source of ATP, the parasites instead relying on glycolysis for energy generation (Suplick et al., 1990). However, a recent study has shown that *Apicomplexa* are able to perform a full TCA cycle to catabolise glucose. Unlike classical systems which utilise pyruvate dehydrogenase (PDH) to convert of pyruvate to acetyl-CoA, *P. berghei* mitochondrial branched chain ketoacid dehydrogenase (BCKDH) can perform this function. *Plasmodium* mitochondria are also essential for various biosynthetic processes including haem biosynthesis, pyrimidine biosynthesis, ubiquinone biosynthesis and iron-sulphur cluster biosynthesis (Mather et al., 2007; Vaidya and Mather, 2009).

A defining characteristic of the apicomplexan phylum is the presence of an apicoplast, a relict plastid originating from a photosynthetic eukaryote (Oborník et al., 2009). Virtual proteome studies have identified approximately 500 nuclear-encoded apicoplast-targeted proteins and 35 proteins encoded within the apicoplast itself (Ralph et al., 2004). As well as various 'housekeeping' functions (such as genome replication, transcription, translation etc.), the apicoplast has been confirmed to be involved in several metabolic pathways including haemozoin synthesis, iron-sulphur cluster biogenesis, fatty acid synthesis and isoprenoid precursor synthesis. Less well defined roles may include import and export of metabolites and energy generation, which are, in addition to the organelle growth and division, are poorly understood (Goodman and McFadden, 2013).

1.7 Invasion of RBCs by *P. falciparum* merozoites

The exterior of the merozoite is covered with abundant surface proteins that function in both immune evasion and RBC invasion. *P. falciparum* can invade erythrocytes via various molecular mechanisms, leading to redundancy in the invasion pathway. It has been known for some time that culture adapted *P. falciparum*, and more recently clinical isolates, have differential invasion efficiencies into enzyme treated (neuraminidase, trypsin, chymotrypsin) RBCs. These protease treatments specifically cleave different receptors on the RBC surface. None of the treatments block invasion entirely in all strains (Bei et al., 2007; Mitchell et al., 1986), indicating various mechanisms for cell entry.

Over 50 parasite proteins have been hypothesised to have a function in invasion, however, the precise role is known for very few of them (Wright and Rayner, 2014). Some of these proteins have been classed into functional groups, MSPs (merozoite surface proteins), PfEBAs (*P. falciparum* erythrocyte binding antigens) and PfRHs (*P. falciparum* reticulocyte binding protein homologues). MSPs are the most abundant proteins on the merozoite surface and are thought to act early in the initial cell contact phase of invasion. PfRHs and PfEBAs are stored in the merozoite secretory organelles and have functions later in invasion (Wright and Rayner, 2014). Invasion of erythrocytes by merozoites is extremely rapid and is concluded, on average, within two minutes of egress (Gilson and Crabb, 2009). This is presumably another method of immune evasion by reducing the length of time that the merozoite is extracellular.

Merozoite invasion is a tightly regulated stepwise process that begins with initial attachment to the RBC surface. A process of reorientation then occurs to align the apex of the merozoite with the RBC membrane, there is also major buckling of the erythrocyte membrane, possibly as the merozoite manipulates the host cytoskeleton (Zuccala and Baum, 2011).

There is a great variety of parasite proteins that are predicted to be involved in erythrocyte initial contact. These proteins are not evenly distributed on the surface and some are concentrated at the merozoite apex, indicating a role in invasion (Sanders et al., 2005). In addition, many have domains involved in protein-protein interactions including the Duffy binding-like (DBL) domains which are specific to *Plasmodium spp.* (Peterson et al., 1995). Some of the families implicated in initial contact, whether directly or indirectly are MSPs and serine repeat antigens (SERAs) protease like family. Although functions are not fully understood, some members of these families are essential and specific antibodies can inhibit invasion, including MSP-1 (Blackman et al., 1994). Many of these proteins are also important vaccine candidates.

Parasite reorientation and active invasion involves multiple proteins that are released from apical organelles in a highly coordinated manner. The differential localisation of proteins into separate organelles, and even within organelles (especially rhoptries), presumably plays a role in this regulation (Riglar et al., 2011). Invasion proteins can be divided into adhesins, which function as binding ligands to host cell receptors, and invasins, which are involved in invasion but not binding directly to host receptors (Cowman and Crabb, 2006). The major adhesins can be grouped into two families, EBL and reticulocyte binding-like homologues (PfRh), examples include EBA-175 which binds to glycophorin A (Sim et al., 1994), PfRH4 which binds to complement receptor 1 (Tham et al., 2010) and PfRh5 which binds basigin (CD147) (Crosnier et al., 2011). Apical membrane antigen-1 (AMA-1), an important vaccine candidate, is the most studied invasin to date. It forms a complex with a group of rhoptry neck proteins called the RON complex, at the moving junction during invasion (Richard et al., 2010).

Formation of the moving junction (also termed tight junction) may be the trigger for the release of proteins from the rhoptry bulbs, providing the lipids and proteins needed to form the PV. The exact functional components of the moving junction are still under investigation, but it is known to link the parasite, erythrocyte membrane and the internal actomyosin motor. AMA-1 forms a ring, and with the RON complex, follows the moving junction (Riglar et al., 2011). A single-headed myosin is thought to provide the force that drives invasion (and gliding motility) of the merozoites (Baum et al., 2006). It is attached to the IMC by a number of proteins, including GAP45 (Frénal et al., 2010). Filaments of actin are also concentrated in this region, and form a ring-like distribution at the moving junction (Angrisano et al., 2012). The parasite is then pushed through into the PV created by rhoptry protein release, and the cell membrane is sealed behind it (Riglar et al., 2011).

1.8 Egress of *P. falciparum* merozoites from infected RBCs

Merozoite egress from infected red blood cells is a complex process, and must be tightly regulated by the parasite, premature or late egress results in non-invasive merozoites (Collins et al., 2013a). To escape the RBC, the parasites must rupture two membranes, the PV and the RBC membrane. For many years the order of rupture of these membranes was contested. However it is now known that the parasites are released by an 'inside-out' egress mechanism, where the PV membrane ruptures prior to the RBC membrane (Sologub et al., 2011; Wickham et al., 2003). The cysteine protease inhibitor E64 can inhibit the rupture of the host cell membrane when the PV has already ruptured (Chandramohanadas et al., 2011). A further study observed that the PV swells a few minutes prior to egress, with the RBC compartment shrinking, suggesting that the parasites draw in water from the host cell cytoplasm to the PV to create space for parasite separation and then the PV ruptures once it reaches critical expansion (Glushakova et al., 2010). Before the parasite can break down the host cell membrane, it must destabilise the RBC cytoskeleton. The progressive loss of α/β-adducin by host calpain-1 proteolysis has been implicated as a major factor in this process (Millholland et al., 2011). Parasite proteases are also essential for egress, examples include the cysteine protease falcipain-2 and the aspartic protease plasmepsin II, which both act to degrade the host cytoskeleton, and a subtilisin-like serine protease PfSUB1. PfSUB1 is secreted from the exonemes into the PV just prior to egress, where it specifically cleaves a range of substrates including MSP proteins and members of the cysteine-like protease SERA (serine repeat antigen) family. While the precise involvement in egress is unknown, activation of PfSUB1 is thought to lead to a proteolytic cascade resulting in egress and the priming of merozoites to make them ready for invasion (Blackman and Carruthers, 2013). Less is known about the related PfSUB2. PfSUB2 is considered the primary merozoite surface sheddase which is secreted onto the merozoite surface where it cleaves MSP1 and AMA1 on the surface of the parasite (Harris et al., 2005).

Recently it has been shown that perforin-like proteins are essential for host cell egress in both *T. gondii* and *P. falciparum*. Perforin-like protein 1 (PLP-1) is released from the micronemes and disrupts host cell membranes to allow the parasite to escape (Garg et al., 2013; Roiko and Carruthers, 2013).

Parasites must also escape host RBCs at the gametocyte stage of their life cycle, the RBC membrane is lost as the parasites form gametes inside the mosquito midgut. Gametocyte

emergence has many similarities to schizont rupture. The parasites also use an 'inside-out' egress mechanism, with the PV rupturing before the host cell membrane (Sologub et al., 2011), although there is an approximately 15 minute delay between the two, and utilises proteases and perforins (Wirth and Pradel, 2012). Osmiophilic bodies are thought to play a somewhat analogous role to exonemes in asexual stage egress, with the contents, including proteins that have egress phenotypes such as Pfg377 and GEST (gametocyte egress and sporozoite traversal), released into the PV just prior to rupture (de Koning-Ward et al., 2008; Talman et al., 2011). Cyclic nucleotide and calcium signalling are thought to be key regulators in parasite egress. This is described in more detail below.

1.9 Secondary messenger signal transduction

All cells must be able to sense the environment around them and respond appropriately. Signal-transduction cascades are responsible for processing the stimuli and moderating the cellular response. Diverse signals can be detected and amplified leading to activation of an appropriate reaction. There are some small, non-polar molecules, such as steroid hormones, that are able to act as direct messengers by diffusing through the cell membrane to the nucleus and binding to proteins that interact with DNA to modulate gene expression. However, most signal messenger molecules are too large or polar to cross the membrane and transport mechanisms do not exist. Therefore, the signal must be passed across the membrane without the messenger molecule entering the cell. Commonly a membrane bound receptor detects the messenger by binding to it and transmits the message. This leads to changes in the concentration of secondary messenger molecules such as calcium ions (Ca^{2+}), inositol 1,4,5-trisphosphate (IP_3), diacylglycerol (DAG) and the cyclic nucleotides cyclic adenosine monophosphate (cAMP) and cyclic guanosine monophosphate (cGMP). Generation of a large number of second messengers leads to amplification of the initial signal.
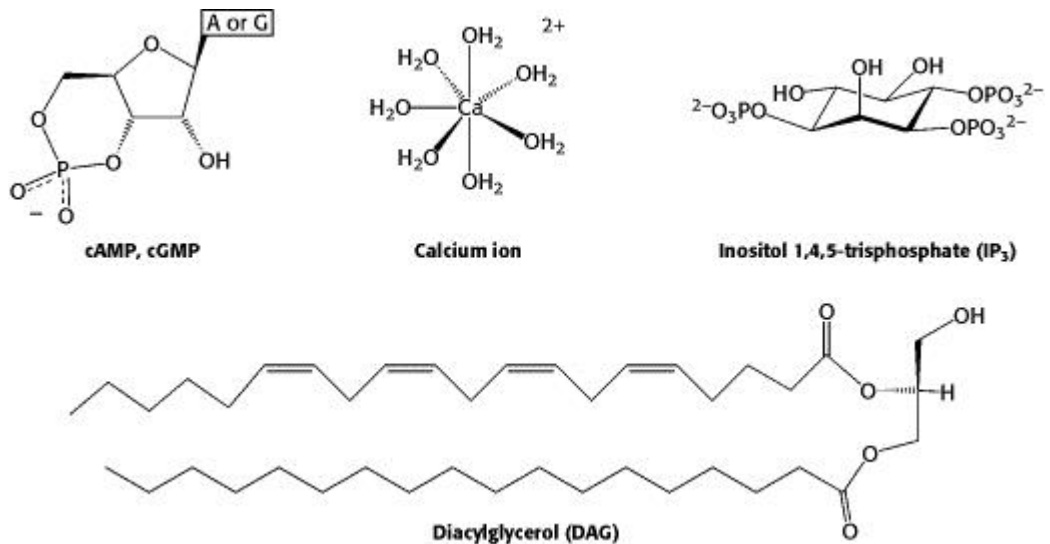
Figure 1.4 Common second messenger molecules
The most abundant second messenger signalling molecules involved in cellular signal transduction. Clockwise, from the top left shows, the cyclic nucleotides, cAMP and cGMP (for a more detailed image see figure 1.5), a calcium ion (Ca^{2+}), inositol 1,4,5-trisphosphate (IP_3) and diacylglycerol (DAG). From (Berg JM, Tymoczko JL, 2002)

Second messengers often convey the signal via activation of protein kinases, which transfer gamma phosphate of ATP phosphoryl groups to specific threonine, tyrosine and serine amino acids in targeted proteins. Protein phosphatases can remove the phosphoryl groups, making protein phosphorylation a reversible reaction (Berg JM, Tymoczko JL, 2002).

1.10 Secondary messenger signal transduction in *P. falciparum*

Malaria parasites utilise several secondary messenger signalling pathways, which are likely to be inextricably linked. Calcium signalling and cyclic nucleotide signalling are of particular importance and regulate many pathways in *Plasmodium* parasites, with an array of conserved and unique component parts when compared to other organisms (Budu and Garcia, 2012).

1.10.1 Calcium signalling in *P. falciparum*

The importance of calcium ions in *Plasmodium* growth and replication has been known since the 1980s. Invasion of RBCs and asexual stage development was found to be dependent on both extracellular and intracellular Ca^{2+} (Wasserman et al., 1982).

Calcium signalling requires the movement of Ca^{2+} from intracellular stores and the extracellular environment. This mobilization and removal of calcium in the cytoplasm is controlled by a series of buffers, pumps and exchangers. Ca^{2+} binds to effectors, such as kinases, that then leads to the stimulation of a number of Ca^{2+} -dependent processes (Verkhratsky and Parpura, 2013).

The erythrocytic cytoplasm calcium concentration is very low (<100 nM), in order to combat the problem of obtaining sufficient calcium ions the malaria parasite maintains a high concentration of Ca^{2+} in the PV (approx. 40 μM) (Gazarini et al., 2003). In addition, the parasite stores Ca^{2+} in the mitochondrion, an acidic store and the endoplasmic reticulum (Gazarini and Garcia, 2004; Marchesini et al., 2000; Passos and Garcia, 1997).

In comparison with other eukaryotic organisms, apicomplexans have fewer calcium related genes, although as with most systems, the genetic information in these organisms is so divergent that others may remain uncharacterised (Moreno et al., 2011). There are at least two calcium pumps acting in the parasite, an apicomplexan unique P-type ATPase, PfATP4 (Krishna et al., 2001), and a sarco/endoplasmic reticulum Ca^{2+} -ATPase (SERCA) orthologue, PfATP6 (Eckstein-Ludwig et al., 2003).

In most mammalian cells, a receptor is coupled to a phospholipase C protein, leading to hydrolysis of phosphatidylinositol 4,5-disphosphate (PIP_2), giving inositol 1,4,5-trisphosphate (IP_3) and diacylglycerol. IP_3 then interacts with the IP_3 receptors on the ER membrane, leading to calcium release through IP_3 gated calcium channel (Ma et al., 2000). There is experimental evidence for inositol 1,4,5-trisphosphate (IP_3)-dependent calcium signalling in *Plasmodia* (Alves

et al., 2011), however no receptors have been identified. Phosphoinositide phospholipase C (PI-PLC) has been identified in *T. gondii* (Fang et al., 2006).

Free calcium ions in the cell interact with calcium binding proteins, generally classed in three main categories, the calcineurin B-like (CBL), calmodulins (CaM) and the calcium-dependent protein kinases (CDPKs). Calcium binding proteins are characterised by the presence of a conserved helix-loop-helix motif, called the EF-hand, which are usually in dimerised pairs and facilitate the binding of two Ca^{2+} ions to each domain. Based on sequence homology, it has been predicted that *P. falciparum* encodes around 70 proteins with an EF-hand domain, currently most of these remain hypothetical with no known function (Moreno et al., 2011). Most apicomplexan genomes encode a putative CaM gene, however only in *T. gondii* has it been cloned and proven to bind Ca^{2+} (Seeber et al., 1999). The CaM inhibitors calmidazolium and trifluoperazine have been shown to inhibit host cell entry by *T. gondii* tachyzoites (Pezzella-D'Alessandro et al., 2001) and parasite development and RBC invasion on *P. falciparum* (Geary et al., 1986; Vaid et al., 2008).

There are seven known CDPKs encoded by malaria parasites (12 in *T. gondii*), related to plant CDPKs (Harper and Harmon, 2005), that regulate many varied processes including stress responses and cell cycle progression. Typically the CDPKs have an amino-terminal serine/threonine kinase domain, then an autoinhibitory domain connecting to a calmodulin-like domain (usually with multiple Ca^{2+} binding domains) at the carboxy terminus (Moreno et al., 2011). In *P. berghei*, CDPK3 is critical for ookinete motility and penetration of the mosquito mid-gut wall, targeted disruption of the PbCDPK3 gene prevented the formation of oocysts (Ishino et al., 2006). *Plasmodium* CDPK4 has been shown to be essential for male-specific events in gametogenesis, particularly genome replication, in *P. berghei* (Billker et al., 2004). *T. gondii* CDPK1 (closest homolog of PfCDPK4) downregulation leads to a reduction in parasite motility, host cell invasion and host cell egress (Lourido et al., 2010). TgCDPK3 (the closest homolog of PfCDPK1) genetic disruption results in a defect in calcium induced egress which can be rescued by complementation with the PfCDPK1 gene (Gaji et al., 2014). PfCDPK5 is essential for RBC egress in asexual blood stages (Dvorin et al., 2010). Recently, it has been shown that PfCDPK7 has a PH (pleckstrin homology) domain which can interact with a PIP_2, and is involved in asexual stage growth. Genetic ablation of PfCDPK7 results in severe asexual growth defects (Kumar et al., 2014).

Calcium signalling is critical for microneme secretion in both *Toxoplasma* and *Plasmodia*. The contents of micronemes can be artificially released with the addition of calcium ionophores,

which can be blocked with the addition of the calcium chelator BAPTA-AM (Carruthers and Sibley, 1999; Gantt et al., 2000). In addition, *T. gondii* egress can be stimulated by addition of calcium ionophores (Endo et al., 1982).

Motility is a key theme in apicomplexan calcium signalling. As mentioned previously, PbCDPK3 is involved in ookinete motility (Ishino et al., 2006; Siden-Kiamos et al., 2006) and TgCDPK1 downregulation reduces motility in tachyzoites (Lourido et al., 2010). In addition, increased cytosolic Ca^{2+} levels have been linked to sporozoite motility in *P. berghei* (Carey et al., 2014). PfCDPK1 is essential in asexual blood stages, and is known to phosphorylate at least two merozoite motor complex components (Green et al., 2008).

As soon as the merozoite is released from the host RBC, it is exposed to low potassium levels, triggering calcium release that activates secretion of invasion proteins onto the merozoite surface (Singh et al., 2010).

1.10.2 Cyclic nucleotide signalling

The cyclic nucleotides 3'-5'-cyclic adenosine monophosphate (cAMP) and 3'-5'-cyclic guanosine monophosphate (cGMP) are ubiquitous signalling molecules found in all eukaryotes, regulating processes as diverse as water reabsorption in the kidney, vision in mammals and chemotaxis in *Dictyostelium* (Baker, 2011).

In mammalian cells, cyclic nucleotide signalling is frequently activated by membrane bound G-protein coupled receptors (GPCRs). GPCRs that stimulate the increase of cNMPs are termed stimulatory G proteins (G_s), there are also inhibitory G proteins (G_i) that act by preventing the formation of cNMPs. GPCRs frequently act in combination with heterotrimeric G proteins. cAMP and cGMP are synthesised by adenylyl cyclase (AC) and guanylyl cyclase (GC), respectively, and hydrolysed by cyclic nucleotide phosphodiesterases (PDEs). By the action of these opposing enzymes, levels of cNMPs can jump over 20-fold from resting state (approximately 10^{-7} M (Bacskai et al., 1993)) in seconds. The primary effector molecule of cAMP is protein kinase A (PKA), and protein kinase G (PKG) for cGMP (Alberts et al., 2002).

PKA and PKG are serine/threonine kinases, they act by phosphorylating specific serine or threonine residues in target proteins, thereby regulating their activity. PKA has both a regulatory and a catalytic subunit. When inactive (in higher eukaryotes at least) PKA is a complex containing two regulatory and two catalytic domains. When cAMP binds to the regulatory domain, the complex dissociates and the active catalytic domains are released, leading to kinase

activity (Reimann et al., 1971; Taylor et al., 2012). The regulatory domains are also responsible for protein localisation within the cell via association with A-kinase anchoring proteins (AKAPs). AKAPs bind the regulatory domain to other components, including membrane associated proteins, the cytoskeleton and other signalling associated molecules, thereby forming a signalling complex called a signalosome (Wong and Scott, 2004). For example, around the nuclear membrane of heart muscle cells, AKAP binds PKA and a phosphodiesterase together. When the cell is unstimulated, the PDE will keep levels of cAMP low locally around the PKA, then becoming saturated when stimulated leading to PKA activity. As soon as the signal stops, the PDE will then rapidly reduce the level of cyclic nucleotide and PKA activity will cease. This arrangement leads to an extremely rapid response to the signal (Röder et al., 2009). In some cases, activation of PKA can lead to a (slower) transcriptional response. Some transcriptional activating proteins contain a cAMP response element (CRE), that is activated by the CRE-binding protein (CREB), a substrate of PKA. For example, in brain cells, the hormone somatostatin initiates a cAMP signalling cascade leading to activation of CREB and upregulation of genes thought to be involved in memory and learning (Brunelli et al., 1976; Kandel, 2012).

cGMP signalling is less ubiquitous than that of cAMP and, unlike PKA, the regulatory and catalytic domains of PKG are contained within the same polypeptide. In humans, there are two PKG families, PKGI and PKGII, encoded by separate genes. In addition, PKGI exists as two different splice variants, PKGIα/β which differ in the N-terminus by roughly 100 amino acids (Francis et al., 2010; Wernet et al., 1989). The catalytic domain is found at the C-terminus of the protein, with the regulatory domain at the N-terminus, containing a leucine zipper motif (for dimerisation and localisation), overlapping autoinhibitory and autophosphorylation domains and cGMP binding domains (Francis et al., 2010). PKG interacting partners (GKIPs) share some analogous features with AKAPs in that they can localise PKG to certain cellular locations, however the characteristics are significantly different. Most GKIPs are PKG substrates, requiring activation by PKG for association (Reger et al., 2014). Example of GKIPs include myosin-binding subunit of myosin light-chain phosphatase (Surks, 1999) and PDE-5 (Thomas et al., 1990). Nitric oxide (NO) signalling is primarily cGMP dependent. NO binds directly to the NO-activated GC, leading to phosphorylation of proteins involved in smooth muscle contraction, cardiac function and platelet activation (Francis et al., 2010).

1.10.3 Cyclic nucleotide signalling proteins in *Plasmodium*

All currently sequenced species of malaria contain homologues of many of the major genes involved in cyclic nucleotide signalling. There are two ACs and two GCs, PKG, catalytic and regulatory subunits of PKA and four PDEs. No receptor proteins have yet been discovered, and there are no recognisable heterotrimeric G proteins in the *Plasmodium* genome.

In the 1990s, it was determined that *P. falciparum* parasites contained AC activity with distinct biochemical properties from that of the erythrocyte. A notable property of PfAC activity was that it was insensitive to the mammalian AC activator forskolin and heterotrimeric G protein activators AlF4^{-} and GTPγS (Read and Mikkelsen, 1991a). In *Plasmodia*, cAMP is synthesised by two ACs, PfACα (PF3D7_1404600) and PfACβ (PF3D7_0802600), that are structurally divergent from mammalian ACs and each other. Full length PfACα contains six predicted transmembrane (TM) domains, and a single C-terminal catalytic domain (CD), however mRNA analysis has shown that PfACα exists as multiple splicing variants, potentially giving rise to proteins with differing numbers of TM domains (Muhia et al., 2003). Structural studies have shown that motifs for catalytic activity and substrate binding are present within the CD. However a homodimer is necessary for activity (Muhia et al., 2003). PfACα has dual predicted functions, in addition to the C-terminal AC catalytic domain there is also an N-terminal potassium channel (Salazar et al., 2012). PfACβ has no predicted TM domains and has two catalytic domains, with substrate binding and catalytic sites spread over the two, implying the need for intramolecular heterodimerisation. Uniquely for *P. falciparum*, the two CDs of PfACβ are broken up by low complexity regions consisting of blocks of highly charged residues, the function of which remains unknown (Salazar et al., 2012). Illumina-based sequencing of *P. falciparum* 3D7 mRNA suggests that PfACα is upregulated in gametocytes and ookinetes and PfACβ in schizonts (López-Barragán et al., 2011). In ACα deficient *P. berghei*, there was more than a 50% reduction in hepatocyte infectivity by sporozoites *in vivo* (Ono et al., 2008). ACβ is homologous to mammalian soluble, bicarbonate sensitive ACs, and has proved refactory to genetic disruption and recombinant expression, however in *P. falciparum* asexual stage culture, addition of specific AC inhibitors resulted in parasite death before completion of schizogony, suggesting an essential asexual function of ACβ. (Salazar et al., 2012).

The two GCs, PfGCα (PF3D7_1138400) and PfGCβ (PF3D7_1360500), are closely related to each other, but have an unusual predicted bifunctional topology, unique to alveolates. The N-terminus is similar to a P-type ATPase, but its function is unknown. The C-terminal end resembles mammalian heterotrimeric G protein-dependent ACs. Notably it is cGMP, not cAMP that is

synthesised however (Carucci et al., 2000; Linder et al., 1999). Each of the domains contains many putative TM domains, giving a predicted 22 overall. Illumina-based sequencing of *P. falciparum* 3D7 mRNA suggests PfGCα is relatively consistently expressed, but somewhat upregulated in late trophozoites. PfGCβ is upregulated in stage V gametocytes (PlasmoDB). Microscopy studies using antibodies against the C-terminus of PfGCα localise to the PV of gametocytes, with little staining in the asexual stages (Carucci et al., 2000), which is unexpected considering the mRNA data. It could be that, like some other *Plasmodium* proteins, the mRNA is transcribed and then suppressed to be translated later in the life cycle (Hall et al., 2005), or that the antibody used lacked specificity. GCβ deficient *P. berghei* parasites were found to have a motility deficiency in ookinetes (Hirai et al., 2006), which will be discussed in more detail in chapter 1.12.9.

PfPKG (PF3D7_1436600), like mammalian PKG, is encoded by a single polypeptide and consists of a C-terminal catalytic domain and a N-terminal regulatory domain (Gurnett et al., 2002). Whilst mammalian PKG proteins have two cGMP binding domains, PfPKG has four (of which three bind cGMP, the fourth is degenerate) (Deng et al., 2003). Studies on the orthologous *Eimeria* PKG have shown that for full activation of the kinase, cGMP must be bound to all three functional cGMP binding domains (Salowe et al., 2002). In other apicomplexan parasites (*Toxoplasma* and *Eimeria*), PKG is found as both a membrane bound and a cytosolic isoform. The membrane attachment is facilitated by dual acylation (Donald and Liberator, 2002), the signatures of which are absent from PfPKG (Diaz et al., 2006). PfPKG does not have any recognisable leucine zipper motif or dimerization domains. mRNA transcript data suggests that PKG is upregulated in trophozoites, schizonts and ookinetes (PlasmoDB).

PfPKA has both a regulatory (PKA-R, PF3D7_1223100) and catalytic subunit (PKA-C, PF3D7_0934800), similar to PKA in higher eukaryotes, that are encoded by separate genes on different chromosomes. PfPKA-R, unlike its mammalian counterpart, is predicted to be a monomer as the N-terminus of PfPKA-R does not contain a similar dimerisation domain. However, it does contain predicted myristylation and palmitylation sites, which presumably localises PKA to a cellular membrane. Therefore, if AKAP binding is involved in *P. falciparum*, a novel mechanism must be present (Haste et al., 2012). There are eleven different experimentally verified phosphorylation sites within PfPKA-R, mostly towards the N-terminus (Lasonder et al., 2012). One of these sites appears to be PKG specific, indicating some degree of crosstalk between the cAMP and cGMP signalling pathways (Christine Hopp, Thesis). PKA-R overexpression has been shown to lead to reduced PKA activity and was detrimental to parasite

growth (Merckx et al., 2008). PKA-C has considerable homology with its mammalian counterparts, however there are disparities in key domains, including domains involved in phosphorylation mechanisms, ATP anchoring, substrate recognition and inhibitor sensitivity (Wurtz et al., 2011).

Plasmodium species encode four PDEs, that have six predicted TM domains at the N-terminal end and a C-terminal catalytic domain. PDEα (PF3D7_1209500) is cGMP specific and is the only PfPDE to have been active when expressed in recombinant form (Wentzinger et al., 2008). Deletion of PfPDEδ (PF3D7_1470500) gave reduced levels of cellular cGMP-PDE activity in gametocytes and a corresponding increase in cellular cGMP levels, strongly suggesting that PDEδ is cGMP specific (Taylor et al., 2008). The cyclic nucleotide specificities of PDEβ (PF3D7_1321500) and PDEγ (PF3D7_1321600) have yet to be proven experimentally. PDEs are discussed in more detail below.

1.11 Cyclic nucleotide phosphodiesterases

Cyclic nucleotide phosphodiesterases (PDEs) have an opposing action to the cyclases, catalysing the hydrolysis of the cyclic nucleotides (figure 1.5), thereby controlling the intracellular concentrations of cAMP and cGMP. Dysregulation of cyclic nucleotide signalling is responsible for many human disorders, including chronic obstructive pulmonary disorder (COPD), acute refractory cardiac failure and erectile dysfunction, amongst many others (Maurice et al., 2014).
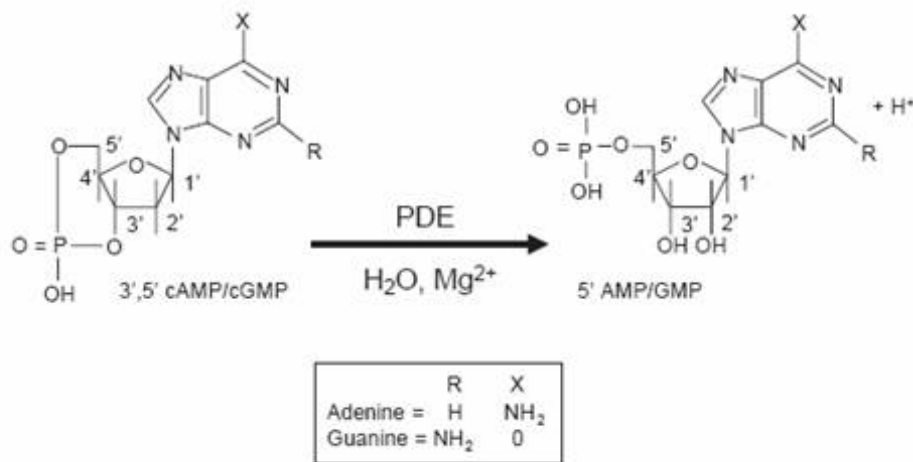
Figure 1.5 Cyclic nucleotide hydrolysis by PDEs
PDEs catalyse the hydrolysis of the cyclic phosphate bond between carbons 3 and 5 of the ribose group (left hand structure) in cAMP and cGMP, in the presence of a divalent cation (such as magnesium). This results in the production of AMP or GMP (right hand structure). The box shows the differences between adenine-based and guanine-based structures (Lugnier, 2006).

The therapeutic potential of targeting PDEs has been long investigated. Shortly after the discovery of the cAMP hydrolytic activity of PDEs, caffeine was shown to be an effective inhibitor (Rall and West, 1963). Indeed, before they were identified as non-selective PDE inhibitors, caffeine and other xanthine derivatives were used clinically in the treatment of asthma, as bronchodilators. However, the broad specificity of these therapies lead to unfavourable side-effects (Schudt et al., 2011). Later studies in the 1970s and 80s identified that there were multiple molecular forms of PDEs, that had the potential to be selectively targeted (Weishaar et al., 1985).

The mammalian superfamily of PDEs can be subdivided into 11 structurally similar, but functionally divergent gene families (PDEs 1-11), most containing several different PDE genes (e.g. PDE1A, PDE1B and PDE1C), that can each be spliced or transcriptionally processed to give

over 100 PDE isoenzymes in total (Maurice et al., 2014). The individual PDEs differ in structure, cyclic nucleotide specificity, function, catalytic properties, regulatory mechanisms and responses to activators, inhibitors and effectors (Conti and Beavo, 2007; Francis et al., 2011).

PDEs are modular proteins that contain a conserved C-terminal catalytic domain and divergent N-terminal regulatory domains.   Different PDE families can hydrolyse different cyclic nucleotides. There are cAMP specific PDEs, (PDEs 4, 7 and 8) cGMP specific PDEs (PDEs 5, 6 and 9) and some that are dual specific (PDEs 1, 2, 3, 10 and 11). The amino terminal domains are responsible for subcellular location targeting, post-translational modifications, responses to regulatory molecules and signals, dimerisation domains, autoinhibitory regulation, allosteric ligand binding, phosphorylation sites, protein-protein interaction sites etc. (figure 1.6) (Kritzer et al., 2012; Maurice et al., 2014).
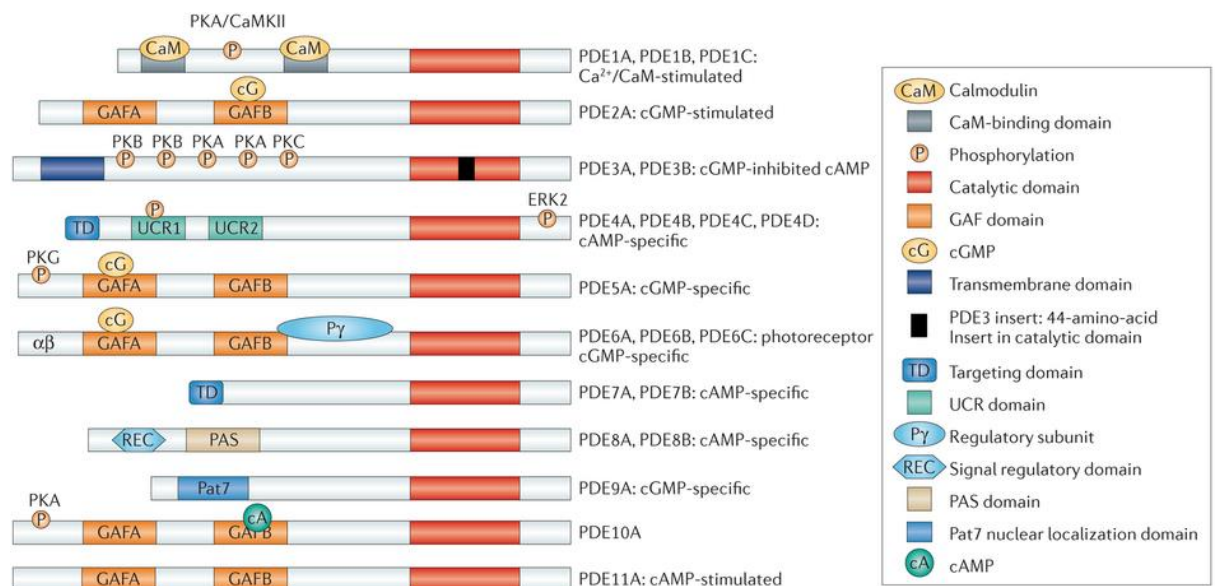
Figure 1.6 Structure and domain organisation of the 11 mammalian PDE families.
The catalytic domain of all mammalian PDEs is conserved at the C-terminus, and many contain N-terminal subdomains and phosphorylation sites. (Maurice et al., 2014)

The mammalian PDE family is extremely complex, and although there is likely to be some redundancy most of the PDE isozymes have been demonstrated to have specific physiological roles (Bender and Beavo, 2006). A brief overview of each PDE family is described below. The PDE1 family are calcium and calmodulin (CaM)-dependent. The binding of a Ca^{+2}/CaM complex to N-terminus stimulates cyclic nucleotide hydrolysis. There are three PDE1 isoforms, PDE1A, PDE1B and PDE1C that have dual-specific cyclic nucleotide activity, although specific affinities

vary (Goraya and Cooper, 2005). PDE1A is involved in regulation of vascular smooth muscle contraction and possibly sperm function. PDE1B is important for immune cell activation and survival as well as dopaminergic signalling. PDE1C has been implicated in sperm function and neuronal signalling and is essential for vascular smooth muscle cell proliferation (Bender and Beavo, 2006). PDE2 is also dual specific and often is involved in cross-talk between cAMP and cGMP pathways. Examples include in adrenal gland aldosterone secretion, phosphorylation of Ca^{+2} channels in the heart and long-term memory function (Bender and Beavo, 2006; Gomez and Breitenbucher, 2013). The two isoforms of PDE3 (PDE3A and PDE3B) are dual specific, however, *in vivo* cAMP hydrolysis can be inhibited by the presence of cGMP. They are activated by phosphorylation by numerous kinases, including PKA. PDE3A has many functions, including cardiac muscle contraction and platelet aggregation. PDE3B is involved in insulin signalling and cell cycle regulation (Ahmad et al., 2012). PDE4 comprises a large family, with four genes (PDE4A-D) each with multiple splicing variants. All PDE4 enzymes are cAMP specific are involved in a large number of functions, including vascular smooth muscle proliferation, immune cell activation and neutrophil infiltration (Bender and Beavo, 2006; Gavaldà and Roberts, 2013). Only one PDE5 gene has been discovered (PDE5A), although several spice variants exist. Amongst other potential functions, PDE5 is involved in NO-cGMP signalling, particularly in the penis and the lungs (Sung et al., 2003). Members of the PDE6 family are involved in cGMP signalling in photoreceptors in the eye and are important in vision (Kerr and Danesh-Meyer, 2009). PDE7A and PDE7B are cAMP specific enzymes, expressed in immune and proinflammatory cells and are implicated in T cell activation (Safavi et al., 2013). The PDE8 family comprises PDE8A and PDE8B which are cAMP specific. Although limited studies exist on PDE8, it is known to regulate Leydig cell steroid production (Shimizu-Albergine et al., 2012). PDE9A, the only member of the PDE9 family, although multiple splice variants exist, is involved in NO-cGMP signalling in the brain (Zhihui, 2013). PDE10 can hydrolyse both cAMP and cGMP *in vitro*, however the *in vivo* specificity is still under investigation. PDE10 is involved in cGMP signalling in the brain and has been implicated in neurodegenerative disorders (Bollen and Prickaerts, 2012). PDE11, described in 2000, is the most recently reported PDE enzyme family (Fawcett et al., 2000). Little is known about PDE11, it is dual specific but can be stimulated by cAMP. It has been implicated in sperm development and dysregulation is associated with major depressive disorder (Bollen and Prickaerts, 2012; Makhlouf et al., 2006).

X-ray crystallography has determined the structures for the catalytic domains of nine of the PDE families, exhibiting a shared topography, roughly 350 amino acids folded into 16 helices. The active site forms a highly conserved, histidine containing, hydrophobic pocket with the PDE-

specific signature motif HD(X$_2$) H(X$_4$)N, and two divalent metal ion binding sites which are essential for catalytic activity (Ke et al., 2011). The catalytic site can be divided into four sub-sites, the metal binding site, core pocket, hydrophobic pocket and the lid region (Sung et al., 2003). The active site pocket contains 11 of the 17 PDE conserved residues (Jin et al., 1992). Two metal ions are necessary for PDE activity, a zinc ion and (usually) a magnesium ion (Conti and Beavo, 2007).

Most of the current PDE inhibitors were generated using classical medicinal chemistry approaches, involving 'black-box' screening, generation of a lead compound and then systematic chemical modification to produce an inhibitor with the desired attributes, such as selectivity, potency and pharmacokinetic properties. Recently, the field is moving towards a more structure-based design approach, using crystal structures of the catalytic sites and PDE-inhibitor complexes for lead optimisation (Card et al., 2005).

At present there are limited PDE inhibitors in widespread clinical use, these include inhibitors against PDEs in three different PDE families (PDE3, PDE4 and PDE5 inhibitors). However there are many more currently in clinical trials. Additionally, whilst not necessarily clinically relevant, inhibitors against all PDE families, with the exception of PDE11, have been developed (Maurice et al., 2014). PDE3 inhibitors include milrinone (Primacor; Astellas Pharma/Sanofi), which can be used for acute treatment of adults with refractory heart failure and those awaiting heart transplants (Movsesian and Kukreja, 2011), and cilostazol (Pletal; Otsuka Pharmaceutical), extensively used to treat intermittent claudication (muscle ache due to peripheral arterial disease) (Kanlop et al., 2011). PDE4 inhibitors, including roflumilast, are used clinically to reducing the risk of exacerbations in patients with chronic bronchitis and COPD, due to the cAMP-mediated anti-inflammatory responses (Fabbri et al., 2009). PDE5 inhibitors, notably sildenafil (Viagra™, Pfizer), are used to treat male erectile dysfunction (Boolell et al., 1996), as well as pulmonary arterial hypertension (Ghofrani et al., 2006). Broader spectrum PDE inhibitors, such as theophylline and caffeine (target all PDE families except PDE8 and PDE9), are used clinically as bronchodilators to treat various pulmonary diseases including COPD, emphysema and asthma (Schudt et al., 2011).

As previously mentioned, certain signalling proteins can specifically interact with each other to form signalosomes. The idea of signalling compartmentalisation was first proposed in the 80s, in a study looking at cAMP specific PKA activation in cardiomyocyte soluble and insoluble fractions (Buxton and Brunton, 1983). This was later confirmed with the identification of AKAPs (Bregman et al., 1989). Individual PDEs are interned within specific signalosomes, for example,

PDE3A, 4B and 4D are all cAMP specific PDEs that are sequestered into different AKAP-based, differentially localised signalosomes that regulate distinct functions all relating to myocardial contraction, allowing cross-talk between signalling networks (Dodge-Kafka et al., 2005; Maurice et al., 2014).

1.11.1 Phosphodiesterases in *Plasmodium falciparum*

The *P. falciparum* genome, and the genomes of all other species of *Plasmodium* sequenced so far, contains four single copy genes encoding for class 1 PDEs, named PDEα-δ. The catalytic domains are closely related to the 11 human PDE families based on the signature $HD(X_2) H(X_4)N$ binding pocket, and similarly to other known class I PDEs, the predicted catalytic domain is at the C-terminus. Unlike most human PDEs, all plasmodial PDEs are integral membrane proteins, containing six transmembrane helices near the N-terminus. Human PDE3 has a single TM domain (Maurice et al., 2014).

In *P. falciparum*, the four PDEs have around 40% amino acid sequence conservation in their predicted catalytic domains, roughly akin to the homology between all the 11 human PDE families, suggesting that the *Plasmodium* proteins each represent a separate family (Conti and Beavo, 2007; Wentzinger et al., 2008). The metal ion binding residues are conserved between, not only the *Plasmodium* PDEs, but all human PDEs as well (Manallack et al., 2005; Wentzinger et al., 2008). Between all currently sequenced *Plasmodium* genomes, the amino acid identity between PDE sub-types is around 50-60% in the catalytic domains (Wentzinger et al., 2008). There are 16 amino acid residues that are conserved across all human PDEs, 13 of these are also conserved in PfPDEs (Howard et al., 2011).

As mentioned above, the PfPDEs are predicted to contain 6 TM domains. The membrane association has been confirmed experimentally. Measurement of total endogenous PDE activity in asexual stage *P. falciparum* lysates has shown that membrane fractions contain more than 95% of cyclic nucleotide hydrolysing activity (Taylor et al., 2008; Wentzinger et al., 2008).

Several attempts have been made to express functional recombinant PfPDEs, both catalytic domains and full length proteins, in a number of different heterologous systems including *E. coli*, *Saccharomyces cerevisiae* and the baculovirus expression system ((Wentzinger et al., 2008) Pfizer, Personal Communication). All attempts thus far have been unsuccessful for PDEβ, PDEγ and PDEδ. The only successful approach was a codon optimised *E. coli* expression system for PDEα catalytic domain, although at very low levels (Wentzinger et al., 2008).

A recent investigation has performed active site similarity modelling between human and PfPDEs. In the absence of crystal structures for the *Plasmodium* enzymes, homology models based on human PDEs were created. The authors found that although the most suitable template for homology model construction was HsPDE9A, PDE1 active site architecture was most similar that that of the PfPDEs. In addition, the authors were able to model the molecular docking of cGMP but not cAMP (Howard et al., 2011).

1.11.2 PDEα

PfPDEα (PF3D7_1209500) is located on chromosome 12 and encodes for a protein of 115 kDa. The polypeptide exists as two different alternative splicing variants. The open reading frame of PfPDEαA is 62 amino acids longer than that of PfPDEαB, due to an additional intron excision (amino acids N^{360}-D^{421}) resulting in the loss of TM helices 4 and 5 (Wentzinger et al., 2008). Consequently PfPDEαA contains 6 TM helices and PfPDEαB contains 4. At the N-terminus, before the start of the TM domains, the section of 260 amino acids has no putative functional domain, although it does contain a predicted phosphorylation motif. This motif (K^{66}KKSDMEY^{73}) has the potential to be phosphorylated by PKA, casein kinase II and tyrosine kinase, and is conserved in other *Plasmodium* species. After the last TM helix, there is an additional casein kinase II target sequence, which is again conserved between *Plasmodium* species. The C-terminal catalytic domain is a predicted 396 amino acids long and shares 22.8% homology with HsPDE4 including more than 93% of all the residues that are conserved between all human PDEs (15 0f 16) (Wentzinger et al., 2008).

Illumina mRNA sequencing indicates that PfPDEα is expressed predominantly in late asexual stages, trophozoites and schizonts, and also potentially in stage V gametocytes (López-Barragán et al., 2011).
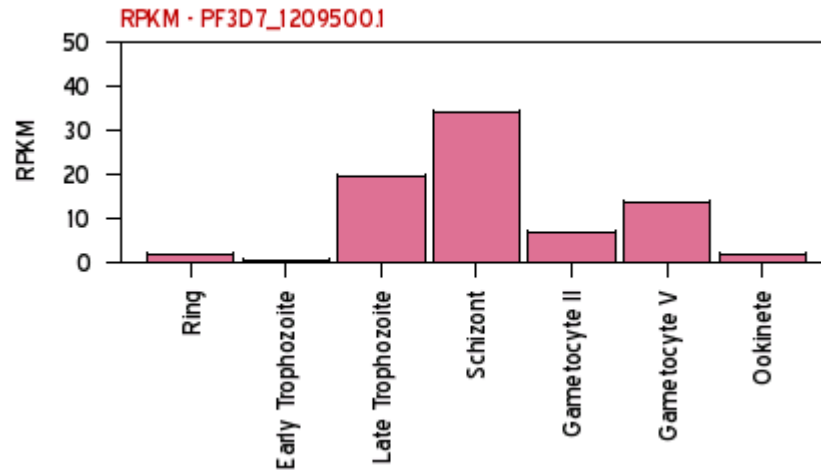
Figure 1.7 Illumina mRNA transcript data for PfPDEα
mRNA was collected from seven different life cycle stages (x-axis) and sequenced using illumina methods. The y-axis shows transcript levels of reads per kilobase of exon model per million mapped reads (RPKM). PfPDEα mRNA is upregulated in late trophozoites and schizonts. Expression data for the splicing variant shows no difference in timing or level of expression (adapted from PlasmoDB).

PDEα is the only *Plasmodium* PDE to have been successfully expressed as a biochemically active recombinant protein. PDE assay data found that it is cGMP specific, no cAMP hydrolysis is observed even under a competitive environment (100 fold excess of cAMP). The K_m for cGMP as a substrate was 2 µM. Wentzinger et al. tested a series of PDE inhibitors that are commercially available, only one, zaprinast, was found to be weakly potent (IC50 of 3-4 µM) (Wentzinger et al., 2008). The others (e.g. IBMX, theophylline, sildenafil), had IC50s above 10 µM.

In a slightly earlier study by Yuasa et al., zaprinast was found to inhibit parasite growth with an IC50 of 35 µM (Yuasa et al., 2005). Dipyridamole, E4021 and sildenafil also demonstrated a moderate inhibitory effect (IC50s 22±0.58, 46±1.8, and 56±11 µM, respectively), all of these compounds are human PDE5 inhibitors (Yuasa et al., 2005).

The metal ion binding activity of the recombinant protein was also investigated. Human PDEs are dependent on the presence of a divalent cation (magnesium, calcium, manganese etc.), and the metal ion binding sites in the PfPDEs are highly conserved. PDE activity was measured in the presence of various cations and the most potent activator of PDEα was found to be Mn^{2+} (in comparison to Mg^{2+} and Ca^{2+}), with maximum activity at 1 mM $MnCl_2$ (Yuasa et al., 2005).

A complete knockout of PDEα resulted in no major discernible phenotype (Wentzinger et al., 2008). There was no visible difference in the morphology between the parental 3D7 and the PDEα-KO lines. However, the authors noted a consistent cell cycle difference between the WT and PDEα-KO line, with the mutant line appearing to grow slightly faster than the WT. Wentzinger et al. found that after synchronisation, ring stages appeared earlier. However, the number of cycles for this to be observed was not consistent, and the authors were unable to quantify the time difference. While PDEα mRNA was ablated in the KO line, mRNA levels of the three other PDEs were not significantly altered compared to the WT, indicating that they are not being upregulated transcriptionally to compensate for the lack of PDEα (Wentzinger et al., 2008).

Overall, in the PDEα-KO line, cGMP hydrolysis decreased by approximately 20% with no effect on cAMP concentrations. This indicates that at least one other PDE can hydrolyse cGMP in the asexual stages (Wentzinger et al., 2008). Addition of greater than the IC50 of the PDE inhibitor zaprinast, decreased cGMP hydrolysis by about 50%, indicative of another PDE that is somewhat sensitive to zaprinast. In addition, cGMP hydrolysis in membrane fractions was severely (>60%) inhibited by a 5-fold excess of cAMP, also indicative of another PDE with cGMP hydrolytic activity that can be inhibited by cAMP. cAMP hydrolysis is significantly reduced in both WT and KO strains in an excess of cGMP (Wentzinger et al., 2008). All these results taken together are highly suggestive that at least one other PDE remains functional in the PDEα-KO line and is a dual specific PDE. Given the expression profile, this is most likely to be PDEβ as it is the only other PDE highly expressed in asexuals.

1.11.3 PDEβ

PfPDEβ (PF3D7_1321500) is located in chromosome 13, and encodes a protein with a deduced molecular mass of 133 kDa, with a predicted six TM domains. There is also a recently characterised alternative splicing variant which leads to a single amino acid change from alanine to threonine (A^{630}→T) (PlasmoDB). Little is known about PDEβ, including the cyclic nucleotide specificity, however the above PDEα-KO suggests it may be dual specific. As with all the *Plasmodium* PDEs, specificity for cAMP or cGMP cannot be predicted from the sequence. It is also presumed to be an essential protein as all attempts to ablate the gene, in both *P. falciparum* and *P. berghei*, have been unsuccessful (David Baker, unpublished). Hidden Markov topography predictions suggest that the catalytic domain faces towards the PV lumen, but this has not been verified experimentally (Gould and de Koning, 2011) and its location remains unknown.

Transcript sequencing data suggests PfPDEβ is expressed most highly in late trophozoites and schizonts (figure 1.8).

Figure 1.8 Illumina mRNA transcript data for PfPDEβ
mRNA was collected from seven different life cycle stages (x-axis) and sequenced using illumina methods. The y-axis shows transcript levels of reads per kilobase of exon model per million mapped reads (RPKM). PfPDEβ mRNA is upregulated in late trophozoites and schizonts. Expression data for the splicing variant shows no difference in timing or level of expression (adapted from PlasmoDB).

1.11.4 PDEγ

PDEγ (PF3D7_1321600) is also on chromosome 13, approximately 3000 bp downstream from PDEβ, transcribed from the opposite strand. This arrangement may have been the result of a gene duplication event in a common *Plasmodium* ancestor. This arrangement can be detected in all currently sequenced *Plasmodium* species but could not be identified in other *Apicomplexa*. It also has six predicted TM domains and encodes for a protein with a deduced molecular weight of 92 kDa, making it the smallest PfPDE protein. mRNA sequencing data (from all the stages examined thus far) suggests that PDEγ is only expressed at very low levels in asexual blood stages, but is upregulated in stage V gametocytes. A knockout of PDEγ showed no aberrant phenotype in asexual blood stages, gametocytes, rounding up or exflagellation (Taylor et al., 2008). However, PfPDEγ is important for sporozoite formation and infectivity (Cathy Taylor, Thesis).
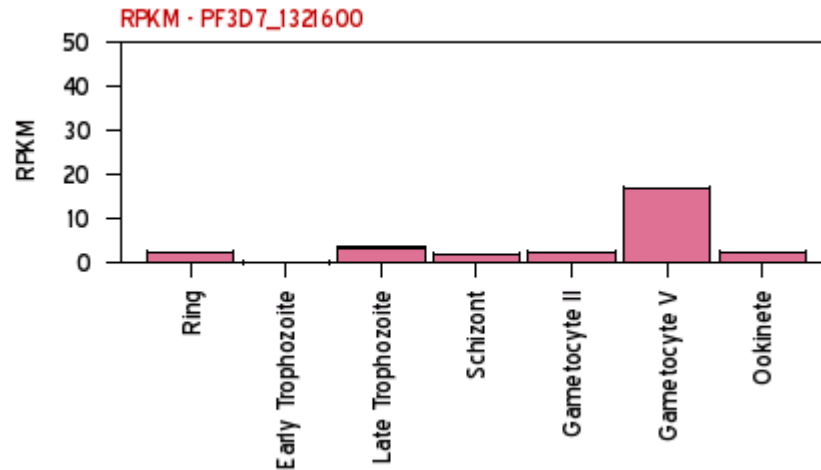
Figure 1.9 Illumina mRNA transcript data for PfPDEγ
mRNA was collected from seven different life cycle stages (x-axis) and sequenced using illumina methods. The y-axis shows transcript levels of reads per kilobase of exon model per million mapped reads (RPKM). PfPDEγ mRNA is upregulated in gametocytes, although the levels never get very high (adapted from PlasmoDB).

1.11.5 PDEδ

The PfPDEδ (PF3D7_1470500) gene is located on chromosome 14, it also has six predicted TM domains and encodes a protein with a deduced molecular weight of 97 kDa. A PfPDEδ-KO was created by Taylor et al., which showed significantly reduced cGMP hydrolysis and corresponding increase in cellular cGMP levels (with no effect on cAMP hydrolysis or levels) compared to WT parasites, indicating that PDEδ is a cGMP specific PDE (Taylor et al., 2008). Illumina mRNA transcript sequencing suggests that PDEδ is expressed in sexual stages only and is highly upregulated in stage V gametocytes and ookinetes (figure 1.10).
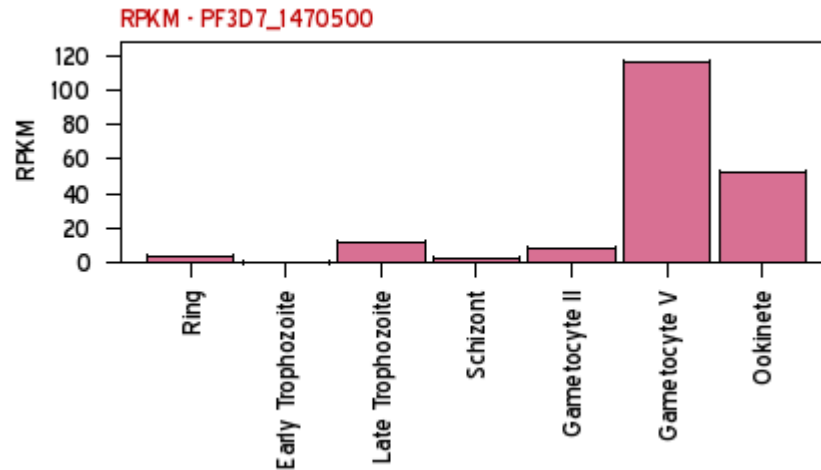
Figure 1.10 Illumina mRNA transcript data for PfPDEδ
mRNA was collected from seven different life cycle stages (x-axis) and sequenced using illumina methods. The y-axis shows transcript levels of reads per kilobase of exon model per million mapped reads (RPKM). PfPDEδ mRNA is upregulated in gametocytes and ookinetes (adapted from PlasmoDB).

The PfPDEδ-KO gametocytes, all the way up to stage V, are morphologically identical to wild-type, however they show an extreme reduction in the number of parasites able to undergo gametogenesis (Taylor et al., 2008) due to an increase in the cGMP levels. In the KO, cGMP-PDE activity was reduced by about 50%, but not completely abolished, suggesting that another PDE is active (and potentially upregulated) in gametocyte stages. Additionally, the mutant gametes were not able to egress from the RBC at the same rate as WT parasites. Addition of zaprinast to WT parasites reduced cGMP-PDE activity by about 75% compared to 100% in KO parasites. It is therefore likely that PDEδ is less sensitive to zaprinast than the enzymes responsible for the residual PDE activity (Taylor et al., 2008). The authors also note that a conserved glycine residue, implicated in interaction between zaprinast and human PDE5, is present in all PfPDEs except PDEδ, potentially explaining its relative insensitivity to the compound (Taylor et al., 2008; Turko et al., 1998).

Interestingly the gametogenesis phenotype was absent in a *P. berghei* PDEδ-KO. Moon et al., instead focused on *P. berghei* ookinete stages, which showed that PbPDEδ is important for transmission to the mosquito vector, ookinete formation and gliding motility. As with PfPDEδ-KO, PbPDEδ-KO cyclic nucleotide levels were measured and cGMP-PDE activity was lower in the PDEδ-KO at gametocyte stages. During ookinete formation, the concentrations got closer together for WT and the mutant and by the time the ookinetes were fully mature, the cGMP-

PDE activity was the same as WT. The same study also created a GCβ-KO, which showed normal rounding up, exflagellation and fertilization *in vitro*, but were much less able to transmit to mosquitoes when measuring oocyst numbers compared to wildtype (Moon et al., 2009). The PDEδ-KO and GCβ-KO total cGMP levels did not vary from WT in ookinetes, suggesting that PDEδ is not the predominant PDE in ookinetes nor is GCβ the predominat GC (Moon et al., 2009). The biological relevance of these findings is discussed in more detail below.

1.12 Roles of cyclic nucleotide signalling in *Plasmodia*

1.12.1 cAMP signalling and sexual commitment

The importance of cyclic nucleotide signalling in malaria was first investigated in the late 70s with the observation that cAMP production is increased in infected RBCs compared to uninfected (Hertelendy et al., 1979). The following year, the remarkable observation that addition of 1 mM cAMP to asexual cultures of *P. falciparum* could trigger almost 100% switching to gametocytes was observed, however this has not been reproduced (Kaushal et al., 1980). Later that decade, it was shown that cAMP-PDE inhibitors could increase the numbers of asexual parasites switching to gametocytes (Trager and Gill, 1989). Further evidence for the role of cAMP signalling in gametocytogenesis was provided by Read and Mikkelsen, when they compared the PKA activities of a gametocyte producing (LE5) and a gametocyte deficient strain (T9/96). Despite basal levels of AC activity being equal, the levels of PKA activity were much higher in the gametocyte producing strain (Read and Mikkelsen, 1991b).

As mentioned previously, the *Plasmodium* genome does not contain any obvious candidate genes for heterotrimeric G proteins based on sequence homology. However, a study by Dyer and Day, utilising cholera and pertussis toxins which are used to study the involvement of stimulatory or inhibitory heterotrimeric G proteins respectively in other systems, suggested the involvement of a heterotrimeric Gsα subunit in *P. falciparum* gametocyte formation (Dyer and Day, 2000). However, a more recent study looking at G protein signalling in sexual commitment, showed that although treatment with cholera toxin or MAS 7 (expected to down-regulate or have no effect of gametocytogenesis through indirect reduction in AC activity by inhibition of an α-subunit of the heterotrimeric G protein) increased the switching rate, only MAS 7 lead to increased cAMP levels. This indicates that although the cholera toxin does increase gametocytogenesis, it is unlikely through the action of heterotrimeric G proteins. The

unexpected MAS 7 result suggests that it acts, directly or indirectly, on the PfAC activity but the authors noted that these results were preliminary and further work was needed to ascertain exactly what role MAS 7 was playing in this study (Peatey et al., 2013).

A study by Harrison et al. in 2003 reported that an erythrocyte G protein-coupled receptor signalling pathway via the β2-adrenergic receptor and heterotrimeric guanine nucleotide–binding protein (Gαs), is involved in RBC entry by *P. falciparum*. An inhibitory Gαs peptide, which blocks interaction with GPCRs and preventing downstream signalling, reduced formation of new rings when added to a *P. falciparum* culture. Conversely, addition of β2-adrenergic receptor agonists increased infection by about two-fold. Additionally, the use of Gαs antagonists in *P. berghei* infected mice was able to reduce parasitaemia in comparison to untreated mice (Harrison et al., 2003). In follow up study, addition of the β2-adrenergic receptor antagonist propranolol also inhibited blood stage parasite growth (Murphy et al., 2006). In mammalian cells, G protein signalling is important in cellular cytoskeleton reorganisation, a process that is also involved in merozoite invasion of RBCs (Vanhauwe et al., 2002). It is possible that host G-protein signalling is responsible for the rapid cytoskeletal reorganisation necessary for malaria RBC invasion.

1.12.2 cAMP and melatonin

Melatonin is a regulator of circadian rhythm in many organisms, in humans it is produced as a response to decreasing light levels in order to promote sleep (Trivedi and Kumar, 2014). Data have been reported that suggest that the synchronicity seen in malaria parasite infection during asexual blood stages is dependent on signalling by host melatonin. Addition of melatonin to Balb/C mice that had undergone removal of the pineal gland, restored the synchronicity of *P. chabaudi*, lost by the surgery, to the levels seen in un-pinealectomized mice. Addition of melatonin resulted in a phospholipase C -dependent calcium release from *Plasmodium* intracellular stores (Hotta et al., 2000), and a 40% increase in cAMP levels leading to a 50% increase in PKA activity (Beraldo et al., 2005). This is highly suggestive of a complex interplay between calcium and cAMP signalling in response to melatonin. Further analysis of this pathway has shown that this is an IP_3 dependent pathway. The authors propose that melatonin activates phospholipase C, generating IP_3, leading to opening of ER-localised IP_3 sensitive Ca^{2+} channels (Alves et al., 2011). A study by Lima et al., identified PfNF-YB as a potential transcription factor regulated by melatonin. The authors also observed that cAMP regulates PfNF-YB expression (Lima et al., 2013).

1.12.3 cAMP in sporozoite stages

In the 1970s, it was shown that sporozoite gliding motility could be induced by albumin *in vitro* (Vanderberg, 1974). Sporozoite motility and hepatocyte invasion is dependent on secretion of adhesin proteins from apical organelles, including CSP and TRAP. In a PbACα-KO strain, sporozoite infectivity is reduced by half due to an impairment in the ability to exocytose in response to cell migration, suggesting that microneme exocytosis is regulated by cAMP. This phenotype could be restored by reintroduction of the PbACα gene (Ono et al., 2008). This study also suggests a role for potassium ions, hypothesising that increased K+ permeability may induce ACα activity. It is possible that Ca^{2+} signalling is linked to cAMP induced exocytosis in sporozoites, as incubation with calcium ionophores can also lead to microneme secretion (Mota et al., 2002). Albumin may act as a signal to simulate calcium release and increase cAMP levels leading to gliding motility (Kebaier and Vanderberg, 2010).

1.12.4 cAMP signalling and anion transport through iRBC membranes

Parasites establish extensive anion transport systems through the host erythrocyte membrane to take up solutes, excrete metabolic waste products and maintain ion gradients (Kirk, 2001). A study by Egee et al. indicated a role for cAMP signalling and endogenous PKA in the regulation of an anion exchange pathway in *P. falciparum* infected RBCs (Egee et al., 2002). However in patch clamp experiments by Merckx et al., it was observed that the addition of recombinant PfPKA regulatory subunit, PKI (mammalian PKA inhibitor) or overexpression of PfPKA-R resulted in a down regulation of anion conductance, suggesting that parasite PKA is also involved in anion transport. The transgenic overexpression line also had a defect in asexual growth that could be repaired by increasing cAMP levels, demonstrating the importance of tightly regulated cAMP levels for parasite growth (Merckx et al., 2008).

1.12.5 cAMP in merozoite stages

As mentioned in chapter 1.7, invasion of merozoites involves formation of a tight junction and secretion of adhesion proteins from apical organelles. One of the key proteins in tight junction formation is AMA1 (Alexander et al., 2006). PfAMA1 is phosphorylated by PKA at serine 610, in the cytoplasmic tail of the protein. When mutated to an alanine, thereby abolishing phosphorylation, invasion was roughly 4% efficient compared to WT, highlighting the importance of PKA in invasion (Leykauf et al., 2010).

A study by Saraiva et al. found that addition of angiotensin II, a peptide hormone involved in vasoconstriction, part of the rennin-angiotensin system (RAS), reduces RBC invasion by merozoites. Angiotensin peptides can modulate PKA activity. The inhibition of invasion could be reversed by addition of 1 μM dibutyryl-cAMP (a membrane permeable cAMP analogue). The authors therefore postulated a role of RAS in *P. falciparum* blood stages (Saraiva et al., 2011).

A recent phosphoproteome study has shown that PKA-dependent phosphorylation is extremely important in schizont stages, and is implicated in number of processes, including chromatin remodelling, cytoskeleton organisation, membrane lipid metabolic, phosphotase and kinase activity and merozoite motility. The study also verified three novel PKA substrates, myosin A, GAP45 and CDPK1, using an *in vitro* kinase assay, which are involved in the merozoite glideosome motor (Lasonder et al., 2012). The phosphorylation of CDPK1 is another example of overlap between the cyclic nucleotide signalling pathways and calcium signalling.

1.12.6 cGMP in schizont stages

The parasite PKG gene is essential in asexual blood stages and is therefore refractory to deletion. There are however, two highly selective compounds that specifically target PKG, named compound 1 (C1) and compound 2 (C2). C1 is a tri-substituted pyrroles identified by Merck as an inhibitor of the coccidian *Emieria* PKG (Gurnett et al., 2002). C2 is an imidazopyridine which was developed later by Merck, using medicinal chemistry, to be more potent and specific than C1 (figure 1.11). Both C1 and C2 are ATP competitive inhibitors that interact with a pocket adjacent to the ATP binding site (Donald et al., 2002). C1 and C2 are low nanomolar inhibitors of recombinant PfPKG (Diaz et al., 2006; McRobert et al., 2008).

Compound 1   Compound 2
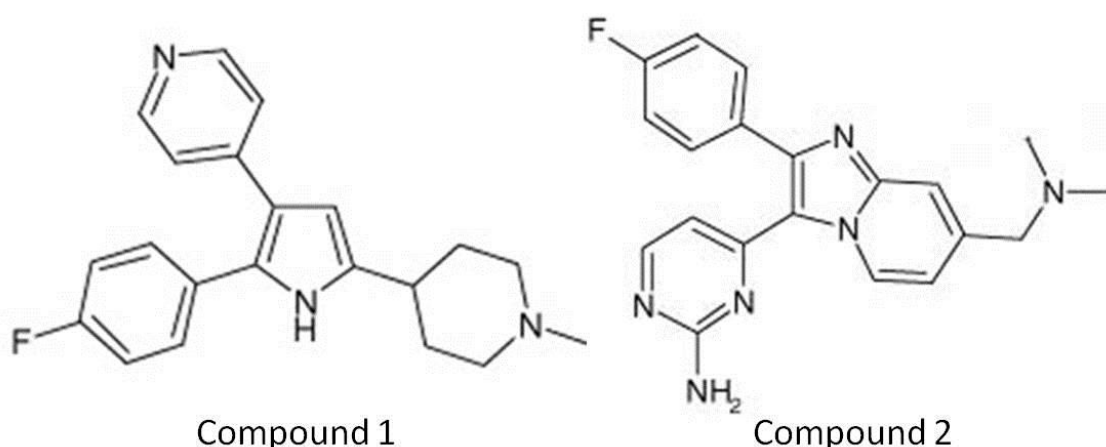
Figure 1.11 Biochemical structure of compound 1 and compound 2

The entry of the fluorophenyl group of C1 and C2 into this small hydrophobic pocket, which connects with the ATP binding pocket, is mediated by a small gatekeeper residue (threonine 618 in PfPKG), that when substituted to a more bulky glutamine side chain to create mutant PfPKG$_{T618Q}$, the fluorophenyl group cannot access this pocket. This reduces the sensitivity of the protein to the inhibitor more than 2000-fold. A transgenic parasite line in which the endogenous PKG was replaced by PKG with the PfPKG$_{T618Q}$ mutation was also created (McRobert et al., 2008).

Addition of C1 to asexual stage parasites prevents formation of new rings by blocking egress of schizont stages. If added to rings, they are able to develop normally up to late schizonts which are then unable to rupture. Merozoite protein localisation by IFA appeared normal and the parasites looked morphologically ready to egress, however the merozoites were unable to escape the RBC. This effect was confirmed as PKG specific as the T618Q mutant was resistant to egress block by C1 and C2, rupturing and reinvading erythrocytes at levels comparable to the DMSO control (Taylor et al., 2010). The sensitivity of T618Q parasites to C2 is about 10 fold less than WT due to some off target activity, however a recent medicinal chemistry effort between the David Baker's laboratory and Medical Research Council Technology has lead to the development of a more potent and specific inhibitor (MRT00207065) with over a 1000 fold difference in IC50.

Inhibition of PfPKG by C1 was found to prevent the functioning of PfSUB1, with the protease unable to process its target substrates, including MSP1 (Dvorin et al., 2010). Conditional knockdown, using the destabilisation domain system, of PfCDPK5 also results in an egress block, yet the SUB1 activity is unaffected. Additionally, manually ruptured CDPK5-DD arrested parasites were able to reinvade erythrocytes, whereas C1 blocked parasites were not. This is suggestive of PKG activity upstream of CDPK5 activity (Dvorin et al., 2010).

1.12.7 cGMP in liver stages

In *P. berghei*, a conditional knockout system was used to remove a large portion of the PbPKG protein. A parasite line containing flippase (FlpL, a temperature dependent site-specific recombinase) under the control of a sporozoite stage promoter, was transfected with a plasmid that inserted two FRT sites into the PKG locus, leading to disruption of the gene within the mosquito (Combe et al., 2009). The resultant PbPKG-KO parasites were able to invade and develop inside the HepG2 human hepatocyte cell line, however release of merosomes and egress of the parasites was severely impaired (Falae et al., 2010).

Addition of C1 to sporozoites was found to reduce motility and block hepatocyte invasion entirely in the sub micromolar range. However, addition of C1 to the PbPKG-KO parasites also prevented invasion, indicating that there is an additional non-PKG target mediating this effect (Panchal and Bhanot, 2010).

1.12.8 cGMP in gametogenesis and exflagellation

As mentioned previously, cGMP signalling has been implicated in gametogenesis, with several lines of evidence strongly indicative of this. The addition of the PDE inhibitor zaprinast to stage V gametocytes can stimulate dose-dependent rounding up and exflagellation in the absence of XA, and without an appropriate pH shift (Taylor et al., 2008; Yuasa et al., 2005). In a GCβ-KO line, reduction of GC activity has no effect on gametogenesis indicating that cGMP levels need to be maintained below a threshold for sexual development to continue (Taylor et al., 2008). In PDEδ-KO parasites exflagellation levels were very low with stimulation both by XA and zaprinast (Taylor et al., 2008). Antibody co-staining with band 3 (a RBC anion exchanger) as a marker for RBC presence showed that mutant gametocytes were unable to escape the erythrocyte (Taylor et al., 2008). Furthermore, the addition of C1 to stage V gametocytes prevents the rounding up of WT parasites, with the PfPKG$_{T618Q}$ parasites able to proceed at normal levels (McRobert et al., 2008). Taken together, the data suggest that high levels of cGMP during the gametocyte stage are very detrimental to the parasites ability to perform gametogenesis, but that rounding up and exflagellation are mediated by PKG. BAPTA-AM, a calcium chelator, did not block rounding up, indicating that cGMP dependent PKG activity is upstream of calcium signalling in gametogenesis (McRobert et al., 2008).

1.12.9 cGMP in ookinetes

In contrast to the findings for PfPDEδ-KO, PbPDEδ-KO parasites can proceed normally through gametogenesis, but have morphologically impaired ookinetes. For the first 12 hours, the ookinetes develop normally, but then the usually banana-shaped cells round up or deteriorate into stumpy forms, resulting in poor oocyst formation. The addition of C1 could reverse the stumpy/rounded up phenotype, as did a double PbPDEδ-KO/PbGCβ-KO mutant (Moon et al., 2009).

PbGCβ-KO parasites undergo normal rounding up, exflagellation and fertilization *in vitro*, however, ookinete motility was severely impaired. The parasites have a very slow average speed and show only occasional slow gliding (Moon et al., 2009). Addition of C1 to WT parasites strongly blocked gliding motility with an IC50 of less than 100 nM.

Interestingly, the round and stumpy forms produced in the PbPDEδ-KO were still viable and able to form oocysts when the ookinetes were injected directly into the mosquito haemcoel, bypassing the midgut epithelium. Salivary gland infections were established at the same level as WT and the parasites were transmissible into mice. GCβ-KO ookinetes were not able to establish oocysts or salivary gland infections (Moon et al., 2009). There may therefore be an additional role of GCβ-KO in the oocyst/sporozoite stage. In the PDEδ-KO, motor function was not abrogated, but the parasites rotated on the spot. Ultrastructure data showing abnormalities in the IMC and subpellicular microtubules supports this finding (Moon et al., 2009).

1.12.10 cGMP and phosphoinositide metabolism

A recent study has revealed a cGMP-PKG link to phosphoinositide metabolism and calcium signalling in *P. falciparum* schizonts and *P. berghei* mosquito stages. As mentioned previously, PKG activity was found to control the level of cytosolic Ca^{2+} necessary for gliding motility of the ookinete in *P. berghei* (Moon et al., 2009), as well as regulation of egress in *P. falciparum* (Taylor et al., 2010). Disruption of these processes, using C2, has a major effect on phosphoinositide metabolism. During ookinete gliding, PKG controls phosphoinositide biosynthesis. Furthermore, in schizonts, inhibition of PKG blocks hydrolysis of phosphatidylinostitol (4,5)-bisphosphate, the precursor of IP_3 (Brochet et al., 2014).

1.13 Phosphodiesterases as a target for anti-malarial drug discovery

Novel antimalarial drug targets are desperately needed to counteract the growing threat of resistance by *Plasmodium* parasites. In the past, drugs countering infectious diseases have been designed to act on targets not present in the human host, as this can result in highly specific drugs with low toxicity, the 'silver bullet' method. Although this principle often works well for bacterial diseases (e.g. antibiotics against bacterial cell walls), eukaryotic pathogens share similar biological systems with the host. More recently there has been a growing trend towards the 'inverted silver bullet', an established target in humans is used to develop a specific drug for its protozoan counterpart. PfPDEs represent good candidates for this type of drug development. PDE inhibitors are well established for a variety of human ailments, including; chronic obstructive pulmonary disease, depression, asthma and erectile dysfunction (Bender and Beavo, 2006; Maurice et al., 2014). Current human PDE inhibitors are often extremely specific for their target, presenting the possibility that a specific, selective *Plasmodium* PDE inhibitor can be developed. In the last few years there has been some advancement towards a PfPDE inhibitor. Two papers by Beghyn et al. have described the discovery of tadalafil based antimalarial compounds that have activity in the sub-low micromolar range. After some optimisation, the authors were able to reduce the selectivity for HsPDE5. The authors noted that potency against malarial PDEs would have to be increased and that no *in vivo* data was available (Beghyn et al., 2011, 2012). However, the therapeutic potential of *Plasmodium* PDEs as a drug target and the potential to reduce the activity against human PDEs was established.

Cyclic nucleotide signalling is essential in many life cycle stages of *Plasmodium* parasites and disruption of many of the components results in aberrant parasite growth and often failure to transform to the next life cycle step. Phosphodiesterases are key regulators of the cAMP and cGMP signalling pathways, and although PDEα, PDEγ and PDEδ are not essential in blood stages *in vivo*, the most easily druggable stage, PDEβ is predicted to be. Therefore this project will focus on validation of PDEβ as a target for antimalarial drug discovery.

Chapter 2: Materials and methods

2.1 *Plasmodium falciparum* culture

2.1.1 General culture

The clonal parasite line 3D7 was maintained in culture following standard culture practices (Trager and Jensen, 1977). The parasites were cultured in A^+ human erythrocytes (National Blood Transfusion Service), with RMPI 1640 (Sigma-Aldrich) supplemented with 50 mg/l hypoxanthine, 3.96 g/l glucose and 1.5 g/l L-glutamine (Sigma-Aldrich) and 0.5% complete Albumax II solution (Fisher-Scientific). The cultures were incubated at 37°C in 5% CO_2 in a static CO_2 incubator (Binder). To sustain a healthy culture the parasites were maintained at less than 5% parasitaemia at 3-5% haematocrit. To monitor the parasitaemia, 0.5 ml of the culture was removed and briefly centrifuged to pellet the RBCs. The pellet was resuspended in an equal volume of culture medium to give 50% haematocrit and a thin blood smear was prepared on a glass slide (VWR). The slide was fixed with methanol and stained with 10% Giemsa solution (Sigma-Aldrich) for 20 minutes. The slide was examined under light microscopy.

Parasite synchronisation to isolate ring stages was carried out according to standard practice with 5% sorbitol (Lambros and Vanderberg, 1979) to retain only the ring stages. The parasites were pelleted by centrifugation, resuspended in five volumes of 5% sorbitol (in H_2O, filter sterile) and incubated at room temperature for two minutes. The culture was spun at 500 x g for two minutes, the sorbitol was removed and the cells were washed twice with warmed culture medium. The pellet was resuspended in culture medium to give 5% haematocrit.

Late stage parasites were purified using magnetic cell separation (MACS). Briefly, mid-trophozoite and schizont cultures were pelleted, resuspended in RPMI 1640 and captured in a magnetic column (Miltenyi Biotec). Uninfected RBCs and early stages flow through and late stages are captured on the magnetic matrix by haemozoin binding. Late stages are eluted with RPMI 1640 in the absence of the magnet.

2.1.2 Thawing and cryopreservation

Parasites were quickly thawed from liquid nitrogen stocks in a 37°C waterbath. The volume was measured and 1/5th of the volume of 12% NaCl (Sigma-Aldrich) was added dropwise, shaking after addition of each drop. The culture was left to stand for two minutes. Ten times the original volume of 1.6% NaCl was added dropwise with mixing, as before. The cell suspension was centrifuged at 500 x g for 5 minutes and the supernatant removed. To wash, the pellet was resuspended in culture medium and again centrifuged. The washing step was repeated 2-3 times. After the final wash step, the pellet was resuspended in 10 ml culture medium and the cell suspension was transferred to a small cell culture flask (T25), and adjusted to 5% haematocrit with fresh erythrocytes. All solutions were pre-warmed to 37°C and filter sterile.

To freeze down parasite stocks, the cultures were pelleted and the medium removed. An equal amount of cryosolution (28% glycerol, 3% sorbitol, 0.65% NaCl, filter sterile through a 0.22 µm membrane) was added to give a 1:1 mix. 0.5-1 ml was added to a cryotube (PAA) and stored in liquid nitrogen. When freezing down, the cultures were at a minimum of 2% ring-stage parasitaemia.

2.1.3 Transfection of *P. falciparum*

Genetic manipulation of *P. falciparum* parasites was achieved using standard transfection methods (Wu et al., 1995). 80 µg of precipitated plasmid DNA was resuspended in 15 µl of 1 x TE buffer (10 mM Tris-HCl, pH8, 1 mM Na_2EDTA). Just before electroporation, 385 µl warmed cytomix (120 mM KCl, 0.15 mM $CaCl_2$, 2 mM EGTA, 5 mM $MgCl_2$, 10 mM K_2HPO_4/KH_2PO_4, 25 mM HEPES (pH7), filter sterile) was added. A culture of synchronised ring-stage parasites at 5-10% parasitaemia was pelleted and all media removed. The DNA-cytomix solution was added to 250 µl of the packed cells, and transferred to a 0.2 cm cuvette (Bio-Rad). The sample was electroporated at 950 microfarad (µF) at a voltage of 0.31 kilovolts (Kv) using a GenePulser Xcell™ (Bio-Rad). The electroporated parasites were moved to a T25 culture flask (VWR) with 10 ml culture medium and enough fresh blood (usually fresh from an LSHTM donor with 50 U/ml) was added to give 5% haematocrit. 24 hours later, the positive selection marker WR99210 was added at 5 nM concentration. WR99210 is a selective inhibitor of the parasite dihydrofolate reductase (DHFR) (Fidock and Wellems, 1997; Fidock et al., 1998). The transfection plasmids encode a mutant human *dhfr* gene which confers resistance to WR99210. After starting positive selection with WR99210, 24 hours post transfection, parasites were visible by Giemsa smear at between 14-28 days. To reduce the presence of episomes, and increase the proportion of

parasites with an integrated plasmid copy, the cultures were cycled off drug for three weeks then on drug until parasites reached 1% parasitaemia for one to four cycles. Integration was monitored by PCR after each cycle, see chapter 2.2.2.

2.1.4 Limiting dilution to generate clonal parasite lines

Transgenic *P. falciparum* lines were cloned by limiting dilution. Ring stage cultures were counted using a haemocytometer to get the number of parasitised cells in a microlitre of packed RBCs. The infected culture was diluted to give 0.25 parasites per well in a 96 well plate at 2% haematocrit. Culture media was replaced every three days. After 14-21 days, positive wells were identified by a lactate dehydrogenase assay.

2.1.5 Lactate dehydrogenase assay

The lactate dehydrogenase (LDH) assay can be used as a colorimetric measure of parasite positive wells. LDH is an enzyme that catalyses conversion of lactate to pyruvate, simultaneously reducing NAD+ (Nicotinamide adenine dinucleotide) to NADH. *P. falciparum* LDH can rapidly reduce 3-acetyl pyridine NAD (APAD), whilst erythrocytic LDH is only able to catalyse this reaction very slowly. An NBT/PES (nitro blue tetrazolium/phenazine ethosulphate) solution is included that converts APADH into a coloured salt, which can be read at 650 nm on a spectrophotometer. The LDH assay was modified from previously described methods (Makler and Hinrichs, 1993; Makler et al., 1993). 20 µl of whole culture was removed from each well and transferred to a replica plate. 100 µl of Malstat reagent (0.1% Triton X-100, 130 mM L-Lactate, 27 mM Tris-HCl, pH 9.0), supplemented with 33 µM APAD (Sigma-Aldrich) was added. 25 µl of NBT/PES solution (2.2 mM nitro blue tetrazolium, 240 µM phenazine ethosulphate) was added to each well and the plate was incubated at 37°C for 30 minutes in the dark. Positive wells can be identified by a colour change to dark blue/purple. Positive wells were expanded for PCR and Southern blotting analysis of the clones.

2.2 Nucleic acid manipulation

2.2.1 Oligonucleotide primer design

All primers were designed by hand assessed for secondary structures and uniqueness using Oligocalc (http://www.basic.northwestern.edu/biotools/-oligocalc.html) and PlasmoDB, respectively, and supplied by Sigma-Aldrich. Working stocks of 10 µM were used in all reactions. For a complete list of primers, see Appendix A1.

2.2.2 Polymerase chain reaction (PCR)

The Polymerase Chain Reaction (PCR) is used to amplify the number of copies of a specific DNA sequence for further analysis. The reaction relies on thermal cycling of the DNA with a thermostable DNA polymerase. The oligonucleotide primers are designed to bind to template DNA flanking the region of interest on the opposing DNA strands. Firstly the double stranded DNA is denatured at 94-95°C. The temperature is then lowered to the optimal primer-template annealing temperature which varies between primers and template, usually 40-60°C. The primer anneals to the complementary template DNA. The temperature is raised to 65°C (although normally 72°C, the AT-rich *P. falciparum* DNA requires a lower elongation temperature) to allow the polymerase to add nucleotides to the primer sequence, extending the complementary strand and creating double stranded DNA. This is the elongation step. The temperature is once again raised to 94°C to denature the DNA. This cycle of denaturation, annealing and elongation is repeated around 30 times to exponentially increase the amount of DNA.

For reactions that required high fidelity, PCR was carried out using PfuUltra II Fusion HS DNA Polymerase (Stratagene), unless otherwise stated. PfuUltra is a proof-reading polymerase, used to reduce the chance of incorporating mutations in the PCR products. Negative controls, without genomic DNA, were also carried out for each experiment. PCR was performed according to the Stratagene protocol for PfuUltra II Fusion HS DNA Polymerase. For reactions where high fidelity was not necessary, BioMix™ Red DNA polymerase (Bioline) was used according to the manufacturer's instructions.

To screen bacteria transformed with plasmids for colonies positive for an insert, Colony PCR was performed. Colony PCR can be carried out on whole bacterial cells straight from an agar plate and is useful for screening plasmids with low efficiencies of ligation or transformation. A master plate is used to refer back to the correct colony. Firstly the appropriate number of PCR reactions

were set up using BioMix™ Red DNA polymerase (Bioline) and primers that are specific for the insert-plasmid junction, in a total volume of 10 μl. A sterile pipette tip was used to touch a single colony from the transformed *E. coli*, streaked on to the master plate and then the tip was put into the PCR tube. The PCR reaction was mixed with the tip and then the tip was discarded. The reaction was cycled as follows; 94°C for 3 minutes, 60°C for 30 seconds, 65°C for 30 seconds, 94°C for 30 seconds, 60°C for 30 seconds, 65°C for 30 seconds, steps 4-6 cycled for 25 times, then 65°C for 3 minutes.

2.2.3 Agarose gel electrophoresis

Agarose gel electrophoresis enables DNA fragments to be separated by size for further analysis or manipulation, and approximate concentrations to be calculated. 0.8-1.2% agarose (BioLine) gels were prepared in TAE Buffer (tris-acetate-ethylenediaminetetraacetic acid (EDTA), 40 mM Tris, 1 mM EDTA pH 8.0, 0.12% glacial acetic acid), with ethidium bromide solution (Sigma) at 0.5 μg/ml. DNA products were mixed with a 1/5 volume of 5x loading buffer (Fermentas) and were loaded and run alongside HyperLadder I (Bioline) to estimate to molecular weight of the bands. The running buffer was TAE, and the gel was run at 100-120 volts (V). The bands were visualised using UV light. If necessary, bands were excised using a sterile scalpel blade to facilitate cloning.

Two different methods were used for purifying DNA after PCR and restriction digests; PCR cleanup (QIAquick PCR Purification, Qiagen) and agarose gel extraction (Qiaquick Gel Extraction Kit, Qiagen). The kits were used to remove proteins (e.g. polymerases and restriction endonucleases), primers, free nucleotides and other DNA fragments which could interfere with further experiments. The kits were used as per the manufacturer's handbook. Agarose gel electrophoresis was used to assess the concentration and purity of the extracted DNA sample.

2.2.4 Restriction digests and DNA ligation reactions

All restriction endonucleases were supplied by Fermantas or New England Biolabs. All digest reactions were incubated at 37°C for three hours, unless otherwise stated.

Ligation reactions, with the digested insert and plasmid, were set up using T4 DNA ligase (Promega). The total reaction volume was 10 μl and the ratio of insert:plasmid was calculated using the manufacturer's formula. The ligation was incubated for 4-18 hours at 15°C.

2.2.5 Transformation of competent *E. coli* cells

Plasmid DNA was amplified using commercially chemically competent XL-1 Blue *E. coli* cells (Agilent). Briefly, the cells were defrosted on ice and 50 µl was aliquoted into pre-chilled round bottom tubes (BD Falcon). 1.7 µl of β-mercaptoethanol was added and the tubes were gently shaken. The cells were incubated on ice for ten minutes. Plasmid DNA, 0.1-50 ng, was added to the tubes. The reaction was then incubated on ice for 30 minutes. The cells were heat-shocked at 42°C for 45 seconds and then incubated on ice for two minutes. 0.9 ml of SOC recovery medium (2% tryptone, 0.5% yeast extract, 10 mM NaCl, 2.5 mM KCl, 10 mM MgCl$_2$ and 20 mM glucose), prewarmed to 37°C, was added and the cell suspension was incubated at 37°C for 1 hour in a shaking incubator. 200 µl of the suspension was spread onto Luria-Bertani (LB) agar (1% tryptone, 0.5% yeast extract, 1% NaCl and 1.5% agar) supplemented with 100 µg per ml ampicillin (Sigma-Aldrich), and incubated at 37°C overnight. Colonies were screened for presence of the insert by colony PCR, positives were grown up for DNA extraction.

2.2.6 Extraction of plasmid DNA from transformed *E. coli* cells

Single colonies of transformed *E. coli* were selected and incubated overnight in LB-broth (as LB-agar without the 1.5% agar) supplemented with ampicillin. The plasmid DNA was isolated from the transformed cells using the QIAprep Spin MiniPrep Kit (Qiagen) or QIAGEN Plasmid Mega Kit, following the supplier's handbook. Glycerol stocks were also created with a 1:1 ratio of cell culture solution to glycerol, and stored at -80°C.

2.2.7 Sequencing of DNA

DNA was sequenced using the BigDye® Terminator v3.1 Cycle Sequencing Kit (Applied Biosystems). The reaction mix contains both deoxynucleotides (dNTPs), which can be incorporated into the amplifying strand, and fluorescently-labelled dideoxynucleotides (ddNTPs) which, when integrated into the DNA strand, result in termination of elongation. This creates many strands of different lengths with a base specific fluorescently-labelled ddNTP which can be read on an ABI3730 capillary sequencer (Applied Biosystems). Reactions were carried out in a 10 µl total volume (1.75 µl BigDye buffer, 0.5 µl BigDye 3.1, 1 µl of 10 µM primer, 3 µl purified DNA and 3.75 µl dH$_2$O). The reaction was cycled as follows; 94°C for 1 minute, 55°C for 1 minute, 65°C for 1 minute, above steps repeated 25 times, and then 65°C for 5 minutes.

The DNA from the sequencing reaction was precipitated, to remove dye, excess nucleotides and proteins, by the addition of 0.3 M sodium acetate, three times the volume of 100% ethanol and

put at -80°C for 30 minutes. This was then spun at 4°C for 30 minutes at 13000 x g. The supernatant was removed and 500 μl of 70% ethanol was added and the reaction was spun again. The supernatant was carefully removed and the tubes were left to dry in the dark. The samples were sequenced using an ABI3730 capillary sequencer using a faculty funded service.

2.2.8 Isolation of *P. falciparum* genomic DNA

P. falciparum genomic DNA (gDNA) was isolated from infected cultures using two different methods, depending on the amount of DNA required. For smaller amounts of gDNA, less than 10 μg, the QIAmp DNA Blood Mini Kit (Qiagen) was used, according to the manufacturer's guide. This kit can extract DNA from up to 200 μl packed cell volume of infected RBCs. For larger volumes, the following protocol was performed. 10 ml of late stage parasite culture was saponin lysed (see chapter 2.3.3), and the pellets resuspended in 400 μl of resuspention buffer A (500 mM NaOAc pH 5.2, 100 mM NaCl, 1 mM EDTA). Half the volume of 10% SDS (sodium dodecyl sulphate) was added, followed by one volume of buffered phenol:choloroform, pH 8, and the solution mixed. The samples were centrifuged at full speed for five minutes at room temperature, by which time the aqueous and organic phases had separated. The DNA remains dissolved in the aqueous phase, which is transferred into a fresh tube and the phenol:chloroform extraction repeated. The aqueous phase is again transferred to a clean tube and the final extraction uses one volume of chloroform. Finally, the DNA pellet is precipitated by adding two volumes of 100% ethanol, spinning at 4°C for 30 minutes at full speed. The pellet is then washed once in 70% ethanol, and resuspended in 20-100 μl 1 x TE buffer.

2.2.9 Southern hybridisation

The purpose of a Southern blot is to detect a specific DNA sequence within a sample. With respect to this project, Southern hybridisation was performed in order to detect integration events and episomal DNA within transgenic parasite lines. 5-10 μg of gDNA was digested for three hours with the appropriate restriction enzymes, at appropriate temperatures (see chapter 3). The digested DNA was precipitated in the same way as for preparing DNA for sequencing (chapter 2.2.7), and resuspended in 20 μl TE buffer. The samples were then run on a 0.7% agarose gel with ethidium bromide (0.5 μg/ml) at 75V for three hours to achieve good separation of the fragments and photographed under UV light. The gel was depurinated for 10 minutes in 0.25 M HCl and denatured in alkaline transfer buffer (0.4 M NaOH) for 30 minutes, with one wash. The gel was then transferred onto a positively charged nylon membrane (Brightstar, Ambion) overnight using capillary action. Once transferred, the DNA was crosslinked onto the

membrane using 1200 joules of UV (UV Stratalinker™ 1800, Stratagene). The membrane was washed twice in 2x saline-sodium citrate (SSC, 20x stock at 3 M NaCl, 0.3 M sodium citrate) buffer. Hybridisation buffer (HYB, containing 10% dextran sulphate, 50 mM Tris, 10 mM EDTA, 5x SSC buffer, 1x Denhardt's solution and 0.2% SDS, pH 7) containing 100 μg/ml of sheared salmon sperm DNA (denatured at 95°C for 5 minutes) was used to pre-hybridise the membrane for 2 hours at 60°C. The specific DNA probes were created using PCR (specific details in chapter 3). 25 ng of probe DNA in TE buffer was denatured at 95°C for 5 minutes, then snap-cooled on ice for a further 5 minutes. The probe was radiolabelled with [^{32}P]dCTP (Perkin-Elmer) using Rediprime II random prime labelling kits (GE Healthcare) following the manufacturer's protocol. Following the 30 minute 37°C incubation period, the probe was separated from the unincorporated nucleotides in an Illustra microspin G-25 column (GE Healthcare) and denatured at 95°C for 5 minutes before being added to the membrane-HYB. Hybridisation with the labelled probe was carried out overnight at 60°C, after which the membrane was rinsed once and washed twice, for one hour, in 2x SSC buffer at 60°C. The membrane was exposed to a phosphor screen for 24-48 hours and developed using a Typhoon PhosphorImager (GE Healthcare).

2.3 Parasite protein manipulation

2.3.1 Immunofluorescence assay (IFA) on blood smears

Thin blood smears were prepared on glass slides (VWR) and wells marked with a hydrophobic PAP pen (Sigma-Aldrich). The slides were fixed in 4% formaldehyde (made up fresh from paraformaldehyde in PBS, pH 7.3, Sigma-Aldrich) for 20 minutes at RT, then washed twice with 1x PBS. The cells were then permeabilised with 0.1% Triton X-100 (Sigma-Aldrich) in 1x PBS for 10 minutes at room temperature and again washed three times with 1x PBS. The slides were incubated for 1 hour at RT or overnight at 4°C in blocking buffer (3% BSA in 1x PBS, Sigma-Aldrich) to prevent unspecific binding, before incubation with the primary antibody, diluted to an appropriate concentration in blocking buffer, for 1 hour at RT. The slides were washed thrice with 1x PBS and incubated with the secondary antibody, diluted 1:500 in blocking buffer, for 1 hour at RT, before being washed for a final three times with 1x PBS. The slides were mounted in Vectashield mounting media (Vector Laboratories) with DAPI, before analysis on the confocal microscope (Zeiss).

Primary antibodies were diluted as follows: monoclonal rat anti-HA (clone 3F10, Roche) at 1:100 and monoclonal mouse anti-HA (clone 16B12, Convance) at 1:500. Rat anti-PfBiP and mouse anti-PfGAP45, obtained from Anthony Holder's laboratory, NIMR, were used at 1:1000. Rabbit antibodies against PfMSP-1 and PfEBA175, obtained from Mike Blackman's laboratory, NIMR, were used at 1:5000, 1:200 and 1:200, respectively. Rabbit anti-PfERD2, from the Malaria Research and Reference Reagent Resource Centre (MR4), was diluted 1:1000. Rabbit anti-PfAKAP, from Anaïs Merckx's laboratory, Université Paris Descartes, was used at 1:500.

Anti-peptide antibodies, provided by Pfizer, were generated by Cambridge Research Biochemicals using the Target™ Antibody service. Short peptide sequences of PfPDEα and PfPDEβ, predicted to be immunogenic by a Pfizer immunogenicity program, were synthesised by Cambridge Research Biochemicals and conjugated to chicken gamma globulin (CGG). The sequences and positions of the peptides are shown in appendix A2. Two peptides were produced for PfPDEα and one for PfPDEβ. The peptide conjugates were then used to immunise rabbits, two rabbits for each peptide. Four booster immunisations were given, two weeks after the previous immunisation. Serum samples were taken pre-immunisation, after each booster and the final bleed at the end of the course. The final bleed was affinity purified using columns coated with the corresponding peptide to obtain specific antibodies. Two elution buffers were used, glycine and triethanolamine (TEA).

The following secondary antibodies were all obtained from Invitrogen and used at 1:500: Alexa Fluor 488 goat anti-rat IgG (H+L), preabsorbed against mouse IgG (A11006), Alexa Fluor 594 goat anti-rat IgG (H+L), preabsorbed against mouse IgG (A11007), Alexa Fluor 594 F(ab')$_2$ goat anti-rabbit IgG (H+L)(A11072), Alexa Fluor 594 goat anti-mouse IgG (H+L), highly cross absorbed (A11037) and Alexa Fluor 488 F(ab')$_2$ goat anti-mouse IgG (H+L), highly cross absorbed (A11017).

2.3.2 Immunofluorescence assay (IFA) with ER-Tracker, in suspension

50 µl of purified late stage parasites were resuspended in 50 µl RPMI 1640 and incubated with 1 µM ER-Tracker™ Blue-White DPX (Molecular Probes, Life Technologies, kindly provided by Theresa Ward (LSHTM)) for 15 minutes at 37°C. The cells were then washed three times with RPMI 1640 and once with 1x PBS at 500 x g. The parasites were fixed with 1 ml fixation solution (4% formaldehyde, 0.01% glutaraldehyde in 1x PBS) for 30 minutes at RT, and then washed 5 times with 1x PBS at 400 x g. The cells were permeabilised with 0.1% Triton X-100 in 1x PBS for 10 minutes at room temperature and washed three times with 1x PBS at 500 x g. The cells were incubated for 1 hour at RT in blocking buffer (3% BSA in 1x PBS), then with an appropriate dilution of primary antibody (1:100 monoclonal rat anti-HA (clone 3F10, Roche)) in blocking solution. The primary antibody was washed away 3 times with 1x PBS, and the cells incubated with 1:500 dilution of the secondary antibody (Alexa Fluor 488 goat anti-rat IgG, Invitrogen), and washed a final 3 times. The cells were mounted in Vectashield mounting media (Vector Laboratories) without DAPI, before analysis on the confocal microscope (Zeiss).

2.3.3 Saponin lysis of erythrocyte membranes

To free parasites from the host cell, packed RBC pellets were resuspended in 5x the volume of 0.15% saponin solution (Sigma-Aldrich) in PBS, containing EDTA-free protease inhibitor cocktail (Roche), and incubated for two minutes at RT. The samples were pelleted for 1 minute at 10,000 x g and washed three times in ice cold 1x PBS, also containing EDTA-free protease inhibitors for 30 seconds at 10,000 x g. The samples were then stored on ice for further work or frozen at -20°C for future analysis.

2.3.4 Solubility assay

Frozen saponin lysed parasite pellets were vigorously resuspended in 2-5 times the volume of ice cold 5 mM Tris-HCl, pH 8.0 containing EDTA-free protease inhibitor cocktail (Roche), and incubated for 10 minutes on ice. The lysate was centrifuged at 16,000 x g for 10 minutes at 4°C, the supernatant removed, recentrifuged to remove residual insoluble material and saved as sample S1. DNAse digestion was performed on the pellet, briefly, the pellet was resuspended in half the volume of DNAse digestion buffer (5 mM Tris-HCl and 2.5 mM MgCl$_2$, plus EDTA-free protease inhibitor cocktail) and 1 µl DNAse I (stock concentration 5 mg/ml) per 100 µl sample was added. The digestion was incubated at RT for 10 minutes and gently mixed every 2 minutes. The sample was centrifuged at 16,000 x g for 10 minutes at 4°C and the supernatant aspirated. The pellet was extracted for 30 minutes with 2-5 pellet volumes of 1% Triton X-100 on ice, then centrifuged at 16,000 x g for 10 minutes at 4°C to obtain the S2 fraction. The final pellet was extracted using insoluble fraction extraction buffer (4% SDS (Sigma-Aldrich), 0.5% Triton X-114 (Sigma-Aldrich), in 0.5x PBS), for 30 minutes at RT. All extractions used the same extraction volume and equal amounts were analysed by immunoblotting.

2.3.5 Sodium dodecyl sulphate polyacrylamide gel electrophoresis (SDS-PAGE)

Polyacrylamide gel electrophoresis is used to separate proteins based on their electrophoretic mobility, dependent on size, charge and conformation of the protein. For all the work in this project, denaturing SDS-PAGE was used. This linearises the protein and the SDS in the buffer gives the protein an overall negative charge, therefore the separation is mostly based on size. Estimations of the size of sample proteins can be made by comparison with proteins of a known molecular weight (Alberts et al., 2002).

4x reducing sample buffer (200 mM Tris-HCl, pH 6.8, 8% SDS, 40% glycerol, 4% β-mercaptoethanol, 50 mM EDTA, 0.08% bromophenol blue) was added to the samples (to give a 1x final volume). The samples were boiled for 5 minutes before running on a Tris-HCl polyacrylamide gel (8 or 10% gels were used, separating gel pH 8.8 (stacking gel pH 6.8, 4% polyacrylamide) Acrylogel 2.6 (40% solution, 37:1 acrylamide to N,N'-methylenebisacrylamide, VWR)). The gel was run in Tris-glycine buffer (25 mM Tris-HCl pH8.3, 250 mM glycine, 0.1% SDS), for 1.5 hours at 120 V. The molecular weight ladders used were Precision Plus Protein™ Standards, Unstained for Coomassie blue staining or All Blue for immunoblotting (both Bio-Rad). The gels where then analysed either by Coomassie blue staining or immunoblotting.

2.3.6 Coomassie blue gel staining

To stain for total protein content, Coomassie blue gel staining was performed. After SDS-PAGE, the gel was soaked in Coomassie blue staining solution (0.25% Coomassie Brilliant Blue R-250, 45% methanol, 10% acetic acid) for 1 hour. After which, the gel was incubated in destaining solution (45% methanol, 10% acetic acid) with gentle shaking for up to 16 hours. The gels were stored in 5% acetic acid solution.

2.3.7 Western blotting

After SDS-PAGE, transfer to nitrocellulose membrane was performed using the Trans-Blot Turbo™ transfer system (Bio-Rad), according to the manufacturer's instructions. Membranes were blocked in 5% milk powder in 1x PBS with 0.1% Tween (Sigma-Aldrich) (PBS-T), at RT for 1 hour or overnight at $4^{o}C$. The membrane was probed with an appropriate primary antibody dilution (see below), at RT for 1 hour or overnight at $4^{o}C$, and washed twice for 15 minutes with PBS-T. The blot was then incubated with a 1:3000 dilution of horse radish peroxidise (HRP)-conjugated secondary antibody (see below) at RT for 1 hour. Finally the blot was washed in PBS-T three times for 10 minutes each. The immunostaining was visualised using Pierce ECL 2 western blotting substrate (Thermo Scientific) and ECL Hyperfilm (GE healthcare) according to the manufactures protocols.

Primary antibodies were diluted as follows: monoclonal rat anti-HA (clone 3F10, Roche) at 1:1000. Polyclonal rabbit anti-human PKG (Enzo Life Sciences) used at 1:3000. Mouse anti-PfGAP45, obtained from Anthony Holder's laboratory, NIMR, was used at 1:3000. Mouse anti-PfGAPDH, obtained from Claudia Danbunberger (Swiss Tropical and Public Health Institute) was used at 1:30000.

The following secondary antibodies were all obtained from Dako and used at 1:3000: polyclonal rabbit anti-rat immunoglobulin/HRP, Ig fraction (P0450); polyclonal goat anti-mouse immunoglobulin/HRP, affinity isolated (P0447); and polyclonal goat anti-rabbit immunoglobulin/HRP, affinity isolated (P0448).

2.4 [³H] Hypoxanthine incorporation growth inhibition assay

Hypoxanthine is the major base used by *Plasmodium* to synthesise the adenylate and guanylate purine nucleotides during DNA synthesis (Webster and Whaun, 1981). In iRBCs, hypoxanthine incorporation is linearly proportional to parasitaemia levels (Chulay et al., 1983) and can be used to assess relative parasite numbers. Parasites are incubated with a drug of interest in a low hypoxanthine environment for a minimum of 24 hours before tritiated ([³H]) hypoxanthine is added, when the parasites are mostly trophozoites. During DNA synthesis, the ^{3}[H] hypoxanthine is incorporated into the genome. Harvesting of the assay captures macromolecules, including gDNA, onto glass fibre filtermats, with the unincorporated radio labelled hypoxanthine washed away. The counts per minute (CPM) are measured using a scintillation counter and used to determine relative parasite numbers.

IC50s (50% maximal inhibitory concentrations) are used to determine the performance of drugs under particular assay conditions to assess whether the drug has desirable properties. IC50 is the half maximal inhibitory concentration, the concentration of drug required in the assay to give 50% inhibition of parasite growth. In a hypoxanthine assay, it is calculated using uninfected RBCs (uRBCs) as 100% inhibition and untreated parasites as 0% inhibition.

Stock solutions of drugs were diluted in low hypoxanthine assay (IV) medium (with RMPI 1640 supplemented with 0.5% complete Albumax II solution and 5 µM cold hypoxanthine) in a 96-well flat bottom plate to give 2x final concentration in the first column, in triplicate. The final DMSO concentration was always lower than 0.5%. Serial dilutions were then performed across the plate to give a final volume of 100 µl. A positive control row, iRBCs and no drug, and a negative control row, uRBCs and no drug, were included on each plate. In addition, a control plate of at least one commercial antimalarial was included in each experiment, usually chloroquine and artemisinin.

Synchronous ring-stage (>70% rings) *P. falciparum* cultures maintained in complete medium were washed twice in RPMI 1640 to remove all the hypoxanthine to ensure maximal uptake of [³H] hypoxanthine. IV medium was used to adjust the culture to 0.5% parasitaemia at 5% haematocrit, resulting in a final 0.5% parasitaemia and 2.5% haematocrit. 100 µl of parasites or uRBCs (5% haematocrit) was added to each well. The plates were incubated at 37°C, 5% CO_2 for 24 or 48 hours.

After 24 hours, 250 nanocurie (nCi) of ^{3}[H] hypoxanthine (Perkin-Elmer) in 25 µl RPMI was added per well. The plates were then incubated for a further 24 or 48 hours depending on the assay. After a total of 48 or 72 hours, the experiment was terminated by freezing in a -80°C incubator. Once frozen, the plates were then thawed and harvested onto glass fibre filtermats (Perkin-Elmer), Meltilex solid scintillant (Perkin-Elmer) added and read using a Wallac BetaLux scintillation counter.

Data analysis was performed using Microsoft Excel and GraphPad Prism. Average positive (drug-free wells) and negative (uRBC wells) controls were calculated for each plate and percentage inhibition was calculated using the following formula:

$$1 - \left(\frac{\text{value} - \text{average negative}}{\text{average positive} - \text{average negative}} \right)$$

Parasite growth was plotted against the logarithm of drug concentrations and IC50s were calculated by the non-linear regression analysis using Prism 6.0 software. For the comparison assays, the difference between the best-fit logIC50 values was assessed using the compare function in Prism 6.0. The level of significance was fixed at P<0.05.

2.5 Parasite growth assays

Parasite growth assays, used to assess differences in growth rate between different parasite strains, or parasites under different conditions, were analysed by flow cytometery, adapted from previously published protocols (Wilson et al., 2010, 2013). Synchronous ring stage parasites were diluted to 0.5% parasitaemia in 2% haematocrit in 6 well plates, 2 ml total volume. The cultures were incubated for six days, according to culture practices in chapter 2.1.1. Culture media was changed daily and 50 μl samples (in duplicate for a technical repeat) were taken at 0 hours and once a day for the six days of incubation. The samples were fixed in an equal volume of FACS fixation solution (4% formaldehyde, 0.01% glutaraldehyde) overnight at 4°C. The fixative was aspirated and the samples were kept in 1x PBS until the end of the assay. After all samples were collected, they were washed twice in 1x PBS. The parasite DNA was stained with SYBR Green I (Life Technologies) nucleic acid stain (excitation 497 nm and emission 520 nm) at a final concentration of 1:5000-1:10000 in 1x PBS, at 37°C for 30 minutes, in the dark. The samples were again washed in 1x PBS three times, and transferred to 1.2 ml microtubes (Starlab) in a total volume of 300 μl. The samples were analysed using a BD™ LSR II flow cytometer system (BD Biosciences). Typically, 50,000-100,000 events were counted for each sample. The assay was analysed using FlowJo, v. 7.6.5 software (Tree Star Inc.). Representative Giemsa smears were performed for a proportion of the samples to monitor the robustness of the flow cytometry based assay. The following gating strategy was applied:
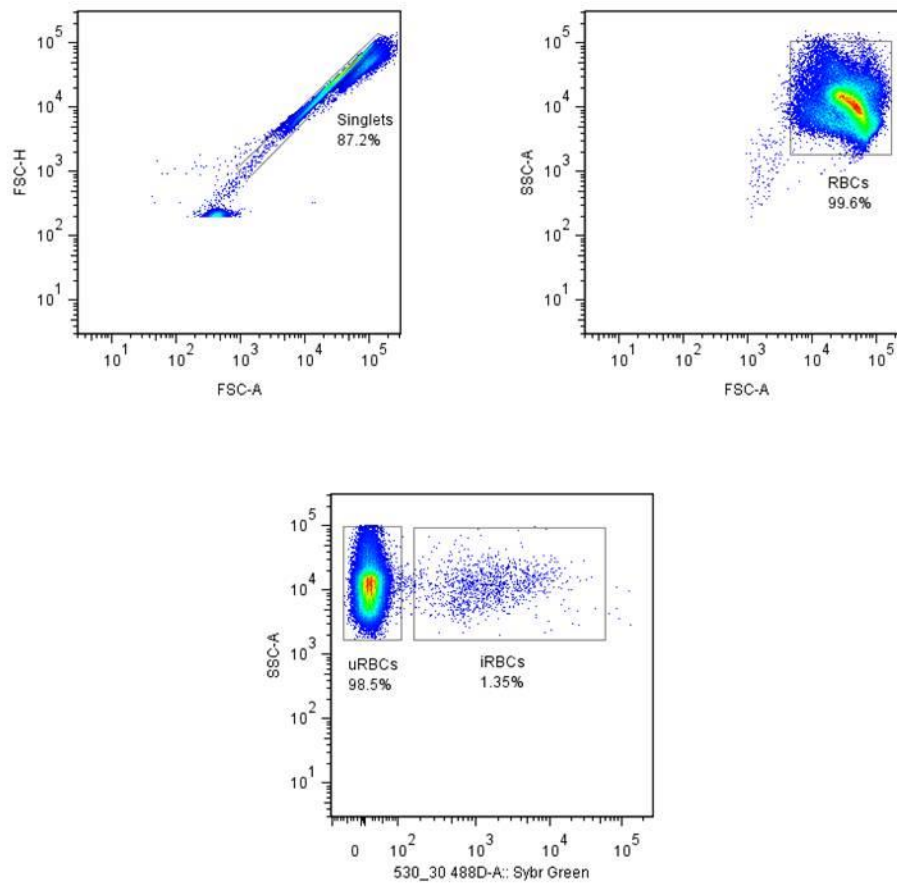
Figure 2.1 Standard gating strategy for growth assays
Gates were used to identify singlets (top left panel), all RBCs based on size (top right panel) and to distinguish between uRBCs and iRBCs based on SYBR Green fluorescence (lower panel).

The assays were performed in triplicate, with three biological repeats, unless otherwise stated. Growth curves were generated using GrapPad Prism (GraphPad Software). Parasitaemias were adjusted to give 0.5% at day 0 to reduce variability in the differences in parasitaemia between experiments.

2.6 Phosphodiesterase activity assays

To measure the PDE activity of a protein sample, a PDE assay was developed using a scintillation proximity assay (SPA). SPA is dependent on the limited energy of a sub-atomic particle to travel through water. When a tritium atom decays, a β-particle is released. This particle is able to excite scintillant in an aqueous solution only if it is less than 1.5 µm away. Scintillant is incorporated into beads coated with a specific molecule, in this case the beads allow direct binding of the primary phosphate groups of non-cyclic 5'AMP or GMP, and the assay relies on the fact that cAMP and cGMP are unable to bind (figure 2.2). The PDE SPA beads (Perkin Elmer, RPNQ0150) are yttrium silicate based. An ion chelation mechanism allows the linear nucleotide to bind to the bead in the presence of zinc sulphate.
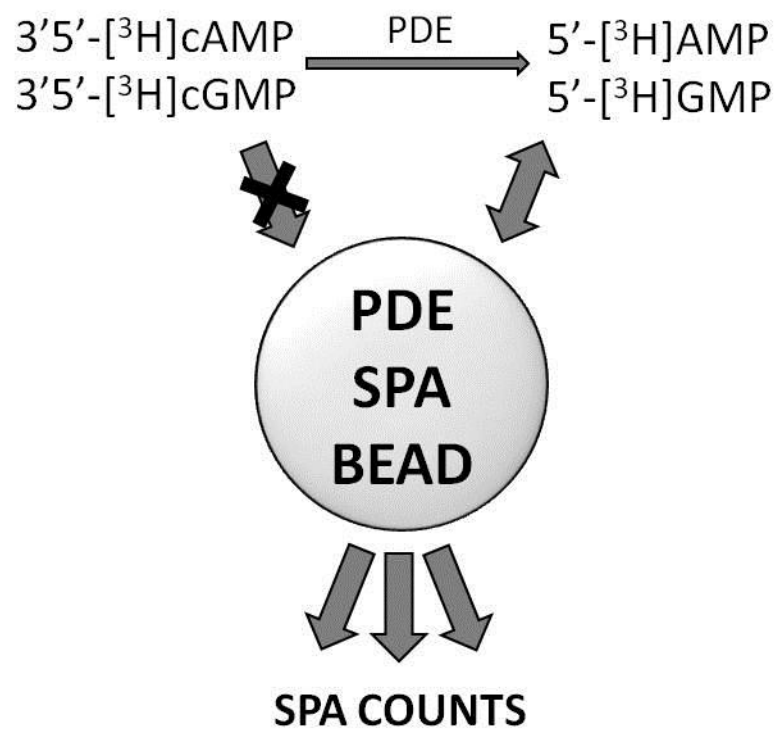
Figure 2.2 Phosphodiesterase assay diagrammatic representation
Cyclic nucleotides are unable to bind to the SPA bead, but when hydrolysed by a PDE the AMP or GMP product will bind the SPA bead and excite the scintillant within the bead.

2.6.1 Parasite lysate preparation

Packed parasite pellets were obtained by saponin lysis and centrifugation (see chapter 2.3.3). The pellet was resuspended in ice cold 5 mM Tris-HCl (with EDTA-free protease inhibitors), centrifuged at 16000 x g for 10 minutes at 4°C and the supernatant aspirated to remove residual RBC material. This was repeated until the supernatant was clear. Any colour in the final sample can affect the number of counts measured. The pellet was then resuspended in 250 μl PDE lysis buffer (10 mM Tris-HCl pH 7.5, 150 mM NaCl, 0.5% Nonidet P-40 and EDTA-free protease inhibitors) per 50 μl of sample, incubated on ice for 30 minutes with occasional mixing and centrifuged at 16000 x g for 20 minutes at 4°C. The supernatant was saved for analysis by PDE assay. When developing the assay, the Tris-HCl (1st wash) sample was saved as the cytosol fraction and the final pellet was further extracted with RIPA buffer (10 mM TrisH-Cl pH 7.5, 150 mM NaCl, 0.1% SDS, 1% Triton X-100, 1% deoxycholate with EDTA-free protease inhibitors). EDTA was left out of all buffers because PfPDEs are magnesium dependent (Ross Cummings, Thesis).

2.6.2 Immunoprecipitation of PDEβ-HA

Pulldowns on the transgenic HA epitope tagged PDEβ-HA were performed using the Anti-HA Affinity Matrix (Roche, 11815016001) that incorporate immobilised rat monoclonal antibody (clone 3F10). Packed parasite pellets of PDEβ-HA were obtained by saponin lysis (see chapter 2.3.3). The pellet was resuspended in 250 μl ice cold PDE lysis buffer (10 mM Tris-HCl pH 7.5, 150 mM NaCl, 0.5% Nonidet P-40 and EDTA-free protease inhibitors) per 50 μl of sample, incubated on ice for 30 minutes with occasional mixing and centrifuged at 16000 x g for 20 minutes at 4°C. The supernatant was transferred to a pre-cooled tube, adjusted to 500 μl with PDE dilution buffer (10 mM Tris-HCl pH 7.5, 150 mM NaCl and EDTA-free protease inhibitors) to give a final detergent concentration of less than 0.2%, and the pellet discarded. A sample of the supernatant was saved for analysis by immunoblotting, referred to as 'input'. 20 μl of the matrix was washed twice with dilution buffer (centrifuged at 30 seconds 13000 x g to pellet the matrix), to equilibrate the anti-HA affinity matrix. The lysate sample was then added to the equilibrated anti-HA affinity matrix, and incubated at RT for 2 hours with constant mixing. After incubation, the matrix was pelleted at 13000 x g, the supernatant removed and a sample saved for analysis by immunoblotting, referred to as 'unbound'. The beads were washed twice with ice cold dilution buffer. A small sample of the beads was saved for analysis by immunoblotting, referred to as 'bound beads'. The remaining beads were saved for analysis by PDE assay.

2.6.3 PDE assay

PDE assays were conducted on parasite lysates, immunoprecipitated samples and putative recombinant proteins. The general protocol is outlined below, with specific details on the relevant chapters.

Assays were conducted in 100 µl volumes using a flexible-96 well plate (Perkin Elmer, 1450-401). Each well contained 90 µl of the enzyme mixture (lysates, immunoprecipitated samples, putative recombinant proteins or commercial bovine brain PDE) diluted in 1x PDE assay buffer (10x buffer contains 500 mM Tris-HCl, 83 mM $MgCl_2$, 17 mM EGTA). 10 µl of a cNMP dilution (5 µl of [^{3}H] cNMP tracer (Perkin Elmer cAMP-NET275250UC, cGMP-NET337250UC) in 995 µl 1x PDE assay buffer) was added to each well to start the reaction. The plates were incubated at 37°C for 1 hour. The reaction was terminated by addition of 50 µl of resuspended PDE SPA beads (reconstituted to 20 mg/ml in distilled H_2O). The plates were sealed with Plateseal (Perkin Elmer) briefly shaken and then incubated for 20 minutes at RT to allow the beads to settle. Scintillation was measured using a Wallac 1450 Microbeta™ Scintillation Counter (Perkin Elmer), with each well counted for 30 seconds.

To determine the dilution needed for the test sample, an initial dose-response assay was performed with doubling dilutions of the sample. This was to ensure the substrate was not depleted during the course of the assay. The initial sample was diluted to give roughly 30% hydrolysis of the cyclic nucleotide.

2.7 Baculovirus expression system

A synthetic gene encoding the *P. vixax* PDEβ was purchased from GeneArt (Invitrogen) and codon optimised for *Spodoptera frugiperda*, the baculovirus insect host, to maximise the production of recombinant protein from the system. Protein expression was performed in collaboration with Avnish Patel (LSHTM) and Meredith Stewart (LSHTM). The donor plasmid, pRN16, the shuttle vector, Bacmid KO *orf*:1629 and the control plasmid pRN42-GFP were kindly provided by Meredith Stewart and Polly Roy (LSHTM) and pAcH10Mistic YMI by Avnish Patel.

2.7.1 Bacmid shuttle vector preparation

The baculovirus genome (KO:1629) was propagated inside *E. coli* as a bacmid, a bacterial artificial chromosome that replicates using a mini-F replicon sequence that mimics the host genome origin of replication thus utilising the genomic replication machinery of the bacterial host, (supplemented with chloramphenicol (50 µg/ml) and kanamycin (50 µg/ml)). pRN42-GFP was used as a GFP control transfer vector to measure transfection efficiency and grown in *E. coli* (supplemented with ampicillin (100 µg/ml)). Alkaline lysis, phenol:chloroform extraction and isopropanol precipitation was used to extract and purify the DNA. Briefly, the bacterial pellet was lysed in an equal volume of Solution I (5 mM Tris-HCl, pH8, 2 mg/ml RNase), Solution II (1% SDS, 0.8% NaOH) and Solution III (29.5% glacial acetic acid, 3 M potassium acetate), until a white precipitate was formed. The sample was centrifuged at 3,500xg for 10 minutes and the supernatant decanted into a fresh tube. Half the volume of phenol:chloroform:isoamyl-alcohol (25:24:1) was added and the sample was centrifuged at 3000xg until the organic and aqueous phases separated. The aqueous phase, containing the DNA, was decanted into a fresh tube and an equal volume of 100% chloroform was added. The sample was again centrifuged and the aqueous phase removed to a new tube. An equal volume of ice-cold isopropanol was added and left at 4°C for a minimum of five minutes. The DNA was centrifuged at 3,500xg for 30 minutes, washed with 70% ethanol and the centrifugation repeated. The ethanol was removed and the pellet dried. The purified DNA was resuspended in nuclease-free water and stored at 4°C.

2.7.2 General *Sf*9 insect cell culture

*Sf*9 insect cells were maintained at 28°C in Insect-Xpress medium (Lonza) supplemented with antibiotics and antimycotic solution (100 µg/ml penicillin streptomycin and 2.5 µg/ml amphotericin B).

2.7.3 Transfection of *Sf*9 cells

Transfection of *Sf*9 cells was performed using the X-tremeGENE HP DNA transfection system (Roche), according to the manufacturer's protocol. Briefly, $1x10^6$ *Sf*9 cells were seeded into a 6 well plate. 100 µl of sterile H_2O was added to 100 ng linear bacmid DNA (digested with *Bsu*361 restriction endonuclease for 2 hours at 37°C) and 500 ng of transfection vector (described in chapter 6). Per reaction, 5 µl of transfection reagent (X-tremeGENE HP) was diluted in 100 µl sterile H_2O and incubated for 5 minutes. The transfection mix was then added to the DNA solution and incubated for 15 minutes at RT. The *Sf*9 cell medium was aspirated and 800 µl of antibiotic and serum free medium was added. The transfection mixture was added to the cells and incubated for four hours with rocking at RT. The transfection mixture was aspirated and fresh culture medium was added to the cells. The cells were then incubated for 3-5 days at 28°C. Transfection efficiency was monitored using light microscopy for cell morphology changes and UV microscopy (Eclipse TS100 inverted microscope, Nikon) with the pRN42-GFP control plasmid.

2.7.4 Baculovirus plaque assay

To quantify the viral titre, plaque assays were performed. Plaque assays work by restricting the spread of new viruses to the neighbouring cells by application of a viscous medium over host cells. When cell lyses due to infection with a virus, those viruses will be unable to diffuse far and will only infect cells in very close proximity to the original infected cell. Over several cycles this will form a 'plaque', a region of cell death next to live, uninfected cells. When the viral stock is sufficiently dilute only a few viral particles will infect per well, individual plaque formation will be visible and the number of plaques will equate to the initial concentration of virus added.

10 fold dilutions of the virus stock in culture medium were created, which were then added to *Sf*9 cell monolayers in 6 or 12 well plates. The plates were put on a rocker and the virus allowed to adhere for 2-3 hours. The supernatant was then aspirated and an agar overlay (3% low gelling temperature agarose in PBS, sterilised by autoclaving), culture media mix at a 1:1 ratio and equilibrated to 42°C, was applied to the wells. The agar overlay was allowed to set for 30

minutes before 0.5-1 ml of medium was added on top. The plates were incubated at 28°C for 3-5 days until plaque formation was visible.

Plaques were visualised with neutral red solution (Sigma) at 1 mg/ml in PBS, filter sterilised, which stains healthy cells. Liquid overlay was removed from the agarose gel and 1 ml of neutral red stain was added. The plates were incubated at 28°C for 3 hours, the stain removed and the plates were then inverted for 1 hour. After this time, the plaques will appear as a clear area and can be counted. Viral titres are expressed as particle forming units (PFU) per ml of the neat solution.

To clone individual viruses, plaques can be picked from the stained plaque assay. Single plaques were removed with a sterile glass pipette and re-cultured on fresh cells.

2.7.5 Viral amplification

To amplify the virus, *Sf*9 cells were infected with low MOIs of virus (0.1-0.2). MOI is multiplicity of infection and is the ratio of virus to cells. Therefore an MOI of 1 is equivalent to 1 virus for every cell. High MOIs (3-5) are used to ensure every cell is infected in the first round of replication, useful for protein expression where you want a high number of viruses and large amount of protein. Low MOIs are used to amplify the viral stocks to give at least one round of cell replication before all cells are infected, thereby when the virus is harvested there will be a much higher concentration in the supernatant. While amplifying the virus, the cells are monitored for signs of viral infection and decreasing viability. After 4-7 days, the virus is harvested and the viral title measured by plaque assay. To monitor protein expression during viral amplification, western blotting and IFAs were performed on the whole cells. For immunoblotting, the cells were pelleted, the supernatant removed and the pellet resuspended in 1 pellet volume of 1x PBS before sample buffer was added. Western blotting was performed as per chapter 2.3.7. The *Sf*9 cell IFA method is shown below.

2.7.6 Immunofluorescence assay

To visualise recombinant protein expression in the *Sf*9 cells, Immunofluorescence assays (IFAs) were performed. Cells were seeded onto sterile glass coverslips in 6-well plates and incubated with virus for 48 hours. The cells were then fixed in 4% formaldehyde for 1 hour at RT, before being washed twice in 1x PBS. The cells were permeabilised with 0.5% Triton X-100 in PBS for 1 hour at RT. The coverslips were washed twice in 1x PBS and the blocking solution (1% BSA in PBS) was added. The cells were blocked for 1 hour to prevent non-specific binding of the antibodies. The primary antibody, mouse monoclonal anti-polyHistidine antibody (clone HIS-1, Sigma-Aldrich) was diluted to 1:300 in blocking solution, and added to the cells for 1 hour at RT, the cells were then washed 3 times with 1x PBS. The secondary antibody, anti-mouse IgG (whole molecule)-FITC antibody produced in goat (Sigma-Aldrich) was diluted in blocking solution and added to the cells for 1 hour in the dark at RT, the cells were then washed 3 times with 1x PBS. The coverslips were then mounted on glass slides with Vectashield mounting media (Vector Laboratories) without DAPI, before analysis on the confocal microscope (Zeiss).

2.7.8 Histidine tagged protein expression and purification

The codon optimised *Pv*PDEβ gene was cloned into the pAcH10Mistic YMI transfer vector using inframe *Bam*HI restriction sites. This construct allows protein expression as an N-terminal 10 times histidine mistic tagged fusion protein. The Mistic tag has been demonstrated to improve the expression of complex membrane proteins (Xu et al., 2013). Recombinant baculovirus was produced by co-transfection using vector and purified KO *orf*:1629 bacmid genome, the virus was then grown to high titre for protein expression. A 100 ml culture of $2x10^6$ *Sf9* cells per ml was infected at an MOI of 10. Expressed protein was purified using immobilised metal affinity chromatography (IMAC).

Insect cells were lysed by dounce homogenisation in one tenth of the culture volume of lysis buffer (1% Triton X-100, 20 mM imidazole (Sigma-Aldrich) in 1x PBS, pH 7.4 with (EDTA-free protease inhibitor cocktail set V (Merck Millipore)). The sample was centrifuged at 15000 x g for 5 minutes, the pellet retained for analysis by SDS-PAGE and immunoblotting as the insoluble fraction. To the supernatant, one hundredth of the volume of nickel fast flow sepharose bead slurry (GE Healthcare) was added and the sample was incubated under agitation for one hour at RT. The beads were pelleted at 3000 x g for 5 minutes, the supernatant retained for analysis by SDS-PAGE and immunoblotting as the unbound fraction. 10 ml of lysis buffer was added to the beads and the sample was incubated under agitation for five minutes at RT. The beads were

again pelleted at 3000 x g for five minutes and the supernatant removed. This wash step was repeated two more times. Protein was eluted off the beads by addition of 500 µl of elution buffer (1% Triton X-100, 400 mM imidazole in 1x PBS, pH 7.4 with (EDTA-free protease inhibitor cocktail), incubated under agitation for five minutes at RT. The beads were pelleted at 5000 x g for five minutes and the supernatant was retained as the purified protein.

Samples were analysed by SDS-PAGE, immunoblotting and PDE assay to determine the success of recombinant protein expression.

Chapter 3: Generation and characterisation of conditional knockdown constructs for *Pf*PDEs

3.1 Introduction

3.1.1 Knockdown systems in *Apicomplexa*

The ability to ablate the expression of a particular gene of interest a very important tool in assigning a function to the gene. This technique is extremely challenging when it comes to essential genes, in particular for *P. falciparum* asexual stages, on which the drug selection is performed.

Transfection for *P. falciparum* is very inefficient and must be performed during asexual stages while the parasite is within the red blood cell. For a successful transfection, the DNA must therefore travel through four separate membranes to reach the inside of the nucleus. It has been estimated that the integration efficiency for *P. falciparum* is around 10^{-6} (O'Donnell et al., 2002).

An additional complication in the generation of genetically manipulated *P. falciparum* parasite lines is the difficulty in creating large transfer plasmids. The strong AT-richness results in larger plasmids being highly unstable in *E. coli*, impeding plasmid production (de Koning-Ward et al., 2000). There is also a limited repertoire of selectable markers suitable for use in *Plasmodium*. In *P. falciparum*, the human dihydrofolate reductase (DHFR), an enzyme involved in folate metabolism, is most commonly used which confers resistance to WR99210 (Fidock and Wellems, 1997). In addition, the fungal blasticidin S deaminase (BSD), bacterial neomycin phosphotransferase II (NEO) and *Saccharomyces cerevisiae* dihydroorotate dehydrogenase (DHOD) that confer resistance to blasticidin, neomycin and atovaquone, respectively, have been adapted for *P. falciparum* (Limenitakis and Soldati-Favre, 2011).

In *P. falciparum,* integration occurs primarily by homologous recombination and the parasites are able to maintain circular plasmids as stable episomes. To generate a stable integrated line, the episome must be lost by successive rounds of drug cycling before the concentration of integrated, episome-free parasites are high enough to clone. With gene targeting strategies that are unfavourable to the parasite, the episomes can form stably replicating forms that are transferred to daughter merozoites even in the absence of selection pressure (O'Donnell, 2001). When performing double homologous crossover it is possible to use negative selection markers

such as the thymidine kinase (TK) from the herpes simplex virus, or the *E. coli* cytosine deaminase, where the addition of ganciclovir or 5-fluorocytosine, respectively, poisons the parasites where single crossover has occurred, favouring parasites that have undergone double homologous recombination events (Duraisingh et al., 2002). However, no such negative selection exists for single crossover recombination. It can take months to generate a stable line and therefore removal of essential asexual stage genes is impossible.

Traditional gene disruption at a specific locus involves double homologous recombination replacing the gene of interest (GOI) with the selectable marker cassette. Single crossover recombination results in integration of the entire plasmid, including the selectable marker cassette, however, single crossovers are able to revert to WT as this process is reversible, therefore once established the mutant parasite line must be continually under drug pressure. Another problem with gene knockouts is with multifunctional proteins, only the earliest essential phenotype can be elucidated as any downstream function will be inaccessible (Carvalho and Ménard, 2005; Thathy et al., 2002). Repeated failure to generate a double crossover knockout line is highly suggestive that the gene is essential (Slavic et al., 2010). However, alternative approaches, including conditional gene disruption, are needed to validate this conclusion.

3.1.2 Conditional gene excision systems

Experimental conditional gene expression control systems, adapted to *Plasmodium* species, fall into four categories which act either by, gene deletions or manipulation of transcription, translation or protein stability.

Inducible gene deletion by site-specific recombinases is the most powerful way to disrupt gene function as it prevents protein expression by removal of the gene, reducing leakiness in expression of the GOI, and is irreversible. However, achieving maximal recombination efficiency while ensuring the recombinase is not expressed inappropriately can be challenging (Pino, 2013).

In *P. berghei*, a flippase (FLP) recombinase technique has been developed. The FLP is able to recognise FLP recombinase target (FRT) sites and excise the sequence in between. A temperature sensitive FLP which is much more active at lower temperatures, is used to achieve temporal control. When the parasites are taken up into the mosquito, the drop in temperature activates the FLP. By flanking the GOI, the sequence can be removed and gene expression prevented. This technique best suited for genes that have functions in the mosquito and hepatic

stages (Combe et al., 2009; Lacroix et al., 2011). FLP/FRT excision has been used in *P. falciparum* to recycle selectable markers, but not for inducible knockout of essential genes (van Schaijk et al., 2010).

Cre-lox excision technology has been utilised in many other organisms since the 1980s. A Cre recombinase recognises two *loxP* sites, resulting in excision of the intervening sequence (Sauer, 1994). Attempts to adapt this technology to *Apicomplexa* were unsuccessful. In *T. gondii*, the use of a stage specific promoter, or even without a promoter, Cre recombinase expression was not tightly controlled enough to prevent inappropriate excision (Brecht et al., 1999). In 2003, DiCre technology was developed. The enzyme was split into two component parts, one fused to FKBP12 (FK506-binding protein) the other to FRB (binding domain of the FKBP12-rapamycin associated protein). The moieties by themselves are inactive, however the addition of rapamycin leads to hetero-dimerisation and Cre activity (Jullien et al., 2003). This was successfully applied to *T. gondii* in the inducible deletion of essential invasion genes (Andenmatten et al., 2013). During the course of this project, the DiCre system was also being adapted to *P. falciparum* in Mike Blackman's laboratory and various strategies exist to conditionally knockdown genes of interest. For this project, the DiCre conditional knockdown system was used to attempt conditional knockout of PDEβ. The results will be discussed later in this chapter.

3.1.3 Gene transcription control strategies

When conditionally controlling gene transcription, there are two strategies that have been applied to the study of malaria parasites, promoter swap and the Tet system. For genes that are not expressed in the asexual stage, simply swapping the promoter for one that is not active in the stage of interest can be effective. For example for PbMyoA, the endogenous promoter was changed to one that is inactive in ookinetes (Siden-Kiamos et al., 2011). However, like the FLP/FRT system, this is limited to genes expressed in mosquito and liver stages. The tetracycline-controlled transcriptional activation (Tet) system, like the *Cre-lox* system, is widely utilised in other organisms, and a modified version had been adapted to *Apicomplexa* (Meissner et al., 2002, 2005). Briefly, a transactivator, composed of the tetracycline repressor (TetRep) fused to an activating domain, binds via the TetRep to tet operator sequences (TetO). The TetO is placed before a minimal promoter and this activates transcription. In the presence of tetracycline (or specific derivatives), binding affinity of the transactivator to TetO is highly diminished, preventing transcription (Pino, 2013). More recently, the identification of transcriptional activation domains from the ApiAP2 family of transcription factors, allowed tetracycline-induced

repression of two essential *P. berghei* genes (Pino et al., 2012). However this system is yet to be adapted to *P. falciparum*.

3.1.4 Strategies to control mRNA translation

In many other organisms, one of the most frequently used knockdown approaches is the use of RNA interference (RNAi). However, *Plasmodium* species lack much of the necessary machinery and reports of limited success (Kolev et al., 2011; McRobert and McConkey, 2002) are therefore controversial. There has been some success using other mRNA translation systems including; long double-stranded RNA (dsRNA) to interfere with mRNA expression (Gissot et al., 2005); targeting ribonuclease P activity to a specific mRNA to promote cleavage (Augagneur et al., 2012) and using riboswitches (autocatalytic RNA), where the cis-acting hammerhead ribozyme N9 integrated near the start of translation was able to downregulate reporter genes in *T. gondii* and *P. falciparum* (Agop-Nersesian et al., 2008). However further work to investigate the broader applications is necessary.

3.1.5 Protein stability manipulation strategies

Conditionally knocking down gene expression at the protein stability level has the potential to be fast responding and reversible, useful aspects for some phenotype analyses. In 2006, Banaszynski et al., developed the destabilisation domain (DD) system by producing mutants of human FKBP12 that, when expressed, are immediately degraded in mammalian cells. When this unstable FKBP12 was fused to a protein of interest (POI), the whole complex was targeted to the proteasome for degradation. In addition, in the presence of a small synthetic ligand, shield-1, which binds to the FKBP, prevented this degradation (Banaszynski et al., 2006) (figure 3.1). Soon after, the DD-system was adapted to *P. falciparum* (Armstrong and Goldberg, 2007) and there have been several publications that effectively utilise this system (including, but not limited to (Dvorin et al., 2010; Jain et al., 2013; Russo et al., 2009).
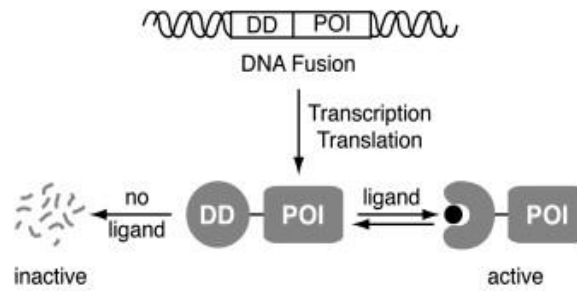
Figure 3.1 Diagrammatic overview of the DD-system
Genetic fusion of a protein of interest (POI) to the destabilisation domain (DD, unstable FKBP12) leads to degradation of the whole fusion protein. Addition of a stabilising ligand (shield-1) prevents degradation (Banaszynski et al., 2006).

3.1.6 Control of gene expression in *P. falciparum* PDEs

Traditional gene knockout has been applied to three of the four PfPDEs, PDEα, γ and δ (Taylor et al., 2008; Wentzinger et al., 2008). As described in chapter 1, none of these knockout lines have an obvious phenotype in asexual blood stage culture. Genetic knockouts of PDEβ have been attempted in both *P. falciparum* and *P. berghei*, but have never been successful (Ross Cummings, thesis; Oliver Bilker, personal communication). It is therefore assumed that PDEβ is indispensable for asexual blood stage growth, however this remains a speculation as absence of parasite growth is insufficient proof. Therefore this project has attempted to generate conditional knockdowns of PfPDEβ. Initially the DD-system was pursued, secondly, in collaboration with Mike Blackman (NIMR), the DiCre system.

3.2 Results

3.2.1 Construction of *Plasmodium falciparum* PDEα and PDEβ destabilisation domain plasmids for parasite transfection

Constructs based on the pJDD41 vector (donated by Jeff Dvorin (Dvorin et al., 2010)) were generated in order to C-terminally tag the endogenous *pdeα/β* locus with both a haemagglutinin (HA) tag and a destabilisation domain (DD). The constructs contained a 1.5 kb C-terminal fragment of the relevant *pfpde* gene, to enable single crossover recombination and without a stop codon, fused to the HA tag and DD tag. Following this was the 3'UTR of *pfhsp86*. The construct also contained a human DHFR gene which confers resistance to the antifolate WR99210. The 3' fragment of *pdeα* was amplified by PCR from genomic DNA (gDNA) using the primers 5'-AGC<u>GCGGCCGC</u> TAA CGATAGATAATACTATACCTACATCGCC-3' (*Not*I restriction site underlined) and 5'-TAG<u>CTCGAG</u> TTCAAA TTTGATGAGCTCAAGTTTGCTTAG-3' (*Xho*I restriction site underlined). The 3' fragment of *pdeβ* was amplified by PCR from genomic DNA (gDNA) using the primers 5'- AGC<u>GCGGCCGC</u> TAA GATTGTATAAGTACTGACAAAGTGGATTTAGA-3' (*Not*I restriction site underlined) and 5'-TAG<u>CTCGAG</u> ATCGGAAACATTcTTTATgAAAAATAGAGTTAAATCAATATAAC-3' (*Xho*I restriction site underlined). The lower case letters c and g indicate where bases have been changed from T and A respectively (without altering the encoded amino acid), in the PDEβ reverse primer to prevent formation of secondary structures. The PCR conditions were as described in chapter 2.2.2, however the annealing temperature was 42°C. These fragments were cloned into pJDD41, which already contained the HA and DD tags, using the *Not*I and *Xho*I restriction endonucleases. The plasmids were verified by restriction digest and sequencing (figure 3.2).
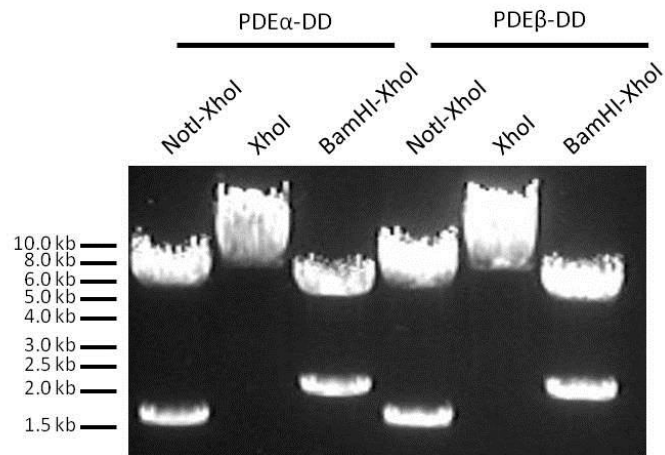
Figure 3.2 Restriction digests to verify the PDE-DD constructs are correct
The expected sizes for both pPDEα-HA-DD and pPDEβ-HA-DD were as follows: *Not*I-*Xho*I double digest, 5.9 kb and 1.5 kb, *Xho*I single digest, 7.4 kb and *BamH*I-*Xho*I double digest, 2 kb and 5.4 kb. Although the gel is overloaded, the sizes are correct for both plasmids. Sequencing of the inserts and junctions was also performed.

Figures 3.3 and 3.4 show the allelic replacement strategy for *pfpdeα* and *pfpdeβ*, respectively. *P. falciparum* parasites were transfected with the plasmids as described above. 0.5 µM of shield-1 was added at the time of transfection, and the parasites were then continually grown in the presence of this stabilising ligand. WR99210 drug-resistant parasites were detected 3-4 weeks post-transfection. Up to four rounds of drug cycling for PfPDEα-HA-DD and PfPDEβ-HA-DD were performed to reduce the presence of the episome and enrich the proportion of parasites containing integrated plasmid. After each cycle, the parasites were screened by integration specific PCR, as described in chapter 2.2.2, to detect successful integration of the plasmid into the correct locus. Integration PCR positive parasites for PfPDEα-HA-DD were detected after two cycles, however integration was never observed for PfPDEβ-HA-DD, even after four cycles (figure 3.5).
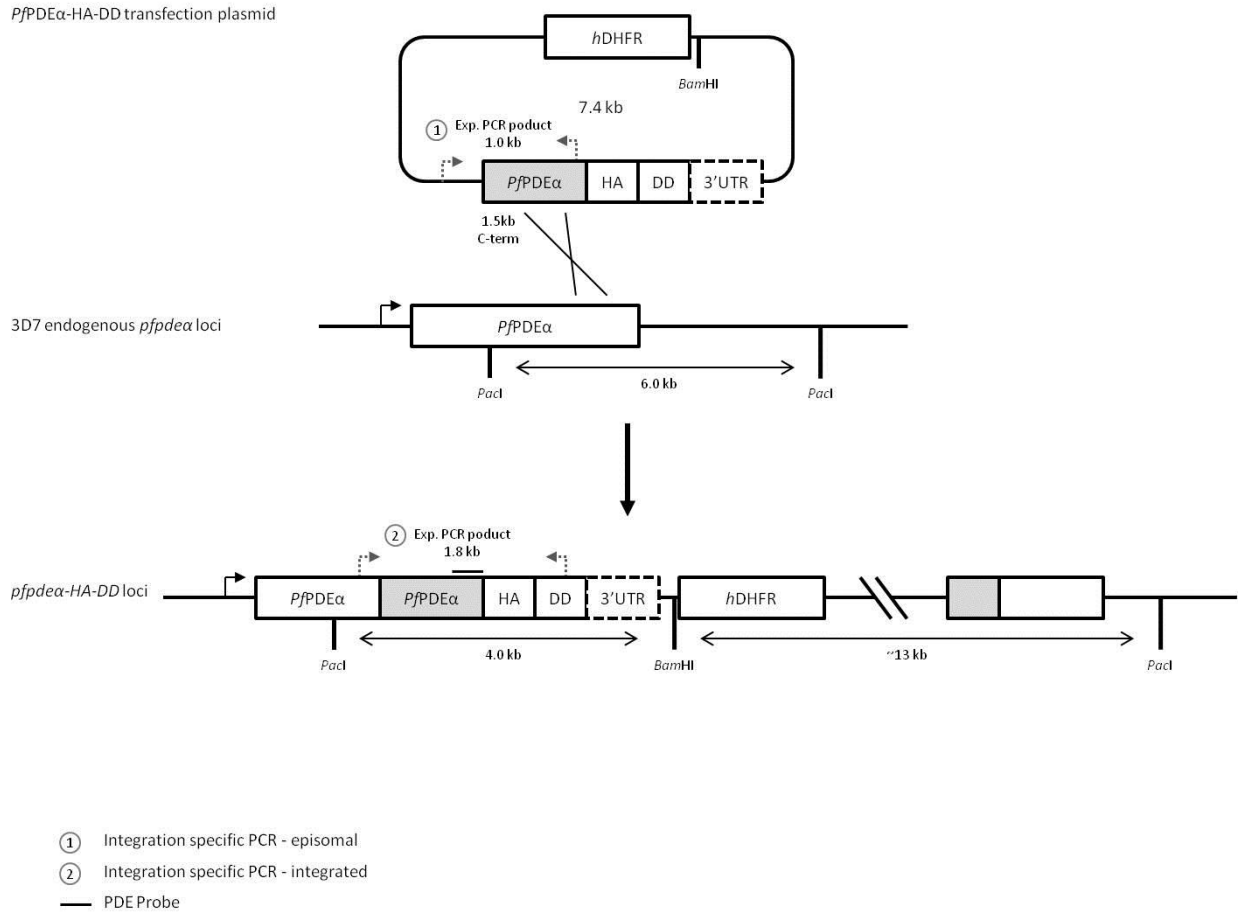
Figure 3.3 Integration strategy for *pfpdeα*

A schematic representation of the transfection plasmids and the *pdeα* locus before and after integration. The 1.5 kb C-terminal fragment promotes recombination by single crossover resulting in a HA and DD tagged gene. The integration PCR primer locations are depicted with dashed arrows and the expected fragments given, 1 kb for presence of the episome and 1.8 kb for an integration event. The diagram also shows the locations of the restriction sites and the PDEα specific probe for Southern blotting. The expected fragment sizes are 7.4 kb for the episome, 6.0 kb for the WT locus and 4.0 kb for the integration event.
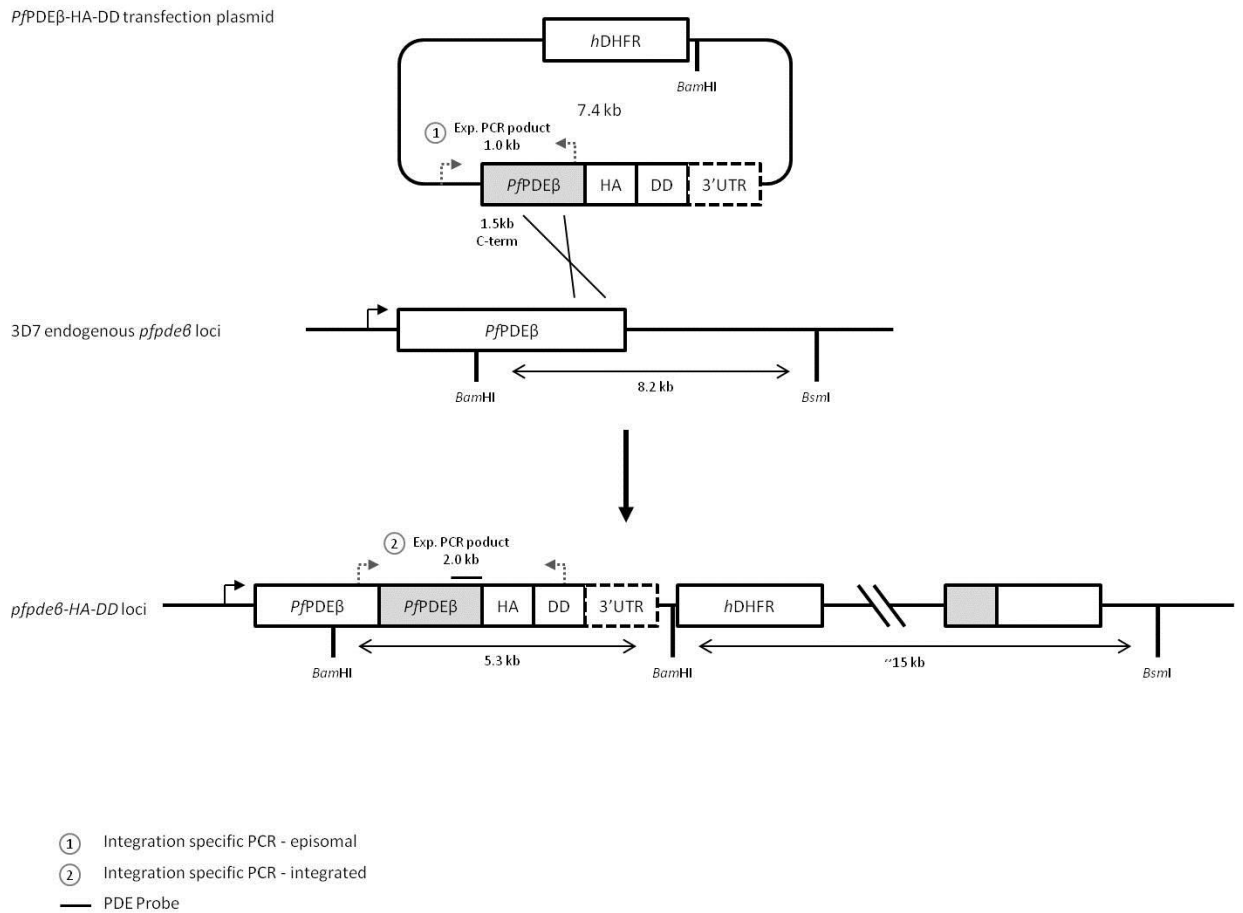
Figure 3.4 Integration strategy for *pfpdeβ*
A schematic representation of the transfection plasmids and the *pdeβ* locus before and after integration. The 1.5 kb C-terminal fragment promotes recombination by single crossover resulting in a HA and DD tagged gene. The integration PCR primer locations are depicted with dashed arrows and the expected fragments given, 1 kb for presence of the episome and 2.0 kb for an integration event. The diagram also shows the locations of the restriction sites and the PDEβ specific probe for Southern blotting. The expected fragment sizes are 7.4 kb for the episome, 8.2 kb for the WT locus and 5.3 kb for the integration event.
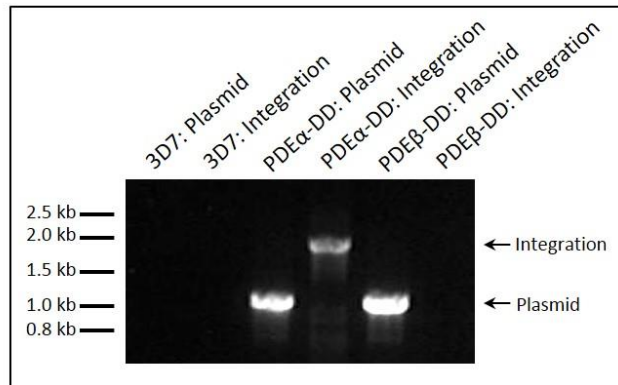
Figure 3.5 Integration specific PCR for PfPDEα-HA-DD and PfPDEβ-HA-DD
Integration specific PCR was performed using the primers shown in figures 3.3 and 3.4 Genomic DNA was extracted from PfPDEα-HA-DD after two cycles and four for PfPDEβ-HA-DD. WT 3D7 gDNA was used as a negative control. The arrows denote the expected product sizes. For both constructs, an episomal band of 1 kb and the integration bands 1.9 kb and 2.0 kb for PDEα and PDEβ, respectively. PfPDEα-HA-DD is positive for integration, PfPDEβ-HA-DD is not.

The PfPDEα-HA-DD transfected line was then cloned by limiting dilution and genotypic analysis was performed by repeating the integration specific PCR on the clones, including a WT control PCR which would only amplify in the absence of integration. The forward primer was located in the genomic PDEα sequence, upstream of the cloned fragment. The reverse primer was located in the endogenous 3'UTR. The expected band size was 2.2 kb. Two clones, positive for integration and negative for the endogenous WT locus, were selected and Southern blotting was performed. The uncloned PfPDEβ-HA-DD transfected line was also genotypically analysed by Southern blotting to test if the lack of an integration band by PCR was due to a problem with the primers used. The integration specific PCR for PfPDEα-HA-DD clones 6 and 7 showed the expected result, they were integration positive and WT negative. The controls on the Southern blot showed the anticipated result, a 7.4 kb band for the plasmid, a 6.0 kb band for the WT and no band for the PDEα-KO. The DNA of the clones was somewhat degraded, however, the two major bands, episomal (7.4 kb) and integration (4.0 kb) were visible. The PDEα-KO line was a gift from (Selina Bopp and Hans-Peter Beck, Swiss Tropical and Public Health Institute). The Southern blot of the PfPDEβ-HA-DD uncloned transfected lines showed very strong bands at the expected episomal size (7.4 kb). The four lanes (1st-4th) contain samples from the individual separate transfection experiments performed with the plasmid. All the transfections show the same pattern. The plasmid DNA was overloaded and it was difficult to infer size and the 3D7 DNA was too dilute. As the PfPDEβ-HA-DD was not positive for integration by PCR or Southern blotting, no further work was performed on this line.
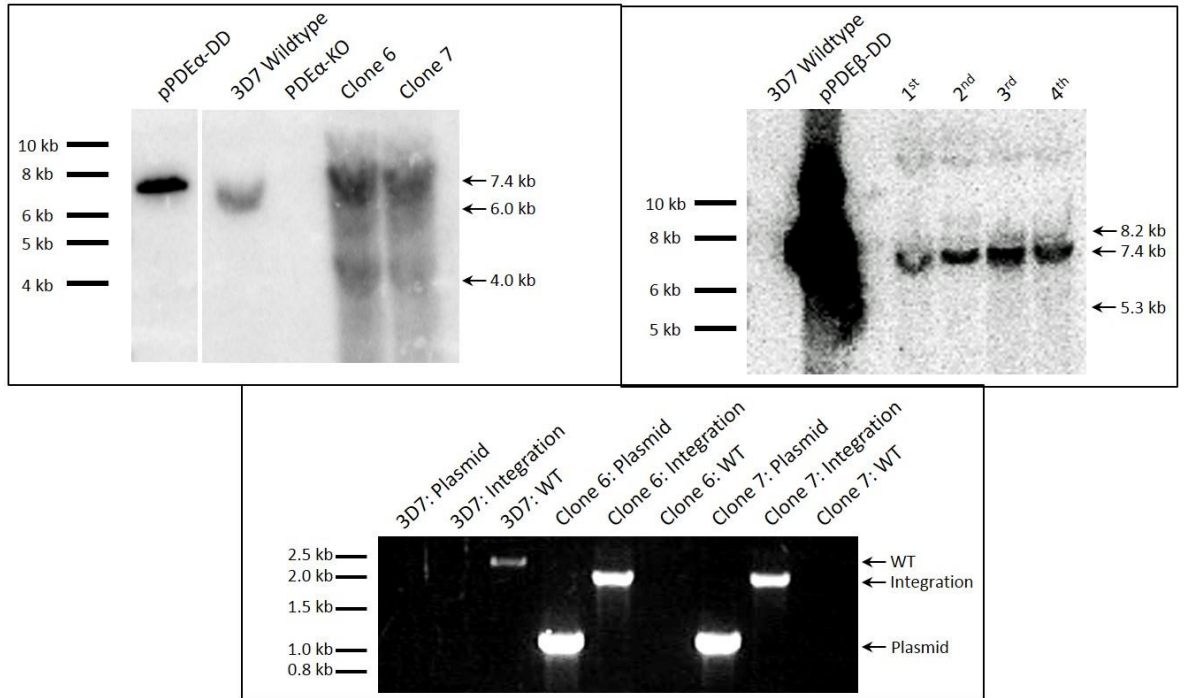
Figure 3.6 Genotypic analysis of PfPDEα-HA-DD and PfPDEβ-HA-DD transfected lines
Southern blotting (top left panel) and integration specific PCR (bottom panel) of PfPDEα-HA-DD cloned lines shows that the plasmid integrated in the correct locus and that there is no WT contamination. The Southern blot shows the correct sized band for the plasmid (7.4 kb) and the 3D7 WT line (6.0 kb), and no band for the PDEα-KO line. The DNA for the clones appears degraded, resulting in smeary lanes, however the major bands are consistent with the expected sizes of 7.4 kb and 4.0 kb. This finding is reinforced by the integration PCR. The 3D7 line shows only the WT band (2.2 kb), whereas both clones shown have episome (1 kb) and integration (1.9 kb) bands present and a negative PCR result for the unmodified locus. The PfPDEβ-HA-DD Southern blot shows the episome band only.

3.2.2 Removal of the stabilising ligand shield-1 does not affect the growth of PDEα-HA-DD mutants

Parasite growth assays, as described in chapter 2.5 were performed on the two PfPDEα-HA-DD clones, referred to as A6 and A7. These assays were carried out initially to compare the growth rate of the mutants to the 3D7 parental line to verify normal growth (data not shown separately), and secondly to assess whether the growth rate changes in the absence of shield-1. Figure 3.7 shows that 3D7 (red lines), A6 (green lines) and A7 (blue lines) do not differ in growth rate. The addition of 0.5 μM shield-1 to 3D7 parasites does not significantly impair their growth. The removal of shield-1 from the PDEα-DD mutants (dashed lines) does not result in a change in growth rate.
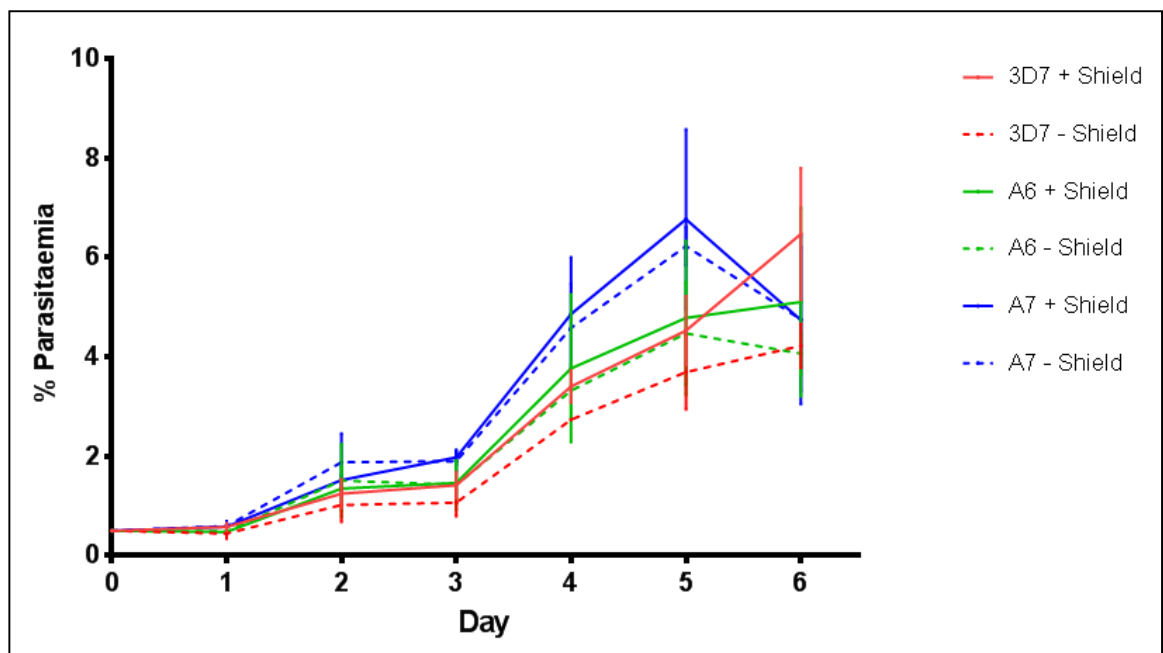
Figure 3.7 The growth rate of 3D7 and PDEα-HA-DD mutants in the presence and absence of shield-1
The growth rates of 3D7 (red), A6 (green) and A7 (blue) are not significantly different either between the strains or in the absence (dashed line) or presence (unbroken line) of the stabilising ligand. The experiment was performed in duplicate and three biological repeats were conducted. The error bars represent standard error of the mean (SEM).

3.2.3 PDEα-KO mutants have a higher replication rate than other parasite strains

The creators of the PfPDEα-KO line, Wentzinger et al., reported a discrepancy in cell cycle timing between WT and knockout strains. The authors noted that after synchronisation, ring stages were detected earlier in the KO than in the WT, although they were unable to quantify the precise timings (Wentzinger et al., 2008). This phenotype was also observed during the course of the present study. Additionally, the parasite line also appeared to grow to a higher parasitaemia than other strains. A growth assay was performed to demonstrate this result. Figure 3.8 shows the growth rate of PfPDEα-KO (purple) compared to 3D7 (red), A6 (green), A7 (blue) and the A4 line (pink). A6 and A7 were kept off shield-1 with the expectation that this would knockdown the levels of PfPDEα. PfPDEα-KO is a non-gametocyte producing line (as was the parent 3D7 line), therefore line A4 was also included to investigate whether this growth phenotype simply resulted from an inability to produce gametocytes. The A4 line has a defect in the ApiAP2-g transcription factor, a master regulator for gametocytogenesis, and therefore is unable to produce gametocytes (Kafsack et al., 2014). The reason for the lack of gametocytes in PfPDEα-KO is unknown. Figure 3.8 demonstrated that PfPDEα-KO grows to a higher parasitaemia than all the other lines, when kept in the same culture conditions.
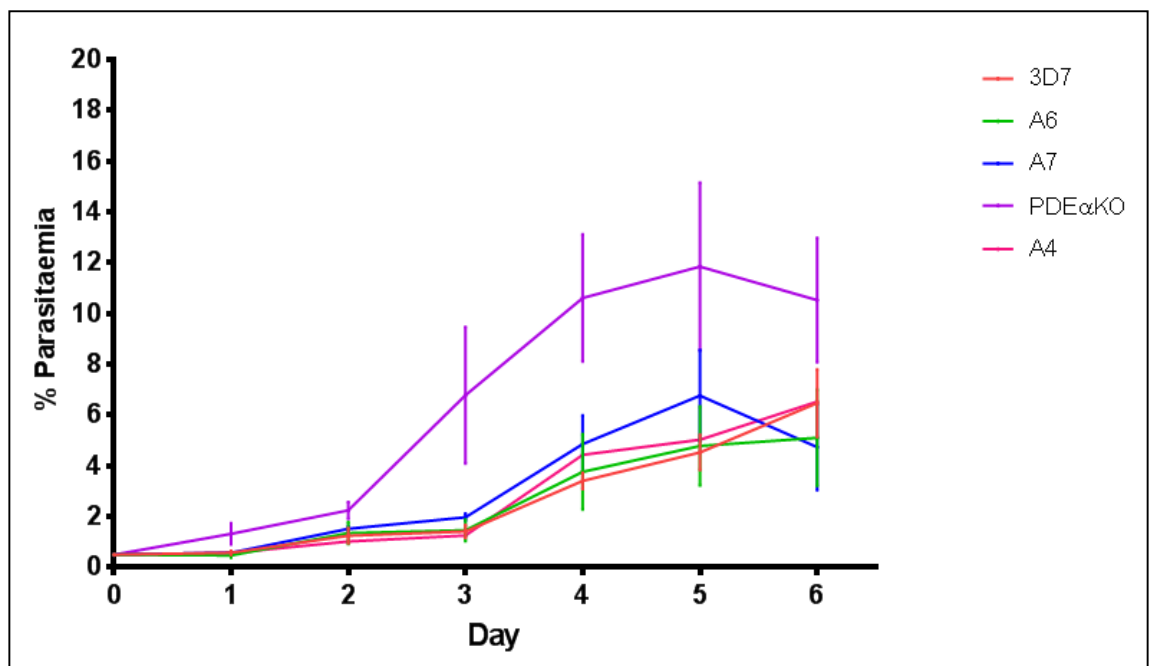
Figure 3.8 The growth rate of PDEα-KO is higher than the other strains
The parasitaemia of PDEα-KO is consistently higher than all other strains after day 2. The A4 line is a non-gametocyte producing line. All strains were grown in the absence of shield-1. The experiment was performed in duplicate and three biological repeats were conducted. The error bars represent standard error of the mean (SEM).

3.2.4 PfPDEα-HA-DD cannot be detected by western blotting or IFA

Western blotting on late stage parasite extracts of PfPDEα-HA-DD A6 and A7, with 3D7 and PfPDEα-KO as negative controls, were performed. The membrane was probed with a monoclonal rat antibody against HA, with an anti-GAPDH antibody as a loading control. The expected size of PfPDEα-HA-DD is 145 kDa (115 kDa protein and a 30 kDa HA-DD tag). No protein was detectable at a primary antibody concentration of 1:1000, although the amount of lysate loaded was lower than for the 3D7 control this assay was repeated several times and no band was ever seen (figure 3.9, left image). To assess whether the concentration of shield-1 was insufficient to prevent protein degradation, increasing concentrations were tested. Clone A6 was cultured with four concentrations of shield-1, between 0 and 2 µM for two cycles. Late stage parasite extracts were then analysed by western blotting. No protein was detected in any of the four concentrations (figure 3.9, right image). Immunofluorescence assays were also performed, with a primary antibody concentration of 1:100, in an effort to detect the protein. There was extremely weak staining with the antibody, but it could not be confidently identified as specific (figure 3.10). The PfPDEα-HA-DD line was not analysed further.
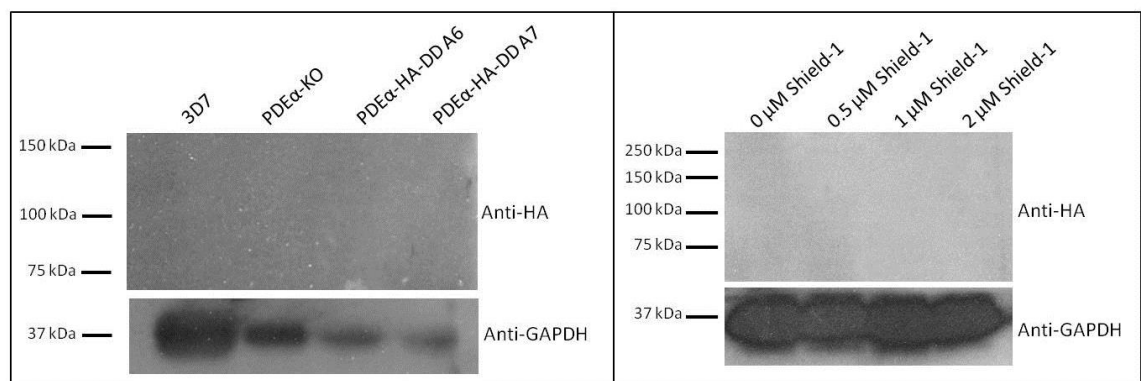
Figure 3.9 Transgenic PfPDEα-HA-DD clones are not detectable by western blotting
Western blots of asexual late stage parasites showed that the HA tag in the PfPDEα-HA-DD lines could not be detected, even with increased amounts of shield-1 (left panel). The predicted size was 145 kDa. Anti-GAPDH (37 kDa) was used as a loading control.
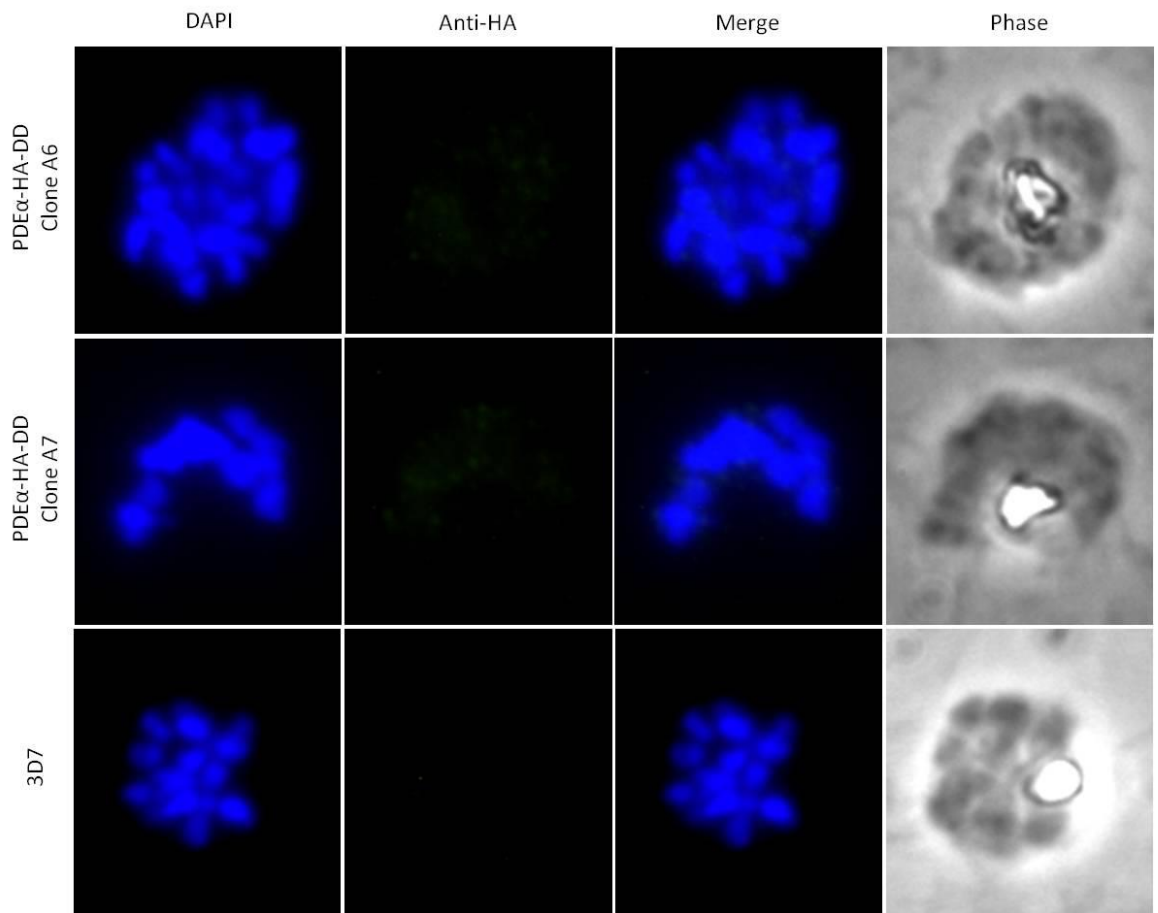
Figure 3.10 Transgenic PfPDEα-HA-DD clones are not detectable by IFA
IFAs using formaldehyde fixed smears of late stage asexual parasites were stained with rat anti-HA antibodies. Representative IFA images are shown alongside the bright field image. DAPI was used to stain the parasite nuclei. The staining for PfPDEα-HA-DD was extremely weak and it could not be confidently distinguished from background staining. For antibody the negative controls, see appendix A3.

3.2.5 Construction of *Plasmodium falciparum* PDEβ 3' replacement DiCre plasmids for parasite transfection

Constructs based on the pHH1_SERA5del3DC vector (obtained through collaboration with Mike Blackman (Collins, et al. 2013)) were generated in order to C-terminally tag the endogenous *pdeβ* locus with both a haemagglutination (HA) tag and a loxP site prior to the 3'UTR. The constructs contained a 0.9 kb C-terminal fragment of the *pfpdeβ* gene to enable single crossover recombination and without a stop codon, fused to the HA tag. Following this was the loxP site and the 3'UTR of *pb*DT. The construct also contained a second loxP site and a human DHFR gene which confers resistance to the antifolate WR99210. The C-terminal fragments of *pfpdeβ* were excised from the pPDEβ-HA-DD plasmid using the endogenous restriction site *Afl*II and *Xho*I, and cloned into pHH1_SERA5del3DC using the same enzymes, creating the pPDEβ-HA-DiCre. The plasmids were verified by restriction digest and sequencing (figure 3.11).
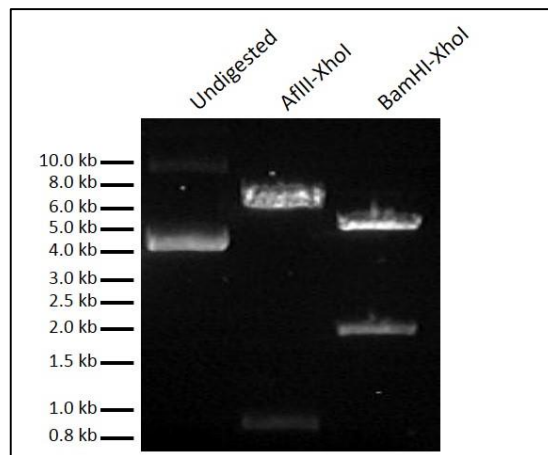
Figure 3.11 Restriction digests to verify the PDEβ-HA-DiCre constructs are correct
The expected sizes for both pPDEβ-HA-DiCre were as follows: *Afl*II-*Xho*I double digest, 5.9 kb and 0.9 kb and *BamH*I-*Xho*I double digest, 2 kb and 4.8 kb. The sizes are correct for the plasmid. Correct sequence of the inserts and junctions was also confirmed.

Figure 3.12 shows the allelic replacement strategy for *pfpdeβ*. *P. falciparum* PreDiCre parasites were transfected with the pPDEβ-HA-DiCre plasmid as described above. The PreDiCre line was generated by the Blackman lab and contains the DiCre cassette integrated by single crossover at the SERA5 locus, with no detrimental effect on the parasite (Collins et al. 2013).

WR99210 drug-resistant parasites were detected 3-4 weeks post transfection. Two rounds of drug cycling were performed to reduce the presence of the episome and enrich the proportion of parasites containing integrated plasmid. After each cycle, the parasites were screened by

integration specific PCR, as described in chapter 2.2.2, to detect successful integration of the plasmid into the correct locus. Integration PCR positive parasites were detected after two cycles (figure 3.13).
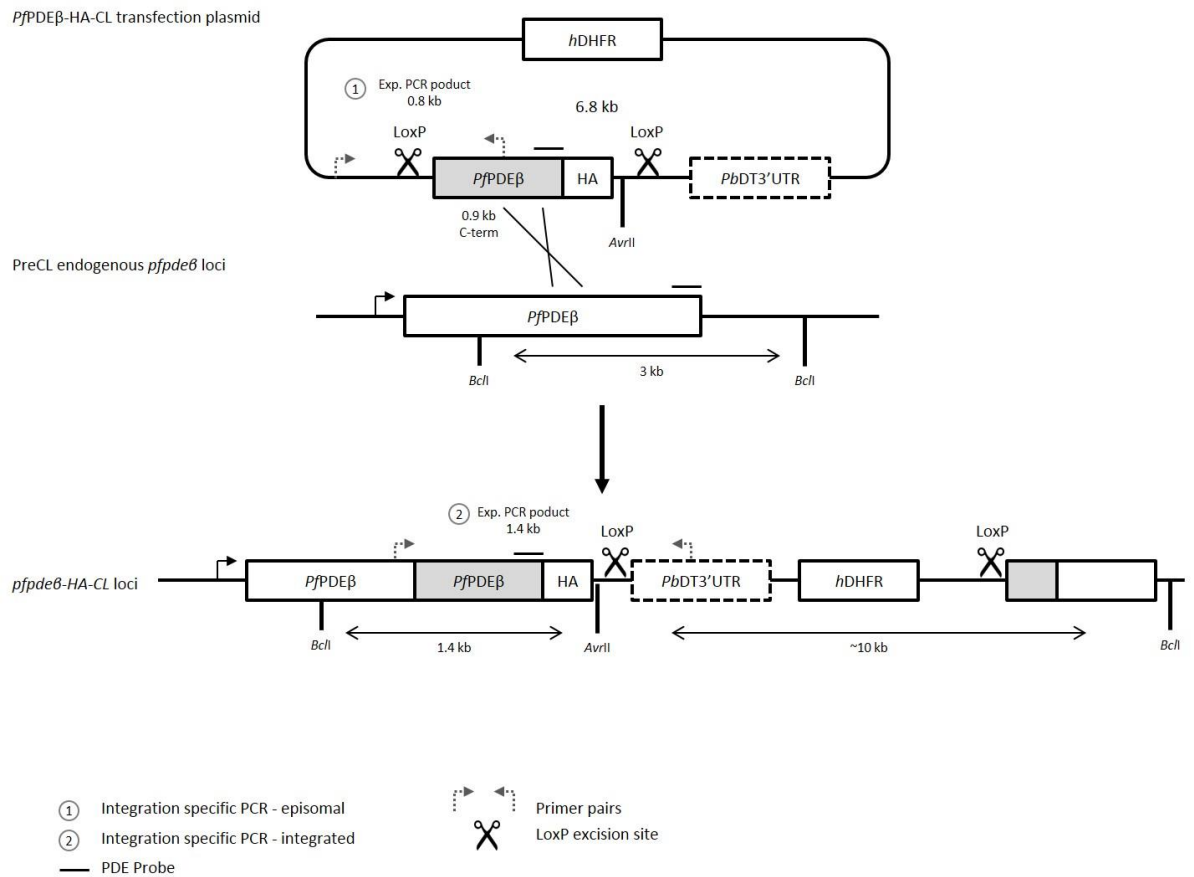
Figure 3.12 Integration strategy for *pfpdeβ*
A schematic representation of the transfection plasmids and the *pdeβ* locus before and after integration. The 0.9 kb C-terminal fragment promotes recombination by single crossover resulting in a HA tagged gene, followed by a LoxP site, the pbDT 3'UTR and a second loxP site. The integration PCR primer locations are depicted with dashed arrows and the expected fragments given, 0.8 kb for presence of the episome and 1.4 kb for an integration event. The diagram also shows the locations of the restriction sites (*Bcl*I and *Avr*II) and the PDEβ specific probe for Southern blotting. The expected fragment sizes are 6.8 kb for the plasmid, 3.0 kb for the WT locus and 1.4 kb for the integration event. There is also potential for a larger band to be present (~10 kb) depending on the location of the crossover as the downstream fragment may also contain the probe sequence.

The PfPDEβ-HA-DiCre transfected line was then cloned by limiting dilution and genotypic analysis was performed by repeating the integration specific PCR on the clones, including a WT control PCR which would only amplify in the absence of integration. The forward primer was located in the genomic PDEα sequence, upstream of the cloned fragment. The reverse primer was located in the endogenous 3'UTR. The expected band size was 2.0 kb. Two clones, positive for integration and negative for the endogenous WT locus, were selected and Southern blotting was performed. The integration specific PCR for PfPDEβ-HA-DiCre clones 4 and 7 (named B4 and B7) showed the expected result, they were integration positive and WT negative (figure 3.13). The controls on the Southern blot showed the anticipated result, a 6.7 kb band for the plasmid and a 3.0 kb band for the WT. For both B4 and B7, the 1.4 kb integration band is present, as is a larger (~8 kb) band that probably indicates the downstream fragment. The presence of a band the same size as the plasmid indicates that multiple copies have integrated. As the plasmid contains only a 0.9 kb fragment of PfPDEβ, not preceded by a promoter and designed to start with a stop codon, it is extremely unlikely to be transcribed (data shown in chapter 3.2.6, figure 3.17).
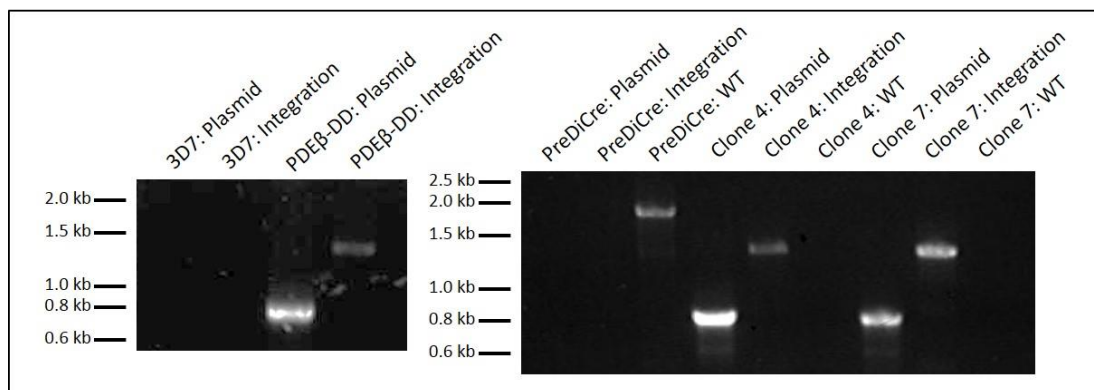
Figure 3.13 Genotypic analysis of PfPDEβ-HA-DiCre transfected lines
Integration specific PCR of PfPDEβ-HA-DiCre uncloned (left) and cloned lines (right) show that the plasmid integrated in the correct locus and that there is no WT contamination.

3.2.6 Addition of the excision inducing compound rapamycin effectively excises the 3' UTR of *pfpdeβ*

To induce excision of the 3' UTR of *pfpdeβ*, the DiCre enzyme was heterodimerised by the addition of 100 nm rapamycin, or 1% DMSO as a negative control, to synchronised ring stage parasites (clones B4 and B7) for four hours. The rapamycin or DMSO was then washed away and the parasites were allowed to develop for a further 24 hours in WR99210 free medium as the expected excision would remove the resistance cassette (figure 3.14). After the parasites had developed to schizonts, gDNA was extracted. The rapamycin treatment was repeated and gDNA was also extracted after 72 hours. The gDNA samples were analysed by excision specific PCR which was designed to distinguish the intact modified locus from the expected DiCre excision genomic product.
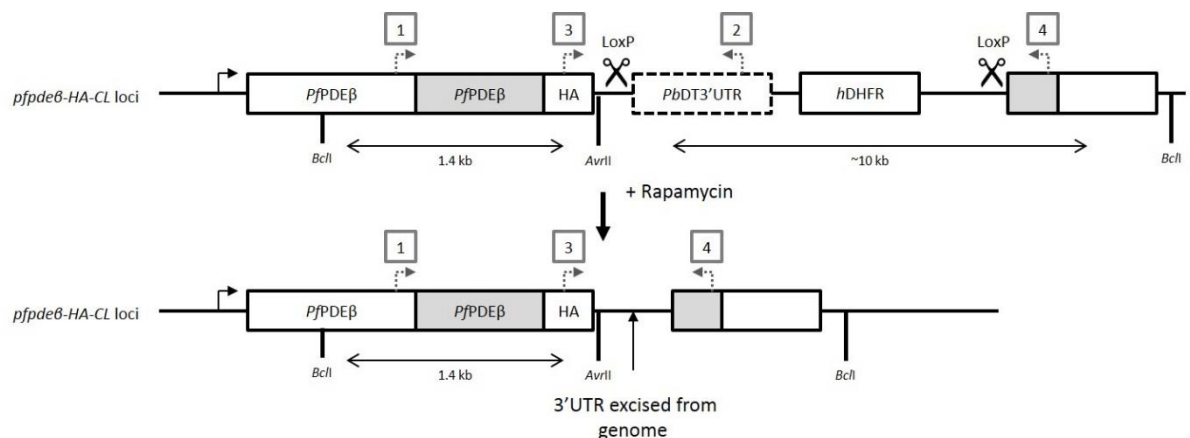
Figure 3.14 Excision strategy for the removal of the 3' UTR of PfPDEβ-HA-DiCre
Addition of rapamycin to PfPDEβ-HA-DiCre parasites is expected to remove the PbDT 3'UTR, the resistance cassette and much of the original plasmid backbone. The upper scheme shows the modified locus pre-excision and the lower scheme shows the expected result of the excision event. The dashed arrows and overhead numbers show the primer binding locations and designation. In the absence of rapamycin, the primer pair 1 and 2 should produce a 1.5 kb band and the primer pair 3 and 4 should produce no product as it would be too large to amplify (>6.0 kb). After rapamycin induced excision, no band should be produced with primer pair 1 and 2 as site 2 will have been excised. Primer pair 3 and 4 will be brought closer together, resulting in a 1.0 kb band. The locations of the restriction sites for Southern blotting are indicated under the loci. The 1.4 kb integration band will still be present, however the larger band will be reduced in size (exact size depends on crossover location), and all extra plasmid copies (6.8 kb) should be absent.

After 24 hours, in the absence of rapamycin, the expected 1.5 kb band was present for both clones, unfortunately this band was not lost with the addition of rapamycin. For B7 with rapamycin, there appeared to be reduced band intensity, however this could be due to

differences in the PCR reaction as it is not quantitative. With rapamycin treatment, primers pairs 3 and 4 produced the expected 1.0 kb band, indicating that the excision event had taken place. There were also faint bands in the non-excised controls, suggesting that there is some leakiness in the control of rapamycin induced DiCre mediated excision. After 72 hours and a second rapamycin treatment, the results were more or less the same (figure 3.15). Monitoring by Giemsa staining showed no differences in growth and morphology between the excised and non-excised lines (data not shown). The B7 line was then cloned by limiting dilution to obtain a pure excised population. Four clones (E1-4) were analysed by excision PCR (figure 3.16). All four clones were positive for integration and negative for any remaining non-excised locus. Clones E1 and E2 were taken forward for further analysis. Southern blotting was also performed on E1 and E2. The 1.4 kb integration band is still present, the larger downstream fragment band has reduced in size to about 3.0 kb, and all additional plasmid copies are absent (figure 3.17).
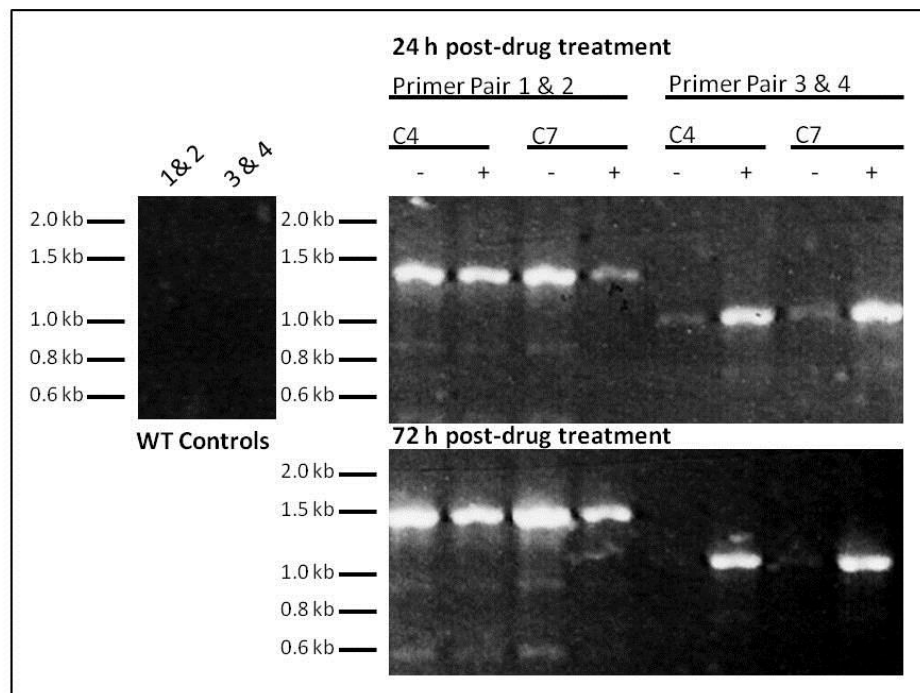
Figure 3.15 Excision PCR on the uncloned rapamycin treated PDEβ-HA-DiCre lines
Addition of a four hour treatment of rapamycin to PDEβ-HA-DiCre resulted in incomplete excision. After 24 hours, the primer pair 3 and 4 showed an increase in excision (1.0 kb band) compared to untreated. Primer pair 1 and 2 showed little difference between treated and untreated control (1.5 kb band), therefore the efficiency was not 100% as the bands for rapamycin treated would have disappeared. After 72 hours and a second treatment, efficiency was not improved. The gel of the left shows the WT controls which are negative, as expected.
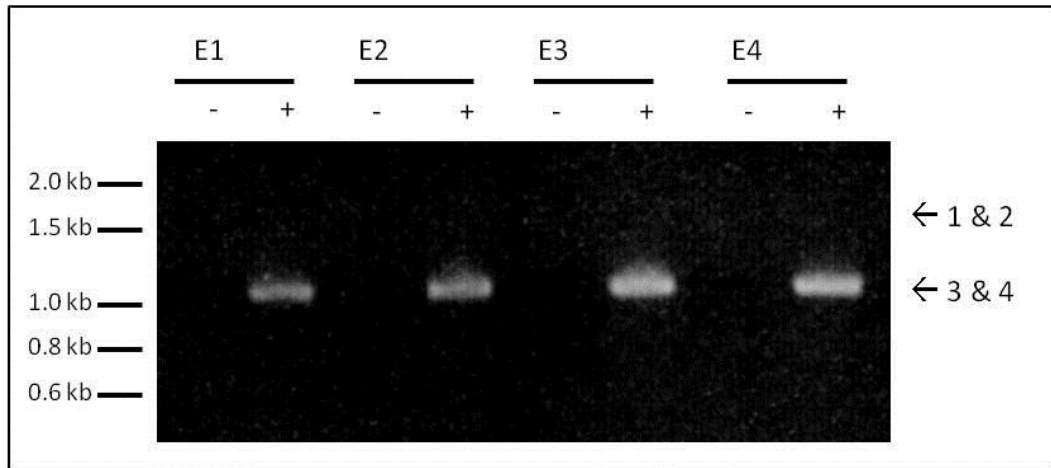
Figure 3.16 Excision PCR on the cloned rapamycin treated PDEβ-HA-DiCre lines
After cloning by limiting dilution, clones E1-4 were analysed by excision PCR. Presence of a 1.0 kb band for primer pair 3 and 4 and loss of the band from primer pair 1 and 2 indicated clonal populations of 3' UTR excised PDEβ-HA-DiCre. Clone E1 and E2 were continued.
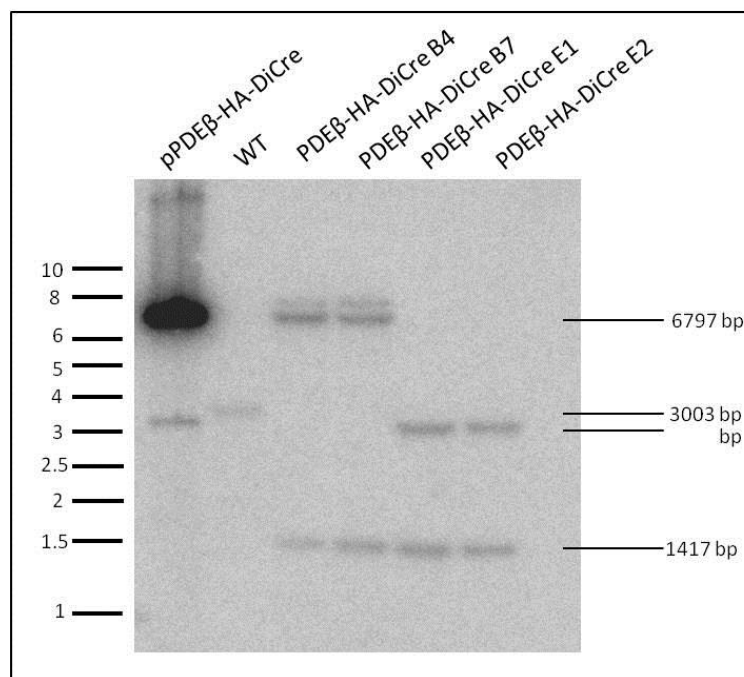
Figure 3.17 Southern blot of PDEβ-HA-DiCre excised and non-exciced lines
gDNA was digested with *Bcl*I and *Avr*II. The *pfpdeβ* fragments detected were as expected. The plasmid pPDEβ-HA-DiCre (major band was 6.8 kb, the smaller band is about the size of the excision event and may represent some minor recombination between the two loxP sites in the plasmid) and WT (3.0 kb) were present. The B4 and B7 lines were positive for the 1.4 kb integration band as well as a larger (~8 kb) downstream fragment band. Presence of a band the size of the plasmid indicates that multiple copies, possibly two as the band intensity is roughly double that of the other bands, have integrated. When treated with rapamycin (clones E1 and E2), the integration band is still present, however the larger band has reduced in size to roughly 3.0 kb and the plasmid copies have been excised.

3.2.7 Addition of the excision inducing compound rapamycin does not reduce the level of PDEβ protein

As PDEβ is expected to be essential, the ability of the rapamycin treated parasites to survive, even to the point of forming a stable line, was a surprise. To determine whether this was due to PDEβ not being essential, or the removal of the 3' UTR no resulting in protein level reduction, phenotypic analysis was performed. Firstly, growth assays were carried out according to the previously described method (chapter 2.5) on the PreDiCre line, non-excised B4 and B7 lines and the excised E1 and E2 lines. No significant growth difference was found, confirming that there was no growth defect in the excised line (figure 3.18). The parasites were also monitored by Giemsa smears which showed no obvious morphological differences between the lines (data not shown).
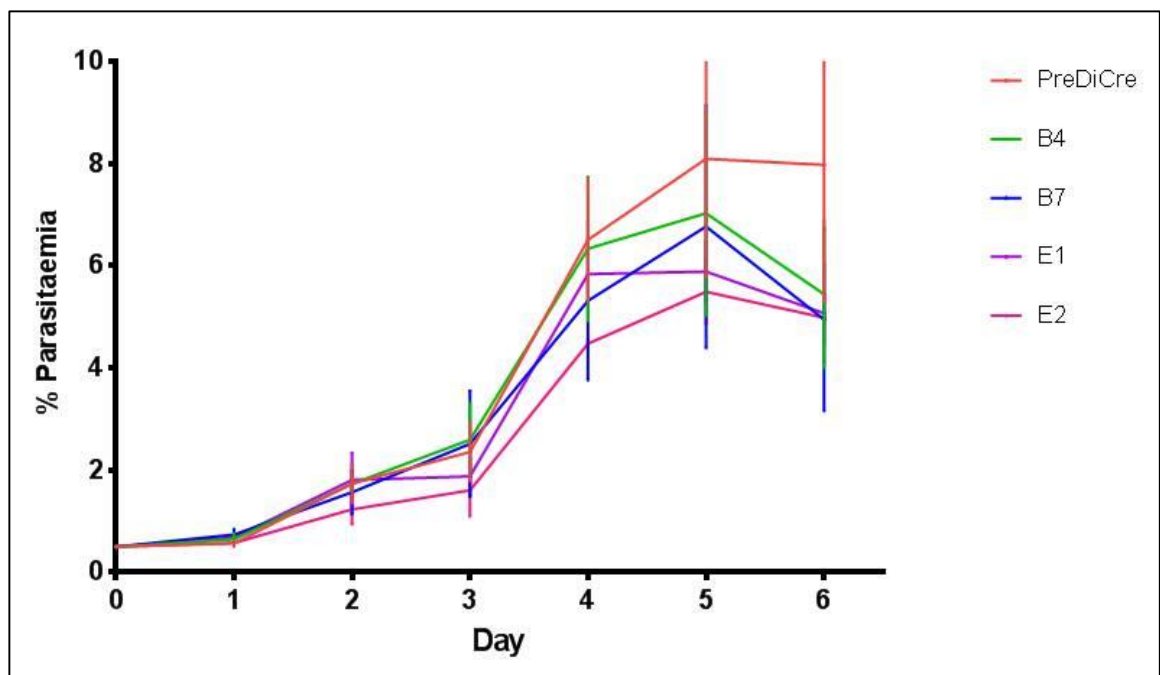
Figure 3.18 The growth rate of PreDiCre and PDEβ-HA-DiCre excised and non-exciced lines
The growth rates of PreDiCre (red), B4 (green), B7 (blue), E1 (purple) and E2 (pink) are not significantly different. The experiment was performed in duplicate and three biological repeats were conducted. The error bars represent standard error of the mean (SEM).

The DiCre knockdown plasmid was also designed to include an HA-tag allowing analysis of protein presence by western blotting and IFA, and protein subcellular localisation by IFA. Western blots on late stage asexual blood stage culture of non-excised B7 and excised E1, probed with rat anti-HA monoclonal antibody, confirmed expression of HA-tagged PfPDEβ. The 136 kDa band is consistent with the expected size of PfPDEβ (133 kDa) plus the epitope tag (3.3

kb). Parental PreDiCre does not react with the anti-HA antibody, as expected. IFAs on mixed stage asexual blood stage culture of non-excised B7 and excised E1, probed with rat anti-HA monoclonal antibody, also confirmed expression of HA-tagged PfPDEβ. The anti-HA staining did not colocalise with the DAPI stained nuclei. Further co-staining experiments are needed to confirm subcellular localisation of PfPDEβ (discussed further in chapter 4). Taken together, the data suggest that 3'UTR excision of PfPDEβ is not sufficient to reduce the level of protein, or have an effect on the growth or morphology of the parasites. The excised lines E1 and E2 were not analysed further. PDEβ-HA-DiCre was exploited further as an epitope tagged line and will be referred to as PDEβ-HA henceforth.
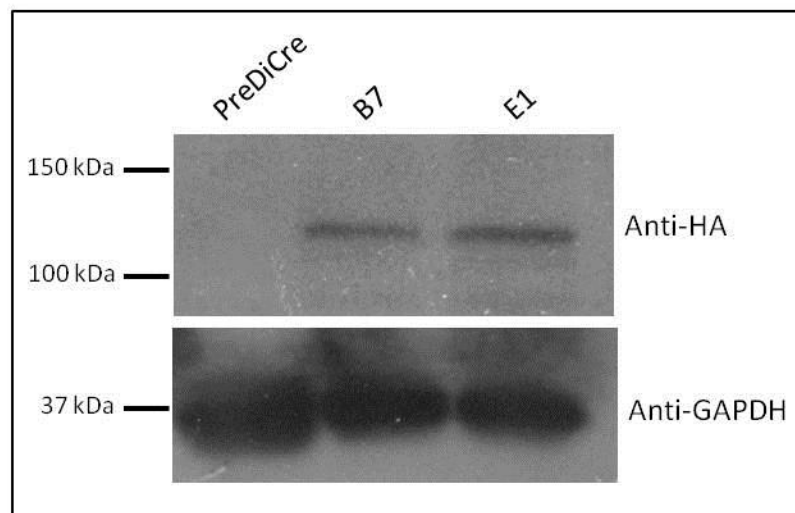
Figure 3.19 Transgenic PDEβ-HA-DiCre excised and non-excised lines express tagged PfPDEβ
Western blots of parental PreDiCre, non-excised B7 and excised E1 were probed with rat anti-HA monoclonal antibody. The predicted epitope tagged form of PfPDEβ (136 kDa) was present in both transgenic lines. As expected, the PreDiCre line is negative. Anti-GAPDH (37 kDa) was used as a loading control.
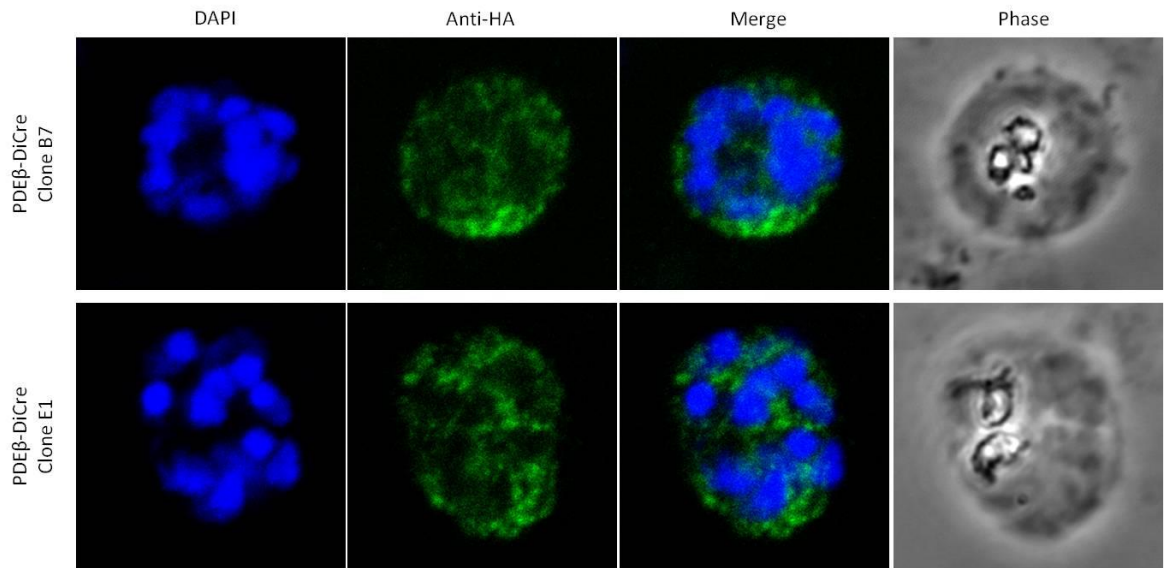
Figure 3.20 Transgenic PDEβ-HA-DiCre excised and non-excised lines express tagged PfPDEβ
IFAs on formaldehyde fixed thin smears of mixed asexual stage non-excised B7 and excised E1 were performed and representative images are shown for each strain. The parasite nuclei were stained with DAPI, and the bright field image is shown on the right. For negative control images, see appendix A3.

3.2.8 Construction of *Plasmodium falciparum* PDEβ internal-loxP DiCre plasmids to mediate conditional knockout

PDEβ contains eight introns, mostly at the C-terminus. After the failure of the transgenic PDEβ-HA-DiCre line to knockdown the level of PDEβ in the cell following excision of the 3' UTR, a construct was designed to insert a loxP site into one of the introns. The predicted catalytic domain of PDEβ contains three introns and the furthest from the C-terminus was chosen as the location for the loxP site. This would effectively cut the catalytic domain in two, hypothetically rendering the protein inactive. A synthetic, partially recodonised (*Spodoptera frugiperda* codon usage) PDEβ, based on the predicted *P. falciparum* 3D7 sequence was synthesised by GenScript. The sequence contained a 5' *Afl*II and a 3' *Xho*I site. Upstream of the third from end intron was a 1.0 kb targeting sequence containing native PDEβ sequence, for recombination by single crossover. The third intron was also native sequence, however a loxP site was inserted 58 bp from the 5' end and 109 bp from the 3' end. 34 bp after the intron also retained native sequence. Insertions into the middle of an intron rather than near the end are less likely to be detrimental to the parasite (Catherine Suarez, NIMR, personal communication). cDNA was used for the final 819 bp of PDEβ which was recodonised to prevent recombination downstream of the loxP site. An HA-tag was added to the end of the sequence, followed by a stop codon (see figure 3.22).

The pPDEβ-HA-DiCre plasmid was digested with *Afl*II and *Xho*I, resulting in the removal of the PDEβ sequence, the HA tag and the 3' loxP site. The synthetic PDEβ containing the internal loxP site and the recodonised sequence was then cloned into the plasmid with the same restriction enzymes. This resulted in the plasmid pPDEβ-IntronLoxP. The plasmids were verified by restriction digest and sequencing (figure 3.21).
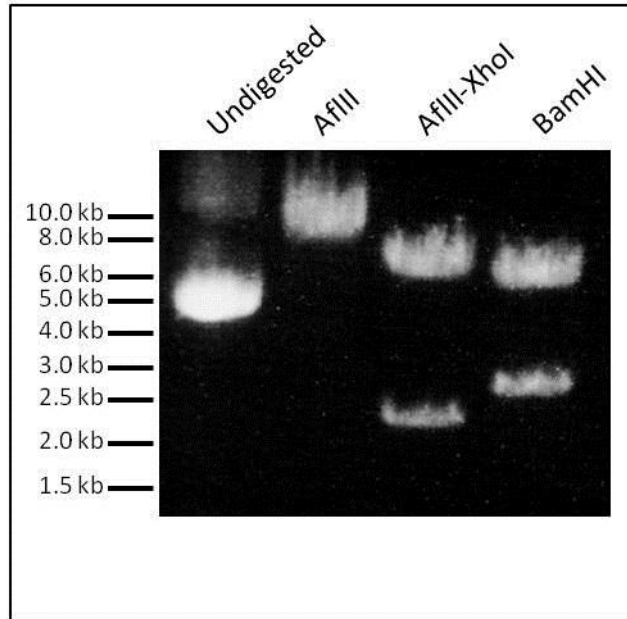
Figure 3.21 Restriction digests to verify the PDEβ-IntronLoxP constructs are correct
The expected sizes for both pPDEβ-IntronLoxP were as follows: *Afl*II single digest, 8.0 kb, *Afl*II-*Xho*I double digest, 5.8 kb and 2.2 kb and *BamH*I single digest, 5.3 kb and 2.6 kb. The sizes are correct for the plasmid. Correct sequence of the inserts and junctions was also confirmed.

Figure 3.22 shows the allelic replacement strategy for *pfpdeβ*. *P. falciparum* PreDiCre parasites were transfected with the pPDEβ-IntronLoxP plasmid as described above. The PreDiCre line was generated by the Blackman lab and contains the DiCre cassette integrated by single crossover at the SERA5 locus, with no detrimental effect on the parasite (Collins et al. 2013). WR99210 drug-resistant parasites were detected 3 weeks post transfection. At the time of writing the parasites were undergoing drug cycling. Figure 3.23 shows the expected product of rapamycin treatment, resulting in excision of the C-terminus of *pfpdeβ*, which is hypothesised to ablate the function of the enzyme.
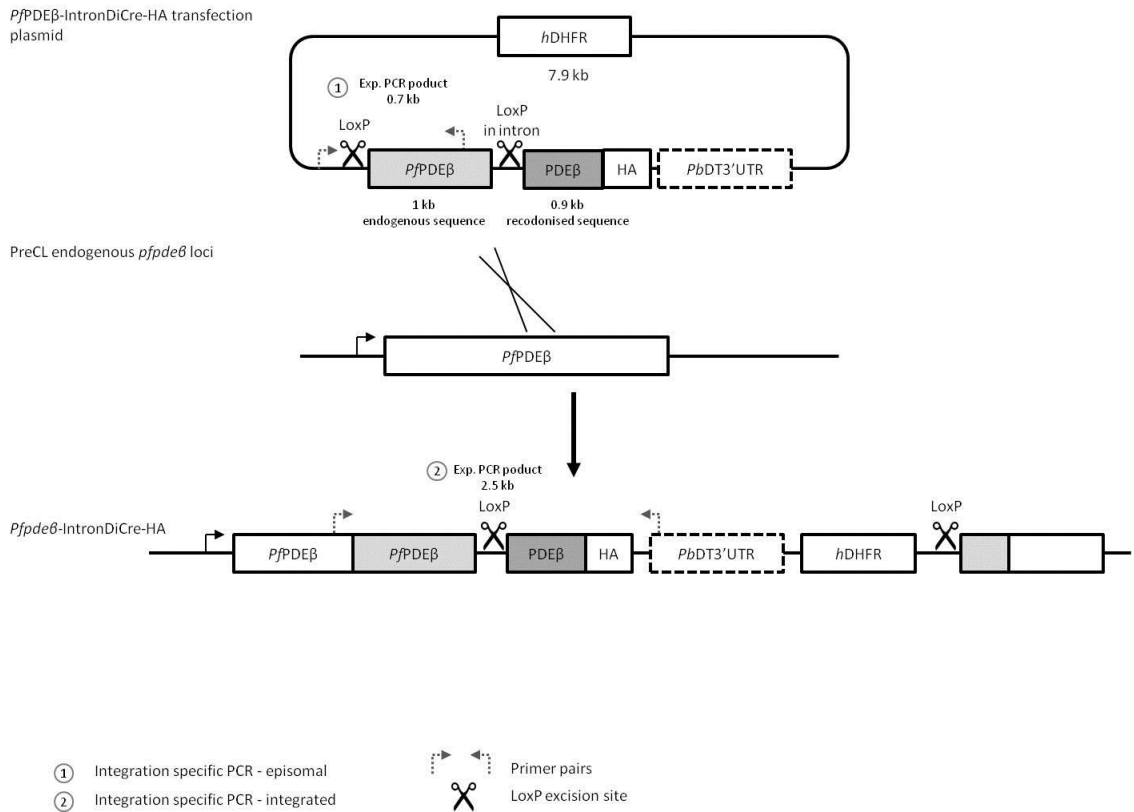
Figure 3.22 Internal loxP integration strategy for *pfpdeβ*
A schematic representation of the transfection plasmid and the *pdeβ* locus before and after integration. The 1.0 kb gDNA fragment of endogenous sequence promotes recombination by single crossover resulting in insertion of a loxP site into an intron within the predicted catalytic domain, followed by 0.9 kb recodonised synthetic sequence (to prevent crossover after the loxP site), an HA-tag, the pbDT 3'UTR and a second loxP site. The integration PCR primer locations are depicted with dashed arrows and the expected fragments given, 0.7 kb for presence of the episome and 2.5 kb for an integration event.
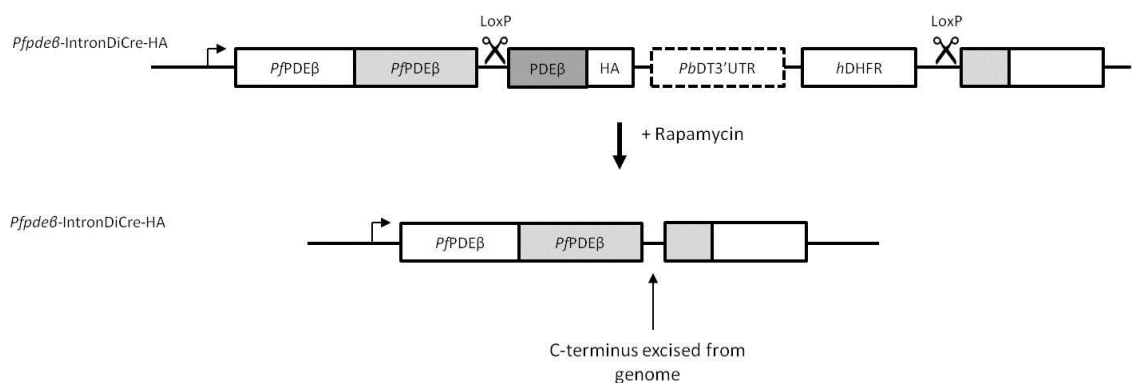
Figure 3.23 Excision strategy for the removal of the C-terminus of pPDEβ-IntronLoxP
Addition of rapamycin to pPDEβ-IntronLoxP parasites is expected to remove the C-terminus of the gene, as well as the resistance cassette and much of the original plasmid backbone. The upper scheme shows the modified locus pre-excision and the lower scheme shows the expected result of the excision event.

3.3 Discussion

3.3.1 The destabilisation domain system and asexual PDEs

The DD system is used in many organisms, including *P. falciparum,* to knockdown the amount of a specific protein in an inducible manner. DD-tagged PDEβ was unable to form a stable integrated parasite line. In the Southern blot showing the four attempted transfections of PDEβ and it appeared that many episomes were present per genome copy, to the point where the genome band was barely visible and the plasmid band was very strong (figure 3.6). This indicates that the plasmid formed highly stable episomes that were not lost with drug cycling, as previously reported (O'Donnell, 2001). As this happened on four separate occasions, it is unlikely that a stable PDEβ-DD line could be produced, perhaps because the DD tag was too detrimental to parasite growth, even in the presence of shield-1. PDEα-HA-DD was able to form a stably integrated line, confirmed by PCR and Southern blotting (figures 3.5 and 3.6). However, the protein was undetectable by either western blotting or IFA, this may be because the protein level is naturally very low or that the HA-tag is inaccessible to the antibody by mis-folding or sequestration in the membrane. As PDEα is not essential, it is also possible that there is no PDEα protein present in the parasites due to degradation. RT-PCR could be used to detect a problem with transcription of the PDEα mRNA. Unfortunately as there is no specific antibody to the PDEα protein, down regulation at the protein level cannot be investigated. Late stage parasites were used for western blotting as this is when expression of PDEα is expected to be highest. For the IFAs, mixed stage cultures were used. As individual parasites can be identified, this would give the highest chance of visualising expression and indicate a rough time course of expression. However, little or no fluorescence above background was detected when the parasites were probed with monoclonal rat anti-HA antibody. As ablation of PDEα is not detrimental to parasite growth, removal of shield-1 was not expected to negatively affect the growth rate of PDEα-HA-DD. 0.5 μM of shield-1 in the culture was used as standard as this was the concentration used in previous studies (Dvorin et al., 2010; Russo et al., 2009), though this concentration does still delay parasite growth to some extent (de Azevedo et al., 2012). Although 0.5 μM of shield-1 is sufficient to stabilise the DD tagged proteins in other published studies, increasing concentrations of shield on PDEα-HA-DD cultures were used and the protein level was assessed by western blotting. Three concentrations of shield-1 (0.5, 1.0 and 2.0 μM), and a no shield control were used, however PDEα-HA-DD was not detected at any concentration. Even if 2 μM or higher was able to stabilise PDEα, this concentration becomes, not only toxic to the parasite, but also prohibitively expensive to use routinely. As there is currently no antibody able to

efficiently detect native PDEα, it is not known whether expression is totally ablated by addition of the tag, expression is below the detection level normally in WT parasites, or the tag is cleaved off within the parasite.

The PfPDEs are transmembrane proteins, with six TM domains. To my knowledge, there is only one study in which apicomplexan integral membrane proteins have been successfully targeted with the DD system. TgAMA1 and TgROM4 levels were efficiently knocked down by DD tagging. TgAMA1 is an integral membrane protein with one TM domain and TgROM4 has six TM domains (Santos et al., 2011). There are no reports of a successful knockdown of a TM protein in *P. falciparum*.

A recent analysis of various aspects of the DD system in *P. falciparum* by de Azevendo et al., noted that proteins that reside in the organelles of *P. falciparum* may be targeted to the proteasome less efficiently that cytoplasmic proteins. Additionally, the authors noted that C-terminally tagged proteins that are co-translationally inserted in the endoplasmic reticulum may escape from proteasome degradation in the absence of shield-1 (de Azevedo et al., 2012).

Reporting bias can be a significant problem in determining the efficiency of a particular system as frequently only the successes are published. Many attempts to DD-tag proteins have failed, either due to rejection of the tag, as with PDEβ, or failure of the tag to regulate protein expression, as is probably the case with PDEα (de Azevedo et al., 2012). Recent attempts to DD-tag many kinases in *P. falciparum* resulted in only a few stable lines that generated efficient knockdown of the target protein. It was estimated that the success rate was around 1 in 10 (Manoj Duraisingh, Harvard School of Public Health, Personal Communication).

3.3.2 The subtle growth phenotype of PDEα-KO

Previous work by Wentzinger et al., reported that their PDEα-KO line had an unusual growth phenotype. The authors noted that when synchronised using sorbitol, rings appeared faster in subsequent generations of PDEα-KO compared with their non-gametocyte forming 3D7 parental line. This phenotype could not be quantified as the phenomenon was not consistent. During the course of this study, it was also observed that the PDEα-KO parasites (used previously in the Wentzinger study) have a shorter lifecycle than the 3D7 line. They also frequently reached a much greater parasitaemia than other strains. When a growth assay was performed, the parasitaemia reached 10% by day four when all other strains were around 4%. PDEα-KO does not produce gametocytes, however the parental 3D7 line was a non-gametocyte producer therefore the effect of PDEα knockout could not be investigated in gametocytes. To investigate

whether the high growth rate of PDEα-KO was due to the lack of gametocyte production, the non-gametocyte producing ApiAP2-g mutant A4 line (Kafsack et al., 2014) was used as a control. The growth rate of A4 was no different from the other strains and significantly lower than that of the PDEα-KO. The high growth rate being a product of the PDEα-KO line's inability to form gametocytes would have been unlikely as the parental line, used for the comparison by Wentzinger et al., was also a non-gametocyte producer.

It cannot be ruled out that the growth rate phenotype could be that when transfected and cloned, there was a mutation somewhere else in the genome that resulted in the observed growth phenotype. Whole genome sequencing of PDEα-KO compared to 3D7 could be employed to determine the differences in the PDEα-KO line at the genome level. The most appropriate 3D7 control would be the original parental line used by Wentzinger. Complementation of the PfPDEα gene could also be performed to see if a normal growth rate resumes when the gene is restored.

The PDEα-HA-DD line, if it had been successful in mediating conditional knockdown, could have been used to assess the growth rate of parasites in the presence or absence of shield-1, however there are many conflicting factors to consider with this. Firstly, shield-1 is known to have a slightly toxic effect on parasite growth, with one study finding that parasite reinvasion was reduced by 11% in a single cycle in the presence of 0.5 µM shield-1 (de Azevedo et al., 2012), which is not ideal when looking at slight differences in growth. Secondly, it was not known if the HA tag was not being detected and that PDEα was active within the cells or if the DD tag resulted in inactive protein, even in the presence of shield-1. PDEα-HA-DD was therefore not an appropriate control for a PDEα-KO growth phenotype.

Although not the main focus of this project, the high growth phenotype of PDEα-KO is extremely interesting and warrants further investigation. To fully examine whether removal of PDEα has a positive impact on *in vitro* growth, a second PDEα-KO line would need to be generated, using a gametocyte producing parental line. This would not only confirm that the PDEα growth phenotype is not a non-gametocyte producer phenotype, but also to investigate the role of PDEα in gametocytes. It may also prove beneficial to attempt to generate a *P. berghei* PDEα-KO to examine whether PDEα is truly indispensable *in vivo* at all stages of the life cycle.

3.3.3 The DiCre system and PDEβ

During the course of this project, the DiCre system was adapted to *P. falciparum*. In collaboration with Mike Blackman, attempts were made to generate a conditional knockdown of PDEβ using this system. Results with the latest strategy are pending at the time of writing. Initially a construct was designed to excise the 3' UTR of the PDEβ gene in an attempt to destabilise the mRNA, and preventing translation and therefore reducing the amount of protein. Both this study, and work by the Blackman group, has found that removal of the 3' UTR, even with 100% efficiency, did not reduce the amount of protein for the genes targeted so far (Collins et al. 2013). Whilst removal of the 3' UTR is employed in studies on different organisms, it is not always successful. As study by Ecker et al. in 2012, found that excision of the 3'UTR of *P. berghei* chloroquine resistance transporter gene (*pbcrt*) by the FLP/FRT system failed to reduce the protein level. This was found to be the result of an alternative polyadenylation sites at the 3' end of the excised locus, that was efficiently able to stabilise the *pbcrt* mRNA. Further studies by Collins et al. showed that the *hsp86* 3' UTR sequence used to regulate transcription of the FRB-Cre60 component of the DiCre cassette, possesses bidirectional transcription termination and polyadenylation functions, and was therefore able to stabilise the mRNA of SERA5. Strangely, the pPDEβ-HA-DiCre transfection plasmid did not contain a second 3' UTR that would be present after rapamycin treatment and the reason for mRNA stability remains unknown, but is plausibly due to a cryptic polyadenylation site. The PDEβ-HA-DiCre line was however detectable with an anti-HA antibody and has been used for further studies on PDEβ, which will henceforth be referred to as PDEβ-HA (see chapter 4).

After the failure of 3' UTR excision to reduce the amount of PDEβ, strategies were considered to remove either part of, or the whole of, the coding sequence. The first published study to successfully employ the DiCre knockdown system in *P. falciparum* was by Yap et al. (2014), where the authors 'floxed' the entire PfAMA1 sequence, which resulted in defective invasion. To achieve this, in the W2mef line, the endogenous PfAMA1 was entirely replaced with the antigenically distinct (to aid analysis) 3D7 gene, flanked by loxP sites at the N- and C-termini. This resulted in excision of the entire gene resulting in a protein knockdown of about 80% within a single intraerytrocytic growth cycle, and was sufficient to have an impact on invasion (Yap et al., 2014). PfAMA-1 coding sequence is only 1.9 kb long, whereas PDEβ is 4.7 kb, with many introns and long stretches of repetitive sequence. It would have been extremely challenging to clone by PCR and would have resulted in a very large transfection plasmid. To have full length cDNA synthetically made would have been too expensive. The Blackman group have employed

a similar approach to that of Yap et al. by tagging the upstream gene from SERA5 with a lox*P* site, and the 3' end of SERA5. With rapamycin treatment, this also resulted in excision of the entire SERA5 locus and lead to ablation of gene function (Mike Blackman, Personal Communication). This approach for PDEβ would also have been extremely challenging as the upstream gene is in the opposite orientation to PDEβ. C-terminally tagging this gene would have resulted in removal of both genes. Instead, a transfection plasmid designed to insert a loxP site into an intron in the middle of the catalytic domain with the second loxP site within the plasmid. This would, hypothetically cut the catalytic domain in half, rendering it inactive (figure 3.24). The construct has been successfully created and transfected into the DiCre containing precursor line, PreDiCre, creating PDEβ-IntronLoxP. Work with this line is currently ongoing.

Although not employed in this study, the recent improvements in *P. falciparum* genome targeting should make transfections and generation of stable, genetically modified parasite lines significantly faster as linearised plasmid can be transfected, reducing the need for drug cycling. Both the use of zinc-finger nucleases (ZFNs) (Straimer et al., 2012) and the clustered regularly interspaced short palindromic repeat targeting of Cas9 (CRISPR/Cas9) (Ghorbal et al., 2014) can mediate specific double strand breakages, mediating editing from this site. Host cell DNA repair machinery is employed and repairs the breakage using a homologous template. As plasmid, with homologous targeting sequences, is added in excess of the genome, the repair machinery will use this as the template to fix the break, thereby inserting the plasmid into the genome.

Chapter 4: Characterisation of the asexual blood stage expression and localisation of *P. falciparum* PDEβ

4.1 Introduction

As mentioned in chapter 1, there are no published studies on PfPDEβ. From the information on PlasmoDB (http://plasmodb.org/plasmo/) (genomic sequence data), *pfpdeβ* is predicted to encode a 133 kDa protein with six transmembrane domains. Illumina-based sequencing of *P. falciparum* 3D7 mRNA on seven life cycle stages suggests that expression, of mRNA at least, peaks in late trophozoites and schizonts. RT-PCR on mRNA transcripts produced in this group also corroborates this finding (Ross Cummings, Thesis). Thus far, there has been very little biological evidence to indicate whether these results correlate with protein expression levels. PDE assays on cell fractions at all life cycle stages have shown highest cyclic nucleotide activity in the membrane fraction, supporting the finding that the PDEs are integral membrane proteins. The subcellular localisation of any of the PfPDEs, prior to this study, has been a mystery. Evidence from mammalian systems suggests that cyclic nucleotide phosphodiesterases are often strictly compartmentalised within the cell (Maurice et al., 2014). In a review of cyclic nucleotide signalling in protozoa, Markov modelling of PDEβ predicted that the catalytic domain projects into the parasitophorous vacuole (Gould and de Koning, 2011).

This chapter aimed to use the HA-tagged PDEβ, outlined in chapter 3, to investigate the expression and localisation of PDEβ in the asexual blood stages of *P. falciparum*. In addition, the specificity of commercially produced antipeptide antibodies against both PDEα and PDEβ, provided by Pfizer, was explored.

4.2 Results

4.2.1 PfPDEβ-HA is located in the membrane fraction of parasite extracts

PDEβ has multiple predicted transmembrane domains, and previous work has indicated that the vast majority of *Plasmodium* PDE activity resides within the membrane fraction of parasite lysate preparations. To further confirm this localisation, the PDEβ-HA epitope tagged parasite line was utilised for solubility assays which were performed as described in chapter 2.3.4. Using sequential extraction buffers on mixed late blood stage parasites, different cell fractions were solubilised. Cytosolic, membrane and insoluble fractions were obtained. Western blotting of the resulting samples was performed and probed with rat anti-HA antibody to detect PfPDEβ-HA. To assess the success of fractionation, the same samples were probed with antibodies that react with PfPKG and PfGap45. PfPKG is mostly cytosolic, but does have some membrane association as it can be detected at low levels with a carbonate extraction (about 50% in very late schizonts), which solubilises membrane-associated (peripheral membrane proteins) but not integral membrane proteins (Hopp et al., 2012). PfGAP45 is N-myristoylated and palmitoylated and should therefore mostly be detected in the integral membrane fraction (Rees-Channer et al., 2006). As expected, PfPKG was mostly found in the cytosolic (S1) fraction in mixed late stage parasites, with a minor band in the membrane fraction (S2). PfGAP45 was detected in both the cytosol and membrane fractions. However, PfPDEβ-HA was detected exclusively in the S2 membrane fraction (extracted with 1% Triton X-100) supporting the sequence evidence that PfPDEβ is an integral membrane protein.
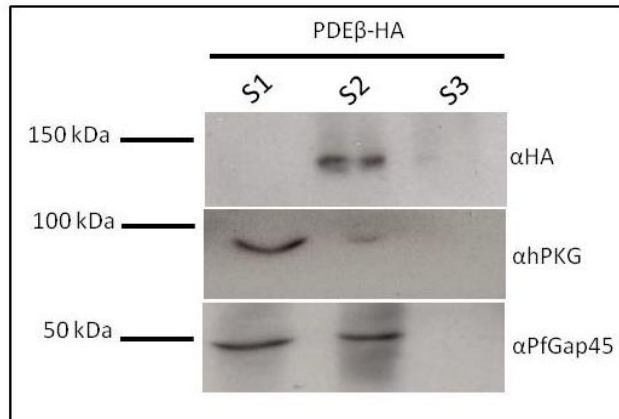
Figure 4.1 Solubility assay of PfPDEβ-HA indicates it is an integral membrane protein
Western blots of sequential solubilisation of cytosolic (S1), membrane (S2) and insoluble (S3) parasite fractions of PfPDEβ-HA. The blot was probed with anti-HA for PfPDEβ (1:1000, top panel), anti-human PKG for PfPKG (1:3000, middle panel) and anti-PfGAP45 (1:.3000, bottom panel). Cytosolic S1 fraction was extracted with a high salt buffer, integral membrane S2 fraction was extracted with 1% Triton X-100 and insoluble S3 fraction was extracted with 4% SDS and 0.5% Triton X-114. Extractions were performed on mixed late stage parasites. Equal volumes of each fraction were loaded and the same stock was used for all three blots.

4.2.2 Expression of PfPDEβ-HA is highest in schizonts

To determine the temporal expression of PfPDEβ-HA, western blotting was performed on synchronised parasites. Samples were taken at three timepoints when the culture was highly enriched for rings (0-8 hours post invasion (h.p.i.)), trophozoites (16-24 h.p.i) and schizonts (32-48 h.p.i). PfPKG, probed with the anti-human PKG antibody, was used as a control. PfPKG peaks in very late schizonts, but can be detected at low levels in trophozoites and very low levels in rings (Hopp et al., 2012). This was reflected in the expression pattern obtained (figure 4.2). PfPDEβ-HA protein expression also peaked in schizonts with a low level of expression in trophozoites and no expression detected in ring stages.

To further study the stage specific expression of PfPDEβ-HA, immunofluorescence assays were performed. Tagged PfPDEβ showed low signal intensity in trophozoites which then peaked in mid to late schizonts, before reducing at very late schizonts. No signal was detected in WT parasites probed with rat anti-HA monoclonal antibody (appendix A3).
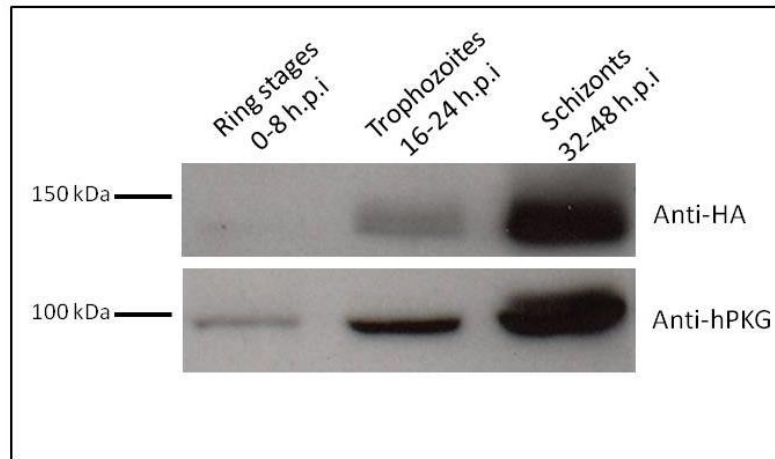
Figure 4.2 Time course assay of PfPDEβ-HA expression indicates it peaks in schizont stages
Western blots of whole parasite lysates taken at three timepoints, 0-8, 16-24 and 32-48 hours
post invasion (h.p.i.). Blots were probed with rat anti-HA (1:1000) to detect PfPDEβ-HA and
anti human PKG (1:2500) to detect PfPKG.
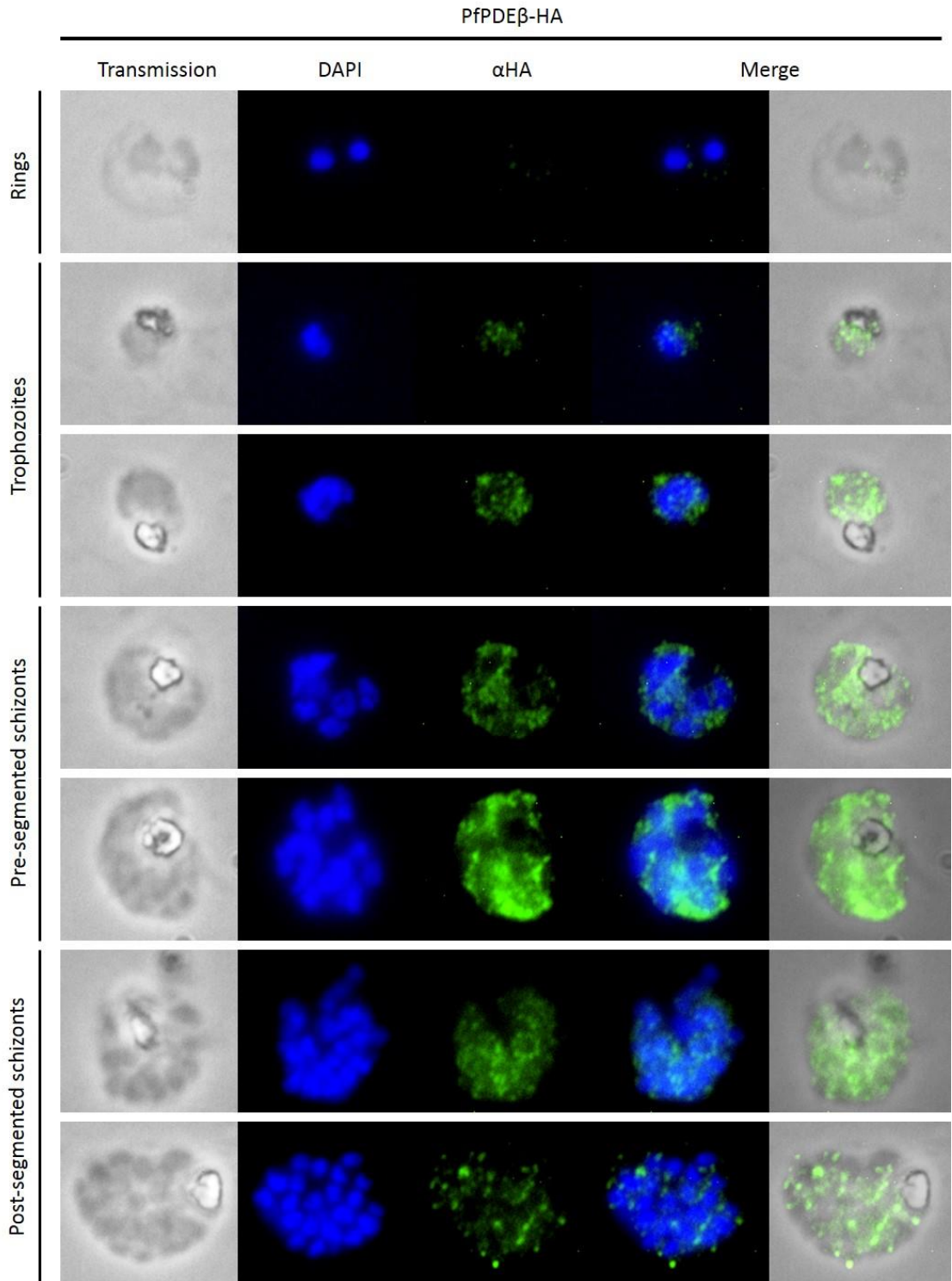
Figure 4.3 Time course assay of PfPDEβ-HA expression indicates it peaks in mid to late schizont stages

Representative images of formaldehyde fixed thin smears of ring, trophozoite and schizont stages of PfPDEβ-HA parasites, probed with rat anti-HA monoclonal antibody. Parasite nuclei are stained with DAPI (second column).

4.2.3 PfPDEβ-HA is located in the parasite endoplasmic reticulum

Subcellular localisation is an important step in fully characterising a protein. From the time course assay, staining of PfPDEβ-HA appeared punctate, with dense focal points in the mid-schizonts and more diffuse in the later schizonts. Co-staining IFAs were performed with proteins of known subcellular location including, PfEBA175 which localises to the micronemes, PfERD2 which localises to the Golgi body, PfGAP45 which localises to the inner membrane complex, PfMSP1 which localises to the merozoite plasma membrane and PfBiP which localises to the lumen of the endoplasmic reticulum.

Dual-labelling of PfPDEβ-HA with anti-HA antibodies and PfBiP resulted in colocalisation, strongly suggesting that PfPDEβ is located in the endoplasmic reticulum (figure 4.4). PfPDEβ-HA did not significantly colocalise with PfEBA175, PfERD2 or PfGAP45 (figure 4.5). Interestingly, although little colocalisation was observed with segmented PfMSP1, significant overlap was seen in earlier, pre-segmentation schizonts (figure 4.6).

In order to confirm the ER localisation of PfPDEβ-HA, IFAs with ER-Tracker™ Blue-White DPX (Molecular Probes, LifeTechnologies) were performed as described in chapter 2.3.2. ER tracker is designed to be used on live parasites however due to that lack of a GFP-tagged PfPDEβ parasite line, staining was performed on fixed parasites. The manufacturer's protocol states that some staining is retained with fixation and permeabilisation, however the signal was very weak. Despite weak staining of both ER-tracker and PfPDEβ-HA, clear overlap can be observed supporting the PfBiP colocalisation data (figure 4.7).

PfPDEβ-HA

| DAPI | αHA | αPfBip | Merge | Transmission |
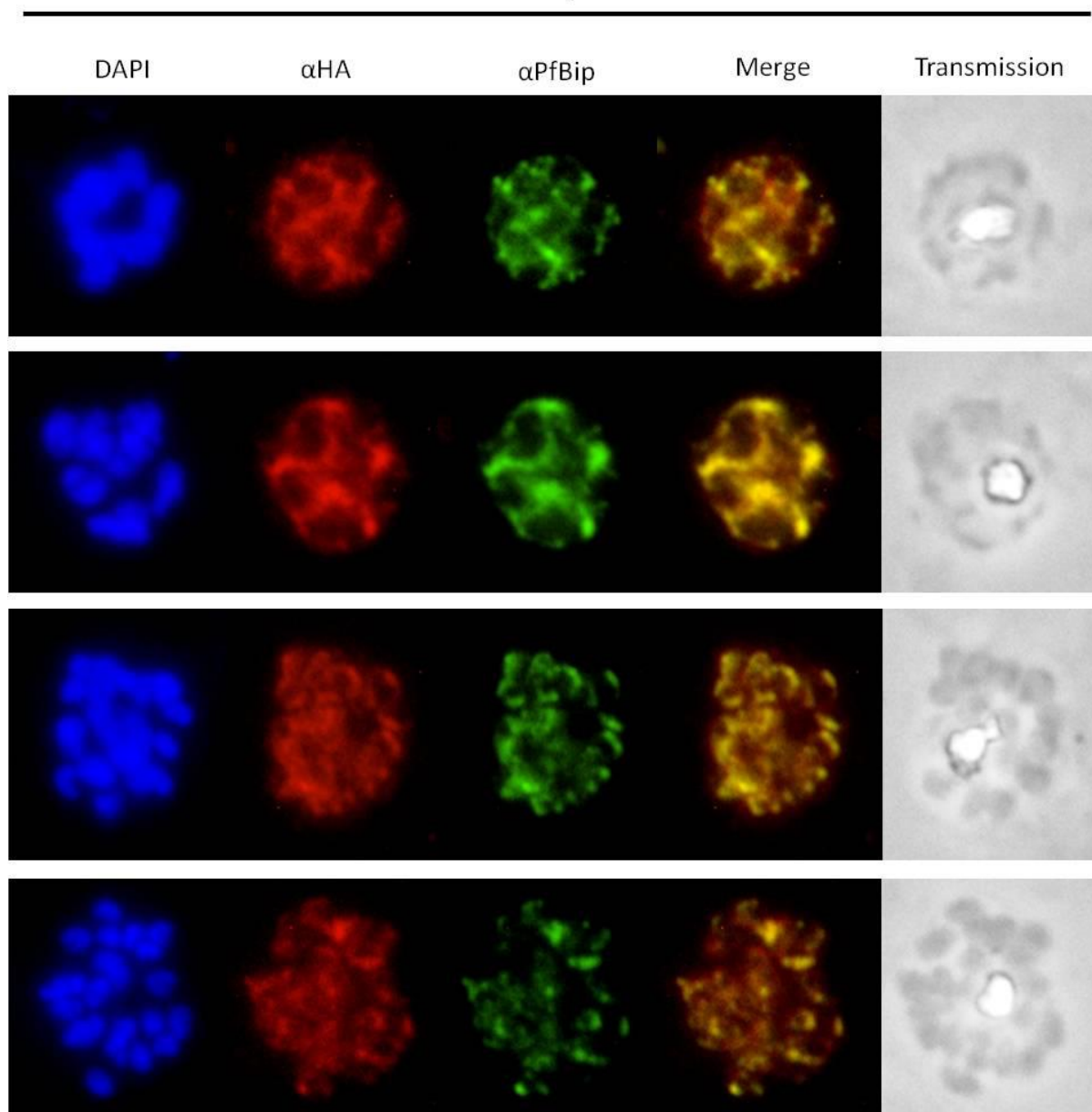
Figure 4.4 PfPDEβ-HA co-localises with PfBiP
Representative images of formaldehyde fixed thin smears of PfPDEβ-HA parasites, probed with
mouse anti-HA monoclonal antibody (red) and rat anti-PfBiP (green). Parasite nuclei are stained
with DAPI (blue, first column) and bright field images are shown on the right.
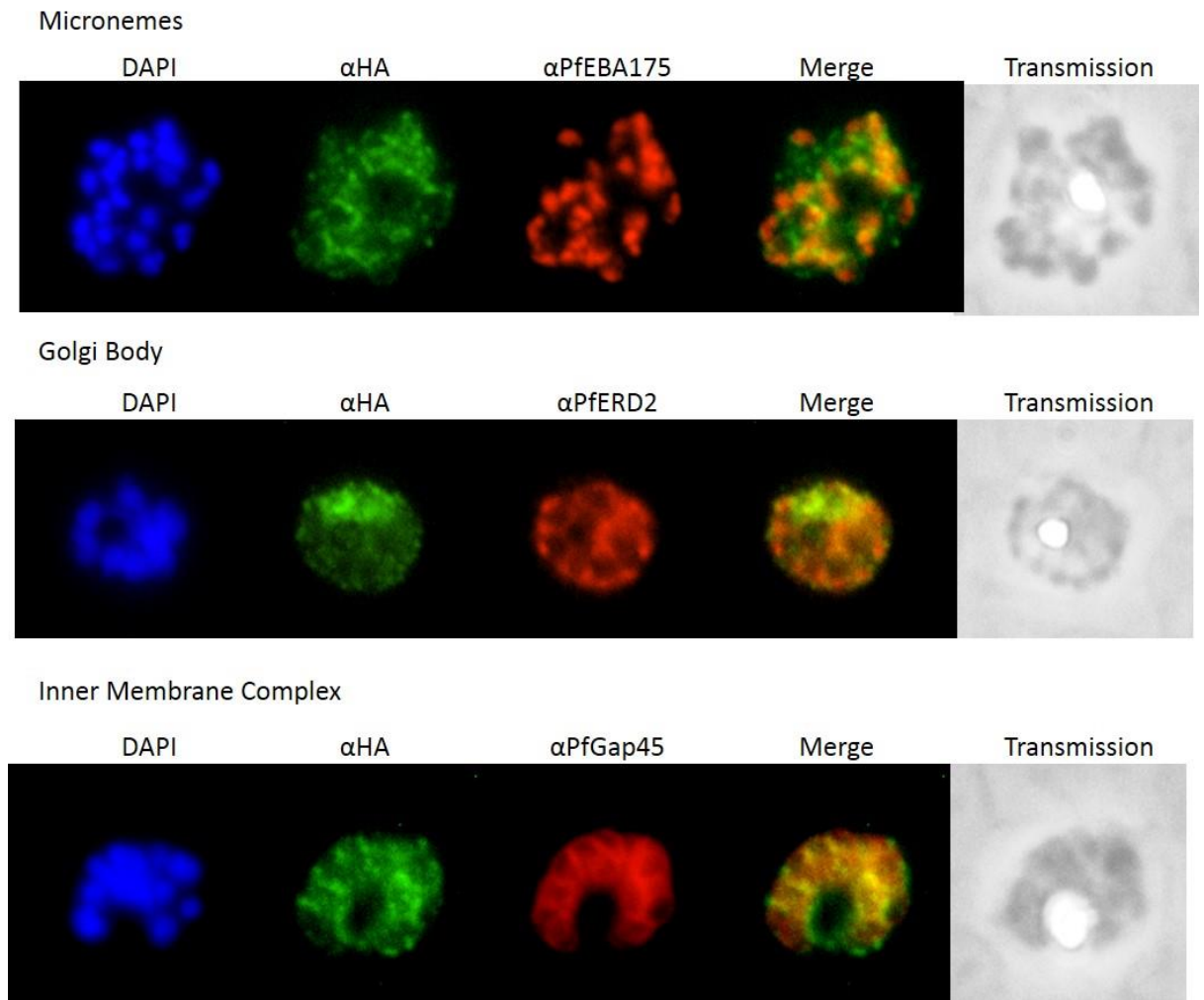
Figure 4.5 PfPDEβ-HA does not co-localises with other cellular locations
Representative images of formaldehyde fixed thin smears of PfPDEβ-HA parasites, probed with rat anti-HA monoclonal antibody (green) and (from top to bottom) PfEBA175, PfERD2 and PfGap45 (all red). Parasite nuclei are stained with DAPI (blue, first column) and bright field images are shown on the right.
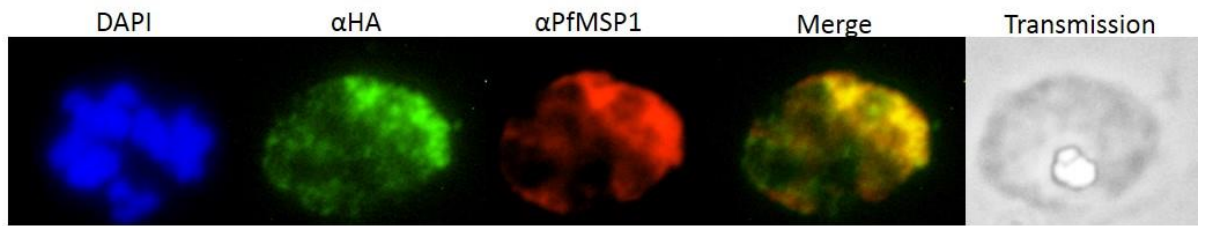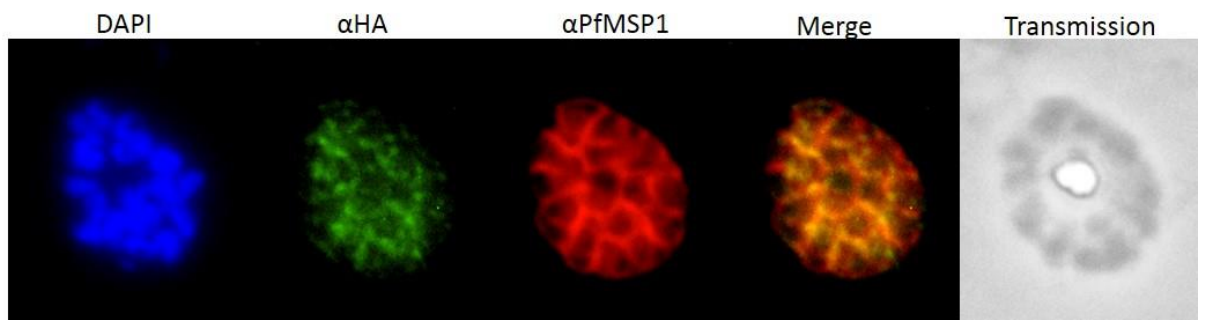
Figure 4.6 PfPDEβ-HA partially co-localises with MSP1 in pre- but not post-segmented schizonts

Representative images of formaldehyde fixed thin smears of PfPDEβ-HA parasites, probed with rat anti-HA monoclonal antibody (green) and PfMSP1 (red). Pre-segmented schizonts are shown in the top row and post-segmented schizonts are the bottom row. Parasite nuclei are stained with DAPI (blue, first column) and bright field images are shown on the right.
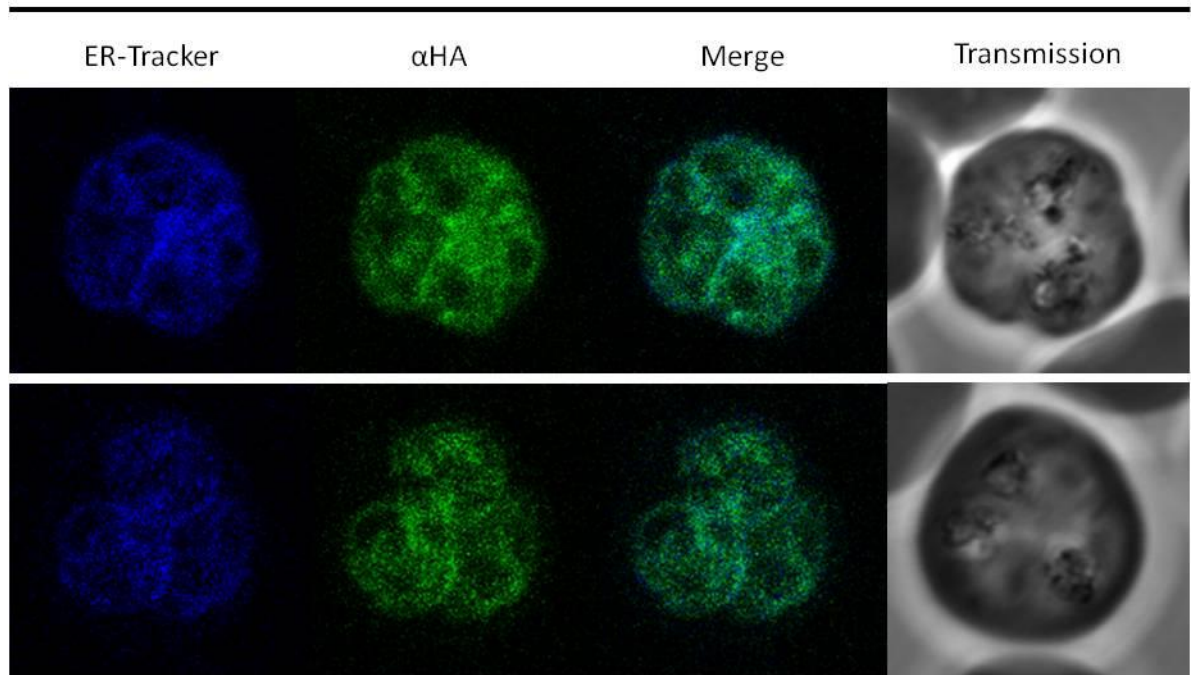
Figure 4.7 PfPDEβ-HA co-localises ER-tracker
Representative images of PfPDEβ-HA parasites, pre-loaded with ER-Tracker™ Blue-White DPX, fixed with formaldehyde, permeabilised and probed with rat anti-HA monoclonal antibody (green) in suspension. Bright field images are shown on the right.

4.2.4 PfPDEβ-HA does not colocalise with an antibody raised to the putative PfAKAP protein

In mammalian systems, signalling molecules are often complexed into signalosomes to compartmentalise and regulate the signalling response. With regards to PKA, often a protein A kinase anchoring protein (AKAP) binds the regulatory domain of PKA to other signalling molecules at a specific subcellular localisation (Dodge-Kafka et al., 2005). PKG interacting partners (GKIPs) have an analogous role to AKAPs in that they associate with PKG and other signalling molecules, thereby compartmentalising the pathway. In *P. falciparum,* only one putative kinase anchoring protein, PfAKAP (PF3D7_0512900), has been identified (Anaïs Merckx, Personal Communication). To determine whether PfAKAP and PfPDEβ-HA are spatially associated and could therefore be part of a signalosome, co-localisation IFAs were performed. The images obtained indicated that PfAKAP and PfPDEβ-HA do not co-localise.
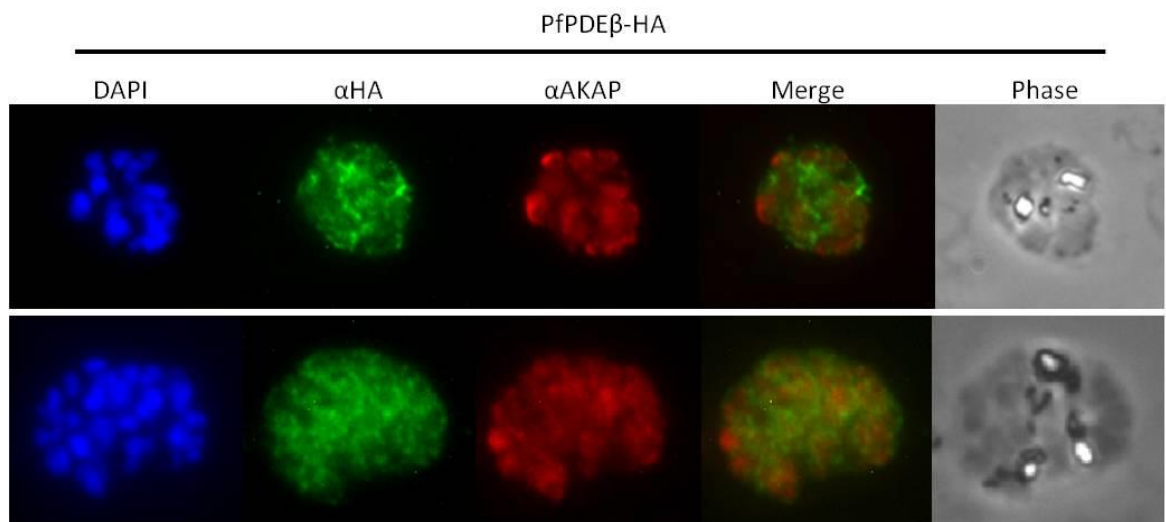
Figure 4.8 PfPDEβ-HA does not colocalise with PfAKAP
Representative images of formaldehyde fixed thin smears of PfPDEβ-HA parasites, probed with rat anti-HA monoclonal antibody (green) and anti-PfAKAP (red). Parasite nuclei are stained with DAPI (blue, first column) and brightfield images are shown on the right.

4.2.5 Screening of antipeptide antibodies against PDEα and PDEβ

Antipeptide antibodies were generated by Cambridge Research Biosciences, commissioned by Pfizer, as described in chapter 2.3.1. To determine the specificity of each purified antibody, the following schemes were applied. For both PDEα and PDEβ, the antibodies were screened initially by IFA and then by western blotting. IFAs were performed as the initial screen as they require much less antibody. The immunogenicity of the pre-bleed, final bleed serum and final bleed affinity purified antibodies was assessed. IFAs were used to test whether the antibodies were reactive and western blotting can determine if they are specific and react with band of the size predicted for each PDE. Anti-PfPDEα was also tested on the PDEα-KO line to look for the loss of detection. Anti-PfPDEβ was also tested on PfPDEβ-HA to determine co-localisation and similar western blotting pattern (with a slight size difference between WT and PfPDEβ-HA parasites relating to the epitope tag). Figures 4.9 and 4.10 outline the screening scheme in more detail.
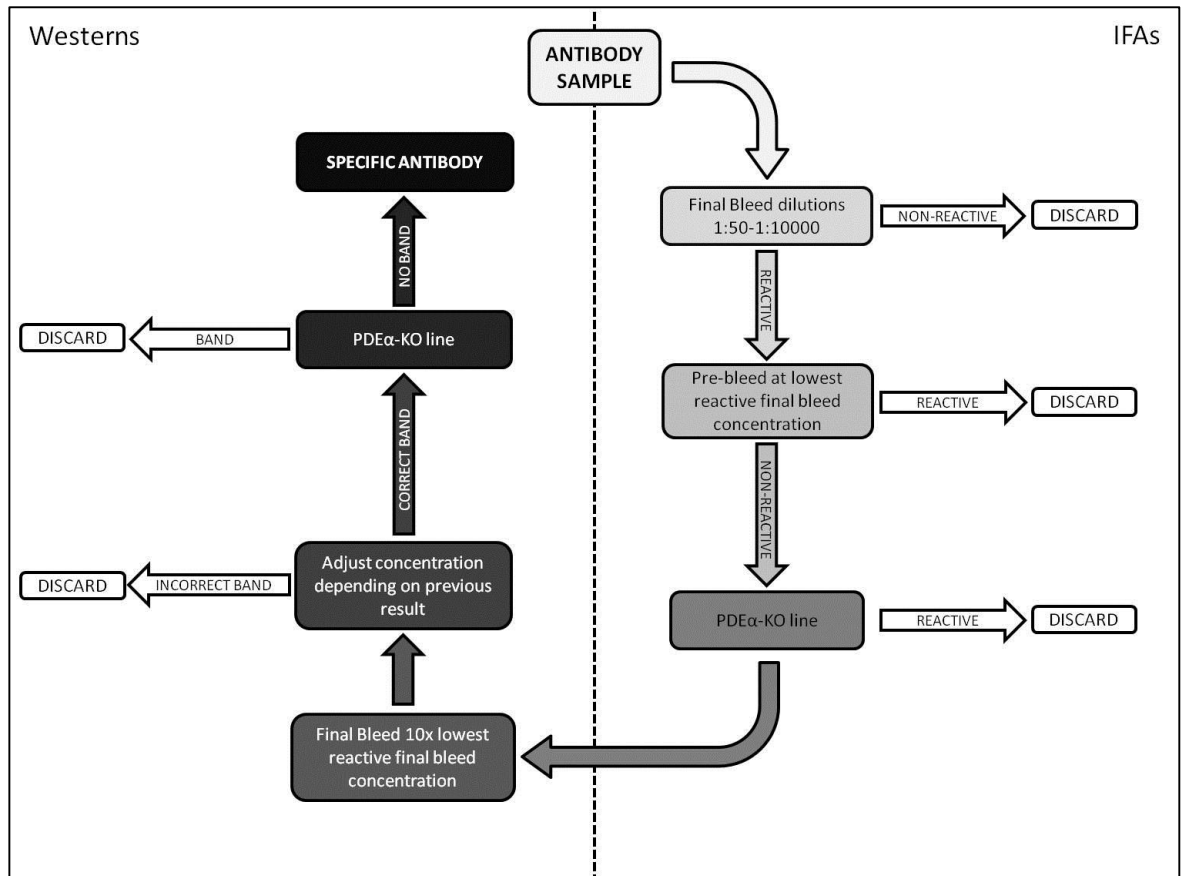
Figure 4.9 Anti-peptide antibody screening strategy for anti-PfPDEα
Initially the final bleed antibodies (sera and affinity purified) were screened by IFA at four different dilutions (1:50, 1:100, 1:2500 and 1:10000). The lowest reactive concentration was then used to screen the pre-bleed serum samples. If the pre-bleed was negative, the samples were then screened on the PDEα-KO line. The PDEα-KO parasites should not react with the antibodies. The samples were then screened by western blotting, initially at 10x the lowest relative final bleed concentration, for example if 1:50 was the lowest reactive concentration by IFA, a 1:500 dilution of the antibody was used for western blotting as it is a more sensitive technique. This concentration was then adjusted as necessary. If a band of the correct size was visualised, the antibody was also tested on the PDEα-KO line.

Westerns   **IFAs**

ANTIBODY SAMPLE

SPECIFIC ANTIBODY

CORRECT BAND

DISCARD ← INCORRECT BAND — PDEβ-HA

CORRECT BAND

DISCARD ← INCORRECT BAND — Adjust concentration depending on previous result

Final Bleed 10x lowest reactive final bleed concentration

Final Bleed dilutions 1:50-1:10000 — NON-REACTIVE → DISCARD

REACTIVE

Pre-bleed at lowest reactive final bleed concentration — REACTIVE → DISCARD

NON-REACTIVE

PDEβ-HA colocalisations — NO COLOCALISATION → DISCARD
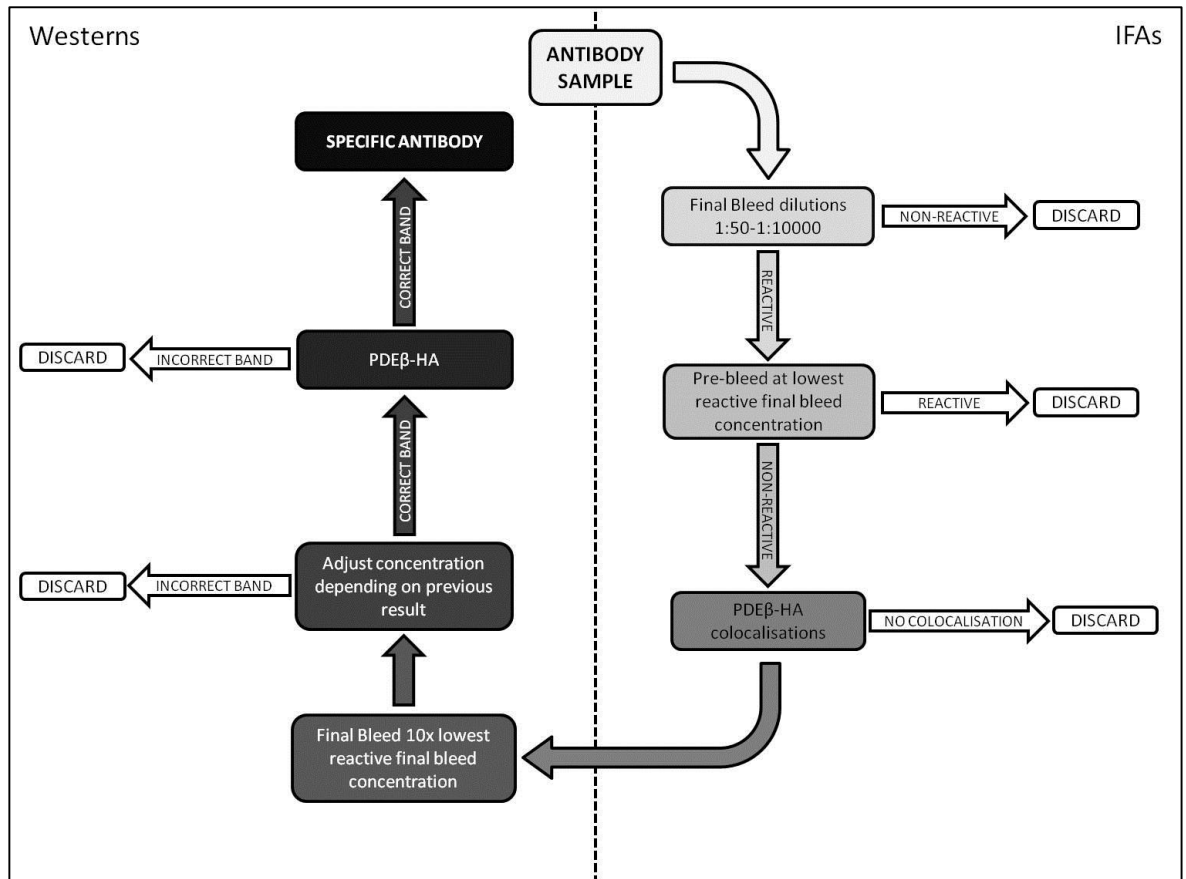
Figure 4.10 Anti-peptide antibody screening strategy for anti-PfPDEβ
Initially the final bleed antibodies (sera and affinity purified) were screened by IFA at four different dilutions (1:50, 1:100, 1:2500 and 1:10000). The lowest reactive concentration was then used to screen the pre-bleed serum samples. If the pre-bleed was negative, the samples were then screened on the PDEβ-HA line. The PDEβ-HA staining should co-localise with the antipeptide antibody. The samples were then screened by western blotting, initially at 10x the lowest relative final bleed concentration, for example if 1:50 was the lowest reactive concentration by IFA, a 1:500 dilution of the antibody was used for western blotting as it is a more sensitive technique. This concentration was then adjusted as necessary. If a band of the correct size was visualised, the antibody was also tested on the PDEβ-HA line, looking for a slight shift in size, corresponding to the epitope tag.

In total, 12 anti-peptide antibodies were screened using the above scheme, eight for PDEα (two peptides each in two rabbits, each with two elution techniques) and four for PDEβ (one peptide each in two rabbits, each with two elution techniques). Table 4.1 summarises the screening results. Generally there was no difference between the TEA (T) and glycine (G) affinity purification elution buffers or the response of the individual rabbits to the same peptide. For PDEα, peptide α3 was not reactive by IFA for either of the two rabbits by both elution buffers, even at a concentration of 1:50 (figure 4.11, upper panel). In some cases, proteins that are not detectable by IFA can still be identified by western blotting. In IFAs the protein is in its native conformation, some epitopes will be hidden or in a conformation that is significantly distinct from the linear peptide used for immunisation. The antibody may be unable to bind these epitopes, resulting in no signal in an IFA. When the protein sample is run on a reducing SDS-PAGE gel, the SDS and β-mercaptoethanol in the sample buffer will denature the protein and the linear polypeptide will be probed, resulting in a greater chance of detection. This is particularly important in anti-peptide antibodies where a short linear peptide is used to elicit an immune response. Therefore, samples 4608 and 4609 were also tested by western blotting, however the antibodies were also non-reactive. Samples from peptide α3 were not tested further. The second PDEα peptide, α4 was reactive at a dilution of 1:100, additionally the pre-bleed sera was not reactive at this concentration suggesting a specific response to the immunisation. The antibody reacted relatively strongly with what appears to be haemozoin crystals or the food vacuole in schizonts, but there was also a more diffuse staining pattern throughout the rest of the infected erythrocyte (figure 4.11, middle panel). Unfortunately the antibody was also reactive to the PDEα-KO parasite line, with the same localisation, therefore samples from peptide α4 were not tested further. The PDEβ peptide, β4 was reactive at a dilution of 1:100 by IFA. The pre-bleed was not reactive at this concentration. Co-localisation IFAs were performed with the PDEβ-HA parasite line. PDEβ-HA did not colocalise with any of the antibody samples. The staining pattern from all of the PDEβ anti-peptide antibodies was generally associated with the merozoite surface (figure4.11, lower panel). This staining pattern could be a result of the antibodies cross reacting with proteins in the parasitophorous vacuole, merozoite surface, or inner membrane complex. Pre-segmentation schizonts did not stain strongly. To confirm that the β4 peptide staining was not due to PDEβ, and to rule out the unlikely possibility that the epitope tag on the PDEβ-HA resulted in a change in localisation, western blotting with one of the samples, 4606, was performed on WT parasites. If the antibody was detecting PDEβ, a band of about 133 kDa should react with the antibody, if the antibody is cross-reacting with a different protein, the band is likely to be a different size. Only an antibody

dilution of 1:500 resulted in a distinct band. The pre-bleed was not reactive at this concentration. PDEβ is predicted to be 133 kDa, unfortunately the band detected was about 150 kDa, too large to be PDEβ (figure 4.12), however it would be beneficial to repeat with a PDEβ-HA control. This was therefore assumed to be a cross reaction with another protein. Samples from peptide β4 were not tested further.

	Peptide	Sample Number	Elution Method	IFA			Western		
				Final Bleed Concentration	Pre-bleed reactive?	PDEα-KO reactive?	Final Bleed Concentration	Pre-bleed reactive?	PDEα-KO reactive?
PDEα	α3	4608	T	Not reactive			Not reactive		
			G	Not reactive			Not reactive		
		4609	T	Not reactive			Not reactive		
			G	Not reactive			Not reactive		
	α4	4668	T	1:100	No	Yes			
			G	1:100	No	Yes			
		4669	T	1:100	No	Yes			
			G	1:100	No	Yes			

	Peptide	Sample Number	Elution Method	IFA			Western		
				Final Bleed Concentration	Pre-bleed reactive?	PDEβ colocalisation?	Final Bleed Concentration	Pre-bleed reactive?	Correct Size?
PDEβ	β4	4606	T	1:100	No	No	1:500	No	No
			G	1:100	No	No	1:500	No	No
		4607	T	1:100	No	No			
			G	1:100	No	No			

Table 4.1 Summary of the results of the anti-peptide antibody screening
The two PDEα peptide antibodies are shown in the first table. Rabbits 4608 and 4609 were immunised with peptide α3 and rabbits 4668 and 4669 were immunised with peptide α4. The PDEβ peptide antibody is shown in the lower table. Rabbits 4606 and 4607 were immunised with peptide β4. Two elution buffers were used for affinity purification for each rabbit final bleed, TEA (T) and glycine (G).
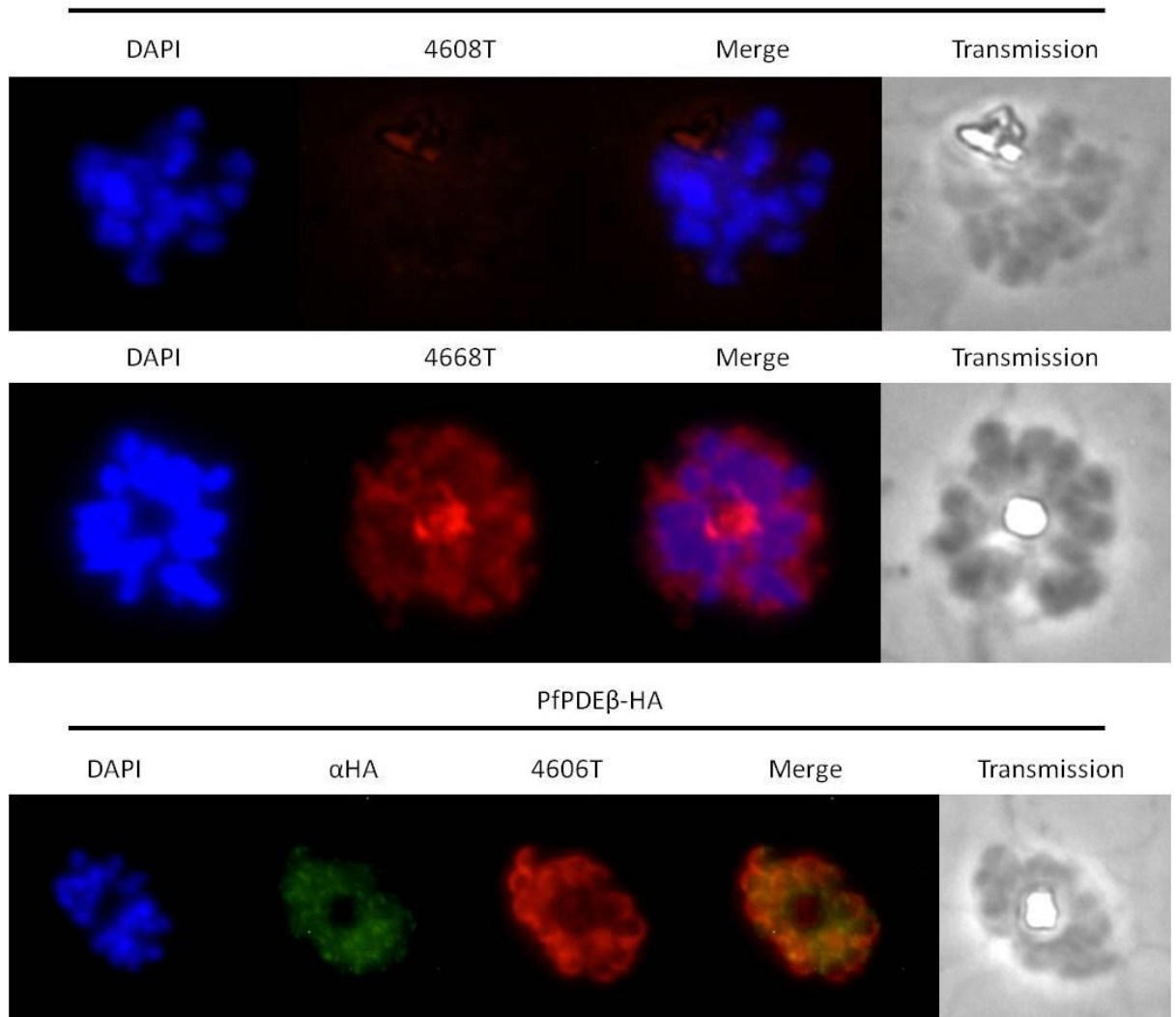
Figure 4.11 Example images of the anti-peptide antibody screening
Representative images of formaldehyde fixed thin smears of 3D7 and PfPDEβ-HA parasites, probed with anti-peptide antibodies (red) and rat anti-HA monoclonal antibody (green). Parasite nuclei are stained with DAPI (blue, first column) and bright field images are shown on the right. One image from each peptide, the final bleed with TEA as the elution buffer, is shown. The top panel shows peptide α3, sample 4608 (1:50), which was non-reactive. The middle panel shows peptide α4, sample 4668 (1:100), which also reacted to the PDEα-KO line. The lower panel shows peptide β4, sample 4606 (1:100), which did not co-localise with PDEβ-HA.
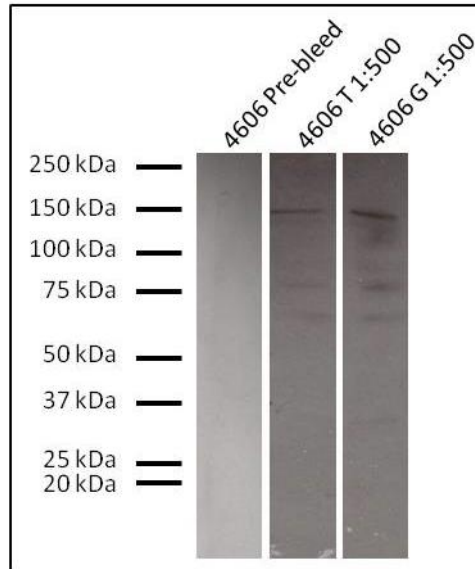
Figure 4.12 Anti-peptide antibody sample 4606 is not specific for PDEβ
An example western blot of 3D7 whole parasite lysates probed with anti-peptide antibodies. The first column was probed with the 4606 pre-bleed sample at a 1:500 dilution. The second column was probed with the 4606 affinity purified, TEA elution buffer at a 1:500 dilution. The third column was probed with the 4606 affinity purified, glycine elution buffer at a 1:500 dilution.

4.3 Discussion

4.3.1 Temporal expression of PfPDEβ-HA

All four PfPDEs contain multiple predicted TM domains and there are several studies confirming the presence of cyclic nucleotide hydrolytic activity in the membrane fraction of whole parasite lysates (Taylor et al. 2008; Wentzinger et al. 2008; Ross Cummings, Thesis). However, there is currently no published evidence to confirm the presence of PDEβ in parasite membranes. Using PfPKG as a cytosol and peripheral membrane control, and PfGAP45 as an integral membrane fraction control, the solubility of PDEβ was investigated. PKG is found primarily in the cytosol fraction of parasite lysates. There is some PKG membrane association (50% in late schizonts) as a carbonate extraction, to solubilise peripheral membrane proteins, is required to completely extract the protein (Hopp et al., 2012). As expected, PKG was mostly found in the cytosol (S1) fraction of the sequential extraction assay. PfGAP45 resides in the parasite IMC and is associated with the parasite membrane via N-myristoylation and palmitoylation motifs (Rees-Channer et al., 2006). PfGAP45 was extracted partially in the S1 fraction, but also in the membrane S2 fraction. Triton X-100, used in the S2 extraction, is a non-ionic surfactant detergent used to solubilise integral membrane proteins. PDEβ-HA was extracted exclusively with the membrane extraction (S2) suggesting that it is an integral membrane protein. The predicted TM domains, previous evidence for PDE activity in the membrane fraction of parasite lysates and the presented solubility data confirms that PDEβ is located in the parasite membrane. To add weight to the solubility assay results, the fractions could also be probed with an antibody against a protein with transmembrane spanning domains. The anti-plasmepsin V (PMV) antibody would be ideal as it is also a TM domain protein located in the parasite ER.

Expression data for PDEβ has so far relied on mRNA transcript level data, which can differ from the stage specific expression of the actual protein. In asexual blood stages, PDEβ mRNA peaks in late trophozoites and schizonts (López-Barragán et al., 2011). Additionally, PDE activity, especially cAMP hydrolytic activity, peaks in schizonts stages (Ross Cummings, Thesis). To determine for the first time when PDEβ is expressed at the protein level and to compare this with the stage specificity of cyclic nucleotide hydrolytic activity, time course western blotting and IFA experiments were performed on the PfPDEβ-HA parasite line. Initially, samples for western blotting were taken at three timepoints over the 48 hour parasite lifecycle to get a broad picture of expression. As predicted from the mRNA data, PfPDEβ-HA was not expressed in ring stages, with expression rising in trophozoites and peaking in schizont stages. PKG

expression was used as a control. PKG detection by western blotting is considerably easier than for PfPDEβ-HA. A much higher antibody concentration and a significantly longer exposure time is needed for a signal to appear for PfPDEβ-HA, compared to both the PKG antibody and the PKG-HA tagged line (data not shown), this could reflect lower abundance of the protein, however, PfPDEβ-HA degrades very easily. A high concentration of protease inhibitors present at all times in the sample is necessary to obtain a clear band. For these reasons, it is difficult to compare PfPDEβ-HA and PKG levels by western blotting, however it is clear that PfPDEβ-HA peaks in schizont stages. For a more focused view of expression, IFAs were performed on the various lifecycle blood stages, concentrating on late trophozoites and schizonts, and images were taken to cover the whole 48 hour cycle. As expected, rings and early trophozoites had very little protein expression. After the initiation of schizogony, the levels of PfPDEβ-HA increased, appearing as a diffuse mottling throughout the iRBC, with intense focal points of fluorescence. As the schizonts matured and segmentation of the merozoites occurred, the pattern changed to a more evenly distributed pattern of protein, distinct from the nuclei. The patches of fluorescence then decreased, both in intensity and size until the merozoites ruptured and there was no visible PfPDEβ-HA. The IFAs corresponded well to the western blot data and mRNA transcript data, however, it could be beneficial to perform a time course western blot on highly synchronised late stage parasites, with samples taken at closer intervals to confirm that the level of PfPDEβ-HA reduces in very late, segmented schizonts and merozoites. Previous work in this group has shown that ring stage parasites have PDE activity (Ross Cummings, Thesis). This activity is predominantly cGMP and the PfPDEβ-HA expression data adds weight to the hypothesis that this is PDEα activity. An interesting point to note about figure 4.2 is that the band for PDEβ appears to be a double band. This is most noticeable in the trophozoite stage band. PDEβ is annotated as highly phosphorylated in PlasmoDB, it is possible that the two bands are different phosphorylation states. For future work it would be interesting to treat the samples with a phosphatase to see if this is indeed the case.

4.3.2 Spatial expression of PfPDEβ-HA

As mentioned above, PfPDEβ-HA IFAs have an interesting pattern of fluorescence that changes over the course of schizogony. Pre-segmentation schizonts have dense focal points of fluorescence, with punctate staining throughout the rest of the iRBC. In segmented schizonts, the fluorescence pattern is more diffuse, and surrounds the merozoites. It is not known whether this change in pattern was due to an active change in localisation of the protein or architectural rearrangements during segmentation. Colocalisation IFAs have shown that PfPDEβ-HA and

PfBiP strongly overlap. PfBiP is located in the lumen of the endoplasmic reticulum (ER) of the parasite.

The endoplasmic reticulum is essential for protein transport in all eukaryotic cells, as well as being the main intracellular calcium store. Protein transport involves precursor polypeptides that contain an amino-terminal signal peptide, as well as cytosolic and ER transport components. Transport into the ER can occur either cotranslationally or posttranslationally. BiP is a heat-shock protein 70 (Hsp70) –type molecular chaperone, located at the luminal face of the ER (Dudek et al., 2014). BiP pulls proteins, posttranslationally into the ER via the ER translocator and distinguishing incorrectly folded proteins, preventing aggregation and further transport through the Golgi (Alberts et al., 2002). Plasmodia also contain BiP which is located in the ER lumen (Kumar et al., 1991).

PfPDEβ-HA and PfBiP co-localisation was consistent throughout the schizont stages. It is therefore likely that the apparent change in staining pattern is rearrangement of the ER rather than relocation of PfPDEβ-HA in very late schizonts. In the mid-schizont stage, the ER comprises an extensive network of reticulated branches extending through the cytosol. In late schizonts, the ER fragments, forming crescent shaped organelles in each merozoite (van Dooren et al., 2005). This is consistent with the morphology seen with PfPDEβ-HA IFAs. PfPDEβ-HA staining was distinct from all other cellular organelles tested by protein co-staining, including the Golgi marker ERD2, suggesting that PfPDEβ-HA does not get transported via the ER, but is a fundamental component. A notable point for the PfPDEβ-HA and PfBiP co-staining is that, unlike all other IFAs, a mouse anti-HA monoclonal antibody was used instead of the usual rat anti-HA antibody. This was due to the fact that the PfBiP antibody was raised in rat and an anti-rat secondary antibody was necessary to stain for BiP, precluding its use for PfPDEβ-HA. The mouse anti-HA antibody was tested on WT parasites by IFA and both WT and PfPDEβ-HA parasites by western blotting and although highly sensitive for the HA tag, it is less specific than the rat anti-HA antibody (data not shown). Therefore, other lines of evidence were pursued to further explore the potential ER localisation of PfPDEβ-HA. Firstly, there is the evidence that prior to segmentation and formation of the merozoite IMC and surface membranes, PfPDEβ-HA and MSP-1 co-localise. Post-segmentation, MSP-1 is located on the outer surface of the merozoites, leading to staining defining the membranes surrounding the daughter cells, the 'bunch of grapes' phenotype (Child et al., 2010). Before reaching their final locations, MSP-1 is presumably trafficked through the ER, during which co-localisation with PfPDEβ-HA occurs (figure 4.6). Secondly, an experiment using ER-tracker was performed. ER-Tracker™ Blue-White DPX (Life

Technologies), a low toxicity, highly specific ER stain. ER tracker is primarily used as a live cell stain, however due to the lack of a PfPDEβ-GFP tagged line, ER tracker loaded parasites were fixed with formaldehyde and stained with rat anti-HA antibodies. As a result, the signal was very weak, both with the ER stain and with the anti-HA staining, however, there was clear overlap between the staining patterns. These three line of evidence, PfBiP co-localisation, MSP1 co-localisation during ER trafficking and ER tracker co-localisation, are strong evidence for PfPDEβ-HA residing within the ER. To provide more evidence for this result, it might be beneficial to perform a full timecourse with PfPDEβ-HA and PfBiP co-staining IFAs to confirm co-localisation throughout the time that PfPDEβ-HA is expressed. It would also be worthwhile to produce a PfPDEβ-GFP tagged line to allow more accurate ER-tracker, live staining experiments. Co-staining with a second ER marker, such as plasmepsin V, ideally not raised in a rat, would also be an important future experiment. It would also be highly beneficial to produce an antibody against the native PDEβ to allow staining of WT parasites and other parasite lines, such as the PDEα-KO line. This would be important to determine conclusively that the epitope tag of PfPDEβ-HA is not resulting in mis-localisation of the parasite. As the parasite line is viable, with no growth defect, it is unlikely that this would be the case. The functional significance of PfPDEβ-HA residing in the ER is unknown.

In many other organisms, signalling molecules form complexes, termed signalosomes, to allow efficient responses to cellular stimuli. By homology detection, a putative AKAP has been identified in *P. falciparum*. However, PfAKAP and PfPDEβ-HA do not colocalise, suggesting that they do not form a complex. As PKG does not reside in the ER, PfPDEβ-HA is unlikely to form a complex with PfPKG either (Hopp et al., 2012). For future work it would be beneficial to investigate interaction between PfPDEβ-HA and PfPKA using a PKA specific antibody. To further investigate PfPDEβ-HA binding partners, immunoprecipitations could be performed, using mass spectrometry to identify the proteins that are co-precipitated. An initial screening immunoprecipitation and subsequent western blotting has shown that PKG is not pulled down with PfPDEβ-HA immunoprecipitation (Oriana Kreutzfeld, LSHTM, MSc Project).

4.3.3 Antipeptide antibodies against PfPDEα and PfPDEβ

Twelve anti-peptide antibodies against two PDEα and one PDEβ peptides, raised in rabbits using a commercial system, were screened by IFA and western blotting. Anti-peptide antibodies were used due to the difficulties encountered by several groups to express recombinant PDE proteins. The peptides were derived from the predicted catalytic domains of the proteins, in regions predicted to be immunogenic. One immunisation and four booster injections were performed as part of the commercial package. The pre-bleed, final bleed and affinity purified antibodies were analysed. The elution of a protein from an immobile ligand (in this case the initial peptide), involves dissociation and recovery of the target molecule using a specific buffer. For elution of the anti-peptide antibodies, buffers of extreme pH were used, TEA at pH 11.5 and glycine at pH 2.5-3.0. However, there was no difference between the sensitivity or specificity of the buffers by IFA or western blotting. The antibody based on the PDEα peptide α3 was non-reactive by IFA and western blotting, even at a dilution of 1:50. The antibody based on the PDEα peptide α4 was also reactive with the PDEα-KO line, implying the antibody was not specific to PDEα. The antibody based on the PDEβ peptide β4 was highly reactive with schizont stages and the pre-bleed sera was non-reactive, however when co-staining was performed with PDEβ-HA, there was no colocalisation, implying that the antibody was not specific to PDEβ. To confirm this result, western blotting was performed which gave a band of approximately 150 kDa, which is too large to be PDEβ (133 kDa), although this would need to be confirmed using the PDEβ-HA line as a positive control.

There has been a previous attempt to generate an anti-peptide antibody against PDEβ using N-terminal peptide sequences by Ross Cummings. Unfortunately the pre-bleeds were quite reactive and there was therefore high background in the final images. Additionally, western blots with the antibody gave a band of around 50 kDa, too small to be PDEβ. It was hypothesised that the final IFA images could show an ER localisation, however in the absence of co-localisations, an incorrectly sized western blot band and a high IFA background, it is unlikely that the antibody was specific to PDEβ (Ross Cummings, Thesis).

Thus far, there has been no antibody produced that is specific to any of the native PfPDEs and all attempts to generate useful anti-peptide antibodies have failed. To improve the likelihood of generating specific antibodies, immunisation with recombinant protein would be ideal. Generation of recombinant proteins will be discussed in more detail in chapter six.

Chapter 5: Investigation of the effects of human phosphodiesterase inhibitors on *P. falciparum*

5.1 Introduction

Phosphodiesterase inhibitors have long been utilised in various studies on *Plasmodium* parasites. In 1978, Martin et al. found that addition of the human PDE4 inhibitor etazolate (SQ-20,009, cGMP specific) and the broad spectrum human PDE inhibitor caffeine, as well as a membrane permeable cAMP derivative (8-bromo-cAMP), could stimulate gametogenesis in the chicken *Plasmodium*, *P. gallinaceum* (Martin et al., 1978). This observation was duplicated in 1982 where caffeine was also shown to enhance gametocytogenesis at 2 mM in *P. falciparum* (Brockelman, 1982). Additionally, the gametogenic property of 8-bromo-cAMP (1 mM) was also duplicated in a 1989 study (Trager and Gill, 1989). Another broad spectrum PDE inhibitor, IBMX (0.5 mM), was found to enhance exflagellation of male gametes in both *P. falciparum* and *P. berghei* (Kawamoto et al., 1990). However, these studies were concentrated on improving the numbers of parasites switching to gametocytes in culture rather than investigating the role of the PDE enzymes themselves in the life cycle of the parasites.

Ross Cummings, a previous PhD student in the Baker group at LSHTM in 2005, focused on the PfPDEs. Several commercial human PDE inhibitors were tested in PDE assays performed on parasite lysate, including IBMX, caffeine and etazolate. However, IBMX and caffeine had little or no effect on PDE activity on any parasite stage, with IC50 values over 200 µM. This calls into question the interpretations made in earlier studies and suggests that specific inhibition of PDE activity may not be responsible for gametogenesis and that other targets may be involved. However some of the earlier work was on *P. gallinaceum* and may represent different inhibitor sensitivities between *Plasmodium* species. The study by Ross Cummings found that dipyridamole (human PDE 5 and 6 specific, cGMP) and etazolate hydrochloride (human PDE4 specific, cAMP) were found to be the most potent compounds and able to inhibit both cAMP and cGMP PDE activity with IC50 values of around 6 and 20 µM, respectively, using asexual blood stage lysates. However, in sexual stages, the compounds were relatively ineffective (>200 µM). The most effective inhibitor tested, and that had activity on both asexual blood stage and gametocytes, was zaprinast. Zaprinast had IC50s of about 12 µM on schizont cAMP hydrolytic activity, 3 µM on schizont cGMP hydrolytic activity and 33 µM stage V gametocyte cGMP hydrolytic activity in the membrane fraction of the parasite lysates. Zaprinast also inhibited ring

stage cGMP hydrolytic activity at an IC50 of about 3.5µM. Zaprinast was therefore the most potent, PfPDE inhibitor tested (Ross Cummings, Thesis).

Zaprinast (previously known as M&B 22948) is a competitive inhibitor of mammalian PDE5 and was originally synthesised as an anti-allergy compound for allergic asthma (Broughton et al., 1974). It was subsequently found to cause vasodilatation and smooth muscle relaxation via nitric oxide induced cGMP production (Gibson, 2001; Merkel et al., 1992). It was also noted that zaprinast treatment facilitated penile erection, which subsequently lead to the development and introduction of a second PDE5 inhibitor, sidenafil citrate, also known as Viagra™(Boolell et al., 1996).

In the two PDEα papers by Yuasa et al. 2005, and Wentzinger et al. 2008, a series of inhibitors were tested on parasite growth, parasite lysates and on recombinant protein. In keeping with data from Ross Cummings, zaprinast was found to be the most potent inhibitor of all three. The EC50 in a *P. falciparum* blood stage growth inhibition assay was 35 µM, the IC50 of zaprinast on PDE activity in parasite lysates was 4.1 µM (Yuasa et al., 2005) and about 3.4 µM on recombinant protein (Wentzinger et al., 2008), which compares quite well with the values obtained by Ross Cummings (thesis). This is about 10 times higher than the expected IC50 on the target hPDE5 (Gibson, 2001). Zaprinast is also able to stimulate rounding up of stage V gametocytes in the absence of XA and in a non-permissive pH, and male gamete exflagellation (McRobert et al., 2008). Recent work has also shown that zaprinast is able to induce egress of blood stage schizonts in a PKG-dependent manner. Addition of 75 µM of zaprinast was able to promote microneme and exoneme discharge, even in unsegmented schizonts, and lead to the premature release of non-invasive merozoites (Collins et al., 2013a).

As part of this project, a small panel of phosphodiesterase inhibitors was provided by Pfizer as a collaborative venture to help address the suitability of malaria PDEs as novel targets for antimalarial drug discovery. Fourteen novel compounds from various development series, as well as eight commercially available compounds including zaprinast were provided. The structures and original human PDE target of the Pfizer compounds were unknown. The names and structures of the commercially available compounds are shown in table 5.1
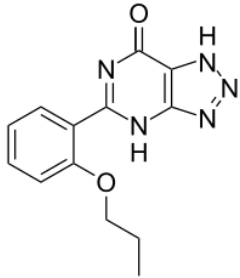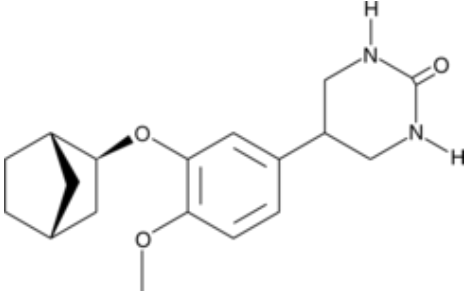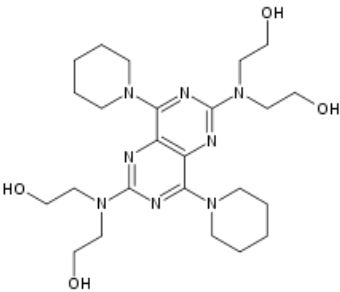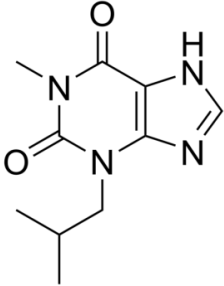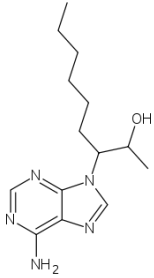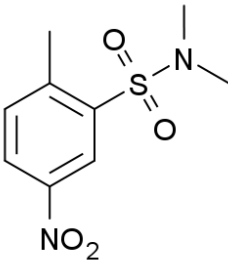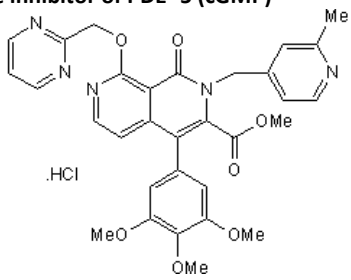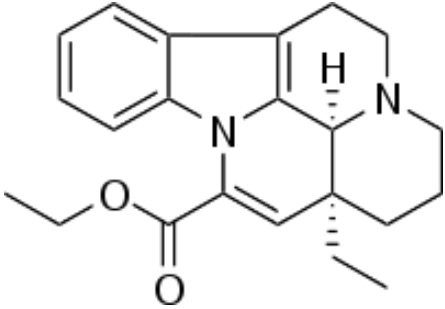
Zaprinast: 5-(2-Propoxyphenyl)-1*H*-[1,2,3]triazolo[4,5-d]pyrimidin-7(4*H*)-one **Selective inhibitor of PDE-5 (cGMP)** 	**CP 80633:** 5-[3-[(1*S*,2*S*,4*R*)-Bicyclo[2.2.1]hept-2-yloxy]-4-methoxyphenyl]tetrahydro-2(1*H*)-pyrimidinone **Selective inhibitor of PDE- 4 (cAMP)**
Dipyridamole: 2,2',2'',2'''-(4,8-di(piperidin-1-yl)pyrimido[5,4-*d*]pyrimidine-2,6-diyl)bis(azanetriyl)tetraethanol **Inhibitor of PDE-5 (cGMP)** 	**IBMX:** 1-methyl-3-(2-methylpropyl)-7H-purine-2,6-dione **Non-selective human PDE inhibitor**
EHNA Hydrochloride: *erythro*-9-(2-Hydroxy-3-nonyl)adenine hydrochloride **Adenosine deaminase inhibitor, also inhibits PDE-2 (cGMP)** 	**BRL 50481:** N,N,2-Trimethyl-5-nitro-benzenesulphonamide **Inhibitor of PDE-7 (cAMP)**
T 0156 Hydrochloride: 1,2-Dihydro-2-[(2-methyl-4-pyridinyl)methyl]-1-oxo-8-(2-pyrimidinylmethoxy)-4-(3,4,5--trimethoxyphenyl)-2,7-naphthyridine-3-carboxylic acid methyl ester hydrochloride **Selective inhibitor of PDE- 5 (cGMP)** 	**Vinpocetine:** (3α,16α)-Eburnamenine-14-carboxylic acid ethyl ester **Selective for PDE-1 (cGMP)**, also blocks voltage-gated Na⁺ channels.

Table 5.1 Commercial phosphodiesterase inhibitors

A table containing the name, structure and primary human PDE target for the eight tested commercial compounds.

5.2 Results

5.2.1 Comparison of 48 hour and 72 hour hypoxanthine growth inhibition assays for PDE inhibitors

Radiolabelled hypoxanthine uptake assays are used to rapidly evaluate the effect of inhibitors on the *in vitro* growth of *P. falciparum*. Hypoxanthine uptake is proportional to the number of parasitised RBCs present (see chapter 2.4). A standard hypoxanthine assay has a 48 hour duration, [^{3}H]hypoxanthine is added to the parasites after 24 hours and the assay is stopped after a further 24 hours. This is extremely effective for fast acting compounds that kill in ring and trophozoites stages. For slower acting compounds or compounds that act very late in the cell cycle, often a 72 hour assay is preferred. This is because the parasites incorporate the radiolabel during DNA synthesis and some drugs will inhibit the parasites growth only in late schizont stages or during invasion, post DNA replication. For example compounds that target PfPKG, delay rupture of the parasite causing a static phenotype. This only becomes cidal (resulting in parasite death) if the egress block is continued for over 6 hours (Taylor et al., 2010). A difference in growth may therefore be missed if the life cycle is extended due to the action of the compounds.
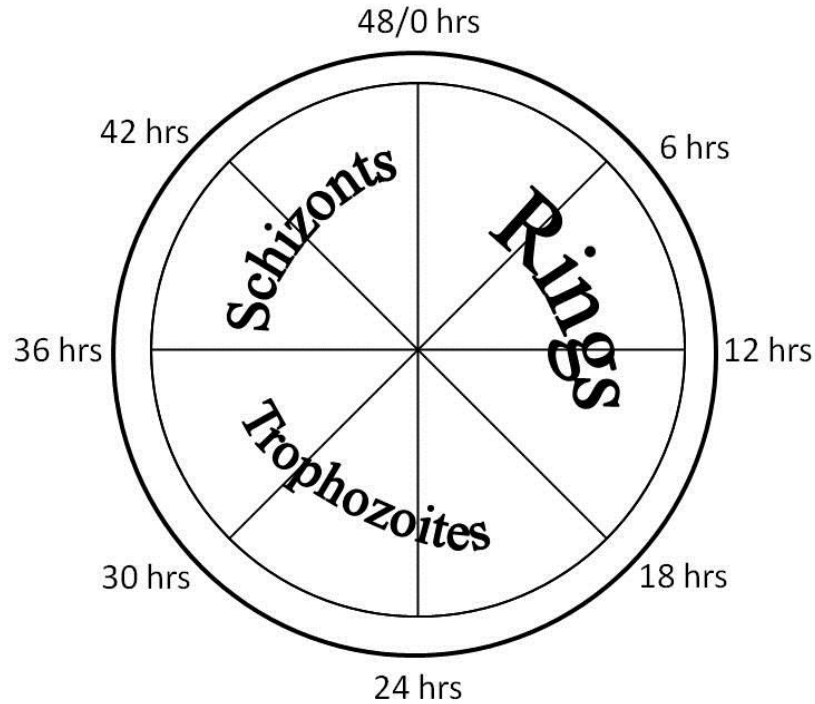
Figure 5.1 The life cycle of *P. falciparum* growth *in vitro*
The life cycle of P. falciparum is 48 hours long. Post invasion, the parasites are ring stages for about 18 hours. They then develop to trophozoites and as DNA synthesis begins, the parasites are classed as schizonts. A hypoxanthine assay is initiated when the parasites are ring stages, usually between 6 and 12 h.p.i (hours post invasion). Tritiated hypoxanthine is added at about 36 h.p.i., as the parasites start to undergo schizogony. The radiolabel will be incorporated into the parasite DNA during DNA replication. If an inhibitory compound is present that kills parasites prior to schizogony, the parasites will not be viable and will not undergo DNA replication. When the assay is stopped 24 hours later, the radiation counts will be lower, reflecting the efficiency of killing. For compounds that are active in the parasite later than schizogony, the counts are likely to be similar at 48 h.p.i. Therefore the assay is continued for a further 24 hours, allowing time for reinvasion of the parasites and the level of reinvasion will be proportional to radiation counts.

As the stage specificity of PDE inhibitors for *P. falciparum* was unknown, although hypothesised to act in schizogony based on PDE protein expression data (see chapter 4), both 48 and 72 hour assays were performed and compared. 72 hour assays were found to be significantly more reliable than 48 hour experiments, in terms of reproducibility. The IC50s of the control drugs artemisinin and chloroquine were not drastically different between the assays (figure 5.2). This is as expected as both compounds can kill the parasites pre schizogony. For the test compounds, results obtained from 48 hour assays resulted in large standard errors and confidence intervals, as well as producing higher IC50s (data shown in appendix A4). 72 hour assays gave much more reproducible results and lower IC50s (full data shown in chapter 5.2.3). Figure 5.3 (representative graph, full IC50 results shown below) shows the six Pfizer compounds with the

lowest IC50s (in both the 48 and 72 hour assays), and the difference between the 48 and 72 hour assays. The standard error of the mean (as shown by the error bars), is much higher in the 48 hour assays. Therefore, the 72 hour assay was used to determine the IC50s of all the compounds tested.
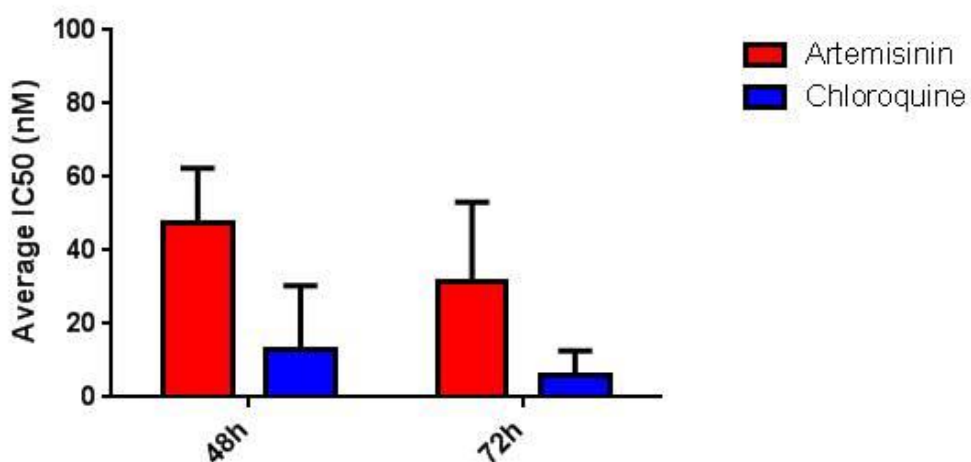
Figure 5.2 Comparison of the IC50s of the control drugs in 48 and 72 hour hypoxanthine uptake assays
The IC50s of artemisinin (red) and chloroquine (blue) are within the expected range for a hypoxanthine uptake assay. Each of the assays was performed in triplicate and the assays were repeated three times. The error bars represent the SEM.
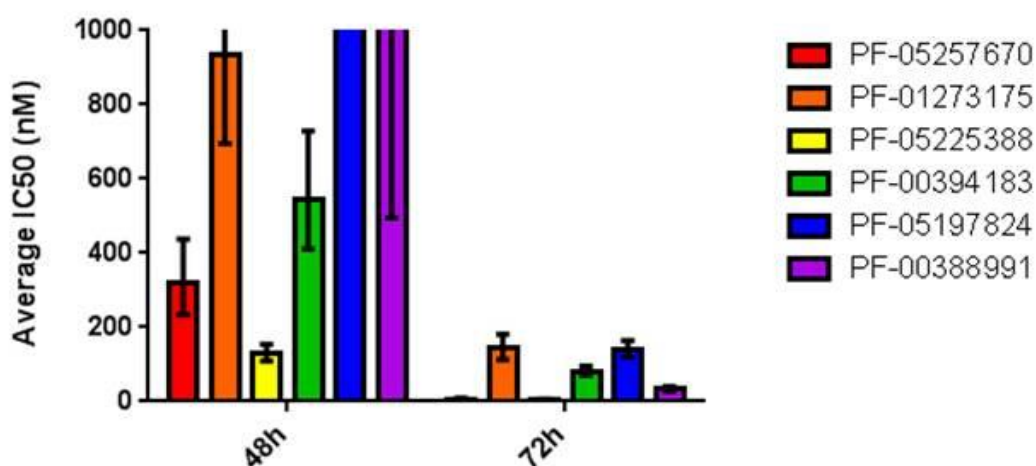
Figure 5.3 Comparison of the IC50s of six of the Pfizer compounds in 48 and 72 hour hypoxanthine uptake assays
The IC50s of six of the Pfizer test compounds for the 48 hour and 72 hour assays are shown. The IC50s are vastly lower for the 72 hour assay, with a much narrower standard error. Each of the assays was performed in triplicate and the assays were repeated three times. The error bars represent the SEM. The graph was capped at 1 µM average IC50.

5.2.3 Results of the 72 hour hypoxanthine growth inhibition assays

72 hour hypoxanthine uptake assays were performed on *P. falciparum* parasites, starting at ring stages, using the eight commercial compounds, fourteen test Pfizer compounds and the control drugs artemisinin and chloroquine. Table 5.2 and figures 5.4 to 5.7 show the average IC50s of three assays. The IC50s of the control drugs artemisinin and chloroquine fall within the expected low nanomolar range, 31 and 6 nM, respectively. The IC50 of zaprinast (26 µM) is similar to what has been reported previously. For the commercially available compounds, IMBX had an IC50 over 100 µM. CP 80633 and BRL50481 also had IC50s greater than 100 µM. EHNA hydrocholate and dipyridamole were the most potent commercial compounds (2.8 and 4.7 µM, respectively). T0156 hydrochloride and vinpocetine had IC50s of 22 and 60 µM, respectively. The IBMX and dipyridamole results are in keeping with results reported by Ross Cummings on inhibition of PDE activity on parasite lysates.

Only one of the Pfizer compounds had an IC50 over 100 µM (PF-03120399), all of the rest were below 20 µM. Seven of the compounds had IC50s in the sub-micromolar range, below 200 nM. The lowest IC50s were for compounds PF-05225388 and PF-05257670 at 5.3 and 7.5 nM, respectively, which compares well with several antimalarials currently in clinical use.

	Average IC50			SE	95% Confidence intervals		
Compound	M	µM	nM	EC50			
PF-05257670	7.47E-09	0.01	7.47	1.08	6.37	to	8.75
PF-04290541	1.03E-05	10.26	10260.00	1.08	8798.00	to	11950.00
PF-03201245	1.74E-05	17.35	17350.00	1.14	13340.00	to	22550.00
PF-03455711	6.42E-06	6.42	6416.00	1.12	5135.00	to	8017
SC-58236	7.78E-06	7.78	7778.00	1.10	6477.00	to	9341.00
PF-03204683	4.03E-06	4.03	4030.00	1.09	3390.00	to	4790.00
PF-03120399		>100					
PF-03455723	1.04E-05	10.41	10410.00	1.08	8951.00	to	12100.00
PF-01273175	1.43E-07	0.14	143.00	1.13	113.00	to	180.9
PF-05184913	1.56E-07	0.16	156.40	5.08	6.18	to	3955
PF-05225388	5.34E-09	0.01	5.34	1.06	4.74	to	6.02
PF-00394183	8.17E-08	0.08	81.73	1.08	70.04	to	95.37
PF-05197824	1.41E-07	0.14	140.50	1.08	120.40	to	163.90
PF-00388991	3.39E-08	0.03	33.86	1.10	28.22	to	40.62
Zaprinast	2.59E-05	25.90	25900.00	1.17	18920.00	to	35450.00
CP 80633		>100					
Dipyridamole	4.66E-06	4.66	4661.00	1.13	3671.00	to	5918.00
IBMX	3.32E-10	>100					
EHNA Hydrochloride	2.8E-06	2.80	2801.00	1.08	2416.00	to	3248.00
BRL 50481		>100					
T 0156 Hydrochloride	2.17E-05	21.69	21690.00	1.20	14990.00	to	31370.00
Vinpocetine	5.99E-05	59.90	59900.00	1.10	49640.00	to	72290.00
Artemisinin	3.15E-08	0.03	31.45	1.30	18.61	to	53.15
Chloroquine	5.85E-09	0.01	5.85	1.48	2.70	to	12.69

Table 5.2 Results of the 72 hour hypoxanthine uptake assay
The average IC50s of three separate assays, each performed in triplicate, are shown in µM and nM. The IC50 is the concentration of inhibitor that gave 50% growth in vitro in comparison to a no drug control. The IC50 values, the standard error of the mean and 95% confidence intervals were calculated using Prism software. >100 denotes sufficient inhibition was not observed and no IC50 could be calculated. The rows in grey are the compounds that have IC50s lower than 160 nM.
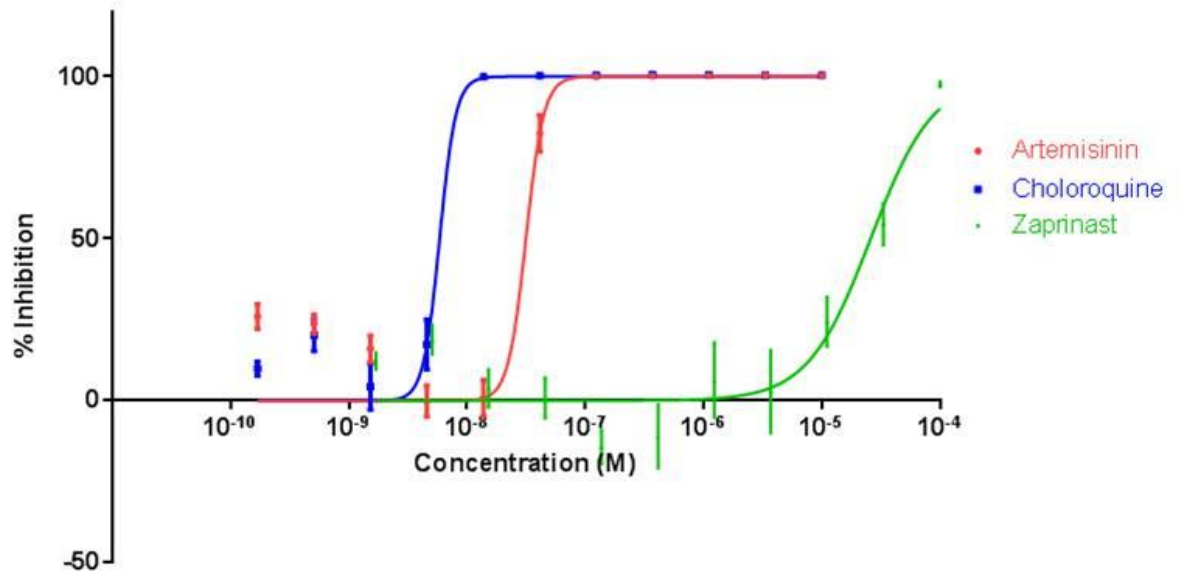
Figure 5.4 Dose-response curves of the control compounds including zaprinast in a hypoxanthine uptake assay
Inhibition profiles are displayed as percentage inhibition relative to absence of inhibitor. The data shown represents three separate assays, each performed in triplicate. Error bars represent standard error of the mean.
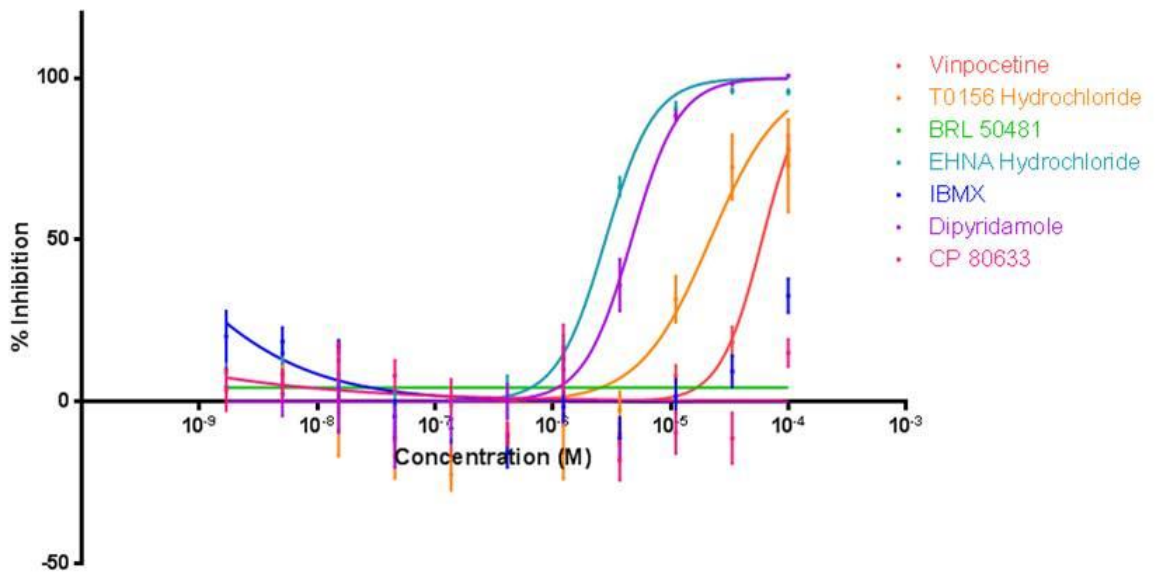
Figure 5.5 Dose-response curves of the commercial compounds in a hypoxanthine uptake assay
Inhibition profiles are displayed as percentage inhibition relative to absence of inhibitor. The data shown represents three separate assays, each performed in triplicate. Error bars represent standard error of the mean.
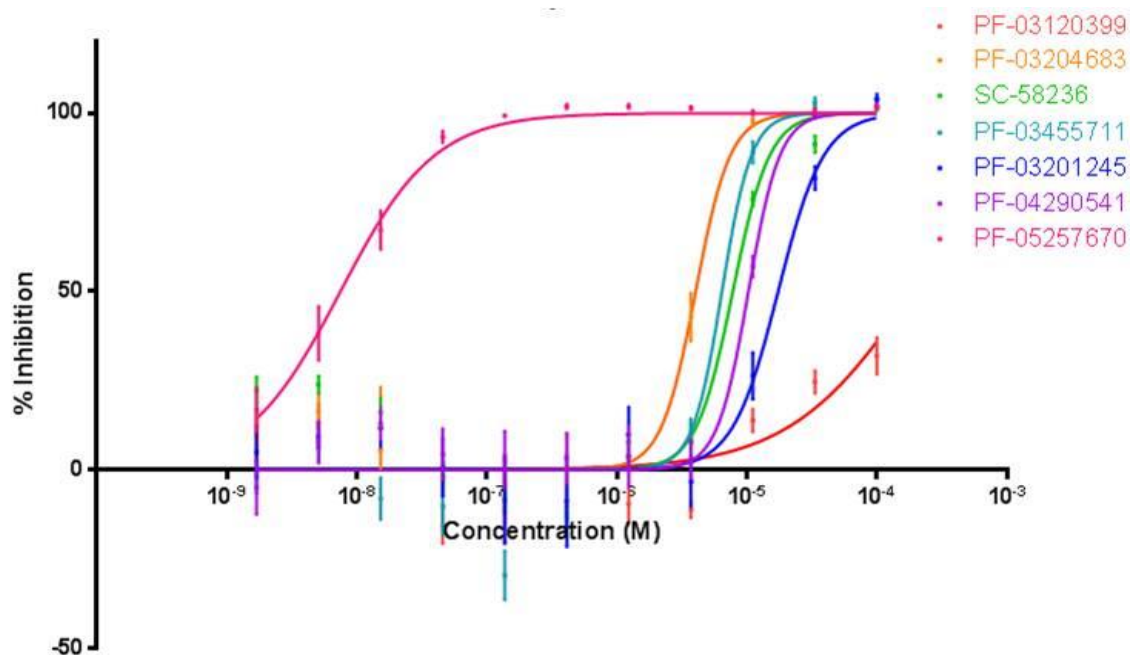
Figure 5.6 Dose-response curves of the first seven Pfizer compounds in a hypoxanthine uptake assay
Inhibition profiles are displayed as percentage inhibition relative to absence of inhibitor. The data shown represents three separate assays, each performed in triplicate. Error bars represent standard error of the mean.
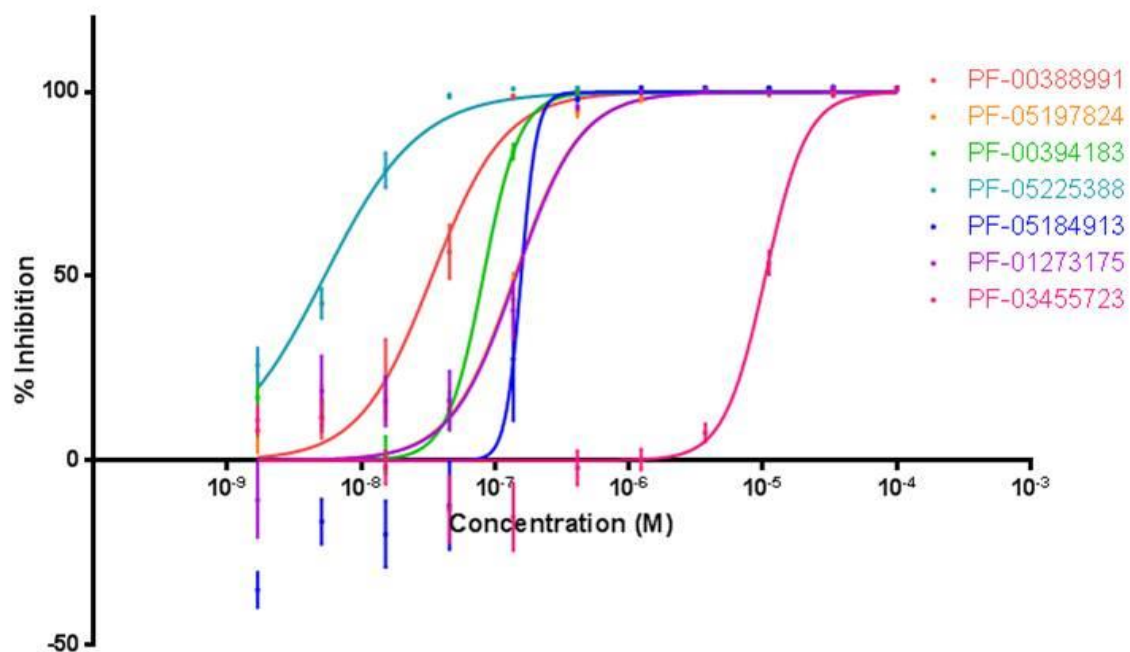
Figure 5.7 Dose-response curves of the final seven Pfizer compounds in a hypoxanthine uptake assay
Inhibition profiles are displayed as percentage inhibition relative to absence of inhibitor. The data shown represents three separate assays, each performed in triplicate. Error bars represent standard error of the mean.

5.2.4 Comparison of wild-type and PfPDEα-KO IC50s in 72 hour growth inhibition assays

mRNA expression data (PlasmoDB) indicate that PDEα and PDEβ are likely to be the two PDEs expressed during *P. falciparum* blood stage development. PDEβ has proved refractory to deletion, but PDEα has been knocked out successfully with only a subtle growth phenotype. It was of great interest to determine whether any of the Pfizer inhibitors was selective for PDEβ as it is presumed that this isoform is essential in the blood stages. To determine whether any of the compounds gave a different inhibition profile in the absence of PDEα, 72 hour hypoxanthine assays were performed on the PDEα-KO parasite line and the parental 3D7 wild type line. Using Prism software, the IC50s were calculated and a comparison between the two was performed, using the extra sum-of-squares F-test. Initially all of the compounds were tested on the PDEα-KO line and compared to the previously determined 3D7 IC50s, however it was difficult to conclude whether there was any difference between the IC50 values as the concentration range was extremely large (~100 µM to 0.1 nM, data not shown). It was there therefore decided to concentrate on the five most potent compounds and zaprinast, using a narrower concentration range in order to plot more points around the IC50. Artemisinin and chloroquine were again used as controls. Unexpectedly, artemisinin and chloroquine gave significant P values for a difference in IC50s between the two strains ($p < 0.001$ and $p = 0.002$). The IC50 for zaprinast was also significantly different between the parasite lines, $p = 0.001$. None of the five tested Pfizer compounds had a significant difference in IC50 between the strains (table 5.3 and figure 5.8), potentially suggesting that PDEα is not a primary target of the compounds. Artemisinin and chloroquine were not expected to have different IC50s as there should be no difference between the two strains, apart from the lack of PDEα and this is not a target of either of the two drugs. However, as there is a significant growth rate difference between the two strains, this could be affecting the results.

Compound	Strain	Molar		uM	nM	R^2	P Value
Artemisinin	3D7	2.11E-08		0.0211	21.13	0.84	<0.001
	PDEα-KO	3.72E-08		0.0372	37.18	0.83	
Chloroquine	3D7	1.26E-08		0.0126	12.55	0.85	0.0021
	PDEα-KO	1.49E-08		0.0149	14.90	0.86	
Zaprinast	3D7	2.77E-05		27.7200	27720.00	0.75	0.0011
	PDEα-KO	4.49E-05		44.8900	44890.00	0.87	
PF-05257670	3D7	5.31E-08		0.0531	53.10	0.83	0.2278
	PDEα-KO	4.29E-08		0.0429	42.86	0.78	
PF-05225388	3D7	9.92E-09		0.0099	9.92	0.88	0.2331
	PDEα-KO	1.16E-08		0.0116	11.57	0.88	
PF-00394183	3D7	6.64E-08		0.0664	66.38	0.85	0.7845
	PDEα-KO	6.86E-08		0.0686	68.55	0.87	
PF-05197824	3D7	4.22E-07		0.4219	421.90	0.68	0.2978
	PDEα-KO	3.59E-07		0.3585	358.50	0.68	
PF-00388991	3D7	4.35E-08		0.0435	43.51	0.93	0.5161
	PDEα-KO	4.74E-08		0.0474	47.42	0.83	

Table 5.3 Results of the 72 hour hypoxanthine assays for 3D7 and PDEα-KO parasite lines
The average IC50s of three separate assays, each performed in triplicate, are shown in µM and nM. The IC50 is the concentration of inhibitor that gave 50% growth in vitro in comparison to a no drug control. The IC50, R^2 and P values (using the extra sum-of-squares F-test) were calculated by Prism software. Significance was set at p<0.05. R^2 is the coefficient of determination, indicating how well the curve fits the data.
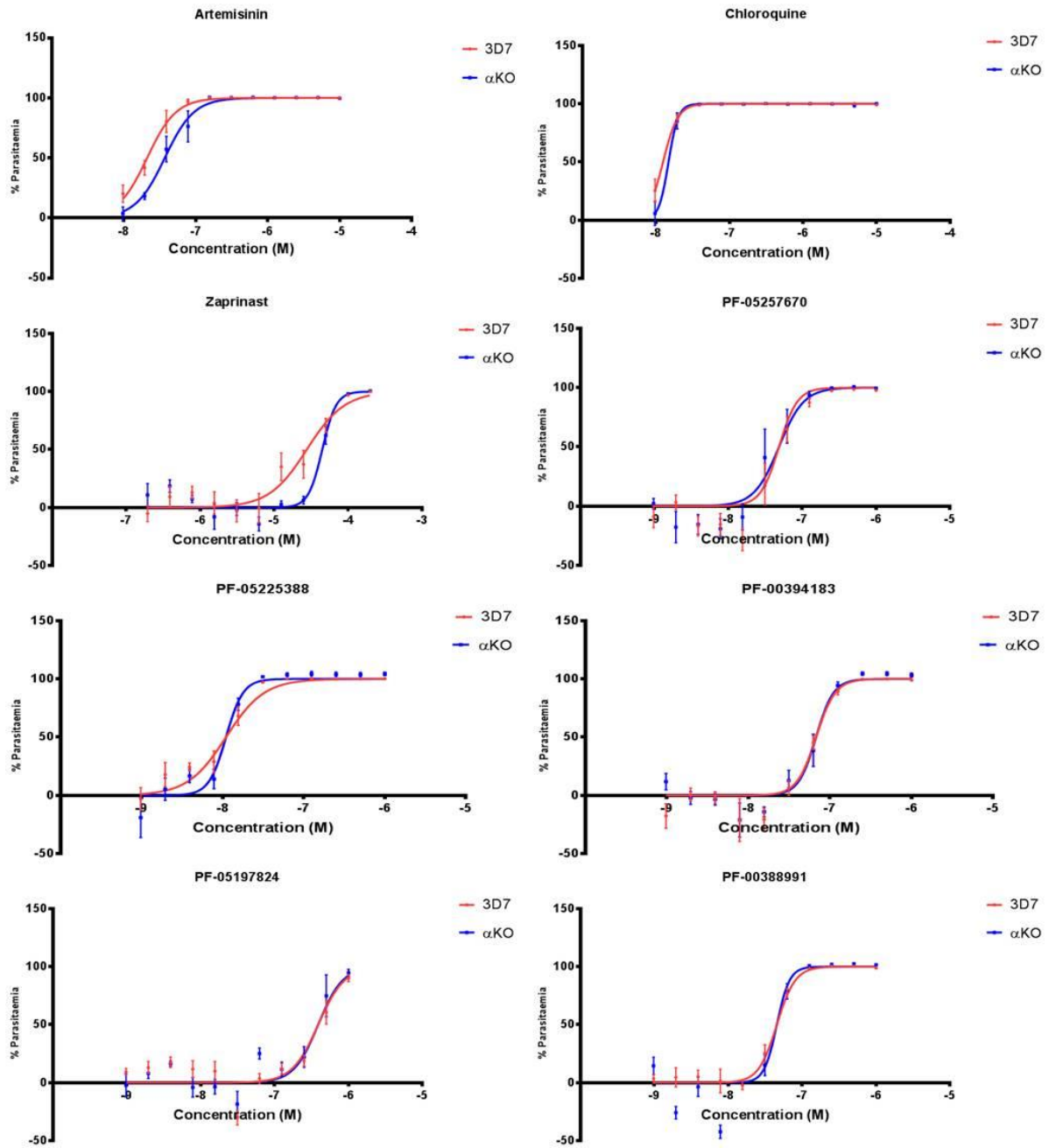
Figure 5.8 Dose-response curves of the comparative hypoxanthine uptake assays for wild type and PDEα-KO parasite lines
Inhibition profiles are displayed as percentage inhibition. Error bars represent standard error of the mean. The wild type IC50 is shown in red and the PDEα-KO is shown in blue.

5.2.5 Development of a native *P. falciparum* phosphodiesterase assay

For this project, a new PDE assay was developed, based on scintillation proximity assay (SPA) beads (Perkin Elmer). The basic protocol was adapted for *P. falciparum* from the PDE assay kit, also produced by Perkin Elmer (Catalogue nos. TRKQ 7090 and TRKQ 7100). The final protocols for the assay and parasite material preparation are described in chapter 2.5. PDE activity was monitored using a discontinuous tritium [^{3}H] based cyclic nucleotide hydrolysis assay. Native enzyme (either from parasite lysate or HA-immunoprecipitation), was incubated with radiolabelled cAMP or cGMP for one hour at 37°C. Any PDE enzyme in the sample will hydrolyse the phosphodiester bond within the cyclic nucleotide. The assay is stopped by addition of the SPA beads. The hydrolysed nucleotide is able to bind to the beads, leading to scintillation which can be measured in a scintillation counter, whereas the intact cyclic nucleotide does not bind. The PDE assay used previously in the group, based on phosphatase enzymatic cleavage of the phosphate group of the hydrolysed cyclic nucleotide and Dowex exchange resin separation, was not used due to unavailability of some of the reagents and the potentially simplified protocol of the SPA based method.

The first steps to optimise the assay used whole parasite lysates. Whole lysate was incubated in the presence or absence of 100 μM of zaprinast (zap). In the absence of the PDE inhibitor, the lysate produced high counts, indicating cNMP hydrolytic activity within the samples. In the presence of zaprinast, this activity was severely reduced, indicating that the hydrolytic activity was the result of phosphodiesterase activity. Commercial PDE enzyme extracted from bovine brain (Enzo Life Sciences) was used as the positive control, which hydrolyses both cAMP and cGMP, with a greater preference for cGMP and could be effectively knocked down with zaprinast (figure 5.9). Additionally, saponin lysed erythrocytes, treated in the same way as the parasite lysate samples, were tested and shown to contain no PDE enzyme activity (data not shown).

When designing the assay buffer for optimal PDE activity, it was necessary to include a divalent cation. All PDEs are predicted to contain two divalent metal ions, zinc and another, usually magnesium (Ke and Wang, 2007). Zn^{2+} is held in the catalytic domain by invariant residues that lead to very strong coordination of the ion. Ross Cummings investigated the effect of different divalent cations (Zn^{2+}, Mg^{2+}, Mn^{2+} and Ca^{2+}) on the PDE activity of parasite lysates. He found that it was not necessary to add zinc to the reaction, presumably due to the strong coordination of Zn^{2+} seen in crystallised PDEs, the ion remains bound to the enzyme in parasite preparations. However, recombinant PDEα requires 20 μM $ZnSO_4$ for full activity (Wentzinger et al., 2008). In an earlier study utilising recombinant PDEα, it was determined that manganese (1 mM $MnCl_2$)

161

was the most potent activator (Yuasa et al., 2005). Ross Cummings found that for whole parasite lysate, highest activity was with Mg^{2+}, followed by Mn^{2+}. Ca^{2+} was not able to support enzyme activity (Ross Cummings, Thesis). Therefore, the PDE assay buffer was supplemented with $MgCl_2$.

To further test the PDE activity assay, negative controls with no enzyme, no substrate and a blank (no enzyme or substrate) were performed. As expected these gave very low readings. The sample that contained the cyclic nucleotide, but no enzyme gave the highest background reading, possibly due to a background scintillation from the cyclic nucleotide or the low level presence of some hydrolysed cyclic nucleotide in the original sample. This background was still very low and was used as the negative control in subsequent experiments. A sample of lysate that had been boiled for 5 minutes at 95°C was also tested. The boiled sample gave a reading comparable to the negative controls, indicating that the hydrolytic activity was a result of a heat labile factor, i.e. a protein (figure 5.10).
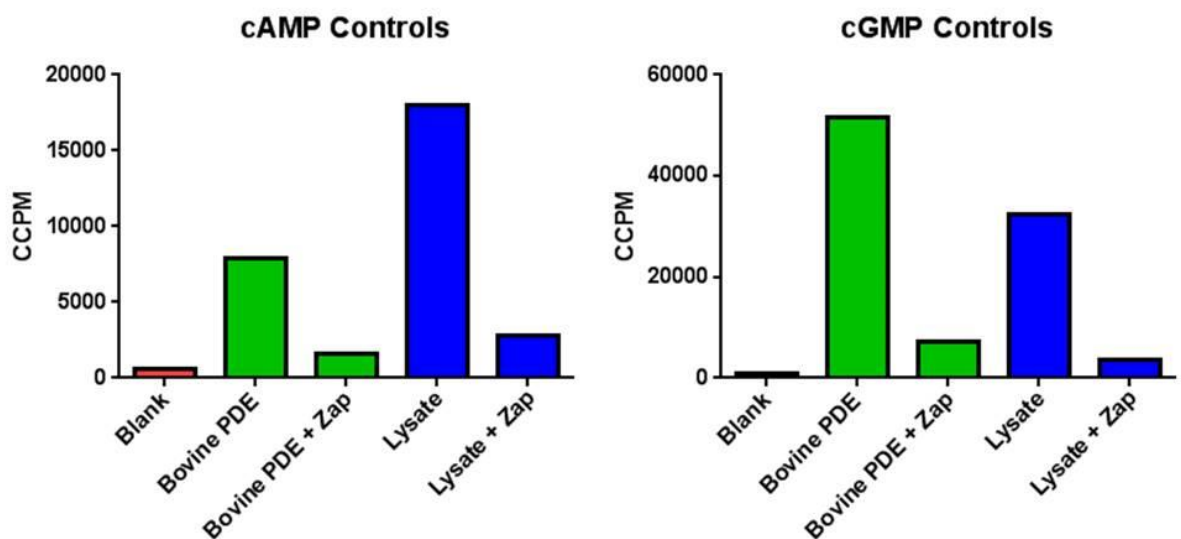
Figure 5.9 Initial assays to characterise native parasite PDE activity
Hydrolysis of cAMP (left) and cGMP (right) by whole parasite lysate displayed in combined counts per minute (CCPM), a relative measure of scintillation. Parasite lysate had PDE activity comparable to the positive control commercial PDE extracted from bovine brain tissue. This activity could be substantially reduced by addition of the PDE inhibitor zaprinast (zap, 100 µM). The blank represents no enzyme and no substrate. The figure contains data from a single representative experiment that was repeated several times.
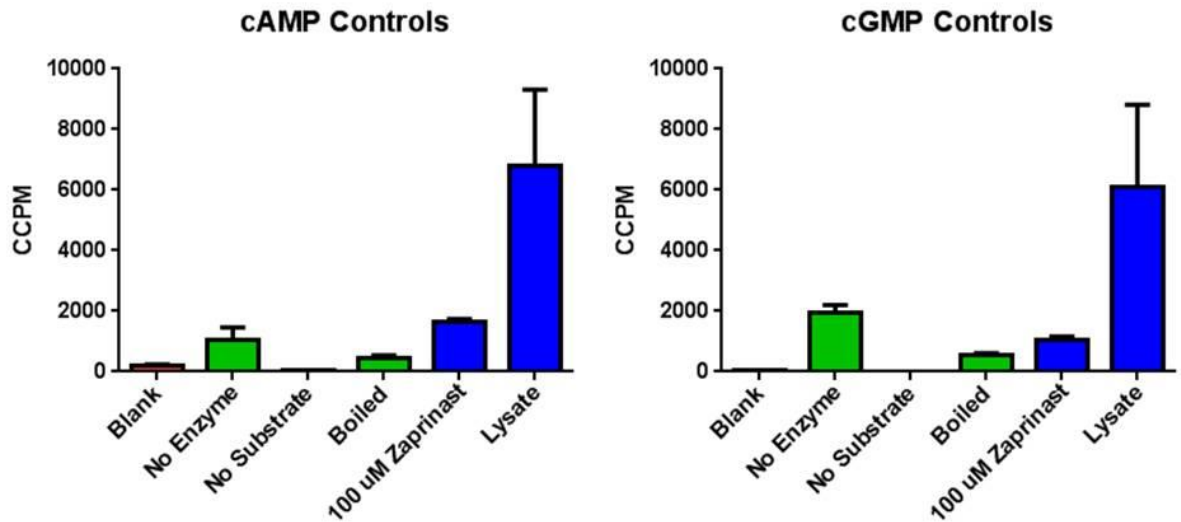
Figure 5.10 Initial assays to characterise parasite PDE activity
Hydrolysis of cAMP (left) and cGMP (right) by whole parasite lysate displayed in combined counts per minute (CCPM), a relative measure of scintillation. Parasite lysate had PDE activity that could be severely reduced by addition of the PDE inhibitor zaprinast (100 µM). The blank represents no enzyme and no substrate. Controls of no enzyme, plus substrate and no substrate plus enzyme were included. Lysate that was boiled for 5 minutes at 95°C ablated PDE activity. The assay was performed in triplicate and the error bars represent standard error of the mean.

Previous studies have identified that PfPDE activity is in the membrane fraction (Wentzinger et al. 2008; Yuasa et al. 2005; Ross Cummings, Thesis). This is consistent with the multiple predicted TM domains within the protein sequences, and with findings in this study, that PfPDEβ-HA is located in the membrane fraction of parasite lysates (see chapter 4.2.1). To confirm the presence of PDE activity in the membrane fraction of parasite lysates, fractionation was performed as described in chapter 2.6.1. The fractionations were performed on the both 3D7 and PfPDEβ-HA parasite lines. Two times the volume of the saponin pellet of extraction buffer was used for the extractions. Western blotting with the rat anti-HA monoclonal antibody was also performed to confirm the presence of PDEβ. PDEα is assumed to be solubilised in the same fraction as PDEβ as it also contains multiple TM domains. Anti-GAPDH antibody was used as a control. As predicted, the majority of PfPDEβ-HA is located in the membrane fraction (S2 – nonidet P-40 extraction), with some residual activity in the S3 fraction (RIPA extraction, a harsher membrane extraction buffer than nonidet P-40). There was no activity in the S1 cytosolic fraction. For future experiments the volume of extraction buffer was increased to five times the volume of the saponin pellet in an attempt to solubilise more of the protein. GAPDH is a cytosolic protein and as expected, was mostly found in the S1 fraction. A lesser amount was

also in the integral membrane S2 fraction which was probably due to the sheer volume of protein present (figure 5.11).
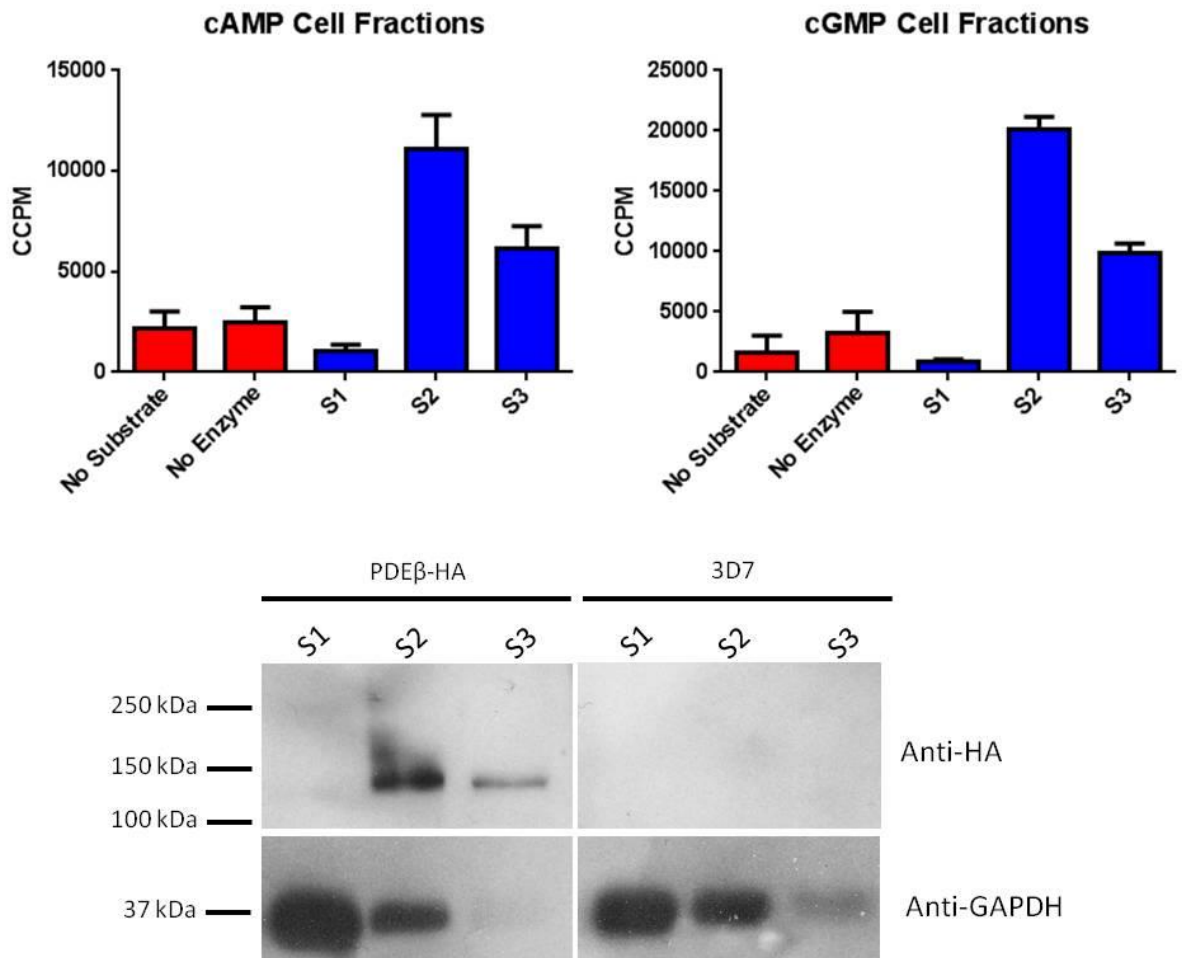
Figure 5.11 PDE activity is in the membrane fraction of the parasite lysate
Upper panel: Hydrolysis of cAMP (left) and cGMP (right) by parasite lysate fractions, displayed as combined counts per minute (CCPM), a relative measure of scintillation. The majority of the PDE activity was in the membrane fraction of the parasite lysate (S2). The cytosol fraction (S1) contained no hydrolytic activity. The S3 fraction contained some PDE activity, but significantly less than the S2 fraction. The results shown are for PfPDEβ-HA, very similar results were obtained for 3D7 (not shown). The assay was performed in triplicate and the error bars represent standard error of the mean. Lower panel: western blot showing the equivalent fractions to the upper PDE assay. The majority of PfPDEβ-HA is found in the S2 extraction, with some activity also in the S3 extraction. This correlates well with the PDE activity assay. Blots were probed with rat anti-HA (1:1000) to detect PfPDEβ-HA and anti-GAPDH (1:30,000) to detect PfGAPDH.

Finally, dose-response curves were performed using the membrane fraction of the parasite lysates. Ten-fold serial dilutions, starting using 10 μl of the extraction sample, were performed and assayed. Both the 10 μl/well and the 1 μl/well saturated the experiment, presumably the

activity of the enzyme exceeded the available cyclic nucleotide concentration. Dose dependent activity is observed at concentrations lower than 1 µl/well. Figure 5.12 shows an example assay. Serial dilutions were performed and assayed prior to each following experiment and the lysate was diluted to give 30% hydrolysis of the substrate.
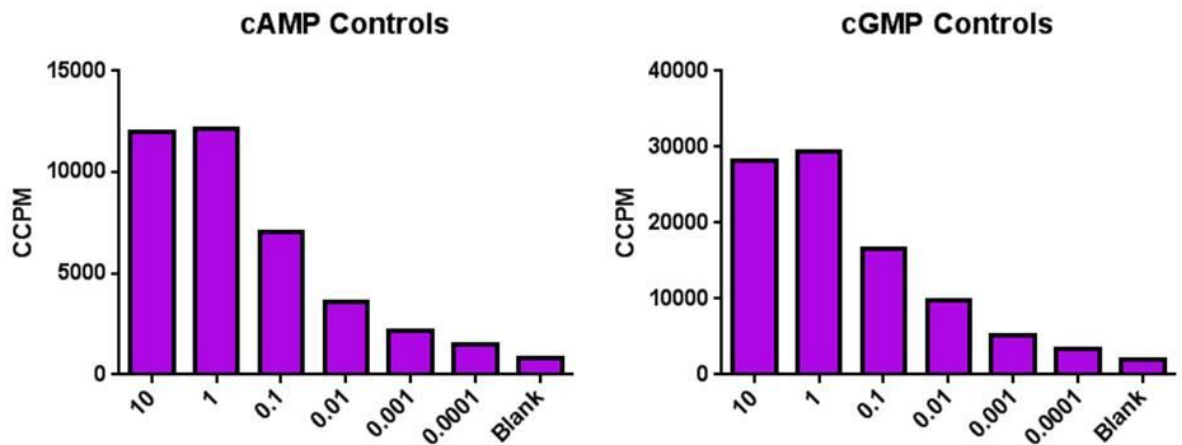
Figure 5.12 PDE activity is dose-dependent
Hydrolysis of cAMP (left) and cGMP (right) by membrane fraction parasite lysate displayed in combined counts per minute (CCPM), a relative measure of scintillation. A dose-response was performed from 10 µl per well at 10-fold serial dilutions. The blank represents no enzyme, plus substrate. This is a representative graph from one assay.

5.2.6 Analysis of the effects of PDE inhibitors on native PDE activity in wild-type parasite lysates

PDE inhibitor assays were performed in order to confirm whether the Pfizer compounds were targeting the PfPDEs. Some of the compounds had very high potency (IC50 values in the low nanomolar range) in the hypoxanthine incorporation assays on parasite growth, however it was not known if the killing was due to on- or off-target effects. All the Pfizer compounds were initially screened at two concentrations, 5 μM and 200 nM in cAMP and cGMP PDE assays. Zaprinast was used as a positive control at 100 μM and 1 μM. Artemisinin and the PKG inhibitor compound 2 were used as negative controls, also at 5 μM and 200 nM. Values were expressed as percent of uninhibited control. Compounds that had IC50s of lower than 250 nM in hypoxanthine incorporation assays are denoted by a star (★), compounds with IC50s below 100 nM are denoted by two stars (★★). As expected, the higher concentration of zaprinast (100 μM) significantly inhibits PDE activity, the lower concentration (1 μM) does not. As previously found by Ross Cummings, Zaprinast inhibits both cAMP- and cGMP-PDE activity, whereas in humans it is selective for PDE5, a cGMP specific PDE. Artemisinin and compound 2 do not reduce PDE activity at either concentration. Of the seven Pfizer compounds that have IC50s of greater than 250 nM in hypoxanthine incorporation assays, none show significant loss in activity in this assay, indicating that they are either off target or not potent enough to inhibit the native *Plasmodium* PDE in this assay. Of the seven compounds that do have IC50s of less than 250nM in parasite growth inhibition assays, five of them, PF-01273175, PF-05184913, PF-05225388, PF-00394183 and PF-00388991, reduce cyclic nucleotide hydrolysis at both 5 μM and 200 nM. This effect is much more pronounced for cAMP hydrolysis. Two of the highly potent inhibitors in hypoxanthine uptake assays, PF-05257670 (IC50 of 7.5 nM) and PF-05197824 (IC50 of 140.5 nM) have no effect on cyclic nucleotide hydrolysis for either cAMP or cGMP. Presumably, they are therefore not primarily hitting a PfPDE in the whole parasite.
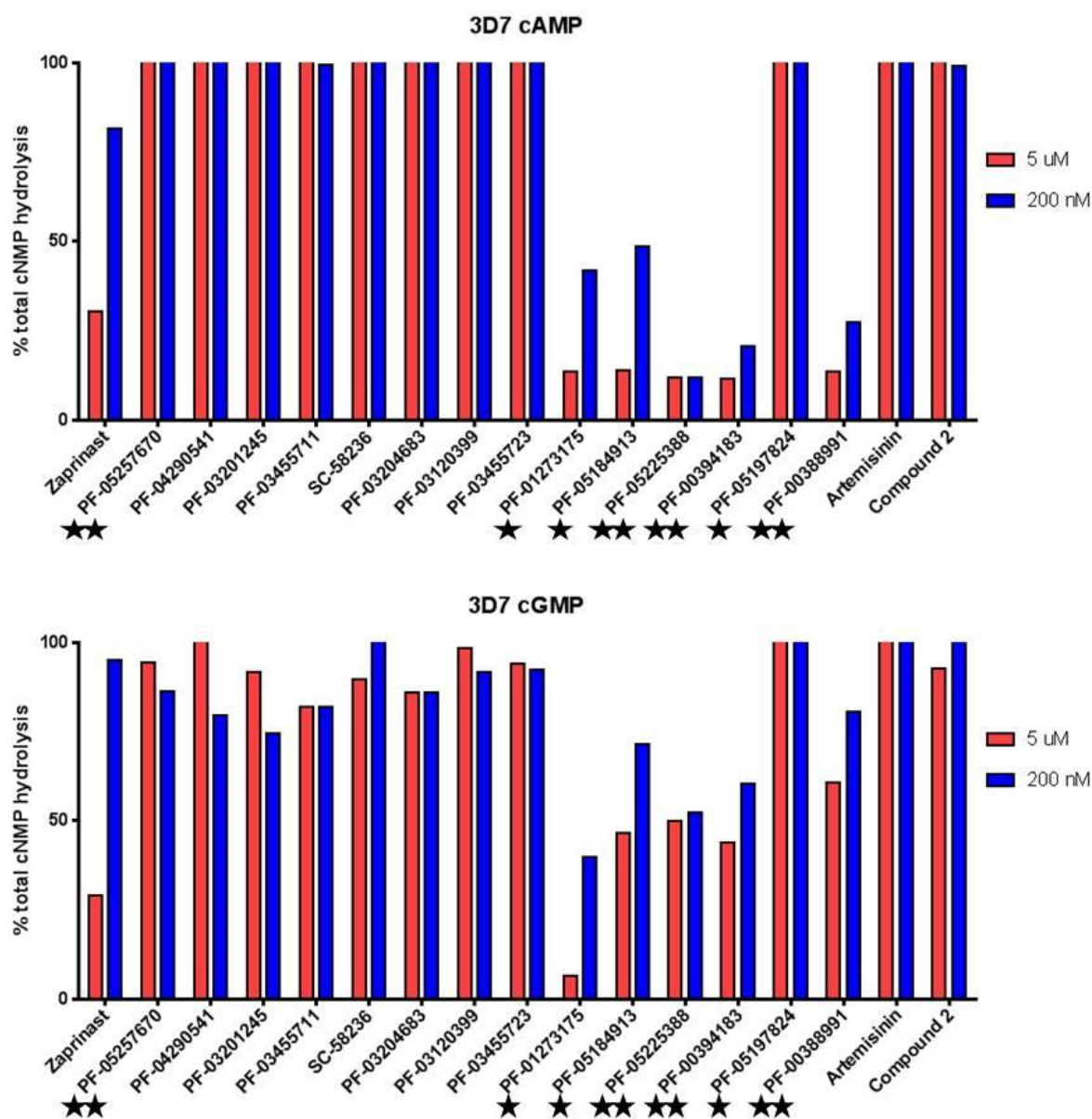
Figure 5.13 Screening of Pfizer inhibitors in a native PDE assay on WT parasites
Hydrolysis of cAMP (upper) and cGMP (lower) by membrane fraction parasite lysate with either
5 µM (red) or 200 nM (blue) of compound. Zaprinast concentrations are 100 µM (red) and 1 µM
(blue) due to the lower potency of the inhibitor. Values are expressed as percent of uninhibited
control. Compounds that had IC50s lower than 250 nM in hypoxanthine incorporation assays
are denoted by a star (★) and compounds with IC50s below 100 nM are denoted by two stars
(★★). Due to time and financial constraints, the results presented represent single data points.
The graph was capped at 100%.

5.2.7 Comparison of the effects of the Pfizer compounds on native PDE activity on wild-type and PfPDEα-KO parasite lysates

The differential results above of the phosphodiesterase screen on 3D7 parasites for cGMP and cAMP were quite unexpected. Although the cAMP hydrolysis levels were highly inhibited in the presence of some of the compounds, the effect was much less pronounced for cGMP hydrolysis. Apart from compound PF-01273175, the pattern was quite different between the cyclic nucleotides. Zaprinast also gave the same pattern between cyclic nucleotides which was expected as it is presumed to be a broad *Plasmodium* PDE inhibitor. PDEα is a cGMP specific phosphodiesterase. Therefore it was hypothesised that some of the inhibitors might be specifically targeting PDEβ and not PDEα, resulting in residual cGMP hydrolytic activity. To test this hypothesis, the assay was repeated on the PDEα-KO line. In the absence of PDEα, the effect of the inhibitors on PDEβ could be dissected. Figure 5.14 shows the screening of inhibitors on the PfPDEα-KO parasite lysates. As with the previous figure, the Pfizer compounds, artemisinin and the PKG inhibitor compound 2 were screened at two concentrations, 5 μM and 200 nM. Zaprinast was used as a positive control at 100 μM and 1 μM. Values are expressed as percent of uninhibited control. Compounds that had IC50s lower than 250 nM in hypoxanthine incorporation assays are again denoted by a star (★), compounds with IC50s below 100 nM are denoted by two stars (★★). As with the 3D7 results, the higher concentration of zaprinast (100 μM) significantly inhibited PDE activity, the lower concentration (1 μM) does not. Artemisinin and compound 2 did not reduce PDE activity at either concentration. The seven Pfizer compounds that have IC50s of greater than 250 nM, and show no cNMP hydrolysis in the WT assay, none showed significant loss in activity in this assay. In both assays, compounds PF-05257670 and PF-05197824 (highly potent in the growth inhibition assay) had no effect on cyclic nucleotide hydrolysis for either cAMP or cGMP, indicating that they have off target effects on the parasite. In the PDEα-KO assay, the inhibition patterns for the five potent, on target inhibitors (PF-01273175, PF-05184913, PF-05225388, PF-00394183 and PF-00388991) is the same for both cAMP and cGMP hydrolysis.

To present this more clearly, figure 5.15 shows a comparison between 3D7 and PDEα-KO phosphodiesterase activity inhibition at the highest (5 μM for the Pfizer inhibitors and 100 μM for zaprinast) concentration. For cAMP hydrolysis inhibition, WT and PDEα-KO parasite lysate shows the same pattern of inhibition. For cGMP hydrolysis inhibition, WT and PDEα-KO parasite lysate show different patterns of inhibition. Zaprinast and PF-01273175 inhibited cGMP hydrolysis equally in WT and PDEα-KO lines. However for PF-05184913, PF-05225388, PF-

00394183 and PF-00388991, cGMP hydrolysis was only partially reduced (about 50% inhibition) in WT lysate, however in PDEα-KO lysate, cGMP hydrolysis was reduced to almost baseline levels. This strongly suggests that zaprinast and PF-01273175 inhibit both PDEα and PDEβ. PF-05184913, PF-05225388, PF-00394183 and PF-00388991 primarily target PDEβ. Since PDEα and PDEβ are the only PDEs expressed in blood stages and the PDEα-KO line retains cAMP and cGMP hydrolytic activity, which can be specifically inhibited with PDE inhibitors, this is also strong evidence that PDEβ is a dual specific PDE.
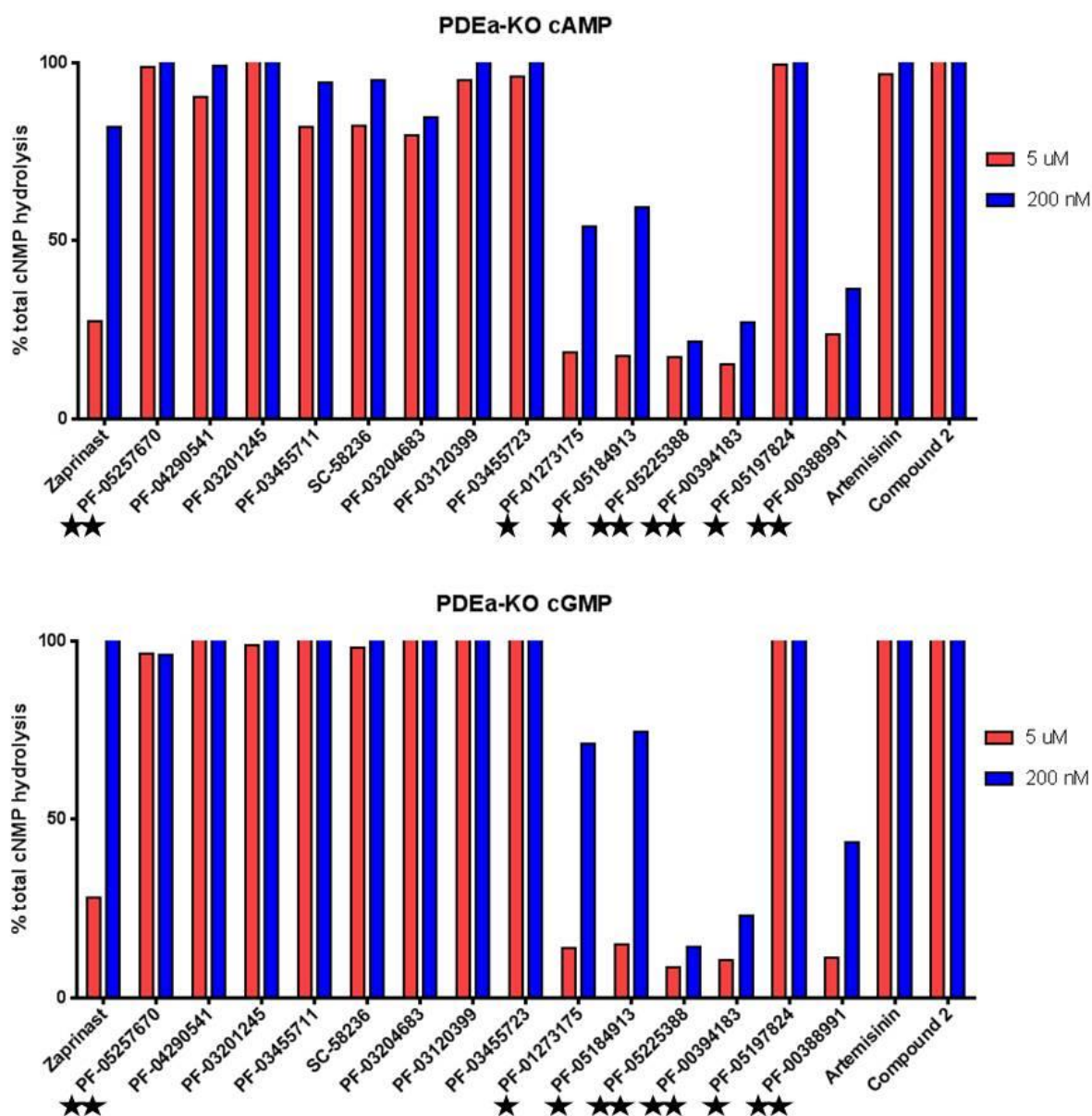
Figure 5.14 Screening of Pfizer inhibitors in a native PDE assay on PDEα-KO parasites
Hydrolysis of cAMP (upper) and cGMP (lower) by membrane fraction parasite lysate with either 5 μM (red) or 200 nM (blue) of compound. Zaprinast concentrations are 100 μM (red) and 1 μM (blue) due to the lower potency of the inhibitor. Values are expressed as percent of uninhibited control. Compounds that had IC50s lower than 250 nM in hypoxanthine incorporation assays are denoted by a star (★) and compounds with IC50s below 100 nM are denoted by two stars (★★). Due to time and financial constraints, the results presented represent single data points. The graph was capped at 100%.

Figure 5.15 Pfizer inhibitors: comparison between 3D7 and PDEα-KO parasites
Hydrolysis of cAMP (left) and cGMP (right) by membrane fraction parasite lysate with either no inhibitor (lysate), 100 μM zaprinast or 5 μM of Pfizer inhibitor. 3D7 parasite PDE activity is shown in green and PDEα-KO activity is shown in blue. Values are expressed as percent of uninhibited control. The graph was capped at 100%.

5.2.8 Phosphodiesterase activity of immunoprecipitated PfPDEβ-HA

To further investigate both the cyclic nucleotide specificity of PDEβ and the specificity of the inhibitors, PDE assays on immunoprecipitated PfPDEβ-HA was performed. Immunoprecipitation was performed as described in chapter 2.6.2. However, for the initial test pulldown and western blot, a Nonidet P-40 based buffer and a RIPA buffer were used sequentially for extraction. Figure 5.16 shows the result of the western blot. A band at about 133 kDa was successfully pulled down with the nonidet P-40 extraction. The nonidet P-40 buffer was therefore used for further immunoprecipitations. To prepare the bead sample for western blotting, the samples were boiled in reducing buffer for 10 minutes, however the majority of the sample remained bound to the beads (figure 5.16). In a separate experiment, the PDEβ protein was eluted using a glycine buffer at acid pH. This was tested by Westen blotting and PDE assay. Very little protein or activity was eluted in this fraction and it was therefore decided to use the bead-protein complex in the PDE assay (data not shown).

Two-fold serial dilutions were performed with the bead-protein complex, from 10 μl to 1.25 μl. Beads only was used as the negative control. Each concentration was performed in duplicate and although the counts were not highly consistent, a dose-response with decreasing bead concentration could be observed. The 30% hydrolysis dilution could not be determined as the highest concentration (10 μl) did not saturate the assay. Therefore, 5 μl of the pulldown sample

was used for a further inhibitor assay as this concentration was within the linear range of the assay (figure 5.17). The immunoprecipitation of PfPDEβ-HA has both cAMP and cGMP hydrolytic activity, confirming for the first time that PDEβ is a dual specific phosphodiesterase.

A selection of the inhibitors was tested in a PDE inhibition assay. Zaprinast was used at 100 μM concentration. The Pfizer inhibitors were all used at a concentration of 100 nM, (lower than the previous screening assay). As a negative control, the off target PF-05257670 inhibitor was included. The five compounds that were previously most potent in the PDE assay were used, PF-01273175, PF-05184913, PF-05225388, PF-00394183 and PF-00388991. Uninhibited lysate was used as a positive control. As predicted, 100 μM zaprinast ablates cyclic nucleotide hydrolysis and PF-05257670 has no effect. At 100 nM, PF-01273175 and PF-05184913 do not significantly inhibit PDEβ activity. This could be likely because their IC50 is above 100 nM, which is likely looking at the data in figure 5.13 where a 5 μM concentration almost totally ablated PDE function whereas 200 nM only reduced the activity by about 60-70%. However, the three remaining compounds do significantly inhibit PDEβ activity. These compounds, PF-05225388, PF-00394183 and PF-00388991, were among the most potent in the parasite growth assays (IC50s of 11 nM, 62 nM and 20 nM, respectively). The combined data indicates that these compounds are potent, on-target, highly PDEβ specific phosphodiesterase inhibitors.
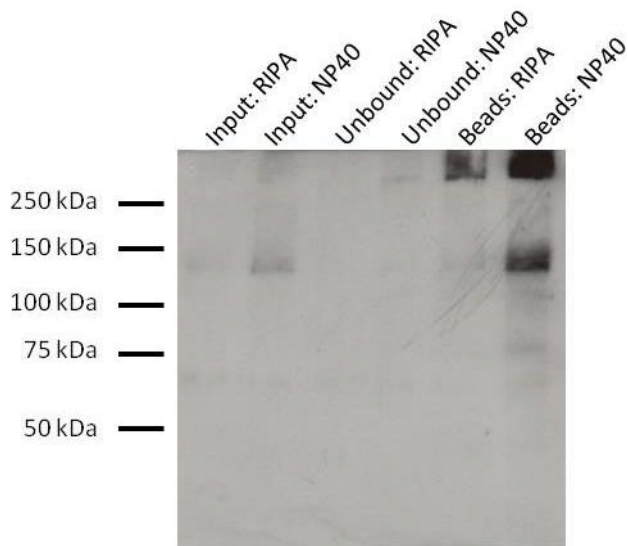
Figure 5.16 Immunoprecipitation of PfPDEβ-HA

Western blot showing the successful immunoprecipitation of PDEβ-HA with a nonidet P-40 based buffer. A protein migrating between 100 and 150 kDa (consistent with the predicted molecular weight of 133 kDa for PDEβ) was successfully isolated. The blot was probed with rat anti-HA monoclonal antibody at 1:1000 dilution.
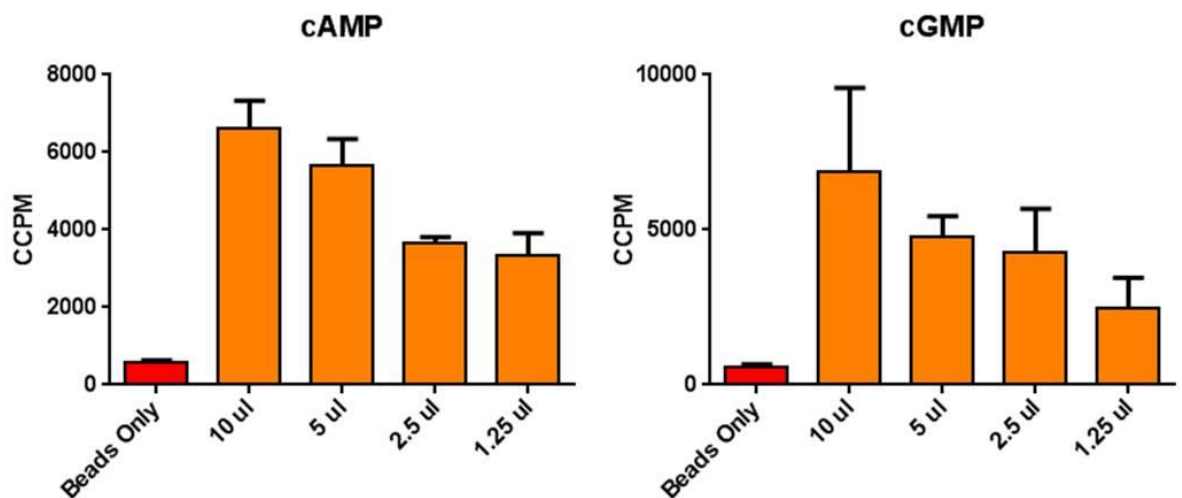
Figure 5.17 Immunoprecipitation of PfPDEβ-HA has cAMP and cGMP hydrolysing activity that is dose-dependent

Hydrolysis of cAMP (left) and cGMP (right) by immunoprecipitaed PfPDEβ-HA is displayed in combined counts per minute (CCPM), a relative measure of scintillation. A dose-response was performed from 10 µl per well at two-fold serial dilutions. The negative control represents anti-HA affinity matrix alone (beads only). 5 µl was used for the subsequent experiments. The assay was performed in duplicate and the error bars represent standard error of the mean.
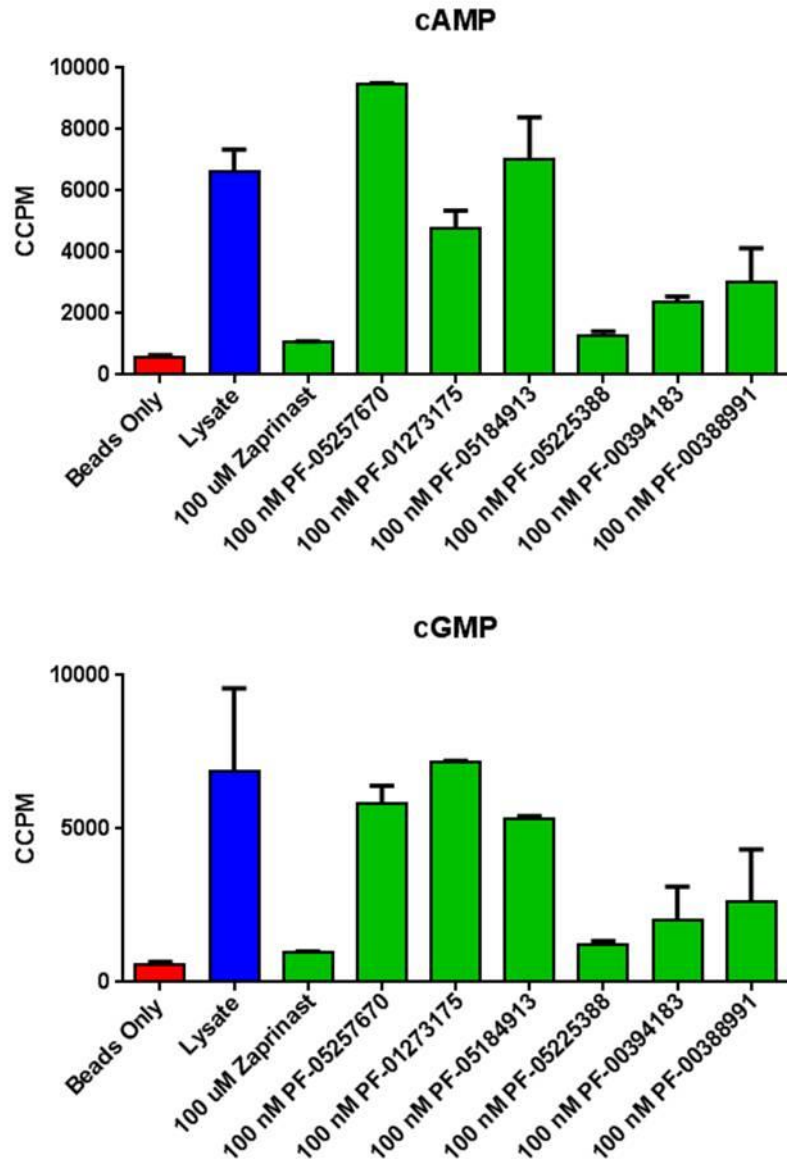
Figure 5.18 Testing of selected inhibitors on immunoprecipitated PfPDEβ-HA
Hydrolysis of cAMP (upper) and cGMP (lower) by immunoprecipitaed PfPDEβ-HA, in the presence of PDE inhibitors is displayed in combined counts per minute (CCPM), a relative measure of scintillation. Zaprinast was used at 100 µM as a positive control and the Pfizer inhibitors were used at 100 nM. The negative control represents anti-HA affinity matrix alone (beads only). The assay was performed in duplicate and the error bars represent standard error of the mean.

5.2.9 Phosphodiesterase inhibitors kill at late schizont and ring stage parasites

To investigate the timing of killing of phosphodiesterase inhibitors, a selection of the Pfizer compounds was added to synchronised asexual blood stage cultures at ring and trophozoite stages. This was a very preliminary assay to visualise the death phenotype. Concentrations of about four times the IC50 determined in the hypoxanthine incorporation assays were used. 0.5% DMSO was used as a negative control. For the first assay, shown in figure 5.19, inhibitors were added to ring stages (T=0). Giemsa stained blood films were examined after 16 hours. Compounds PF-05225388, PF-00394183, PF-00388991 and zaprinast were tested. The most potent PDEβ inhibitor, PF-05225388, is shown in the figure as a representative sample. After 16 hours, the DMSO treated parasites had progressed to trophozoites. Parasites treated with 100 μM zaprinast or 20 nM PF-05225388 appeared to have died at ring stages. Parasites treated with PF-00394183 and PF-00388991 also resulted in parasite death at ring stages (not shown). For the second assay, shown in figure 5.20, inhibitors were added to trophozoite stages (T=0). Giemsa stained blood films were examined after 4 and 16 hours. Compounds PF-05225388, PF-00394183, PF-00388991 and zaprinast were tested. The most potent PDEβ inhibitor, PF-05225388, is shown in the figure as a representative sample. After four hours all three samples had progressed to early-mid schizonts and looked healthy. However after 16 hours, only the DMSO sample contained healthy, reinvaded parasites. Two different phenotypes were present for the inhibitor treated samples. Many of the parasites appeared to have ruptured, releasing merozoites that were unable to reinvade, resulting in a 'burst schizont' phenotype. Some of the merozoites may have attached to RBCs and invaded. These parasites then died at ring stages, as seen in figure 5.19. For some of the parasites it was difficult to tell if they had managed to reinvade or if the merozoite was attached to the RBC surface. Figure 5.20 shows an example of each of these phenotypes for the two compounds. It was not possible to quantify the numbers of each of these phenotypes by Giemsa stained blood films because the burst schizonts made it difficult to count. Further work will be necessary to investigate the stage of killing more thoroughly.
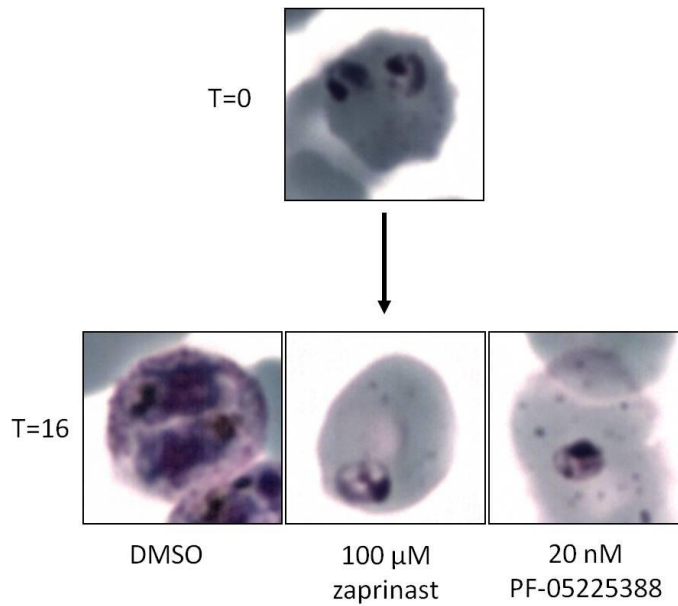
Figure 5.19 PDE inhibitors kill at ring stages
Inhibitor (or DMSO) was added to ring stage parasites at T=0. After 16 hours, DMSO parasites had developed into trophozoites. Parasites in the presence of 100 µM zaprinast or 20 nM PF-05225388 appeared to be dead.
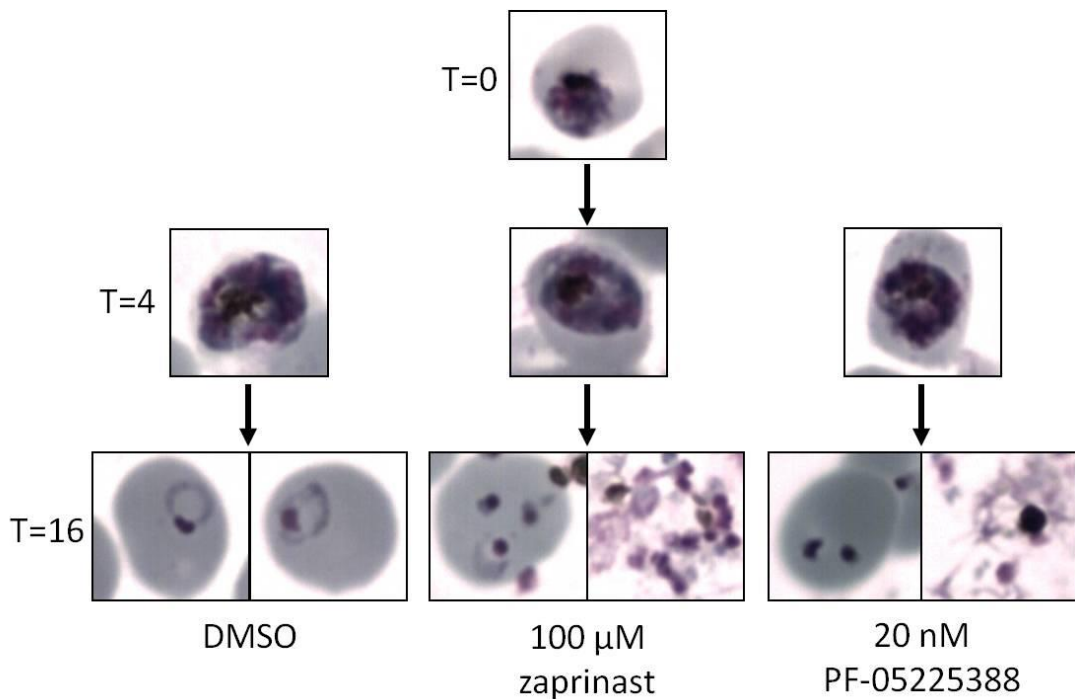
Figure 5.20 PDE inhibitors kill at ring and late schizont stages
Inhibitor (or DMSO) was added to trophozoite stage parasites at T=0. After 4 hours, all the samples contained healthy looking mid-schizonts. After 16 hours, DMSO treated parasites had successfully reinvaded to form new rings. Parasites in the presence of 100 µM zaprinast or 20 nM PF-05225388 appeared to be dead. All of the samples containing PDE inhibitors contained a mixture of what appeared to be burst schizonts and dead merozoites/rings.

5.3 Discussion

As part of this project, fourteen potential PDE inhibitors were obtained from Pfizer. Originally developed as a part of lead compound optimisation for various human PDE series, very little was known about the compounds. In addition, some of the compounds provided were guanylyl cyclase inhibitors although it was not known which. Additionally, eight commercially available PDEs were tested, including the previously characterised, broad spectrum PfPDE inhibitor zaprinast. The current antimalarials artemisinin and chloroquine were used as positive controls.

5.3.1 Hypoxanthine incorporation assays

The first step that was taken in characterising the compounds for potency and specificity against the PfPDEs was with a parasite growth inhibition assay. All 24 compounds were screened using hypoxanthine incorporation assays. A standard hypoxanthine uptake assay is 48 hours long, however in some instances a 72 hour assay is preferred. For the PDE inhibitors this was indeed the case. A 72 hour growth inhibition assay was necessary to obtain reliable IC50 curves. In addition to producing robust results, the necessity of a 72 hour assay may also indicate that the compounds are toxic at the schizont, merozoite or very early ring stages, targets that are less amenable to a 48 hour assay. A late schizont stage target would be expected from the previously determined expression profile of PDEβ. Microscopy of *P. falciparum* parasites in the presence of the inhibitors also indicates that the schizont and early ring stages are killed (figures 5.19 and 5.20). Detailed conclusions about inhibitor potency are discussed in more detail below. However it is important to note that the IC50 of zaprinast was consistent with previous studies (approximately 26 μM) and that a number of the Pfizer inhibitors were far more potent, with IC50s in the low nanomolar range.

Wild-type parasites are predicted to express two different PDEs in asexual blood stages, PDEα and PDEβ. As PDEα is non-essential it can be supposed that the death of the parasites results from inhibition of PDEβ, although antagonistic effects of inhibiting both PDEs cannot be discounted. In an attempt to determine the IC50 of the compounds in hypoxanthine incorporation assays in the absence of PDEα, and to determine whether there is a difference between inhibiting PDE(s) in the WT and the PDEα-KO line, comparison IC50s were performed. Prior to this experiment, any selectivity of the Pfizer compounds was totally unknown. As PDEα is not essential in asexual blood stage parasites there may be no difference in the IC50s between the two lines, especially if a compound inhibited both PDEs equally well and all cyclic nucleotide function was ablated. However, if the compounds only inhibited PDEβ then a difference in IC50

177

may potentially be seen. In one scenario, inhibition of PDEβ in WT parasites could only inhibit the cAMP signalling pathway as PDEα is still able to hydrolyse cGMP, a cAMP specific phenotype may be seen. However inhibition of PDEβ in the absence of PDEα would remove all PDE function from the cell, resulting in a cGMP and cAMP phenotype. The PDEs may also be distinct in function and a PDEβ specific death phenotype would be observed. The five most potent compounds along with zaprinast, artemisinin and chloroquine were tested at a narrower concentration range than for the previous growth inhibition assays. Artemisinin and chloroquine do not target the PfPDEs which should therefore result in a consistent IC50 between the different parasite lines. Zaprinast is known to inhibit PDEα, and as it kill the parasite, presumably PDEβ as well. It should also therefore result in comparable IC50s between the lines. The specificity of the Pfizer compounds was unknown.

Unexpectedly, the hypoxanthine incorporation assay IC50s of some of the control compounds was different between the 3D7 and the PDEα-KO lines. For artemisinin, chloroquine and zaprinast the IC50 was lower in the 3D7 line. There was no difference between the IC50s of the Pfizer compounds. When looking at the IC50 curves (figure 5.8), the differences were quite slight and could have been the result of variation between the replicates. Additionally, the faster and higher growth rate of the PDEα could have resulted in the difference between the IC50s of the controls. This could then mask any true difference in inhibition profile between the WT and PDEα-KO line. Unfortunately this assay was performed before it was determined that compound PF-01273175 inhibits both PDEα and PDEβ as it could have been a useful addition to the PDEα-KO/3D7 comparison experiment. Comparative hypoxanthine assays were not used further due to the complexity in assessing the results. This assay would be well suited to analysis of IC50s of PDEβ in a PDEα conditional knockdown system as the stains used for comparison would be from the same (or one removed) generation rather than a distant parental line. Additionally, if a second PDEα-KO line was generated that did not have a growth rate phenotype (i.e. it is the result of an off target effect) then that would also be a good line to use in this assay system.

5.3.2 Phosphodiesterase activity assays

A PDE assay had previously been developed for *Plasmodium* PDEs at LSHTM, however some of the reagents were no longer commercially available which necessitated the development of an alternative method. A PDE assay kit is produced by Perkin Elmer, however the cost was prohibitively high. A key element of the kit is the PDE specific scintillation proximity assay beads, which are also available separately from Perkin Elmer. These beads were used to develop a PDE assay suitable for analysing PfPDEs. PDEs are dependent on divalent cations as co-factors for activity. Ross Cummings had previously analysed presence of metal ions in the assay buffer for optimal activity. Magnesium, closely followed by manganese results in the highest activity level. Studies on PDEα have shown that Mn^{2+} gives the highest level of PDE activity (Wentzinger et al., 2008; Yuasa et al., 2005). It is possible that Mg^{2+} is the primary co-factor for PDEβ and Mn^{2+} is the co-factor for PDEα. Due to time constraints, this could not be investigated in depth, but would be best with the PDEβ-HA pulldown.

Initially this PDE assay was tested with parasite lysate and commercially available PDE enzyme, both of which showed high levels of activity which was effectively inhibited by zaprinast. Additionally, lysate that was boiled for five minutes at 95°C had no PDE activity, indicating that a protein (i.e. enzyme) is responsible for the activity.

Previous studies, as well as transmembrane domain predictions have indicated that PfPDEs are located in the parasite membranes. In chapter 4.2.1, PDEβ-HA located to the integral membrane fraction in a sequential solubility assay. Sequential protein extractions on PDEβ-HA parasite lysates, were performed and analysed by PDE assay and western blotting. The presence of the protein and the PDE activity in the sample strongly correlate. This is further confirmation that PDEβ is an integral membrane protein.

PDEβ was also successfully immunoprecipitated using an HA-affinity matrix. A protein of approximately 136 kDa was observed by western blotting which correlated to PDE activity. This sample had both cAMP and cGMP hydrolysing activity, confirming for the first time that PDEβ is a dual specific phosphodiesterase.

The Pfizer compounds and zaprinast were also tested on both whole parasite lysates and the PDEβ-HA pulldown, initially on 3D7 parasites at two different concentrations. What was most evident from this experiment was that the inhibition profile was very different for cAMP hydrolysis compared to cGMP hydrolysis. Although the potency of specific compounds will be discussed below, the most active compounds significantly reduced cAMP hydrolysis. These

same compounds tended to reduce cGMP hydrolysis but not to the same magnitude as the cAMP hydrolysis (about 50% inhibition shifting to over 90% inhibition, respectively). As PDEα is cGMP specific and PDEβ is dual specific, the decrease in potency of the compounds (screening of inhibitors on native PDE activity, figure 5.13) for cGMP hydrolysis could be explained by residual PDEα activity if the inhibitors were specifically targeting PDEβ. This hypothesis was tested by repeating the assay on the PDEα-KO parasite line. As part of the study in which the PDEα-KO line was generated, the levels of cyclic nucleotide hydrolysis were measured compared to the parental (WT) line. cGMP hydrolysis was found to be reduced by 20% and cAMP hydrolysis levels were unchanged (Wentzinger et al., 2008). In this study, the PDEα-KO line and the 3D7 line had very similar cAMP hydrolysis levels in the presence of the inhibitors. This was expected as PDEα does not hydrolyse cAMP and PDEβ is predicted to be the only other PDE active in asexual parasites. A key point is that the cGMP hydrolytic activity was substantially inhibited by the potent Pfizer compounds in the PDEα-KO line compared to the WT line. In the PDEα-KO line, the levels of cGMP hydrolysis are highly similar to those seen in the cAMP hydrolysis experiment. The only compounds for which this was not the case were zaprinast and PF-01273175 where inhibition of cAMP and cGMP hydrolysis was not different for 3D7 parasite lysate or PDEα-KO lysate. This is shown clearly in figure 5.15. The conclusion of this assay is that some of the potent PDE inhibitors are specific to PDEβ and do not target PDEα. These compounds are PF-05225388, PF-00394183 and PF-00388991. Zaprinast and PF-01273175 target both PDEβ and PDEα. Compound PF-05184913 is less potent than the other PDEβ specific inhibitors, but is also likely to predominantly target PDEβ. A further conclusion from these data is that two of the compounds that were highly potent in the hypoxanthine uptake assays, PF-05257670 and PF-05197824 (IC50s of 7.5 nM and 140.5 nM, respectively), are not PDE inhibitors. They are potentially some of the guanylyl cyclase inhibitors that were included in the panel of drugs, however this remains unknown (summary table 5.4, below).

5.3.3 Overview of inhibitor potency

During the course of the experiments, almost all details about the Pfizer compounds were unknown, including whether they were indeed PDE inhibitors, rather than guanylyl cyclase inhibitors. Recently, the human PDE target of the five most potent, on-target inhibitors has been divulged. PF-01273175 is a human PDE9 inhibitor, PF-05184913, PF-05225388, PF-00394183 and PF-00388991 are human PDE5 inhibitors (see summary table 5.4). Interestingly, zaprinast (IC50 of 26 μM), T0156 hydrochloride (IC50 of 22 μM) and dipyridamole (IC50 of 4.7 μM), three of the effective commercial compounds, are also PDE5 inhibitors. Although EHNA hydrochloride

(IC50 of 2.8 μM), the most potent commercial compound in the growth inhibition assay, is an inhibitor of PDE2, its primary target in humans is adenosine deaminases. *P. falciparum* also contains an adenosine deaminase (ADA) which catalyses the conversion of adenosine to inosine and is critical in the purine salvage pathway. EHNA has been tested against PfADA, and was found to be weakly active against recombinant protein. It was not however, tested in a growth inhibition assay (Ivanov and Matsumura, 2012). It is possible that the primary target of EHNA is not a PDE, but another protein within the parasite, potentially PfADA. A similar picture emerges with vinopocetine (IC50 of 60 μM), a human PDE1 inhibitor which also blocks voltage gated sodium channels. A brief search for 'voltage gated sodium channel' on PlasmoDB and NCBI did not turn up any obvious annotated candidate genes in the *P. falciparum* genome, however it is possible that the growth inhibition occurs due to a PDE independent effect. CP 80633, a human PDE4 inhibitor and BRL 50481, a human PDE7 inhibitor, did not affect parasite growth (IC50s over 200 μM). In keeping with results by Ross Cummings, IBMX (a broad spectrum PDE inhibitor) had no effect on parasite proliferation.

Mammalian PDE5 is a cGMP specific phosphodiesterase encoded by a single gene. Three variants of PDE5A mRNA have been discovered, PDE5A1-PDE5A3, which differ at their N-termini. PDE5 contains two GAF domains, one of which, GAF-A binds with high affinity to cGMP. GAF domains are allosteric regulation sites which, upon cGMP binding, promote cGMP hydrolysis (Maurice et al., 2014). Several human PDEs contain these domains, PfPDEs do not. PDE5 is phosphorylated by PKG at an N-terminal serine, upstream of the GAF domains. Under certain conditions this site can also be phosphorylated by PKA. This phosphorylation increases the affinity of cGMP binding to the GAF domain and it has been predicted that this mechanism is a feedback loop for prolonging the activation of PDE5 (Bender and Beavo, 2006). Interestingly, in a recent quantitative phosphorylation proteome study, PDEβ was found to be phosphorylated in a cGMP-dependent manner at Serine 156 (Alam et al., 2014). This could potentially result in a feedback mechanism similar to that seen in PDE5.

PDE9 is notable as having the highest affinity for cGMP of all of the PDE families discovered so far. Like PDE5, PDE9 exists as a single gene copy, but has complex mRNA processing with 19 variants identified. PDE9 contains no GAF domains, but does contain a Pat7 nuclear localisation domain. Little is known about the function of PDE9 although a PDE9 inhibitor (PF-04447943) has undergone clinical trials as a treatment for Alzheimer's disease, however no effect was reported on improvement of cognition, behaviour or global change (Schwam et al., 2014). Like

the PfPDEs, PDE9 is insensitive to many of the common broad spectrum PDE inhibitors including caffeine and IBMX.

	IC50 in Growth inhibition Assay		Probable PfPDE Target	Human PDE Target
	µM	nM		
Zaprinast	25.9	25900	Broad	PDE5
PF-05257670	0.01	7.47	Off-target	
PF-01273175	0.14	143.00	PDEα and PDEβ	PDE9
PF-05184913	0.16	156.40	PDEβ	PDE5
PF-05225388	0.01	5.34	PDEβ	PDE5
PF-00394183	0.08	81.73	PDEβ	PDE5
PF-05197824	0.14	140.50	Off-target	
PF-00388991	0.03	33.86	PDEβ	PDE5

Table 5.4 An overview of the properties of the seven Pfizer compounds with the lowest IC50 and zaprinast *in vivo*
IC50s in micromolar and nanomolar of seven of the most potent Pfizer compound with their presumed PfPDE target and the human PDE target, if known.

In summary, this project, along with previous studies, has highlighted differences between PfPDEs and human PDEs in terms of their inhibition profile. Many widely studied broad spectrum PDE inhibitors are ineffective on PfPDEs. Prior to this study, the most potent mammalian PDE inhibitor in terms of effects on the parasite was zaprinast with an IC50 value 35 µM (Yuasa et al., 2005). However, the present study has identified 5 compounds which are about 1000-fold more potent than this, representing a big step forward. Four of these target human PDE5 and, looking at the PDE assay results, are highly PDEβ specific. Additionally, a PDE9 inhibitor was active against both PfPDEα and PfPDEβ. This selectivity was unexpected and therefore the compounds will be valuable tools for future functional analysis, as well as promising lead compounds for future antimalarial drug discovery.

A robust PDE assay has been developed for PfPDEs that is much simpler than those previously used, notably with less handling of radioisotopes. The fundamental differences between human and *Plasmodium* PDEs indicates that selective inhibitors could be developed that selectively target the PfPDEs, resulting in compounds with a good safety profile. This will be further discussed in chapter 7.

Chapter 6: Expression of recombinant PvPDEβ protein

6.1 Introduction

There have been several previous attempts to generate recombinant PfPDE proteins. PDEα is currently the only active PfPDE successfully expressed so far (Wentzinger et al., 2008; Yuasa et al., 2005). The predicted catalytic domain of PfPDEα was expressed in an *E. coli* based recombinant expression system. All of the other PfPDEs have been attempted in a variety of systems including *E. coli* and the baculovirus insect cell system with no success (Ross Cummings, Thesis; Pfizer, personal communication; Thomas Seebeck, University of Bern, personal communication). The reasons for failure are unknown but there have been problems with solubility. Also, often the catalytic domain only was expressed, it is possible that the TM domains or cryptic regulatory features within the rest of the protein are key to activity. *P. falciparum* proteins are notoriously challenging to express. Although the reasons for this are uncertain, it has been postulated that as a result of the AT rich codon bias, some tRNAs used by *P. falciparum* may be rare in heterologous systems, and atypical signal peptides and export motifs contribute to poor recombinant expression (Birkholtz et al., 2008). Also, the high AT content, repetitive amino acid stretches and bias towards unusual codons likely make both the presence of the DNA sequence and subsequent protein unstable in the expression host organism (Zenonos et al., 2014). For these reasons, baculovirus expression of the closely related, and also significant from a public heath perspective (Anstey et al., 2012), *P. vivax* PDEβ (PVX_122885) will be attempted. To our knowledge, expression of the *P. vivax* PDEβ gene had not been attempted. The sequence was recodonised to *Spodoptera frugiperda* codon usage.

Baculovirus expression technology has been exploited for over 30 years (Bishop, 1990). Protein expression within a eukaryotic *S. frugiperda* insect cell line allows complex proteins to be produced with a high yield and post-translationally modified (Kost et al., 2005; Miller, 1993). The major species of baculovirus used for recombinant protein expression is the dsDNA virus *Autographa californica* multiple nucleopolyhedrosis virus (AcMNPV). AcMNPV is a lytic virus to both the insect cells in culture and its natural reservoir, larval stages of Lepidoptera (Blissard and Rohrmann, 1990). The genome of AcMNPV has been manipulated to remove the polyhedrin gene. Polyhedrin is expressed to very high levels in the natural infection cycle of AcMNPV, but is not essential for the growth of the virus in culture (Smith et al., 1983). By insertion of genes into this locus by homologous recombination between the baculovirus genome and a plasmid transfer vector, the protein of interest can be expressed at high levels. In order to remove all

the background, non-recombinant baculoviruses, a segment of an essential gene, *orf1629*, has also been deleted from the genome. This gene is then added to the transfer vector, complementing the baculovirus genome and resulting in rescue of only the recombinant viruses (Zhao et al., 2003).

The his-tagged full length PvPDEβ portion of this study was performed with help from Meredith Stewart (LSHTM), mistic-tagged full length PvPDEβ was expressed in collaboration with Avnish Patel (LSHTM).

6.2 Results

6.2.1 Expression of His-tagged full length PvPDEβ

The synthetic gene of *P. vivax* PDEβ was purchased from GeneArt (Invitrogen). The gene sequence was codon optimised for *Spodoptera frugiperda*, the baculovirus insect host cells, to maximise the production of recombinant protein from the system. The PvPDEβ gene and the pRN16 plasmid were digested with *Bam*HI and *Pst*I restriction endonucleases and ligated using procedures described in Chapter 2. Plasmid DNA was extracted from transformed colonies and analysed by restriction digest and sequencing to ensure the PDE insert was correct. A C-terminal His-tag was also included to enable purification and analysis of the expressed protein. *Sf*9 cells were transfected, and the virus amplified using the methods described in chapter 2.7. The transgenic virus (AcPvPDEβ-6xHis) was cloned by plaque purification. After a few rounds of viral passage to maximise the viral titre or the cloned viruses, IFAs were performed on the infected insect cells in order to visualise the expressed protein and to estimate which clones had the highest expression levels. IFAs, using antibodies against the C-terminal 6x His-tag, were performed as described in chapter 2.7.6. Two of the clones, clone 1 and clone 5, showed punctate fluorescence above the level of the negative control (uninfected Sf9 cells). The fluorescence was mostly in 2-4 foci at the periphery of the infected insect cell. Clone 5 appeared to have more expression of the protein as the staining was stronger. This could be due to increased viral titre in the culture as the insect cells also appeared to have greater cytopathic effects (reduced cell numbers due to cell lysis and irregular shaped cells caused by virus replication) than the clone 1 Sf9 cells (and the uninfected insect cells), or the protein itself could be cytopathic as increased expression correlates with this phenotype (figure 6.1).
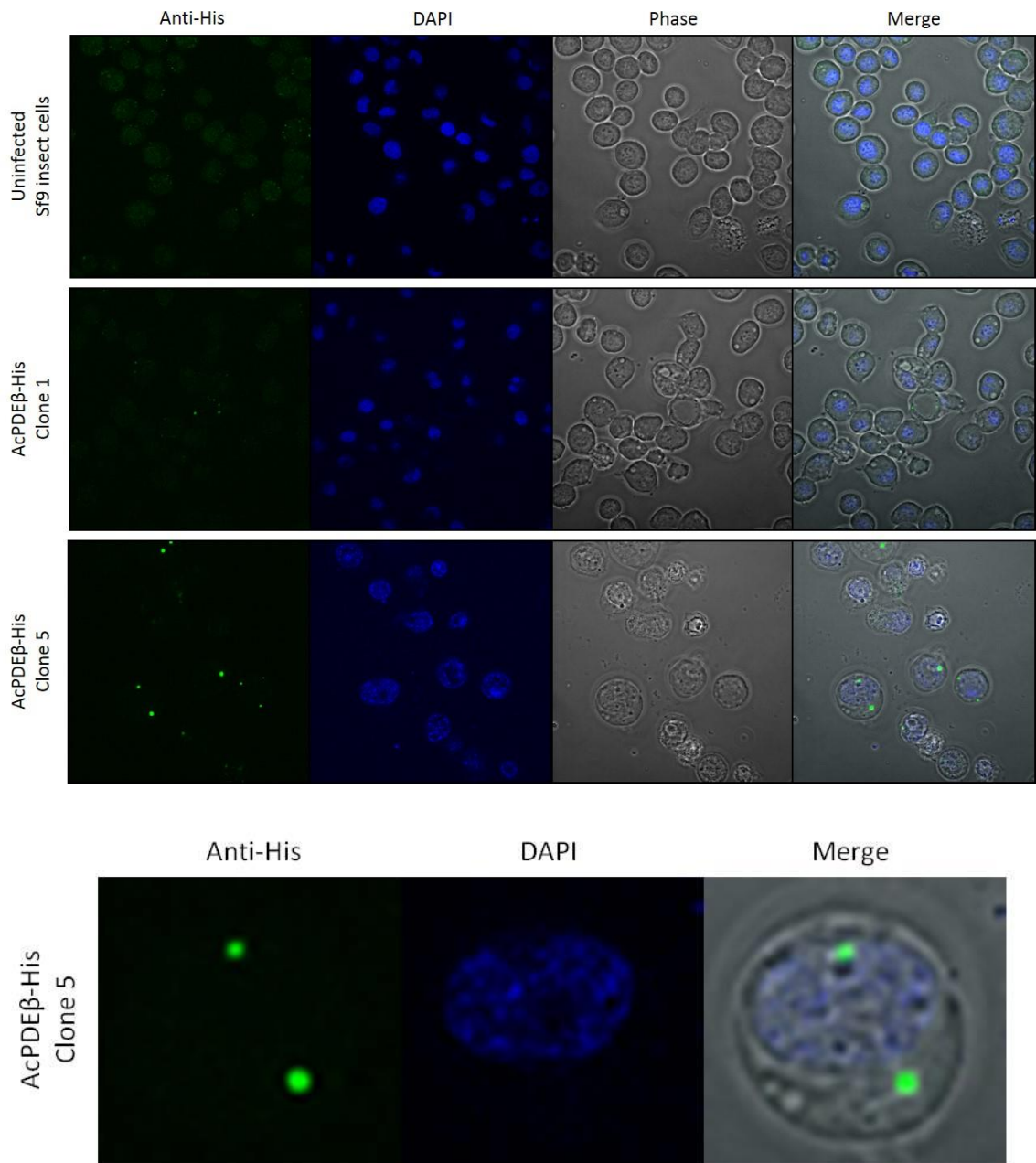
Figure 6.1 Sf9 insect cells positive for His-tagged expression of PvPDEβ

IFAs on formaldehyde fixed Sf9 cells infected with virus clone 1 (middle), clone 5 (lower) or uninfected (upper), were performed and representative images are shown for each. The insect cell nuclei were stained with DAPI, and the phase image is shown. PvPDEβ was stained with mouse monoclonal anti-His antibody (1:3000). The lower figure shows a cell at high magnification from the AcPvPDEβ-6xHis clone 5 infected cells showing two focal areas of fluorescence.

SDS-PAGE and western blotting was performed on whole cell lysates of the infected insect cells to investigate whether the expressed protein was of the expected size. Coomassie stained SDS-PAGE of whole infected insect cell lysates did not give any obvious differences between

AcPvPDEβ-6xHis infected and wild type baculovirus infected cells (figure 6.2). Western blotting was performed several times. Initially a very weak signal was seen, roughly consistent with the expected size (135 kDa) (figure 6.2), however the signal decreased with subsequent virus passages. Sf21 cells were also infected but gave no greater expression than the Sf9 cell line.
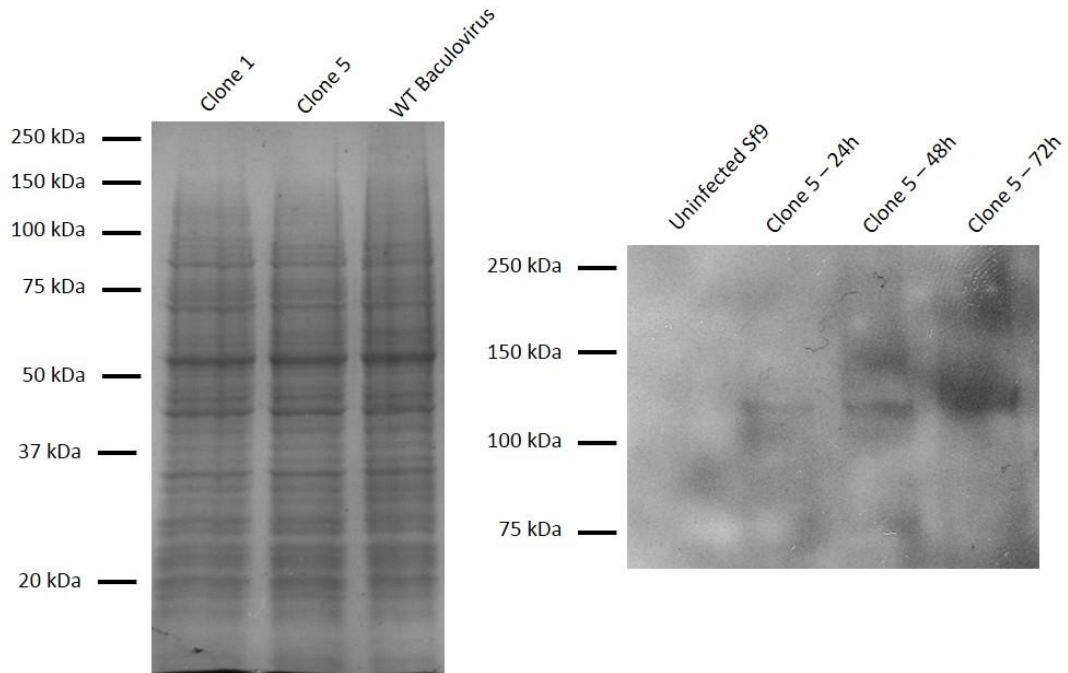
Figure 6.2 Western blot and SDS-PAGE of insect cell lysates
SDS-PAGE of whole infected cell lysate (left) showing AcPvPDEβ-6xHis (clones 1 and 5) compared to WT baculovirus infected cells. western blot showing a time course assay for PvPDEβ-6xHis compared to Uninfected Sf9 cells. The blot was probed with monoclonal mouse anti-His antibody at 1:3000.

6.2.2 Expression of Mistic-tagged full length PvPDEβ

The diminishing of the signal from the His-tag by western blot was not accompanied by a decrease in viral titre of the infection efficiency. It was postulated that the His-tag was unstable or difficult to detect with the antibody. Without an antibody specific to the protein it was not possible to purify the protein. To address the issue of low expression of this membrane protein, potentially due to cryptic translocation signals in an orthogonal system and instability of the His-tag, a second construct was designed utilising a Mistic-tag and a more stable 10x His-tag. A second reason for using a longer His-tag is that proteins sequestered in the membrane can sterically occlude binding between the tag and the affinity resin.

Integral membrane proteins can be extremely difficult to express. Membrane proteins have to be trafficked to the membrane which requires targeting signals that could be unrecognisable to the insect cell (or other expression system). Often, membrane proteins are targeted to inculsion bodies instead which necessitates renaturation of the protein from misfolded insoluble deposits which has had limited success (Laage and Langosch, 2001).

Mistic (<u>M</u>embrane <u>I</u>ntegrating <u>S</u>equence for <u>T</u>ranslation of <u>I</u>ntegral membrane protein <u>C</u>onstructs) is a 13 kDa (for sequence see appendix A5) integral membrane protein derived from *Bacillius subtilis* which is able to fold autonomously into cell membranes and drive the insertion of downstream peptides. This process is independent of the cellular translocon machinery (Roosild et al., 2005). The Mistic protein has been adapted to form a fusion tag that has been shown to dramatically increase yield and expression success of integral membrane proteins when expressed N-terminally to the gene of interest (Deniaud et al., 2011; Xu et al., 2013).

The full length PvPDEβ was cloned into the pAcH10Mistic YMI plasmid, containing an dual N-terminal 10x His-tag followed by the Mistic-tag and a glycine serine flexible linker of the sequence 2x(GGGS), using *Bam*HI endonucleases, to generate AcPvPDEβ-Mistic. Plasmid DNA was extracted from the transformed colonies and analysed by restriction digest and sequencing to ensure the PDE insert was correct and in frame. *Sf*9 cells were transfected, and the virus amplified using the materials and methods described in chapter 2.7.

SDS-PAGE and western blotting was performed on lysates of the infected insect cells to see if PvPDEβ-Mistic was successfully expressed and of the expected size. Coomassie stained SDS-PAGE of whole infected insect cell lysates did not give any obvious differences between AcPvPDEβ-Mistic infected and wild type baculovirus infected cells (data not shown). Western blotting using mouse monoclonal anti-His antibody showed two strong bands that were absent

in the uninfected insect cells. However these proteins were much smaller than expected at about 60 and 50 kDa; PvPDEβ with a 10x his tag and the Mistic tag is predicted to be about 151 kDa (figure 6.3). This protein was His-purified using the protocol described in chapter 2.7.8. Figure 6.3 shows the His-purified AcPvPDEβ-Mistic compared to lysates of uninfected insect cells. Very strong bands are present at about 70 and 50 kDa.
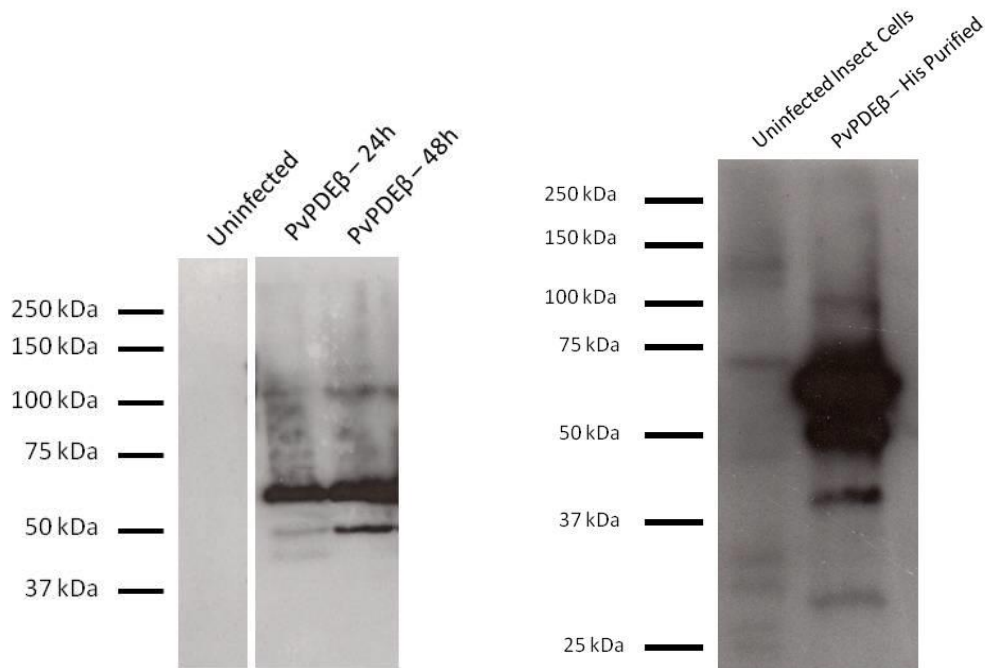
Figure 6.3 PvPDEβ-Mistic in whole cell lysate and His-purified
Western blots of whole infected cell lysate (left) and His-purified PvPDEβ-Mistic (right). Uninfected Sf9 cells were used as a control for both experiments. The blots were probed with monoclonal mouse anti-His antibody at 1:3000.

To test whether the purified PvPDEβ-Mistic contained cyclic nucleotide hydrolysing activity, PDE assays were performed. In addition to testing eluted protein, the nickel sepharose beads used in the purification were utilised to test for residual activity that could not be eluted. Uninfected Sf9 cells, treated identically to the AcPvPDEβ-Mistic infected cells, were used as a negative control. Hydrolysis of both cAMP and cGMP was measured. Purified PvPDEβ-Mistic did not show any activity in either the bead sample or the eluted sample for cAMP or cGMP. This was unsurprising as the His-tag is located at the N-terminal end of the protein and the catalytic domain of PvPDEβ is located at the C-terminus, it was unlikely that the expressed AcPvPDEβ-Mistic could result in an active enzyme (see figure 6.4) as the recombinant protein must be C-

terminally truncated. Curiously, the uninfected Sf9 bead sample showed high cAMP-PDE activity. This could be due to residual insect cell PDEs becoming trapped in the bead sample. This was not seen in the infected cell sample, possibly because the baculovirus efficiently shuts down many host cell functions, potentially including cell signalling (Du and Thiem, 1997).
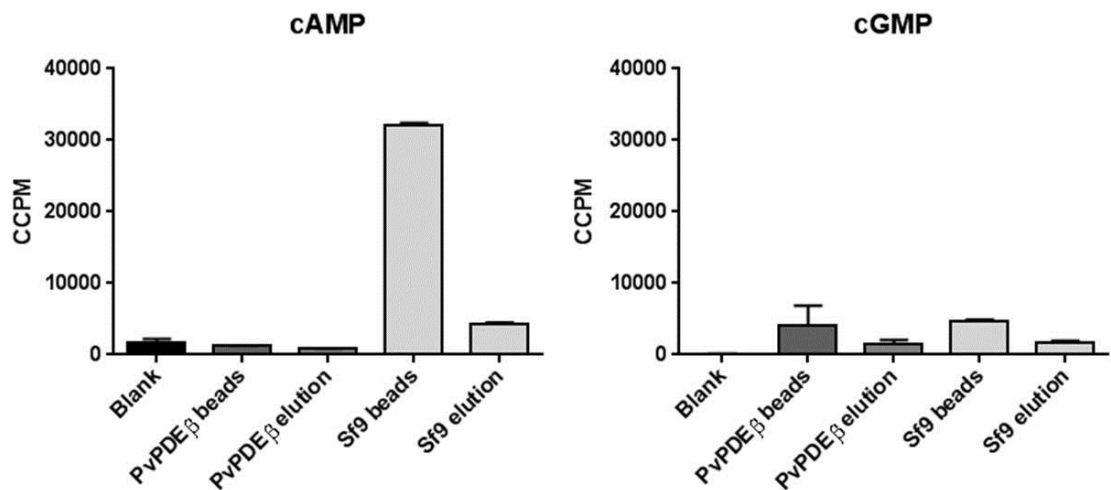
Figure 6.4 The PDE assay with His-purified PvPDEβ-Mistic was negative
Hydrolysis of cAMP (left) and cGMP (right) by PvPDEβ-Mistic or Sf9 cells, purified using nickel sepharose beads. Samples from the eluted fraction and the residual activity on the beads was tested. Activity is displayed as combined counts per minute (CCPM), a relative measure of scintillation. The assay was performed in duplicate and the error bars represent standard error of the mean.

6.3 Discussion

Two different approaches were attempted in order to generate recombinant PvPDEβ, using a C-terminal 6x His-tag and also an N-terminal 10x His-tag in conjunction with a Mistic tag. Unfortunately neither method resulted in a purified active enzyme. The AcPvPDEβ-6xHis construct initially produced a protein of approximately the correct estimated molecular weight, however it could not be detected following subsequent viral passages and the expression level was low. This could have been due to instability of the His-tag or removal of the tag by the host cell machinery, which made it impossible to purify the protein. The second approach AcPvPDEβ-Mistic, used a more stable 10x His-tag and a Mistic-tag to help traffic the protein to the cell membrane. There are currently no published results which utilise the Mistic-tag for *Plasmodium* proteins but it has lead to successful expression of a number of proteins in other organisms that were previously challenging to express (Xu et al., 2013). Although in this case AcPvPDEβ-Mistic resulted in a potentially truncated protein, the Mistic-tag may be useful for expressing other integral membrane *Plasmodium* proteins.

One potential application of the purified PvPDEβ-Mistic could be in generation of an antibody. Expression of PvPDEβ-Mistic does not result in a full length protein, however if the protein was proven by mass spectrometry to contain ~50 kDa of PvPDEβ then it could be significantly more immunogenic than the antipeptide antibodies. One potential complication could be whether a PvPDEβ antibody would cross-react with *P. falciparum* PDEβ orthologue, which is much more experimentally tractable species as *P. vivax* cannot be cultured *in vitro*. This could also be used in conjunction with the PDEβ-HA tagged line to validate the localisation studies in chapter 3. The most conserved part of the protein is the catalytic domain which is C-terminal and will not be present on the truncated PvPDEβ-Mistic as the His-tag used for purification is at the N-terminus. However, mass spectrometery would provide the sequence of the protein and it can be determined from these results whether it is worth using the PvPDEβ-Mistic to immunise animals.

Chapter 7: General discussion

7.1 Overview of the project

One of the aims of this project was to investigate the potential of asexual PfPDEs as targets for lead compound development as novel antimalarials. Through collaboration with Pfizer, a panel of human PDE inhibitors was made available to aid this objective. In addition to drug target validation, this project aimed to advance knowledge of the cell biology of phosphodiesterases in the asexual blood stages of *P. falciparum*. Phosphodiesterase β was the main focus of this project due to its predicted essential nature.

Prior to this study there was very little known about PfPDEβ. All previous attempts to knockout the gene have failed (David Baker, unpublished). Previous difficulty with generating reagents such as PDEβ specific antibodies, epitope tagged lines, recombinant protein and specific inhibitors has prevented progress in studying this molecule. This project has aimed to develop novel tools to aid the study of malaria parasite phosphodiesterases and the cyclic nucleotide signalling pathway.

7.2 Conditional knockdown of PfPDEβ

There are four PfPDEs, three of which can be knocked out in asexual blood stages. For two of the PDEs, the reason they could be genetically removed in asexual blood stages is that they are mosquito stage specific. PDEγ has a role in sporozoite formation and infectivity (Cathy Taylor, Thesis) and PDEδ is essential for gametogenesis in *P. falciparum* (Taylor et al., 2008) and ookinete formation and motility in *P. berghei* (Moon et al., 2009). Therefore disruption of these genes had no effect on blood stage proliferation and selection of transgenic parasites. PDEα, on the other hand, is predicted to be most highly expressed in late trophozoites and schizonts according to mRNA transcript data (López-Barragán et al., 2011), however removing the gene did not lead to any obvious phenotype in *in vitro* culture (Wentzinger et al., 2008). There have been several attempts to knock out PDEβ in both *P. falciparum* (David Baker, unpublished) and *P. berghei* (Oliver Bilker, personal communication), none of which have been successful. Therefore one of the major aims of this study was to attempt to develop a conditional knockdown system for PDEβ.

This project commenced before the initial development of the DiCre system and therefore, at the time, the DD-system was the only conditional knockdown system available to attempt. PDEα

was also included in this experiment, primarily as a positive control as it is not essential. Both the pPDEα-HA-DD and pPDEβ-HA-DD plasmids were successfully generated and used to transfect *P. falciparum* parasites. Unfortunately, despite repeated attempts the PDEβ-HA-DD plasmid did not integrate into the parasite genome. Southern blotting of the individual separate transfection experiments after four rounds of drug cycling indicated that the plasmid had formed stable episomes containing multiple copies of the plasmid. This phenomenon has been reported previously, particularly in cases where the presence of the plasmid was detrimental to the health of the parasite (O'Donnell, 2001). As the *pdeβ* locus was subsequently successfully epitope tagged with the HA-tag, it is possible that the DD-tag is in some way disadvantageous to the parasite, even in the absence of shield-1. A PDEα-HA-DD cloned line was successfully produced, however the presence or absence of shield had no effect on parasite growth and the HA-tag could never be detected with an anti-HA antibody. The reasons for this are unknown but it could be that the DD-tag is preventing appropriate expression or trafficking of PDEα. Ablation of PDEα would not be detected as the protein is not essential *in vitro* and there is no specific antibody that could detect a change in expression compared to the parental line. Regrettably, generation of conditionally regulated PDE-DD proteins was unsuccessful.

Towards the end of this project, the DiCre system was adapted for use with *P. falciparum*. Using this system, PDEβ became one of the first proteins to be targeted by conditional Cre-mediated genomic excision, in collaboration with Mike Blackman. The first strategy tested involved excision of the 3' UTR of *pdeβ* by inserting a pair of loxP sites at either end of this region. This approach has been effectively applied to the conditional knockout of essential genes in *T. gondii* (Andenmatten et al., 2013). Unfortunately, *P. falciparum* appears to be able to stabilise mRNA in this scenario, perhaps using cryptic polyadenylation functions in several genes tested (Mike Blackman, personal communication; Collins et al. 2013). This also seems to be true for PDEβ as, although the plasmid integrated and expression of the HA tag could be detected, 3' UTR excision does not lead to a decrease in the amount of protein expressed. As a result, a second construct was generated that aimed to induce excision of a fragment of the gene by insertion of the 5' loxP site into an intron within the predicted PDE catalytic domain. This construct has been successfully generated and used to transfect a PreDiCre *P. falciparum* line, generated in the Blackman lab, which already contains the DiCre recombinase gene. At the time of writing, the PDEβ-IntronLoxP parasite line was undergoing drug cycling in an attempt to create a stable, integrated line. However, a positive IFA result with the HA antibody has indicated successful integration of the plasmid. Colleagues in the Baker lab are currently carrying out rapamycin-

mediated cleavage and detecting excision using PCR as well as monitoring blood stages for any growth phenotype.

Generating parasite lines with integrated plasmids has traditionally been extremely time consuming. Very recently, there have been reports of major improvements in the ability to target specific areas of the *P. falciparum* genome using the CRISPR/Cas9 (clustered regularly interspaced short palindromic repeats) system. Briefly, CRISPR/Cas is used by bacteria as an adaptive immune defence system and has been adapted as an efficient genome modification tool. CRISPR RNAs (crRNAs), complexed with CRISPR associated (Cas) proteins result in double stranded DNA breaks of specific gene sequences. For genome editing, single guide RNAs (sgRNAs) can target the Cas9 protein to a particular locus of interest, lead to double strand DNA breaks, allowing insertion of a linearised plasmid using host cell repair machinery (Hsu et al., 2014; Mali et al., 2013). For *P. falciparum* this technique can generate stable parasite lines in a much shorter time frame than previously used methods as linear DNA can be transfected, eliminating the need for time consuming drug cycling (Ghorbal et al., 2014). This system will be extremely useful in generating new parasite lines to study all aspects of *P. falciparum*, including further characterisation of the PfPDEs. The following discussion sections include potential future work to continue this project, the CRISPR/Cas9 system could potentially be utilised to create many more transgenic parasite lines. Additionally, if the current PDEβ-IntronLoxP proves inefficient, CRISPR/Cas9 could be used to insert a LoxP site into a different region of PDEβ, or in the 5' non-coding region upstream of the gene to remove the entire gene.

7.3 Temporal and spatial expression of PfPDEβ

Despite not leading to a conditional knockdown of PDEβ, the attempt to create rapamycin induced 3' UTR removal did result in a PDEβ-HA stable parasite line. In this line the PDEβ protein could be detected using monoclonal anti-HA antibodies.

Prior to this study, most of the knowledge of PDEβ was based on what could be inferred from the gene sequence. For temporal expression, mRNA transcript data suggested that the levels of PDEβ peak in late trophozoites and schizonts (López-Barragán et al. 2011; Ross Cummings, Thesis). Additionally, Ross Cummings performed PDE assays on parasite lysates at different life cycle stages. He found that in asexual blood stages, both cAMP and cGMP PDE activity peaked in schizonts. Late ring stages and late trophozoites also had significant levels of PDE activity, with early trophozoites containing least cyclic nucleotide hydrolytic activity. In general the level of cGMP-PDE activity was higher than cAMP-PDE activity and this was most pronounced in

schizont and late ring stages. Work during this project has confirmed that PDEβ is most highly expressed in schizonts (figure 4.2). Signal obtained in immunofluorescence assays indicated that mid-trophozoites contain the highest levels of PDEβ protein, with levels decreasing in very late schizonts (figure 4.3). It would also be beneficial to perform further western blots on tightly synchronised PDEβ-HA parasites over a greater number of time points, particularly around the schizont stages to further investigate the apparent decrease in PDEβ protein expression in very late schizonts. If possible it would also be interesting to perform western blotting on merozoite stages. As ring stages contain cyclic nucleotide hydrolytic activity and PDEβ-HA has not been detected in this stage, it is possible that PDEα is the major PDE at this stage. This would also fit with the observation that cGMP-PDE activity is predominant at this stage as PDEα has been shown to be cGMP specific. To fully dissect the temporal expression of the asexual PfPDEs, it will be necessary to generate a PDEα-tagged line and/or a PDEα specific antibody. A very preliminary experiment looking at the stage specificity of Pfizer PDE inhibitor induced killing of *P. falciparum in vitro* has implied that addition of the drugs to ring stages or schizont stages leads to rapid death of the parasites. Addition of the drugs to trophozoites does not result in death of the parasites until later in the cycle (figure 5.20). This would fit with the PDE activity data, however the lack of PDEβ detected in ring stages is surprising considering this result. From mRNA transcript data, none of the four PDEs are predicted to be expressed in ring stages. Potentially the highly PDEβ specific Pfizer inhibitors such as PF-05225388, PF-00394183 or PF-00388991 on both the 3D7 and PDEα-KO lines at different life cycle stages could be used to determine which PDE is predominantly responsible for this activity. It is also important to consider the possibility that there may be off target effects of the inhibitors.

Before this study, PDEβ was assumed to be an integral membrane protein on the basis of six predicted transmembrane domains in its deduced amino acid sequence and due to the fact that all previous studies have identified PfPDE activity in the membrane fraction of parasite lysates only (Yuasa et al. 2005; Wentzinger et al. 2008; Ross Cummings, Thesis). This has been confirmed by solubility assays during this project (figure 4.1), as well as PDE assays on sequentially solubilised parasite lysate fractions (figure 5.11).

The PDEβ-HA tagged line was also used to determine spatial expression. Prior to this study, the only implied subcellular location of PDEβ was the bioinformatics prediction that the catalytic domain projected into the PV lumen, using hidden Markov topography (Gould and de Koning, 2011). Through colocalisation studies in this project, this seems to be incorrect and that PDEβ colocalises with markers of the endoplasmic reticulum (ER). Three lines of evidence point

towards PDEβ being located in the ER. Firstly, PDEβ-HA strongly colocalises with the ER marker BiP (figure 4.4). This is consistent in all life cycle stages tested which also implies that PDEβ does not change location throughout the *P. falciparum* asexual blood stage life cycle but remains within the ER. Interestingly, PDEβ-HA does not colocalise with ERD2, suggesting that its function is ER-specific and it is not trafficked through the Golgi. Secondly, PDEβ-HA partially colocalises with MSP1 before it becomes merozoite surface associated, presumably as it is trafficked through the ER. Thirdly, PDEβ-HA colocalises with ER-Tracker, a commercial ER stain. This signal was very weak as the stain is predominantly for use with live cell staining. It would be extremely useful to produce a PDEβ-GFP tag to enable live cell studies of PDEβ. It has been known for proteins to be mislocalised to the endoplasmic reticulum as a result of C-terminal epitope tagging.   In mammalian cells, a KDEL (lysine-aspartic acid-glutamic acid-leucine) motif is important for retention of certain proteins within the ER (Cancino et al., 2013). In *P. falciparum*, a SDEL (serine-aspartic acid-glutamic acid-leucine) motif has been shown to play a homologous role, and indeed PfBiP contains this sequence at its C-terminus (Kumar et al., 1991). However, this seems to be more important for soluble proteins, plasmepsin V, an integral membrane protein that is also localised to the ER does not contain the SDEL sequence (PlasmoDB). PfPDEβ also does not contain the SDEL motif. ER retention of membrane proteins appears to be more complex, with several different mechanisms proposed such as lysine-lysine-X-X sequence at the C-terminus (Jackson et al., 1990) or the retention factor p11 with the sequence (histidine/lysine)-X-lysine-X-X-X (Renigunta et al., 2006).   Additionally, multi-spanning transmembrane proteins often use the first TM domain in place of the signal peptide (Rapoport, 2007). No ER integral membrane retention factors have been described for *P. falciparum*. It cannot be fully ruled out that PDEβ-HA is being mislocalised to the ER, however as it is an essential protein, it must be able to perform appropriate functions in the ER as the parasites do not have a growth phenotype. One possibility is that a portion of PDEβ is being targeted to the appropriate subcellular localisation and the HA-tag is cleaved (resulting in no signal at the appropriate localisation). To conclusively prove that PfPDEβ is an ER resident protein, a PDEβ specific antibody would need to be generated. Assuming that PfPDEβ is localised to the ER, it would also be interesting to determine whether the catalytic domain projects into the cytoplasm or the ER lumen. This could be determined by immunogold labelling electron microscopy. As future work it would also be very interesting to generate a PDEα-HA tagged line, (potentially in combination with a DiCre mediated conditional knockdown system) to determine the temporal and spatial localisation of PDEα.

A major feature of cyclic nucleotide signalling pathways in mammalian systems is the presence of signalosomes, complexes of signalling associated molecules that are spatially organised to result in maximum efficiency of the response. In mammalian systems, PKA signalling molecules, including PDEs, are often complexed with A-kinase anchoring proteins (AKAPs) and PKG signalling with PKG interacting partner (GKIP) proteins (see chapter 1.10.2). In *P. falciparum*, only one putative PfAKAP (PF3D7_0512900) protein has been identified on the basis of sequence homology. PfAKAP antipeptide antibodies (through collaboration with Anaïs Merckx) were tested in dual staining IFAs with PDEβ-HA and no colocalisation was observed. Dual staining IFAs were also performed with the commercial PKG antibody on PDEβ-HA, unfortunately the signal was too weak to infer any colocalisation. However, previous work in the group had identified partial overlap between PfPKG and the ER marker PfBiP. It is therefore likely that this association would hold with PKG and PDEβ-HA. However preliminary data using immunoprecipitation and subsequent western blotting of PDEβ-HA did not co-precipitate PKG (Oriana Kreutzfeld, LSHTM, MSc Project). It would be worthwhile to perform colocalisations and co-immunoprecipitations with other known cyclic nucleotide signalling protein such as PKA regulatory and catalytic domains, and the cyclases to try to identify potential signalosomes in *P. falciparum*. Interestingly, a study into the Rab GTPases, important regulators of vesicular trafficking, reported that the catalytic domain of PKA (PKA-C) is recruited to PfRab5A+ and PfRab7+ vesicles. The authors suggested that these Rab proteins may act as pseudo-AKAP proteins (Rached et al., 2012). A comparison may also be drawn to mammalian Rab4 and Rab11A which are able to bind D-AKAP2 and recruit PKA to endosomes, where it regulates transferrin receptor recycling (Eggers et al., 2009).

An emerging role of cyclic nucleotide signalling in malaria parasites is in calcium release or mobalisation, which in itself has a link with the endoplasmic reticulum. As mentioned in chapter 1.10.1, calcium ions are important secondary signalling molecules. The ER is thought to be one of the major Ca^{2+} stores within the parasite cell (Passos and Garcia, 1997). IP_3 signalling leads to release of Ca^{2+} from the ER, resulting in a rise in the cytosolic calcium concentration (Ma et al., 2000). As discussed in chapter 1.12, there are many overlaps between cyclic nucleotide and calcium signalling including, but not limited to; microneme secretion in sporozoites (Mota et al., 2002), motility in merozoite (Lasonder et al., 2012) and ookinete (Moon et al., 2009) stages, gametocyte activation (McRobert et al., 2008), egress in schizont stages (Dvorin et al., 2010; Taylor et al., 2010) and phosphoinositide metabolism (Brochet et al., 2014). One potential function of PDEβ in these instances could be to keep cyclic nucleotide levels low to prevent inappropriate calcium release from the ER.

In one particular example, a recent study by Collins et al. into PKG mediated merozoite secretory organelle discharge and egress, found that addition of zaprinast (a PDE inhibitor) to very late stage schizonts, lead to discharge of the secretory organelles and resulted in premature egress of the merozoites. Usually, BAPTA-AM (a calcium chelator), prevents merozoite egress. Notably in this study, this egress block could be overcome by addition of 75 µM of zaprinast. The authors hypothesised that stimulation of PfPKG by zaprinast (through inhibition of PDE activity and elevation of cGMP levels) may lead to increased levels of calcium signalling, resulting in egress (Collins et al. 2013). Much more work is necessary before the precise roles of PDEα and PDEβ can be elucidated in egress, however the characterisation of highly specific PDEβ inhibitors should be able to help pinpoint whether this phenotype is PDEβ specific.

7.4 Biochemical properties of PfPDEβ

One of the major aims of this project was to determine the cyclic nucleotide specificity of PDEβ. It was previously assumed to be a dual specific PDE on the basis that PDEα is cGMP specific (Yuasa et al., 2005), and that in a PDEα-KO line, both cAMP- and cGMP-PDE activity was present (Wentzinger et al., 2008). As PDEβ is the only other predicted asexual blood stage PDE, it was assumed that it was able to hydrolyse both cyclic nucleotides in the absence of PDEα. In 2004, Zhang et al, proposed a mechanism for cyclic nucleotide selectivity by the mammalian PDEs. An invariant glutamine was identified as key to detection of the purine moiety in the cyclic nucleotide. The surrounding residues anchor the glutamine in a different orientation for cAMP than cGMP, and in dual specific PDEs, a nearby histidine residue allowed the glutamine to shift between the two conformations. This was termed the 'glutamine switch' (Zhang et al., 2004). However this has been shown to be significantly more complex than previously thought, and not all the PDE families conform to this theory (Ke et al., 2011). As part of his thesis (2005), Ross Cummings modelled the active site of PDEβ (and PDEδ) using the Deep View Swiss-PdbViewer (v3.7). Using this he proposed that PDEβ was dual specific as the invariant glutamine (Q_{1052} in PfPDEβ) would be able to rotate freely, as proposed by Zhang et al. Ross Cummings also proposed that PDEδ was a cGMP specific PDE using this modelling method, which was later confirmed by Taylor et al. in 2008. The current study has provided the first direct evidence that PDE beta has dual specificity using immunoprecipitated PDEβ-HA in a PDE activity assay. PDEβ-HA is able to hydrolyse both cAMP and cGMP. With this enzyme it will now be possible to determine the specific kinetic properties of PDEβ including specific substrate affinity by determining the K_m (the Michaelis constant, the substrate concentration at which the reaction rate is at half-maximum) of cAMP and cGMP hydrolysis. A further point to note is that for future

PDE assays it would be highly useful to perform a Bradford assay on the samples to be able to equate the amount of protein to the PDE activity. This will be particularly important when calculating the kinetic constants.

PDEs are dependent on two divalent metal cofactors. All PDEs are predicted to contain a tightly bound Zn^{2+} ion, coordinated by conserved histidines and aspartates (Wang et al., 2005). This ion has been described as structurally important and essential for enzyme function (Conti and Beavo, 2007). The second metal ion binds less tightly to the enzyme, several divalent cations are able to support catalysis *in vitro*, but it is predicted that manganese or magnesium are usually the relevant physiological ion (Houslay et al., 1997). One possible explanation for lower affinity binding is the presence of five water molecules that coordinate this ion with other residues (Xu et al., 2000). Ross Cummings found that Mg^{2+} supported the highest level of PDE activity in asexual blood stage parasite lysates of 3D7. Interestingly recombinant PDEα shows greatest activity when supplemented with Mn^{2+} (Yuasa et al., 2005). It is possible that Mn^{2+} is the most potent activator of PDEα and Mg^{2+} is for PDEβ. This could explain the discrepancy between recombinant PDEα enzyme and parasite lysate metal ion dependent activity. With the immunoprecipitated PDEβ-HA is should be possible to determine if this is the case by supplementing the buffer with different metal ions.

7.5 PfPDEα

PDEα was not the main focus of this project, however to fully understand the role of phosphodiesterases in the context of the cyclic nucleotide signalling pathways in malaria it is essential to gain a better understanding of all the PDEs. PDEα is not essential in asexual blood stage culture as it has been successfully knocked out. This PDEα-KO line has a subtle growth phenotype. Wentzinger et al., noted that ring stages appear earlier after synchronisation than for the parental line. This study also showed that the line reaches a higher parasitaemia, more quickly than all other parasite lines tested. This phenomenon was discussed in greater detail in chapter 3.3.2. However the phenotype is interesting and needs further investigation to validate that it is PDEα specific. For future work it would be important to generate a second PDEα-KO line. Even if this line does not have a growth phenotype it would be extremely interesting to also put PDEβ under DiCre conditional knockout control (if possible) to create a line that would have no asexual PDEs when excision is induced. It would also be important to generate an antibody against PfPDEα. Ideally a PDEα specific antibody would also be produced. As a recombinant catalytic domain of PDEα can be expressed it should be possible to use this to

generate an antibody. However it would also be useful to create an HA- or GFP-tagged line, although the HA tag could not be detected in the PDEα-HA-DD line the reasons for this were unknown. It could be that the DD tag was preventing expression of the protein. An HA- or GFP-tag alone could feasibly be less detrimental to the parasite. Other potential ways to investigate the growth rate phenotype of PDEα-KO would be to complement the gene or perform whole genome sequencing of the parasite compared to WT. Even if the phenotype is not PDEα specific, whole genome sequencing would be informative to determine what is different compared to the WT and may point towards another gene that is responsible. It could also determine the reason why PDEα-KO does not produce gametocytes.

Additionally any future transgenic studies should be performed on gametocyte producing lines to confirm that PDEα does not have a role in gametocytogenesis. It would also be worthwhile to create a *P. berghei* knockout to confirm that PDEα is truly indispensable and not an artefact of culture conditions. A *P. berghei* knockout could also determine if PDEα has a function in any mosquito or liver stages of the lifecycle.

7.6 PfPDEβ as a target for antimalarial drug discovery

One approach for drug development for infectious diseases has relied on targeting proteins or pathways that are absent in their mammalian host, this is called the 'silver bullet' paradigm. Eukaryotic parasites such as *Plasmodium* spp. are genetically similar and metabolic pathways are highly related to those of the human host. This can make drug development according to the silver bullet theory challenging. However, the field is shifting towards more of an 'inverted silver bullet' approach. Established drug targets in humans are explored and the current drugs repurposed through rational drug design to become highly specific for the pathogen and not the host. Phosphodiesterases represent a potential avenue to explore in the context of antimalarials. Additionally, PDEs in members of the kinetoplastid family such as *Trypanosoma brucei*, the protozoan causative agent of African sleeping sickness, are currently being explored as potential drug targets (Amata et al., 2014; Jansen et al., 2013).

Phosphodiesterases are established drug targets for many human diseases. Despite the large number of members of the PDE family in mammalian cells, PDE inhibitors can be highly specific for their target. There is therefore the potential to develop inhibitors that are exclusively specific for the PfPDEs. Two PfPDEs are essential at key stages of the parasite life cycle that have the potential to be targeted with antimalarials. PfPDEβ, as explored in this project, is essential for asexual blood stage growth, the cause of clinical pathology of malaria. PfPDEδ is essential for

transmission to the mosquito. Compound that target these enzymes have the potential to prevent clinical disease and block onward transmission.

This project has demonstrated that specific PDEβ inhibitors are lethal to the parasite *in vitro* with IC50s comparable to current clinically available drugs such as chloroquine and artemisinin. This is a first important step in validating phosphodiesterase inhibitors as potential antimalarials. The compounds PF-01273175, PF-05184913, PF-05225388, PF-00394183 and PF-00388991 should be taken forward as lead compounds for further medicinal chemistry development. Animal studies using *P. berghei* infected mice are an essential step to test the validity of these compounds as effective drugs. Bioavailabilty, amongst other complex factors in the setting of infection of whole organisms may be limiting. If the compounds are not active in mice then there would be several other experiments to attempt. It is possible that the compounds are highly specific for PfPDEβ and are less active against *P. berghei* PDEβ. To combat this a *P. berghei* strain could be modified to replace the PbPDEβ with PfPDEβ. It would also be beneficial to perform pharmacokinetic studies on the compounds to determine absorption and half life rates to ensure that the drug is available to the parasite long enough for drug activity. If the pharmacokinetics are unfavourable, a chemistry programme could be carried out to improve this whilst retaining potency against *P. falciparum in vivo*.

Of the 14 PF- compounds provided by Pfizer, seven have IC50s of less than 160 nM against the parasite. Of these, five were shown to be potent inhibitors of PDE activity within the parasite. It is likely that the other two compounds are guanylyl cyclase inhibitors and also have the potential to be useful in future studies on the cyclic nucleotide signalling pathways. Three of the compounds, PF-05225388, PF-00394183 and PF-00388991, which are based on the human PDE5 inhibitor series, have PDEβ specific activity and are active against the parasite at IC50s of between 5 and 82 nM. Compound PF-05225388 is over 5000 times more potent than zaprinast against the parasite.

In summary, this project has demonstrated that PfPDEβ represents a novel target for antimalarial drug development. Inhibitors exist within current human drug libraries that are highly potent and specific for PfPDEβ. These compounds not only inhibit enzyme activity but also kill the parasite at concentrations comparable to those of current antimalarials. The pathways that PfPDEβ is involved with are essential for parasite survival. The results of this thesis are to be used in an application to the Tres Cantos Open lab to explore GSK compound libraries for PDEβ inhibitors. In addition, this study has also begun to develop the tools necessary for further study of the role of the PfPDEs in the context of malaria infection, such as the PDEβ-

HA tagged line which can provide active enzyme for an effective PDE activity assay developed for this project. Previously little was known about the biology of PfPDEβ but this study has confirmed its dual specific cyclic nucleotide activity and tentatively identified its subcellular location as the endoplasmic reticulum. Work to generate a conditional knockdown of PfPDEβ is ongoing as the detailed biology of this essential drug target still largely remains elusive, however this study has paved the way for future insights.

References

Abay, S.M. (2013). Blocking malaria transmission to Anopheles mosquitoes using artemisinin derivatives and primaquine: a systematic review and meta-analysis. Parasit. Vectors *6*, 278.

Achan, J., Talisuna, A.O., Erhart, A., Yeka, A., Tibenderana, J.K., Baliraine, F.N., Rosenthal, P.J., and D'Alessandro, U. (2011). Quinine, an old anti-malarial drug in a modern world: role in the treatment of malaria. Malar. J. *10*, 144.

Agnandji, S.T., Lell, B., Soulanoudjingar, S.S., Fernandes, J.F., Abossolo, B.P., Conzelmann, C., Methogo, B.G.N.O., Doucka, Y., Flamen, A., Mordmüller, B., et al. (2011). First results of phase 3 trial of RTS,S/AS01 malaria vaccine in African children. N. Engl. J. Med. *365*, 1863–1875.

Agnandji, S.T., Lell, B., Fernandes, J.F., Abossolo, B.P., Methogo, B.G.N.O., Kabwende, A.L., Adegnika, A.A., Mordmüller, B., Issifou, S., Kremsner, P.G., et al. (2012). A phase 3 trial of RTS,S/AS01 malaria vaccine in African infants. N. Engl. J. Med. *367*, 2284–2295.

Agop-Nersesian, C., Pfahler, J., Lanzer, M., and Meissner, M. (2008). Functional expression of ribozymes in Apicomplexa: towards exogenous control of gene expression by inducible RNA-cleavage. Int. J. Parasitol. *38*, 673–681.

Ahmad, F., Degerman, E., and Manganiello, V.C. (2012). Cyclic nucleotide phosphodiesterase 3 signaling complexes. Horm. Metab. Res. *44*, 776–785.

Alam, M.M., Solyakov, L., Bottrill, A.R., Flueck, C., Siddiqui, F., Singh, S., Mistry, S., Viskaduraki, M., Lee, K., Hopp, C.S., et al. (2014). Phosphoproteomics reveals malaria parasite Protein Kinase G as a signalling hub regulating egress and invasion.

Alberts, B., Johnson, A., Lewis, J., Raff, M., Roberts, K., and Walter, P. (2002). Molecular Biology of the Cell.

Alexander, D.L., Arastu-Kapur, S., Dubremetz, J.-F., and Boothroyd, J.C. (2006). Plasmodium falciparum AMA1 binds a rhoptry neck protein homologous to TgRON4, a component of the moving junction in Toxoplasma gondii. Eukaryot. Cell *5*, 1169–1173.

Alves, E., Bartlett, P.J., Garcia, C.R.S., and Thomas, A.P. (2011). Melatonin and IP3-induced Ca2+ release from intracellular stores in the malaria parasite Plasmodium falciparum within infected red blood cells. J. Biol. Chem. *286*, 5905–5912.

Amata, E., Bland, N.D., Hoyt, C.T., Settimo, L., Campbell, R.K., and Pollastri, M.P. (2014). Repurposing human PDE4 inhibitors for neglected tropical diseases: Design, synthesis and evaluation of cilomilast analogues as Trypanosoma brucei PDEB1 inhibitors. Bioorg. Med. Chem. Lett. *24*, 4084–4089.

Andenmatten, N., Egarter, S., Jackson, A.J., Jullien, N., Herman, J.-P., and Meissner, M. (2013). Conditional genome engineering in Toxoplasma gondii uncovers alternative invasion mechanisms. Nat. Methods *10*, 125–127.

Angrisano, F., Riglar, D.T., Sturm, A., Volz, J.C., Delves, M.J., Zuccala, E.S., Turnbull, L., Dekiwadia, C., Olshina, M.A., Marapana, D.S., et al. (2012). Spatial localisation of actin filaments across developmental stages of the malaria parasite. PLoS One *7*, e32188.

Anstey, N.M., Douglas, N.M., Poespoprodjo, J.R., and Price, R.N. (2012). Plasmodium vivax: clinical spectrum, risk factors and pathogenesis. Adv. Parasitol. *80*, 151–201.

Ariey, F., Witkowski, B., Amaratunga, C., Beghain, J., Langlois, A.-C., Khim, N., Kim, S., Duru, V., Bouchier, C., Ma, L., et al. (2014). A molecular marker of artemisinin-resistant Plasmodium falciparum malaria. Nature *505*, 50–55.

Armstrong, C.M., and Goldberg, D.E. (2007). An FKBP destabilization domain modulates protein levels in Plasmodium falciparum. Nat. Methods *4*, 1007–1009.

Augagneur, Y., Wesolowski, D., Tae, H.S., Altman, S., and Ben Mamoun, C. (2012). Gene selective mRNA cleavage inhibits the development of Plasmodium falciparum. Proc. Natl. Acad. Sci. U. S. A. *109*, 6235–6240.

De Azevedo, M.F., Gilson, P.R., Gabriel, H.B., Simões, R.F., Angrisano, F., Baum, J., Crabb, B.S., and Wunderlich, G. (2012). Systematic analysis of FKBP inducible degradation domain tagging strategies for the human malaria parasite Plasmodium falciparum. PLoS One *7*, e40981.

Bacskai, B.J., Hochner, B., Mahaut-Smith, M., Adams, S.R., Kaang, B.K., Kandel, E.R., and Tsien, R.Y. (1993). Spatially resolved dynamics of cAMP and protein kinase A subunits in Aplysia sensory neurons. Science *260*, 222–226.

Baer, K., Klotz, C., Kappe, S.H.I., Schnieder, T., and Frevert, U. (2007). Release of hepatic Plasmodium yoelii merozoites into the pulmonary microvasculature. PLoS Pathog. *3*, e171.

Baker, D.A. (2011). Cyclic nucleotide signalling in malaria parasites. Cell. Microbiol. *13*, 331–339.

Balaji, S., Babu, M.M., Iyer, L.M., and Aravind, L. (2005). Discovery of the principal specific transcription factors of Apicomplexa and their implication for the evolution of the AP2-integrase DNA binding domains. Nucleic Acids Res. *33*, 3994–4006.

Banaszynski, L.A., Chen, L.-C., Maynard-Smith, L.A., Ooi, A.G.L., and Wandless, T.J. (2006). A rapid, reversible, and tunable method to regulate protein function in living cells using synthetic small molecules. Cell *126*, 995–1004.

Bannister, L., and Mitchell, G. (2003). The ins, outs and roundabouts of malaria. Trends Parasitol. *19*, 209–213.

Bannister, L.H., and Mitchell, G.H. (2009). The malaria merozoite, forty years on. Parasitology *136*, 1435–1444.

Bannister, L.. H., Hopkins, J.. M., Fowler, R.. E., Krishna, S., and Mitchell, G.. H. (2000). A brief illustrated guide to the ultrastructure of Plasmodium falciparum asexual blood stages. Parasitol. Today *16*, 427–433.

Baum, J., Richard, D., Healer, J., Rug, M., Krnajski, Z., Gilberger, T.-W., Green, J.L., Holder, A.A., and Cowman, A.F. (2006). A conserved molecular motor drives cell invasion and gliding motility across malaria life cycle stages and other apicomplexan parasites. J. Biol. Chem. *281*, 5197–5208.

Beghyn, T.B., Charton, J., Leroux, F., Laconde, G., Bourin, A., Cos, P., Maes, L., and Deprez, B. (2011). Drug to genome to drug: discovery of new antiplasmodial compounds. J. Med. Chem. *54*, 3222–3240.

Beghyn, T.B., Charton, J., Leroux, F., Henninot, A., Reboule, I., Cos, P., Maes, L., and Deprez, B. (2012). Drug-to-genome-to-drug, step 2: reversing selectivity in a series of antiplasmodial compounds. J. Med. Chem. *55*, 1274–1286.

Bei, A.K., Membi, C.D., Rayner, J.C., Mubi, M., Ngasala, B., Sultan, A.A., Premji, Z., and Duraisingh, M.T. (2007). Variant merozoite protein expression is associated with erythrocyte invasion phenotypes in Plasmodium falciparum isolates from Tanzania. Mol. Biochem. Parasitol. *153*, 66–71.

Bender, A.T., and Beavo, J.A. (2006). Cyclic nucleotide phosphodiesterases: molecular regulation to clinical use. Pharmacol. Rev. *58*, 488–520.

Beraldo, F.H., Almeida, F.M., da Silva, A.M., and Garcia, C.R.S. (2005). Cyclic AMP and calcium interplay as second messengers in melatonin-dependent regulation of Plasmodium falciparum cell cycle. J. Cell Biol. *170*, 551–557.

Berg JM, Tymoczko JL, S.L. (2002). Signal-Transduction Pathways: An Introduction to Information Metabolism.

Billker, O., Lindo, V., Panico, M., Etienne, A.E., Paxton, T., Dell, A., Rogers, M., Sinden, R.E., and Morris, H.R. (1998). Identification of xanthurenic acid as the putative inducer of malaria development in the mosquito. Nature *392*, 289–292.

Billker, O., Dechamps, S., Tewari, R., Wenig, G., Franke-Fayard, B., and Brinkmann, V. (2004). Calcium and a Calcium-Dependent Protein Kinase Regulate Gamete Formation and Mosquito Transmission in a Malaria Parasite. Cell *117*, 503–514.

Birkholtz, L.-M., Blatch, G., Coetzer, T.L., Hoppe, H.C., Human, E., Morris, E.J., Ngcete, Z., Oldfield, L., Roth, R., Shonhai, A., et al. (2008). Heterologous expression of plasmodial proteins for structural studies and functional annotation. Malar. J. *7*, 197.

Bishop, D.H. (1990). Gene expression using insect cells and viruses. Curr. Opin. Biotechnol. *1*, 62–67.

Blackman, M.J., and Carruthers, V.B. (2013). Recent insights into apicomplexan parasite egress provide new views to a kill. Curr. Opin. Microbiol. *16*, 459–464.

Blackman, M.J., Scott-Finnigan, T.J., Shai, S., and Holder, A.A. (1994). Antibodies inhibit the protease-mediated processing of a malaria merozoite surface protein. J. Exp. Med. *180*, 389–393.

Blissard, G.W., and Rohrmann, G.F. (1990). Baculovirus diversity and molecular biology. Annu. Rev. Entomol. *35*, 127–155.

Bollen, E., and Prickaerts, J. (2012). Phosphodiesterases in neurodegenerative disorders. IUBMB Life *64*, 965–970.

Boolell, M., Allen, M.J., Ballard, S.A., Gepi-Attee, S., Muirhead, G.J., Naylor, A.M., Osterloh, I.H., and Gingell, C. (1996). Sildenafil: an orally active type 5 cyclic GMP-specific phosphodiesterase inhibitor for the treatment of penile erectile dysfunction. Int. J. Impot. Res. *8*, 47–52.

Brancucci, N.M.B., Bertschi, N.L., Zhu, L., Niederwieser, I., Chin, W.H., Wampfler, R., Freymond, C., Rottmann, M., Felger, I., Bozdech, Z., et al. (2014). Heterochromatin Protein 1 Secures Survival and Transmission of Malaria Parasites. Cell Host Microbe *16*, 165–176.

Brecht, S., Erdhart, H., Soete, M., and Soldati, D. (1999). Genome engineering of Toxoplasma gondii using the site-specific recombinase Cre. Gene *234*, 239–247.

Bregman, D.B., Bhattacharyya, N., and Rubin, C.S. (1989). High affinity binding protein for the regulatory subunit of cAMP-dependent protein kinase II-B. Cloning, characterization, and expression of cDNAs for rat brain P150. J. Biol. Chem. *264*, 4648–4656.

Brochet, M., Collins, M.O., Smith, T.K., Thompson, E., Sebastian, S., Volkmann, K., Schwach, F., Chappell, L., Gomes, A.R., Berriman, M., et al. (2014). Phosphoinositide Metabolism Links cGMP-Dependent Protein Kinase G to Essential Ca2+ Signals at Key Decision Points in the Life Cycle of Malaria Parasites. PLoS Biol. *12*, e1001806.

Brockelman, C.R. (1982). Conditions favoring gametocytogenesis in the continuous culture of Plasmodium falciparum. J. Protozool. *29*, 454–458.

Broughton, B.J., Chaplen, P., Knowles, P., Lunt, E., Pain, D.L., Wooldridge, K.R., Ford, R., Marshall, S., Walker, J.L., and Maxwell, D.R. (1974). New inhibitor of reagin-mediated anaphylaxis. Nature *251*, 650–652.

Brunelli, M., Castellucci, V., and Kandel, E.R. (1976). Synaptic facilitation and behavioral sensitization in Aplysia: possible role of serotonin and cyclic AMP. Science *194*, 1178–1181.

Budu, A., and Garcia, C.R.S. (2012). Generation of second messengers in Plasmodium. Microbes Infect. *14*, 787–795.

Buxton, I.L., and Brunton, L.L. (1983). Compartments of cyclic AMP and protein kinase in mammalian cardiomyocytes. J. Biol. Chem. *258*, 10233–10239.

Campbell, T.L., De Silva, E.K., Olszewski, K.L., Elemento, O., and Llinás, M. (2010). Identification and genome-wide prediction of DNA binding specificities for the ApiAP2 family of regulators from the malaria parasite. PLoS Pathog. *6*, e1001165.

Camps, M., Arrizabalaga, G., and Boothroyd, J. (2002). An rRNA mutation identifies the apicoplast as the target for clindamycin in Toxoplasma gondii. Mol. Microbiol. *43*, 1309–1318.

Cancino, J., Jung, J.E., and Luini, A. (2013). Regulation of Golgi signaling and trafficking by the KDEL receptor. Histochem. Cell Biol. *140*, 395–405.

Card, G.L., Blasdel, L., England, B.P., Zhang, C., Suzuki, Y., Gillette, S., Fong, D., Ibrahim, P.N., Artis, D.R., Bollag, G., et al. (2005). A family of phosphodiesterase inhibitors discovered by cocrystallography and scaffold-based drug design. Nat. Biotechnol. *23*, 201–207.

Carey, A.F., Singer, M., Bargieri, D., Thiberge, S., Frischknecht, F., Ménard, R., and Amino, R. (2014). Calcium dynamics of Plasmodium berghei sporozoite motility. Cell. Microbiol. *16*, 768–783.

Carruthers, V.B., and Sibley, L.D. (1999). Mobilization of intracellular calcium stimulates microneme discharge in Toxoplasma gondii. Mol. Microbiol. *31*, 421–428.

Carucci, D.J., Witney, A.A., Muhia, D.K., Warhurst, D.C., Schaap, P., Meima, M., Li, J.L., Taylor, M.C., Kelly, J.M., and Baker, D.A. (2000). Guanylyl cyclase activity associated with putative bifunctional integral membrane proteins in Plasmodium falciparum. J. Biol. Chem. *275*, 22147–22156.

Carvalho, T.G., and Ménard, R. (2005). Manipulating the Plasmodium genome. Curr. Issues Mol. Biol. *7*, 39–55.

Chandramohanadas, R., Park, Y., Lui, L., Li, A., Quinn, D., Liew, K., Diez-Silva, M., Sung, Y., Dao, M., Lim, C.T., et al. (2011). Biophysics of malarial parasite exit from infected erythrocytes. PLoS One *6*, e20869.

Child, M.A., Epp, C., Bujard, H., and Blackman, M.J. (2010). Regulated maturation of malaria merozoite surface protein-1 is essential for parasite growth. Mol. Microbiol. *78*, 187–202.

Clyde, D.F., McCarthy, V.C., Miller, R.M., and Hornick, R.B. (1973). Specificity of protection of man immunized against sporozoite-induced falciparum malaria. Am. J. Med. Sci. *266*, 398–403.

Coleman, B.I., Skillman, K.M., Jiang, R.H.Y., Childs, L.M., Altenhofen, L.M., Ganter, M., Leung, Y., Goldowitz, I., Kafsack, B.F.C., Marti, M., et al. (2014). A Plasmodium falciparum Histone Deacetylase Regulates Antigenic Variation and Gametocyte Conversion. Cell Host Microbe *16*, 177–186.

Collins, C.R., Hackett, F., Strath, M., Penzo, M., Withers-Martinez, C., Baker, D.A., and Blackman, M.J. (2013a). Malaria parasite cGMP-dependent protein kinase regulates blood stage merozoite secretory organelle discharge and egress. PLoS Pathog. *9*, e1003344.

Collins, C.R., Das, S., Wong, E.H., Andenmatten, N., Stallmach, R., Hackett, F., Herman, J.-P., Müller, S., Meissner, M., and Blackman, M.J. (2013b). Robust inducible Cre recombinase activity in the human malaria parasite Plasmodium falciparum enables efficient gene deletion within a single asexual erythrocytic growth cycle. Mol. Microbiol. *88*, 687–701.

Combe, A., Giovannini, D., Carvalho, T.G., Spath, S., Boisson, B., Loussert, C., Thiberge, S., Lacroix, C., Gueirard, P., and Ménard, R. (2009). Clonal conditional mutagenesis in malaria parasites. Cell Host Microbe *5*, 386–396.

Conti, M., and Beavo, J. (2007). Biochemistry and physiology of cyclic nucleotide phosphodiesterases: essential components in cyclic nucleotide signaling. Annu. Rev. Biochem. *76*, 481–511.

Coronado, L.M., Nadovich, C.T., and Spadafora, C. (2014). Malarial hemozoin: From target to tool. Biochim. Biophys. Acta *1840*, 2032–2041.

Coulson, R.M.R., Hall, N., and Ouzounis, C.A. (2004). Comparative genomics of transcriptional control in the human malaria parasite Plasmodium falciparum. Genome Res. *14*, 1548–1554.

Cowman, A.F., and Crabb, B.S. (2006). Invasion of red blood cells by malaria parasites. Cell *124*, 755–766.

Cox, F.E.G. (2002). History of human parasitology. Clin. Microbiol. Rev. *15*, 595–612.

Crosnier, C., Bustamante, L.Y., Bartholdson, S.J., Bei, A.K., Theron, M., Uchikawa, M., Mboup, S., Ndir, O., Kwiatkowski, D.P., Duraisingh, M.T., et al. (2011). Basigin is a receptor essential for erythrocyte invasion by Plasmodium falciparum. Nature *480*, 534–537.

Dahl, E.L., and Rosenthal, P.J. (2008). Apicoplast translation, transcription and genome replication: targets for antimalarial antibiotics. Trends Parasitol. *24*, 279–284.

Dahl, E.L., Shock, J.L., Shenai, B.R., Gut, J., DeRisi, J.L., and Rosenthal, P.J. (2006). Tetracyclines specifically target the apicoplast of the malaria parasite Plasmodium falciparum. Antimicrob. Agents Chemother. *50*, 3124–3131.

Deitsch, K.W., Lukehart, S.A., and Stringer, J.R. (2009). Common strategies for antigenic variation by bacterial, fungal and protozoan pathogens. Nat. Rev. Microbiol. *7*, 493–503.

Deng, W., Parbhu-Patel, A., Meyer, D.J., and Baker, D.A. (2003). The role of two novel regulatory sites in the activation of the cGMP-dependent protein kinase from Plasmodium falciparum. Biochem. J. *374*, 559–565.

Deniaud, A., Bernaudat, F., Frelet-Barrand, A., Juillan-Binard, C., Vernet, T., Rolland, N., and Pebay-Peyroula, E. (2011). Expression of a chloroplast ATP/ADP transporter in E. coli membranes: behind the Mistic strategy. Biochim. Biophys. Acta *1808*, 2059–2066.

Diaz, C.A., Allocco, J., Powles, M.A., Yeung, L., Donald, R.G.K., Anderson, J.W., and Liberator, P.A. (2006). Characterization of Plasmodium falciparum cGMP-dependent protein kinase (PfPKG): antiparasitic activity of a PKG inhibitor. Mol. Biochem. Parasitol. *146*, 78–88.

Dodge-Kafka, K.L., Soughayer, J., Pare, G.C., Carlisle Michel, J.J., Langeberg, L.K., Kapiloff, M.S., and Scott, J.D. (2005). The protein kinase A anchoring protein mAKAP coordinates two integrated cAMP effector pathways. Nature *437*, 574–578.

Donald, R.G.., and Liberator, P.A. (2002). Molecular characterization of a coccidian parasite cGMP dependent protein kinase. Mol. Biochem. Parasitol. *120*, 165–175.

Donald, R.G.K., Allocco, J., Singh, S.B., Nare, B., Salowe, S.P., Wiltsie, J., and Liberator, P.A. (2002). Toxoplasma gondii cyclic GMP-dependent kinase: chemotherapeutic targeting of an essential parasite protein kinase. Eukaryot. Cell *1*, 317–328.

Doolan, D.L., Dobaño, C., and Baird, J.K. (2009). Acquired immunity to malaria. Clin. Microbiol. Rev. *22*, 13–36, Table of Contents.

Van Dooren, G.G., Marti, M., Tonkin, C.J., Stimmler, L.M., Cowman, A.F., and McFadden, G.I. (2005). Development of the endoplasmic reticulum, mitochondrion and apicoplast during the asexual life cycle of Plasmodium falciparum. Mol. Microbiol. *57*, 405–419.

Douglas, A.D., Williams, A.R., Illingworth, J.J., Kamuyu, G., Biswas, S., Goodman, A.L., Wyllie, D.H., Crosnier, C., Miura, K., Wright, G.J., et al. (2011). The blood-stage malaria antigen PfRH5 is susceptible to vaccine-inducible cross-strain neutralizing antibody. Nat. Commun. *2*, 601.

Douglas, A.D., Williams, A.R., Knuepfer, E., Illingworth, J.J., Furze, J.M., Crosnier, C., Choudhary, P., Bustamante, L.Y., Zakutansky, S.E., Awuah, D.K., et al. (2014). Neutralization of Plasmodium falciparum merozoites by antibodies against PfRH5. J. Immunol. *192*, 245–258.

Dowse, T., and Soldati, D. (2004). Host cell invasion by the apicomplexans: the significance of microneme protein proteolysis. Curr. Opin. Microbiol. *7*, 388–396.

Du, X., and Thiem, S.M. (1997). Responses of insect cells to baculovirus infection: protein synthesis shutdown and apoptosis. J. Virol. *71*, 7866–7872.

Dudek, J., Pfeffer, S., Lee, P.-H., Jung, M., Cavalié, A., Helms, V., Förster, F., and Zimmermann, R. (2014). Protein Transport into the Human Endoplasmic Reticulum. J. Mol. Biol.

Duffy, M.F., Selvarajah, S.A., Josling, G.A., and Petter, M. (2013). Epigenetic regulation of the Plasmodium falciparum genome. Brief. Funct. Genomics elt047 – .

Duraisingh, M.T., Triglia, T., and Cowman, A.F. (2002). Negative selection of Plasmodium falciparum reveals targeted gene deletion by double crossover recombination. Int. J. Parasitol. *32*, 81–89.

Duraisingh, M.T., Voss, T.S., Marty, A.J., Duffy, M.F., Good, R.T., Thompson, J.K., Freitas-Junior, L.H., Scherf, A., Crabb, B.S., and Cowman, A.F. (2005). Heterochromatin silencing and locus repositioning linked to regulation of virulence genes in Plasmodium falciparum. Cell *121*, 13–24.

Dvorin, J.D., Martyn, D.C., Patel, S.D., Grimley, J.S., Collins, C.R., Hopp, C.S., Bright, A.T., Westenberger, S., Winzeler, E., Blackman, M.J., et al. (2010). A plant-like kinase in Plasmodium falciparum regulates parasite egress from erythrocytes. Science *328*, 910–912.

Dyer, M., and Day, K. (2000). Expression of Plasmodium falciparum trimeric G proteins and their involvement in switching to sexual development. Mol. Biochem. Parasitol. *108*, 67–78.

Eckstein-Ludwig, U., Webb, R.J., Van Goethem, I.D.A., East, J.M., Lee, A.G., Kimura, M., O'Neill, P.M., Bray, P.G., Ward, S.A., and Krishna, S. (2003). Artemisinins target the SERCA of Plasmodium falciparum. Nature *424*, 957–961.

Egee, S., Lapaix, F., Decherf, G., Staines, H.M., Ellory, J.C., Doerig, C., and Thomas, S.L.Y. (2002). A stretch-activated anion channel is up-regulated by the malaria parasite plasmodium falciparum. J. Physiol. *542*, 795–801.

Eggers, C.T., Schafer, J.C., Goldenring, J.R., and Taylor, S.S. (2009). D-AKAP2 interacts with Rab4 and Rab11 through its RGS domains and regulates transferrin receptor recycling. J. Biol. Chem. *284*, 32869–32880.

Endo, T., Sethi, K.K., and Piekarski, G. (1982). Toxoplasma gondii: calcium ionophore A23187-mediated exit of trophozoites from infected murine macrophages. Exp. Parasitol. *53*, 179–188.

Epstein, J.E., and Richie, T.L. (2013). The whole parasite, pre-erythrocytic stage approach to malaria vaccine development: a review. Curr. Opin. Infect. Dis. *26*, 420–428.

Fabbri, L.M., Calverley, P.M.A., Izquierdo-Alonso, J.L., Bundschuh, D.S., Brose, M., Martinez, F.J., and Rabe, K.F. (2009). Roflumilast in moderate-to-severe chronic obstructive pulmonary disease treated with longacting bronchodilators: two randomised clinical trials. Lancet *374*, 695–703.

Falae, A., Combe, A., Amaladoss, A., Carvalho, T., Menard, R., and Bhanot, P. (2010). Role of Plasmodium berghei cGMP-dependent protein kinase in late liver stage development. J. Biol. Chem. *285*, 3282–3288.

Fang, J., Marchesini, N., and Moreno, S.N.J. (2006). A Toxoplasma gondii phosphoinositide phospholipase C (TgPI-PLC) with high affinity for phosphatidylinositol. Biochem. J. *394*, 417–425.

Fawcett, L., Baxendale, R., Stacey, P., McGrouther, C., Harrow, I., Soderling, S., Hetman, J., Beavo, J.A., and Phillips, S.C. (2000). Molecular cloning and characterization of a distinct human phosphodiesterase gene family: PDE11A. Proc. Natl. Acad. Sci. U. S. A. *97*, 3702–3707.

Fidock, D.A., and Wellems, T.E. (1997). Transformation with human dihydrofolate reductase renders malaria parasites insensitive to WR99210 but does not affect the intrinsic activity of proguanil. Proc. Natl. Acad. Sci. U. S. A. *94*, 10931–10936.

Fidock, D.A., Nomura, T., and Wellems, T.E. (1998). Cycloguanil and its parent compound proguanil demonstrate distinct activities against Plasmodium falciparum malaria parasites transformed with human dihydrofolate reductase. Mol. Pharmacol. *54*, 1140–1147.

Flueck, C., and Baker, D.A. (2014). Malaria Parasite Epigenetics: When Virulence and Romance Collide. Cell Host Microbe *16*, 148–150.

Flueck, C., Bartfai, R., Niederwieser, I., Witmer, K., Alako, B.T.F., Moes, S., Bozdech, Z., Jenoe, P., Stunnenberg, H.G., and Voss, T.S. (2010). A major role for the Plasmodium falciparum ApiAP2 protein PfSIP2 in chromosome end biology. PLoS Pathog. *6*, e1000784.

Foth, B.J., Zhang, N., Mok, S., Preiser, P.R., and Bozdech, Z. (2008). Quantitative protein expression profiling reveals extensive post-transcriptional regulation and post-translational modifications in schizont-stage malaria parasites. Genome Biol. *9*, R177.

Francia, M.E., and Striepen, B. (2014). Cell division in apicomplexan parasites. Nat. Rev. Microbiol. *12*, 125–136.

Francis, S.H., Busch, J.L., Corbin, J.D., and Sibley, D. (2010). cGMP-dependent protein kinases and cGMP phosphodiesterases in nitric oxide and cGMP action. Pharmacol. Rev. *62*, 525–563.

Francis, S.H., Blount, M.A., and Corbin, J.D. (2011). Mammalian cyclic nucleotide phosphodiesterases: molecular mechanisms and physiological functions. Physiol. Rev. *91*, 651–690.

Franke-Fayard, B., Fonager, J., Braks, A., Khan, S.M., and Janse, C.J. (2010). Sequestration and tissue accumulation of human malaria parasites: can we learn anything from rodent models of malaria? PLoS Pathog. *6*, e1001032.

Frénal, K., Polonais, V., Marq, J.-B., Stratmann, R., Limenitakis, J., and Soldati-Favre, D. (2010). Functional dissection of the apicomplexan glideosome molecular architecture. Cell Host Microbe *8*, 343–357.

Gaji, R.Y., Checkley, L., Reese, M., Ferdig, M.T., and Arrizabalaga, G. (2014). Expression of the essential kinase PfCDPK1 from Plasmodium falciparum in Toxoplasma gondii facilitates the discovery of novel antimalarial drugs. Antimicrob. Agents Chemother.

Gamo, F.-J. (2014). Antimalarial drug resistance: new treatments options for Plasmodium. Drug Discov. Today. Technol. *11*, 81–88.

Gantt, S., Persson, C., Rose, K., Birkett, A.J., Abagyan, R., and Nussenzweig, V. (2000). Antibodies against Thrombospondin-Related Anonymous Protein Do Not Inhibit Plasmodium Sporozoite Infectivity In Vivo. Infect. Immun. *68*, 3667–3673.

Gardner, M.J., Hall, N., Fung, E., White, O., Berriman, M., Hyman, R.W., Carlton, J.M., Pain, A., Nelson, K.E., Bowman, S., et al. (2002). Genome sequence of the human malaria parasite Plasmodium falciparum. Nature *419*, 498–511.

Garg, S., Agarwal, S., Kumar, S., Yazdani, S.S., Chitnis, C.E., and Singh, S. (2013). Calcium-dependent permeabilization of erythrocytes by a perforin-like protein during egress of malaria parasites. Nat. Commun. *4*, 1736.

Gavaldà, A., and Roberts, R.S. (2013). Phosphodiesterase-4 inhibitors: a review of current developments (2010 - 2012). Expert Opin. Ther. Pat. *23*, 997–1016.

Gazarini, M.L., and Garcia, C.R.S. (2004). The malaria parasite mitochondrion senses cytosolic Ca2+ fluctuations. Biochem. Biophys. Res. Commun. *321*, 138–144.

Gazarini, M.L., Thomas, A.P., Pozzan, T., and Garcia, C.R.S. (2003). Calcium signaling in a low calcium environment: how the intracellular malaria parasite solves the problem. J. Cell Biol. *161*, 103–110.

Geary, T.G., Divo, A.A., and Jensen, J.B. (1986). Effect of calmodulin inhibitors on viability and mitochondrial potential of Plasmodium falciparum in culture. Antimicrob. Agents Chemother. *30*, 785–788.

Genton, B., Betuela, I., Felger, I., Al-Yaman, F., Anders, R.F., Saul, A., Rare, L., Baisor, M., Lorry, K., Brown, G. V, et al. (2002). A recombinant blood-stage malaria vaccine reduces Plasmodium falciparum density and exerts selective pressure on parasite populations in a phase 1-2b trial in Papua New Guinea. J. Infect. Dis. *185*, 820–827.

Ghofrani, H.A., Osterloh, I.H., and Grimminger, F. (2006). Sildenafil: from angina to erectile dysfunction to pulmonary hypertension and beyond. Nat. Rev. Drug Discov. *5*, 689–702.

Ghorbal, M., Gorman, M., Macpherson, C.R., Martins, R.M., Scherf, A., and Lopez-Rubio, J.-J. (2014). Genome editing in the human malaria parasite Plasmodium falciparum using the CRISPR-Cas9 system. Nat. Biotechnol.

Gibson, A. (2001). Phosphodiesterase 5 inhibitors and nitrergic transmission—from zaprinast to sildenafil. Eur. J. Pharmacol. *411*, 1–10.

Gilson, P.R., and Crabb, B.S. (2009). Morphology and kinetics of the three distinct phases of red blood cell invasion by Plasmodium falciparum merozoites. Int. J. Parasitol. *39*, 91–96.

Ginsburg, H. (1990). Some reflections concerning host erythrocyte-malarial parasite interrelationships. Blood Cells *16*, 225–235.

Gissot, M., Briquet, S., Refour, P., Boschet, C., and Vaquero, C. (2005). PfMyb1, a Plasmodium falciparum transcription factor, is required for intra-erythrocytic growth and controls key genes for cell cycle regulation. J. Mol. Biol. *346*, 29–42.

Glushakova, S., Humphrey, G., Leikina, E., Balaban, A., Miller, J., and Zimmerberg, J. (2010). New stages in the program of malaria parasite egress imaged in normal and sickle erythrocytes. Curr. Biol. *20*, 1117–1121.

Gluzman, I.Y., Francis, S.E., Oksman, A., Smith, C.E., Duffin, K.L., and Goldberg, D.E. (1994). Order and specificity of the Plasmodium falciparum hemoglobin degradation pathway. J. Clin. Invest. *93*, 1602–1608.

Golenser, J., Waknine, J.H., Krugliak, M., Hunt, N.H., and Grau, G.E. (2006). Current perspectives on the mechanism of action of artemisinins. Int. J. Parasitol. *36*, 1427–1441.

Gomez, L., and Breitenbucher, J.G. (2013). PDE2 inhibition: potential for the treatment of cognitive disorders. Bioorg. Med. Chem. Lett. *23*, 6522–6527.

Goodman, C.D., and McFadden, G.I. (2013). Targeting apicoplasts in malaria parasites. Expert Opin. Ther. Targets *17*, 167–177.

Goraya, T.A., and Cooper, D.M.F. (2005). Ca2+-calmodulin-dependent phosphodiesterase (PDE1): current perspectives. Cell. Signal. *17*, 789–797.

Gould, M.K., and de Koning, H.P. (2011). Cyclic-nucleotide signalling in protozoa. FEMS Microbiol. Rev. *35*, 515–541.

Graewe, S., Rankin, K.E., Lehmann, C., Deschermeier, C., Hecht, L., Froehlke, U., Stanway, R.R., and Heussler, V. (2011). Hostile takeover by Plasmodium: reorganization of parasite and host cell membranes during liver stage egress. PLoS Pathog. *7*, e1002224.

Green, J.L., Rees-Channer, R.R., Howell, S.A., Martin, S.R., Knuepfer, E., Taylor, H.M., Grainger, M., and Holder, A.A. (2008). The motor complex of Plasmodium falciparum: phosphorylation by a calcium-dependent protein kinase. J. Biol. Chem. *283*, 30980–30989.

Griffin, C.E., Hoke, J.M., Samarakoon, U., Duan, J., Mu, J., Ferdig, M.T., Warhurst, D.C., and Cooper, R.A. (2012). Mutation in the Plasmodium falciparum CRT protein determines the stereospecific activity of antimalarial cinchona alkaloids. Antimicrob. Agents Chemother. *56*, 5356–5364.

Gurnett, A.M., Liberator, P.A., Dulski, P.M., Salowe, S.P., Donald, R.G.K., Anderson, J.W., Wiltsie, J., Diaz, C.A., Harris, G., Chang, B., et al. (2002). Purification and molecular characterization of cGMP-dependent protein kinase from Apicomplexan parasites. A novel chemotherapeutic target. J. Biol. Chem. *277*, 15913–15922.

Haldar, K., Mohandas, N., Samuel, B.U., Harrison, T., Hiller, N.L., Akompong, T., and Cheresh, P. (2002). Protein and lipid trafficking induced in erythrocytes infected by malaria parasites. Cell. Microbiol. *4*, 383–395.

Hall, N., Karras, M., Raine, J.D., Carlton, J.M., Kooij, T.W.A., Berriman, M., Florens, L., Janssen, C.S., Pain, A., Christophides, G.K., et al. (2005). A comprehensive survey of the Plasmodium life cycle by genomic, transcriptomic, and proteomic analyses. Science *307*, 82–86.

Harper, J.F., and Harmon, A. (2005). Plants, symbiosis and parasites: a calcium signalling connection. Nat. Rev. Mol. Cell Biol. *6*, 555–566.

Harris, P.K., Yeoh, S., Dluzewski, A.R., O'Donnell, R.A., Withers-Martinez, C., Hackett, F., Bannister, L.H., Mitchell, G.H., and Blackman, M.J. (2005). Molecular identification of a malaria merozoite surface sheddase. PLoS Pathog. *1*, 241–251.

Harrison, T., Samuel, B.U., Akompong, T., Hamm, H., Mohandas, N., Lomasney, J.W., and Haldar, K. (2003). Erythrocyte G protein-coupled receptor signaling in malarial infection. Science *301*, 1734–1736.

Haste, N.M., Talabani, H., Doo, A., Merckx, A., Langsley, G., and Taylor, S.S. (2012). Exploring the Plasmodium falciparum cyclic-adenosine monophosphate (cAMP)-dependent protein kinase (PfPKA) as a therapeutic target. Microbes Infect. *14*, 838–850.

Haynes, R.K. (2001). Artemisinin and derivatives: the future for malaria treatment? Curr. Opin. Infect. Dis. *14*, 719–726.

Hemingway, J. (2014). The role of vector control in stopping the transmission of malaria: threats and opportunities. Philos. Trans. R. Soc. Lond. B. Biol. Sci. *369*, 20130431.

Hertelendy, F., Toth, M., and Fitch, C.D. (1979). Malaria enhances cyclic AMP production by immature erythrocytes in vitro. Life Sci. *25*, 451–455.

Hinterberg, K., Mattei, D., Wellems, T.E., and Scherf, A. (1994). Interchromosomal exchange of a large subtelomeric segment in a Plasmodium falciparum cross. EMBO J. *13*, 4174–4180.

Hirai, M., Arai, M., Kawai, S., and Matsuoka, H. (2006). PbGCbeta is essential for Plasmodium ookinete motility to invade midgut cell and for successful completion of parasite life cycle in mosquitoes. J. Biochem. *140*, 747–757.

Hollingdale, M.R., and Leland, P. (1982). Detection of exoerythrocytic stages of Plasmodium berghei in fixed liver tissue and cultured cells by an immunoperoxidase antibody technique. Trans. R. Soc. Trop. Med. Hyg. *76*, 624–626.

Homewood, C.A., Warhurst, D.C., Peters, W., and Baggerly, V.C. (1972). Lysosomes, pH and the Anti-malarial Action of Chloroquine. Nature *235*, 50–52.

Hopp, C.S., Flueck, C., Solyakov, L., Tobin, A., and Baker, D.A. (2012). Spatiotemporal and functional characterisation of the Plasmodium falciparum cGMP-dependent protein kinase. PLoS One *7*, e48206.

Hoppe, H.C., van Schalkwyk, D.A., Wiehart, U.I.M., Meredith, S.A., Egan, J., and Weber, B.W. (2004). Antimalarial quinolines and artemisinin inhibit endocytosis in Plasmodium falciparum. Antimicrob. Agents Chemother. *48*, 2370–2378.

Hotta, C.T., Gazarini, M.L., Beraldo, F.H., Varotti, F.P., Lopes, C., Markus, R.P., Pozzan, T., and Garcia, C.R. (2000). Calcium-dependent modulation by melatonin of the circadian rhythm in malarial parasites. Nat. Cell Biol. *2*, 466–468.

Houslay, M.D., Scotland, G., Erdogan, S., Huston, E., Mackenzie, S., McCallum, J.F., McPhee, I., Pooley, L., Rena, G., Ross, A., et al. (1997). Intracellular targeting, interaction with Src homology 3 (SH3) domains and rolipram-detected conformational switches in cAMP-specific PDE4A phosphodiesterase. Biochem. Soc. Trans. *25*, 374–381.

Howard, B.L., Thompson, P.E., and Manallack, D.T. (2011). Active site similarity between human and Plasmodium falciparum phosphodiesterases: considerations for antimalarial drug design. J. Comput. Aided. Mol. Des. *25*, 753–762.

Hsu, P.D., Lander, E.S., and Zhang, F. (2014). Development and Applications of CRISPR-Cas9 for Genome Engineering. Cell *157*, 1262–1278.

Hviid, L., and Staalsoe, T. (2004). Malaria immunity in infants: a special case of a general phenomenon? Trends Parasitol. *20*, 66–72.

Hyde, J.E. (2005). Exploring the folate pathway in Plasmodium falciparum. Acta Trop. *94*, 191–206.

Hyde, J.E. (2007). Drug-resistant malaria – an insight. FEBS J. *274*, 4688–4698.

Ishino, T., Orito, Y., Chinzei, Y., and Yuda, M. (2006). A calcium-dependent protein kinase regulates Plasmodium ookinete access to the midgut epithelial cell. Mol. Microbiol. *59*, 1175–1184.

Ivanov, A., and Matsumura, I. (2012). The adenosine deaminases of Plasmodium vivax and Plasmodium falciparum exhibit surprising differences in ligand specificity. J. Mol. Graph. Model. *35*, 43–48.

Jackson, M.R., Nilsson, T., and Peterson, P.A. (1990). Identification of a consensus motif for retention of transmembrane proteins in the endoplasmic reticulum. EMBO J. *9*, 3153–3162.

Jain, S., Rathore, S., Asad, M., Hossain, M.E., Sinha, D., Datta, G., and Mohmmed, A. (2013). The prokaryotic ClpQ protease plays a key role in growth and development of mitochondria in Plasmodium falciparum. Cell. Microbiol. *15*, n/a – n/a.

Janse, C.J., and Waters, A.P. (2007). The exoneme helps malaria parasites to break out of blood cells. Cell *131*, 1036–1038.

Jansen, C., Wang, H., Kooistra, A.J., de Graaf, C., Orrling, K.M., Tenor, H., Seebeck, T., Bailey, D., de Esch, I.J.P., Ke, H., et al. (2013). Discovery of novel Trypanosoma brucei phosphodiesterase B1 inhibitors by virtual screening against the unliganded TbrPDEB1 crystal structure. J. Med. Chem. *56*, 2087–2096.

Jiang, L., Mu, J., Zhang, Q., Ni, T., Srinivasan, P., Rayavara, K., Yang, W., Turner, L., Lavstsen, T., Theander, T.G., et al. (2013). PfSETvs methylation of histone H3K36 represses virulence genes in Plasmodium falciparum. Nature *499*, 223–227.

Jin, S.L., Swinnen, J. V, and Conti, M. (1992). Characterization of the structure of a low Km, rolipram-sensitive cAMP phosphodiesterase. Mapping of the catalytic domain. J. Biol. Chem. *267*, 18929–18939.

Jofuku, K.D., den Boer, B.G., Van Montagu, M., and Okamuro, J.K. (1994). Control of Arabidopsis flower and seed development by the homeotic gene APETALA2. Plant Cell *6*, 1211–1225.

Jullien, N., Sampieri, F., Enjalbert, A., and Herman, J.-P. (2003). Regulation of Cre recombinase by ligand-induced complementation of inactive fragments. Nucleic Acids Res. *31*, e131.

Kafsack, B.F.C., Rovira-Graells, N., Clark, T.G., Bancells, C., Crowley, V.M., Campino, S.G., Williams, A.E., Drought, L.G., Kwiatkowski, D.P., Baker, D.A., et al. (2014). A transcriptional switch underlies commitment to sexual development in malaria parasites. Nature.

Kandel, E.R. (2012). The molecular biology of memory: cAMP, PKA, CRE, CREB-1, CREB-2, and CPEB. Mol. Brain *5*, 14.

Kanlop, N., Chattipakorn, S., and Chattipakorn, N. (2011). Effects of cilostazol in the heart. J. Cardiovasc. Med. (Hagerstown). *12*, 88–95.

Kats, L.M., Black, C.G., Proellocks, N.I., and Coppel, R.L. (2006). Plasmodium rhoptries: how things went pear-shaped. Trends Parasitol. *22*, 269–276.

Kaushal, D.C., Carter, R., Miller, L.H., and Krishna, G. (1980). Gametocytogenesis by malaria parasites in continuous culture. Nature *286*, 490–492.

Kawamoto, F., Alejo-Blanco, R., Fleck, S.L., Kawamoto, Y., and Sinden, R.E. (1990). Possible roles of Ca2+ and cGMP as mediators of the exflagellation of Plasmodium berghei and Plasmodium falciparum. Mol. Biochem. Parasitol. *42*, 101–108.

Ke, H., and Wang, H. (2007). Crystal structures of phosphodiesterases and implications on substrate specificity and inhibitor selectivity. Curr. Top. Med. Chem. *7*, 391–403.

Ke, H., Wang, H., and Ye, M. (2011). Structural insight into the substrate specificity of phosphodiesterases. Handb. Exp. Pharmacol. 121–134.

Kebaier, C., and Vanderberg, J.P. (2010). Initiation of Plasmodium sporozoite motility by albumin is associated with induction of intracellular signalling. Int. J. Parasitol. *40*, 25–33.

Kelly, J.M., McRobert, L., and Baker, D.A. (2006). Evidence on the chromosomal location of centromeric DNA in Plasmodium falciparum from etoposide-mediated topoisomerase-II cleavage. Proc. Natl. Acad. Sci. U. S. A. *103*, 6706–6711.

Kerr, N.M., and Danesh-Meyer, H. V (2009). Phosphodiesterase inhibitors and the eye. Clin. Experiment. Ophthalmol. *37*, 514–523.

Kirk, K. (2001). Membrane transport in the malaria-infected erythrocyte. Physiol. Rev. *81*, 495–537.

Klayman, D.L. (1985). Qinghaosu (artemisinin): an antimalarial drug from China. Science *228*, 1049–1055.

Klonis, N., Tan, O., Jackson, K., Goldberg, D., Klemba, M., and Tilley, L. (2007). Evaluation of pH during cytostomal endocytosis and vacuolar catabolism of haemoglobin in Plasmodium falciparum. Biochem. J. *407*, 343–354.

Klonis, N., Xie, S.C., McCaw, J.M., Crespo-Ortiz, M.P., Zaloumis, S.G., Simpson, J.A., and Tilley, L. (2013). Altered temporal response of malaria parasites determines differential sensitivity to artemisinin. Proc. Natl. Acad. Sci. U. S. A. *110*, 5157–5162.

Kolev, N.G., Tschudi, C., and Ullu, E. (2011). RNA interference in protozoan parasites: achievements and challenges. Eukaryot. Cell *10*, 1156–1163.

De Koning-Ward, T.F., Janse, C.J., and Waters, A.P. (2000). The development of genetic tools for dissecting the biology of malaria parasites. Annu. Rev. Microbiol. *54*, 157–185.

De Koning-Ward, T.F., Olivieri, A., Bertuccini, L., Hood, A., Silvestrini, F., Charvalias, K., Berzosa Díaz, P., Camarda, G., McElwain, T.F., Papenfuss, T., et al. (2008). The role of osmiophilic bodies and Pfg377 expression in female gametocyte emergence and mosquito infectivity in the human malaria parasite Plasmodium falciparum. Mol. Microbiol. *67*, 278–290.

Kost, T.A., Condreay, J.P., and Jarvis, D.L. (2005). Baculovirus as versatile vectors for protein expression in insect and mammalian cells. Nat. Biotechnol. *23*, 567–575.

Krishna, S., Woodrow, C., Webb, R., Penny, J., Takeyasu, K., Kimura, M., and East, J.M. (2001). Expression and functional characterization of a Plasmodium falciparum Ca2+-ATPase (PfATP4) belonging to a subclass unique to apicomplexan organisms. J. Biol. Chem. *276*, 10782–10787.

Kritzer, M.D., Li, J., Dodge-Kafka, K., and Kapiloff, M.S. (2012). AKAPs: the architectural underpinnings of local cAMP signaling. J. Mol. Cell. Cardiol. *52*, 351–358.

Krogstad, D.J., Gluzman, I.Y., Kyle, D.E., Oduola, A.M.J., Martin, S.K., Milhous, W.K., and Schlesinger, P.H. (1987). Efflux of chloroquine from Plasmodium falciparum: Mechanism of chloroquine resistance. Science (80-.). *238*, 1283–1285.

Krotoski, W.A., Krotoski, D.M., Garnham, P.C., Bray, R.S., Killick-Kendrick, R., Draper, C.C., Targett, G.A., and Guy, M.W. (1980). Relapses in primate malaria: discovery of two populations of exoerythrocytic stages. Preliminary note. Br. Med. J. *280*, 153–154.

Krotoski, W.A., Collins, W.E., Bray, R.S., Garnham, P.C., Cogswell, F.B., Gwadz, R.W., Killick-Kendrick, R., Wolf, R., Sinden, R., Koontz, L.C., et al. (1982). Demonstration of hypnozoites in sporozoite-transmitted Plasmodium vivax infection. Am. J. Trop. Med. Hyg. *31*, 1291–1293.

Kumar, N., Koski, G., Harada, M., Aikawa, M., and Zheng, H. (1991). Induction and localization of Plasmodium falciparum stress proteins related to the heat shock protein 70 family. Mol. Biochem. Parasitol. *48*, 47–58.

Kumar, P., Tripathi, A., Ranjan, R., Halbert, J., Gilberger, T., Doerig, C., and Sharma, P. (2014). Regulation of Plasmodium falciparum development by Calcium-Dependent Protein Kinase 7 (PfCDPK7). J. Biol. Chem. *289*, 20386–20395.

Laage, R., and Langosch, D. (2001). Strategies for Prokaryotic Expression of Eukaryotic Membrane Proteins. Traffic *2*, 99–104.

Lacroix, C., Giovannini, D., Combe, A., Bargieri, D.Y., Späth, S., Panchal, D., Tawk, L., Thiberge, S., Carvalho, T.G., Barale, J.-C., et al. (2011). FLP/FRT-mediated conditional mutagenesis in pre-erythrocytic stages of Plasmodium berghei. Nat. Protoc. *6*, 1412–1428.

Lambros, C., and Vanderberg, J.P. (1979). Synchronization of Plasmodium falciparum erythrocytic stages in culture. J. Parasitol. *65*, 418–420.

Langreth, S.G., Jensen, J.B., Reese, R.T., and Trager, W. (1978). Fine structure of human malaria in vitro. J. Protozool. *25*, 443–452.

Lasonder, E., Green, J.L., Camarda, G., Talabani, H., Holder, A.A., Langsley, G., and Alano, P. (2012). The Plasmodium falciparum schizont phosphoproteome reveals extensive phosphatidylinositol and cAMP-protein kinase A signaling. J. Proteome Res. *11*, 5323–5337.

Leykauf, K., Treeck, M., Gilson, P.R., Nebl, T., Braulke, T., Cowman, A.F., Gilberger, T.W., and Crabb, B.S. (2010). Protein kinase a dependent phosphorylation of apical membrane antigen 1 plays an important role in erythrocyte invasion by the malaria parasite. PLoS Pathog. *6*, e1000941.

Lima, W.R., Moraes, M., Alves, E., Azevedo, M.F., Passos, D.O., and Garcia, C.R.S. (2013). The PfNF-YB transcription factor is a downstream target of melatonin and cAMP signalling in the human malaria parasite Plasmodium falciparum. J. Pineal Res. *54*, 145–153.

Limenitakis, J., and Soldati-Favre, D. (2011). Functional genetics in Apicomplexa: potentials and limits. FEBS Lett. *585*, 1579–1588.

Linder, J.U., Engel, P., Reimer, A., Krüger, T., Plattner, H., Schultz, A., and Schultz, J.E. (1999). Guanylyl cyclases with the topology of mammalian adenylyl cyclases and an N-terminal P-type ATPase-like domain in Paramecium, Tetrahymena and Plasmodium. EMBO J. *18*, 4222–4232.

López-Barragán, M.J., Lemieux, J., Quiñones, M., Williamson, K.C., Molina-Cruz, A., Cui, K., Barillas-Mury, C., Zhao, K., and Su, X. (2011). Directional gene expression and antisense transcripts in sexual and asexual stages of Plasmodium falciparum. BMC Genomics *12*, 587.

Lourido, S., Shuman, J., Zhang, C., Shokat, K.M., Hui, R., and Sibley, L.D. (2010). Calcium-dependent protein kinase 1 is an essential regulator of exocytosis in Toxoplasma. Nature *465*, 359–362.

Lugnier, C. (2006). Cyclic nucleotide phosphodiesterase (PDE) superfamily: a new target for the development of specific therapeutic agents. Pharmacol. Ther. *109*, 366–398.

Ma, H.T., Patterson, R.L., van Rossum, D.B., Birnbaumer, L., Mikoshiba, K., and Gill, D.L. (2000). Requirement of the inositol trisphosphate receptor for activation of store-operated Ca2+ channels. Science *287*, 1647–1651.

Mair, G.R., Braks, J.A.M., Garver, L.S., Wiegant, J.C.A.G., Hall, N., Dirks, R.W., Khan, S.M., Dimopoulos, G., Janse, C.J., and Waters, A.P. (2006). Regulation of sexual development of Plasmodium by translational repression. Science *313*, 667–669.

Makhlouf, A., Kshirsagar, A., and Niederberger, C. (2006). Phosphodiesterase 11: a brief review of structure, expression and function. Int. J. Impot. Res. *18*, 501–509.

Makler, M.T., and Hinrichs, D.J. (1993). Measurement of the lactate dehydrogenase activity of Plasmodium falciparum as an assessment of parasitemia. Am. J. Trop. Med. Hyg. *48*, 205–210.

Makler, M.T., Ries, J.M., Williams, J.A., Bancroft, J.E., Piper, R.C., Gibbins, B.L., and Hinrichs, D.J. (1993). Parasite lactate dehydrogenase as an assay for Plasmodium falciparum drug sensitivity. Am. J. Trop. Med. Hyg. *48*, 739–741.

malERA Consultative Group on Vaccines. (2011). A research agenda for malaria eradication: vaccines. PLoS Med. *8*, e1000398.

Mali, P., Yang, L., Esvelt, K.M., Aach, J., Guell, M., DiCarlo, J.E., Norville, J.E., and Church, G.M. (2013). RNA-guided human genome engineering via Cas9. Science *339*, 823–826.

Manallack, D.T., Hughes, R.A., and Thompson, P.E. (2005). The next generation of phosphodiesterase inhibitors: structural clues to ligand and substrate selectivity of phosphodiesterases. J. Med. Chem. *48*, 3449–3462.

Marchesini, N., Luo, S., Rodrigues, C.O., Moreno, S.N., and Docampo, R. (2000). Acidocalcisomes and a vacuolar H+-pyrophosphatase in malaria parasites. Biochem. J. *347 Pt 1*, 243–253.

Martin, S.K., Miller, L.H., Nijhout, M.M., and Carter, R. (1978). Plasmodium gallinaceum: induction of male gametocyte exflagellation by phosphodiesterase inhibitors. Exp. Parasitol. *44*, 239–242.

Mather, M.W., Darrouzet, E., Valkova-Valchanova, M., Cooley, J.W., McIntosh, M.T., Daldal, F., and Vaidya, A.B. (2005). Uncovering the molecular mode of action of the antimalarial drug atovaquone using a bacterial system. J. Biol. Chem. *280*, 27458–27465.

Mather, M.W., Henry, K.W., and Vaidya, A.B. (2007). Mitochondrial drug targets in apicomplexan parasites. Curr. Drug Targets *8*, 49–60.

Maurice, D.H., Ke, H., Ahmad, F., Wang, Y., Chung, J., and Manganiello, V.C. (2014). Advances in targeting cyclic nucleotide phosphodiesterases. Nat. Rev. Drug Discov. *13*, 290–314.

McRobert, L., and McConkey, G.A. (2002). RNA interference (RNAi) inhibits growth of Plasmodium falciparum. Mol. Biochem. Parasitol. *119*, 273–278.

McRobert, L., Taylor, C.J., Deng, W., Fivelman, Q.L., Cummings, R.M., Polley, S.D., Billker, O., and Baker, D.A. (2008). Gametogenesis in malaria parasites is mediated by the cGMP-dependent protein kinase. PLoS Biol. *6*, e139.

Meissner, M., Schlüter, D., and Soldati, D. (2002). Role of Toxoplasma gondii myosin A in powering parasite gliding and host cell invasion. Science *298*, 837–840.

Meissner, M., Krejany, E., Gilson, P.R., de Koning-Ward, T.F., Soldati, D., and Crabb, B.S. (2005). Tetracycline analogue-regulated transgene expression in Plasmodium falciparum blood stages using Toxoplasma gondii transactivators. Proc. Natl. Acad. Sci. U. S. A. *102*, 2980–2985.

Menendez, C. (2006). Malaria during pregnancy. Curr. Mol. Med. *6*, 269–273.

Merckx, A., Nivez, M.-P., Bouyer, G., Alano, P., Langsley, G., Deitsch, K., Thomas, S., Doerig, C., and Egée, S. (2008). Plasmodium falciparum regulatory subunit of cAMP-dependent PKA and anion channel conductance. PLoS Pathog. *4*, e19.

Merkel, L.A., Rivera, L.M., Perrone, M.H., and Lappe, R.W. (1992). In vitro and in vivo interactions of nitrovasodilators and zaprinast, a cGMP-selective phosphodiesterase inhibitor. Eur. J. Pharmacol. *216*, 29–35.

Meshnick, S.R., and Dobson, M.J. (2001). The History of Antimalarial Drugs. 15–25.

Meshnick, S.R., Taylor, T.E., and Kamchonwongpaisan, S. (1996). Artemisinin and the antimalarial endoperoxides: from herbal remedy to targeted chemotherapy. Microbiol. Rev. *60*, 301–315.

Miller, L.K. (1993). Baculoviruses: high-level expression in insect cells. Curr. Opin. Genet. Dev. *3*, 97–101.

Miller, L.H., and Su, X. (2011). Artemisinin: discovery from the Chinese herbal garden. Cell *146*, 855–858.

Miller, L.H., Baruch, D.I., Marsh, K., and Doumbo, O.K. (2002). The pathogenic basis of malaria. Nature *415*, 673–679.

Miller, L.H., Ackerman, H.C., Su, X., and Wellems, T.E. (2013). Malaria biology and disease pathogenesis: insights for new treatments. Nat. Med. *19*, 156–167.

Millholland, M.G., Chandramohanadas, R., Pizzaro, A., Wehr, A., Shi, H., Darling, C., Lim, C.T., and Greenbaum, D.C. (2011). The malaria parasite progressively dismantles the host erythrocyte cytoskeleton for efficient egress. Mol. Cell. Proteomics *10*, M111.010678.

Mitchell, G.H., Hadley, T.J., McGinniss, M.H., Klotz, F.W., and Miller, L.H. (1986). Invasion of erythrocytes by Plasmodium falciparum malaria parasites: evidence for receptor heterogeneity and two receptors. Blood *67*, 1519–1521.

Moon, R.W., Taylor, C.J., Bex, C., Schepers, R., Goulding, D., Janse, C.J., Waters, A.P., Baker, D.A., and Billker, O. (2009). A cyclic GMP signalling module that regulates gliding motility in a malaria parasite. PLoS Pathog. *5*, e1000599.

Moreno, S.N.J., Ayong, L., and Pace, D.A. (2011). Calcium storage and function in apicomplexan parasites. Essays Biochem. *51*, 97–110.

Mota, M.M., Hafalla, J.C.R., and Rodriguez, A. (2002). Migration through host cells activates Plasmodium sporozoites for infection. Nat. Med. *8*, 1318–1322.

Movsesian, M.A., and Kukreja, R.C. (2011). Phosphodiesterase inhibition in heart failure. Handb. Exp. Pharmacol. 237–249.

Muhia, D.K., Swales, C.A., Eckstein-Ludwig, U., Saran, S., Polley, S.D., Kelly, J.M., Schaap, P., Krishna, S., and Baker, D.A. (2003). Multiple splice variants encode a novel adenylyl cyclase of possible plastid origin expressed in the sexual stage of the malaria parasite Plasmodium falciparum. J. Biol. Chem. *278*, 22014–22022.

Müller, I.B., and Hyde, J.E. (2010). Antimalarial drugs: modes of action and mechanisms of parasite resistance. Future Microbiol. *5*, 1857–1873.

Murphy, S.C., Harrison, T., Hamm, H.E., Lomasney, J.W., Mohandas, N., and Haldar, K. (2006). Erythrocyte G protein as a novel target for malarial chemotherapy. PLoS Med. *3*, e528.

Noedl, H., Se, Y., Schaecher, K., Smith, B.L., Socheat, D., and Fukuda, M.M. (2008). Evidence of artemisinin-resistant malaria in western Cambodia. N. Engl. J. Med. *359*, 2619–2620.

Nussenzweig, R.S., Vanderberg, J., Most, H., and Orton, C. (1967). Protective immunity produced by the injection of x-irradiated sporozoites of plasmodium berghei. Nature *216*, 160–162.

O'Donnell, R.A. (2001). An alteration in concatameric structure is associated with efficient segregation of plasmids in transfected Plasmodium falciparum parasites. Nucleic Acids Res. *29*, 716–724.

O'Donnell, R.A., Freitas-Junior, L.H., Preiser, P.R., Williamson, D.H., Duraisingh, M., McElwain, T.F., Scherf, A., Cowman, A.F., and Crabb, B.S. (2002). A genetic screen for improved plasmid segregation reveals a role for Rep20 in the interaction of Plasmodium falciparum chromosomes. EMBO J. *21*, 1231–1239.

Oborník, M., Janouskovec, J., Chrudimský, T., and Lukes, J. (2009). Evolution of the apicoplast and its hosts: from heterotrophy to autotrophy and back again. Int. J. Parasitol. *39*, 1–12.

Ono, T., Cabrita-Santos, L., Leitao, R., Bettiol, E., Purcell, L.A., Diaz-Pulido, O., Andrews, L.B., Tadakuma, T., Bhanot, P., Mota, M.M., et al. (2008). Adenylyl cyclase alpha and cAMP signaling mediate Plasmodium sporozoite apical regulated exocytosis and hepatocyte infection. PLoS Pathog. *4*, e1000008.

Panchal, D., and Bhanot, P. (2010). Activity of a trisubstituted pyrrole in inhibiting sporozoite invasion and blocking malaria infection. Antimicrob. Agents Chemother. *54*, 4269–4274.

Passos, A., and Garcia, C. (1997). Characterization of Ca2 transport activity associated with a non-mitochondrial calcium pool in the rodent malaria parasite P. chabaudi. IUBMB Life *42*, 919–925.

Peatey, C.L., Dixon, M.W.A., Gardiner, D.L., and Trenholme, K.R. (2013). Temporal evaluation of commitment to sexual development in Plasmodium falciparum. Malar. J. *12*, 134.

Peel, S.A. (2001). The ABC transporter genes of Plasmodium falciparum and drug resistance. Drug Resist. Updat. *4*, 66–74.

Peterson, D.S., Miller, L.H., and Wellems, T.E. (1995). Isolation of multiple sequences from the Plasmodium falciparum genome that encode conserved domains homologous to those in erythrocyte-binding proteins. Proc. Natl. Acad. Sci. U. S. A. *92*, 7100–7104.

Pezzella-D'Alessandro, N., Le Moal, H., Bonhomme, A., Valere, A., Klein, C., Gomez-Marin, J., and Pinon, J.M. (2001). Calmodulin distribution and the actomyosin cytoskeleton in Toxoplasma gondii. J. Histochem. Cytochem. *49*, 445–454.

Pino, P. (2013). From technology to biology: a malaria genetic toolbox for the functional dissection of essential genes. Mol. Microbiol. *88*, 650–654.

Pino, P., Sebastian, S., Kim, E.A., Bush, E., Brochet, M., Volkmann, K., Kozlowski, E., Llinás, M., Billker, O., and Soldati-Favre, D. (2012). A tetracycline-repressible transactivator system to study essential genes in malaria parasites. Cell Host Microbe *12*, 824–834.

Pradel, G., Garapaty, S., and Frevert, U. (2002). Proteoglycans mediate malaria sporozoite targeting to the liver. Mol. Microbiol. *45*, 637–651.

Rached, F. Ben, Ndjembo-Ezougou, C., Chandran, S., Talabani, H., Yera, H., Dandavate, V., Bourdoncle, P., Meissner, M., Tatu, U., and Langsley, G. (2012). Construction of a Plasmodium

falciparum Rab-interactome identifies CK1 and PKA as Rab-effector kinases in malaria parasites. Biol. Cell *104*, 34–47.

Raj, D.K., Nixon, C.P., Nixon, C.E., Dvorin, J.D., DiPetrillo, C.G., Pond-Tor, S., Wu, H.-W., Jolly, G., Pischel, L., Lu, A., et al. (2014). Antibodies to PfSEA-1 block parasite egress from RBCs and protect against malaria infection. Science (80-.). *344*, 871–877.

Rall, T.W., and West, T.C. (1963). The potentiation of cardiac inotropic responses to norepinephrine by theophylline. J. Pharmacol. Exp. Ther. *139*, 269–274.

Ralph, S.A., van Dooren, G.G., Waller, R.F., Crawford, M.J., Fraunholz, M.J., Foth, B.J., Tonkin, C.J., Roos, D.S., and McFadden, G.I. (2004). Tropical infectious diseases: metabolic maps and functions of the Plasmodium falciparum apicoplast. Nat. Rev. Microbiol. *2*, 203–216.

Ranson, H., N'guessan, R., Lines, J., Moiroux, N., Nkuni, Z., and Corbel, V. (2011). Pyrethroid resistance in African anopheline mosquitoes: what are the implications for malaria control? Trends Parasitol. *27*, 91–98.

Rapoport, T.A. (2007). Protein translocation across the eukaryotic endoplasmic reticulum and bacterial plasma membranes. Nature *450*, 663–669.

Read, L.K., and Mikkelsen, R.B. (1991a). Plasmodium falciparum-infected erythrocytes contain an adenylate cyclase with properties which differ from those of the host enzyme. Mol. Biochem. Parasitol. *45*, 109–119.

Read, L.K., and Mikkelsen, R.B. (1991b). Comparison of adenylate cyclase and cAMP-dependent protein kinase in gametocytogenic and nongametocytogenic clones of Plasmodium falciparum. J. Parasitol. *77*, 346–352.

Rees-Channer, R.R., Martin, S.R., Green, J.L., Bowyer, P.W., Grainger, M., Molloy, J.E., and Holder, A.A. (2006). Dual acylation of the 45 kDa gliding-associated protein (GAP45) in Plasmodium falciparum merozoites. Mol. Biochem. Parasitol. *149*, 113–116.

Reger, A.S., Yang, M.P., Koide-Yoshida, S., Guo, E., Mehta, S., Yuasa, K., Liu, A., Casteel, D.E., and Kim, C. (2014). Crystal Structure of the cGMP Dependent Protein Kinase II Leucine Zipper and Rab11b Complex Reveals Molecular Details of G-Kinase Specific Interactions. J. Biol. Chem.

Reimann, E.M., Brostrom, C.O., Corbin, J.D., King, C.A., and Krebs, E.G. (1971). Separation of regulatory and catalytic subunits of the cyclic 3', 5'-adenosine monophosphate-dependent protein kinase(s) of rabbit skeletal muscle. Biochem. Biophys. Res. Commun. *42*, 187–194.

Renigunta, V., Yuan, H., Zuzarte, M., Rinné, S., Koch, A., Wischmeyer, E., Schlichthörl, G., Gao, Y., Karschin, A., Jacob, R., et al. (2006). The retention factor p11 confers an endoplasmic reticulum-localization signal to the potassium channel TASK-1. Traffic *7*, 168–181.

Richard, D., MacRaild, C.A., Riglar, D.T., Chan, J.-A., Foley, M., Baum, J., Ralph, S.A., Norton, R.S., and Cowman, A.F. (2010). Interaction between Plasmodium falciparum apical membrane antigen 1 and the rhoptry neck protein complex defines a key step in the erythrocyte invasion process of malaria parasites. J. Biol. Chem. *285*, 14815–14822.

Riglar, D.T., Richard, D., Wilson, D.W., Boyle, M.J., Dekiwadia, C., Turnbull, L., Angrisano, F., Marapana, D.S., Rogers, K.L., Whitchurch, C.B., et al. (2011). Super-resolution dissection of coordinated events during malaria parasite invasion of the human erythrocyte. Cell Host Microbe *9*, 9–20.

Riley, E.M., and Stewart, V.A. (2013). Immune mechanisms in malaria: new insights in vaccine development. Nat. Med. *19*, 168–178.

Roberts, D.J., Craig, A.G., Berendt, A.R., Pinches, R., Nash, G., Marsh, K., and Newbold, C.I. (1992). Rapid switching to multiple antigenic and adhesive phenotypes in malaria. Nature *357*, 689–692.

Le Roch, K.G., Johnson, J.R., Florens, L., Zhou, Y., Santrosyan, A., Grainger, M., Yan, S.F., Williamson, K.C., Holder, A.A., Carucci, D.J., et al. (2004). Global analysis of transcript and protein levels across the Plasmodium falciparum life cycle. Genome Res. *14*, 2308–2318.

Le Roch, K.G., Chung, D.-W.D., and Ponts, N. (2012). Genomics and integrated systems biology in Plasmodium falciparum: a path to malaria control and eradication. Parasite Immunol. *34*, 50–60.

Röder, I.V., Lissandron, V., Martin, J., Petersen, Y., Di Benedetto, G., Zaccolo, M., and Rudolf, R. (2009). PKA microdomain organisation and cAMP handling in healthy and dystrophic muscle in vivo. Cell. Signal. *21*, 819–826.

Roiko, M.S., and Carruthers, V.B. (2013). Functional dissection of Toxoplasma gondii perforin-like protein 1 reveals a dual domain mode of membrane binding for cytolysis and parasite egress. J. Biol. Chem. *288*, 8712–8725.

Roosild, T.P., Greenwald, J., Vega, M., Castronovo, S., Riek, R., and Choe, S. (2005). NMR structure of Mistic, a membrane-integrating protein for membrane protein expression. Science *307*, 1317–1321.

Rottmann, M., McNamara, C., Yeung, B.K.S., Lee, M.C.S., Zou, B., Russell, B., Seitz, P., Plouffe, D.M., Dharia, N. V, Tan, J., et al. (2010). Spiroindolones, a potent compound class for the treatment of malaria. Science *329*, 1175–1180.

Russo, I., Oksman, A., Vaupel, B., and Goldberg, D.E. (2009). A calpain unique to alveolates is essential in Plasmodium falciparum and its knockdown reveals an involvement in pre-S-phase development. Proc. Natl. Acad. Sci. U. S. A. *106*, 1554–1559.

Safavi, M., Baeeri, M., and Abdollahi, M. (2013). New methods for the discovery and synthesis of PDE7 inhibitors as new drugs for neurological and inflammatory disorders. Expert Opin. Drug Discov. *8*, 733–751.

Salazar, E., Bank, E.M., Ramsey, N., Hess, K.C., Deitsch, K.W., Levin, L.R., and Buck, J. (2012). Characterization of Plasmodium falciparum adenylyl cyclase-β and its role in erythrocytic stage parasites. PLoS One *7*, e39769.

Salowe, S.P., Wiltsie, J., Liberator, P.A., and Donald, R.G.K. (2002). The Role of a Parasite-Specific Allosteric Site in the Distinctive Activation Behavior of Eimeria tenella cGMP-Dependent Protein Kinase. Biochemistry *41*, 4385–4391.

Sanders, P.R., Gilson, P.R., Cantin, G.T., Greenbaum, D.C., Nebl, T., Carucci, D.J., McConville, M.J., Schofield, L., Hodder, A.N., Yates, J.R., et al. (2005). Distinct protein classes including novel merozoite surface antigens in Raft-like membranes of Plasmodium falciparum. J. Biol. Chem. *280*, 40169–40176.

Santos, J.M., Ferguson, D.J.P., Blackman, M.J., and Soldati-Favre, D. (2011). Intramembrane cleavage of AMA1 triggers Toxoplasma to switch from an invasive to a replicative mode. Science *331*, 473–477.

Saraiva, V.B., de Souza Silva, L., Ferreira-DaSilva, C.T., da Silva-Filho, J.L., Teixeira-Ferreira, A., Perales, J., Souza, M.C., Henriques, M. das G., Caruso-Neves, C., and de Sá Pinheiro, A.A. (2011). Impairment of the Plasmodium falciparum erythrocytic cycle induced by angiotensin peptides. PLoS One *6*, e17174.

Sauer, B. (1994). Site-specific recombination: developments and applications. Curr. Opin. Biotechnol. *5*, 521–527.

Van Schaijk, B.C.L., Vos, M.W., Janse, C.J., Sauerwein, R.W., and Khan, S.M. (2010). Removal of heterologous sequences from Plasmodium falciparum mutants using FLPe-recombinase. PLoS One *5*, e15121.

Scherf, A., Carter, R., Petersen, C., Alano, P., Nelson, R., Aikawa, M., Mattei, D., Pereira da Silva, L., and Leech, J. (1992). Gene inactivation of Pf11-1 of Plasmodium falciparum by chromosome breakage and healing: identification of a gametocyte-specific protein with a potential role in gametogenesis. EMBO J. *11*, 2293–2301.

Scherf, A., Hernandez-Rivas, R., Buffet, P., Bottius, E., Benatar, C., Pouvelle, B., Gysin, J., and Lanzer, M. (1998). Antigenic variation in malaria: in situ switching, relaxed and mutually exclusive transcription of var genes during intra-erythrocytic development in Plasmodium falciparum. EMBO J. *17*, 5418–5426.

Scherf, A., Pouvelle, B., Buffet, P.A., and Gysin, J. (2001). Molecular mechanisms of Plasmodium falciparum placental adhesion. Cell. Microbiol. *3*, 125–131.

Schlitzer, M. (2008). Antimalarial drugs - what is in use and what is in the pipeline. Arch. Pharm. (Weinheim). *341*, 149–163.

Schudt, C., Hatzelmann, A., Beume, R., and Tenor, H. (2011). Phosphodiesterase inhibitors: history of pharmacology. Handb. Exp. Pharmacol. 1–46.

Schwam, E.M., Nicholas, T., Chew, R., Billing, C.B., Davidson, W., Ambrose, D., and Altstiel, L.D. (2014). A multicenter, double-blind, placebo-controlled trial of the PDE9A inhibitor, PF-04447943, in Alzheimer's disease. Curr. Alzheimer Res. *11*, 413–421.

Seeber, F., Beuerle, B., and Schmidt, H.H. (1999). Cloning and functional expression of the calmodulin gene from Toxoplasma gondii. Mol. Biochem. Parasitol. *99*, 295–299.

Shanks, G.D., and Edstein, M.D. (2005). Modern malaria chemoprophylaxis. Drugs *65*, 2091–2110.

Shimizu-Albergine, M., Tsai, L.-C.L., Patrucco, E., and Beavo, J.A. (2012). cAMP-specific phosphodiesterases 8A and 8B, essential regulators of Leydig cell steroidogenesis. Mol. Pharmacol. *81*, 556–566.

Siden-Kiamos, I., Ecker, A., Nybäck, S., Louis, C., Sinden, R.E., and Billker, O. (2006). Plasmodium berghei calcium-dependent protein kinase 3 is required for ookinete gliding motility and mosquito midgut invasion. Mol. Microbiol. *60*, 1355–1363.

Siden-Kiamos, I., Ganter, M., Kunze, A., Hliscs, M., Steinbüchel, M., Mendoza, J., Sinden, R.E., Louis, C., and Matuschewski, K. (2011). Stage-specific depletion of myosin A supports an essential role in motility of malarial ookinetes. Cell. Microbiol. *13*, 1996–2006.

Sidjanski, S., and Vanderberg, J.P. (1997). Delayed migration of Plasmodium sporozoites from the mosquito bite site to the blood. Am. J. Trop. Med. Hyg. *57*, 426–429.

Sim, B.K., Chitnis, C.E., Wasniowska, K., Hadley, T.J., and Miller, L.H. (1994). Receptor and ligand domains for invasion of erythrocytes by Plasmodium falciparum. Science *264*, 1941–1944.

Sinden, R.E. (2002). Molecular interactions between Plasmodium and its insect vectors. Cell. Microbiol. *4*, 713–724.

Singh, B., Kim Sung, L., Matusop, A., Radhakrishnan, A., Shamsul, S.S.G., Cox-Singh, J., Thomas, A., and Conway, D.J. (2004). A large focus of naturally acquired Plasmodium knowlesi infections in human beings. Lancet *363*, 1017–1024.

Singh, S., Alam, M.M., Pal-Bhowmick, I., Brzostowski, J.A., and Chitnis, C.E. (2010). Distinct external signals trigger sequential release of apical organelles during erythrocyte invasion by malaria parasites. PLoS Pathog. *6*, e1000746.

Sinha, A., Hughes, K.R., Modrzynska, K.K., Otto, T.D., Pfander, C., Dickens, N.J., Religa, A.A., Bushell, E., Graham, A.L., Cameron, R., et al. (2014). A cascade of DNA-binding proteins for sexual commitment and development in Plasmodium. Nature.

Slavic, K., Straschil, U., Reininger, L., Doerig, C., Morin, C., Tewari, R., and Krishna, S. (2010). Life cycle studies of the hexose transporter of Plasmodium species and genetic validation of their essentiality. Mol. Microbiol. *75*, 1402–1413.

Smith, G.E., Fraser, M.J., and Summers, M.D. (1983). Molecular Engineering of the Autographa californica Nuclear Polyhedrosis Virus Genome: Deletion Mutations Within the Polyhedrin Gene. J. Virol. *46*, 584–593.

Sologub, L., Kuehn, A., Kern, S., Przyborski, J., Schillig, R., and Pradel, G. (2011). Malaria proteases mediate inside-out egress of gametocytes from red blood cells following parasite transmission to the mosquito. Cell. Microbiol. *13*, 897–912.

Spillman, N.J., Allen, R.J.W., McNamara, C.W., Yeung, B.K.S., Winzeler, E.A., Diagana, T.T., and Kirk, K. (2013). Na(+) regulation in the malaria parasite Plasmodium falciparum involves the cation ATPase PfATP4 and is a target of the spiroindolone antimalarials. Cell Host Microbe *13*, 227–237.

Srivastava, I.K., Rottenberg, H., and Vaidya, A.B. (1997). Atovaquone, a broad spectrum antiparasitic drug, collapses mitochondrial membrane potential in a malarial parasite. J. Biol. Chem. *272*, 3961–3966.

Srivastava, I.K., Morrisey, J.M., Darrouzet, E., Daldal, F., and Vaidya, A.B. (1999). Resistance mutations reveal the atovaquone-binding domain of cytochrome b in malaria parasites. Mol. Microbiol. *33*, 704–711.

Straimer, J., Lee, M.C.S., Lee, A.H., Zeitler, B., Williams, A.E., Pearl, J.R., Zhang, L., Rebar, E.J., Gregory, P.D., Llinás, M., et al. (2012). Site-specific genome editing in Plasmodium falciparum using engineered zinc-finger nucleases. Nat. Methods *9*, 993–998.

Sturm, A., Amino, R., van de Sand, C., Regen, T., Retzlaff, S., Rennenberg, A., Krueger, A., Pollok, J.-M., Menard, R., and Heussler, V.T. (2006). Manipulation of host hepatocytes by the malaria parasite for delivery into liver sinusoids. Science *313*, 1287–1290.

Sung, B.-J., Hwang, K.Y., Jeon, Y.H., Lee, J.I., Heo, Y.-S., Kim, J.H., Moon, J., Yoon, J.M., Hyun, Y.-L., Kim, E., et al. (2003). Structure of the catalytic domain of human phosphodiesterase 5 with bound drug molecules. Nature *425*, 98–102.

Suplick, K., Morrisey, J., and Vaidya, A.B. (1990). Complex transcription from the extrachromosomal DNA encoding mitochondrial functions of Plasmodium yoelii. Mol. Cell. Biol. *10*, 6381–6388.

Surks, H.K. (1999). Regulation of Myosin Phosphatase by a Specific Interaction with cGMP-Dependent Protein Kinase I. Science (80-.). *286*, 1583–1587.

Sutherland, C.J., Tanomsing, N., Nolder, D., Oguike, M., Jennison, C., Pukrittayakamee, S., Dolecek, C., Hien, T.T., do Rosário, V.E., Arez, A.P., et al. (2010). Two nonrecombining sympatric forms of the human malaria parasite Plasmodium ovale occur globally. J. Infect. Dis. *201*, 1544–1550.

Talman, A.M., Lacroix, C., Marques, S.R., Blagborough, A.M., Carzaniga, R., Ménard, R., and Sinden, R.E. (2011). PbGEST mediates malaria transmission to both mosquito and vertebrate host. Mol. Microbiol. *82*, 462–474.

Taylor, W.R.J., and White, N.J. (2004). Antimalarial drug toxicity: a review. Drug Saf. *27*, 25–61.

Taylor, C.J., McRobert, L., and Baker, D.A. (2008). Disruption of a Plasmodium falciparum cyclic nucleotide phosphodiesterase gene causes aberrant gametogenesis. Mol. Microbiol. *69*, 110–118.

Taylor, H.M., McRobert, L., Grainger, M., Sicard, A., Dluzewski, A.R., Hopp, C.S., Holder, A.A., and Baker, D.A. (2010). The malaria parasite cyclic GMP-dependent protein kinase plays a central role in blood-stage schizogony. Eukaryot. Cell *9*, 37–45.

Taylor, S.S., Keshwani, M.M., Steichen, J.M., and Kornev, A.P. (2012). Evolution of the eukaryotic protein kinases as dynamic molecular switches. Philos. Trans. R. Soc. Lond. B. Biol. Sci. *367*, 2517–2528.

Tham, W.-H., Wilson, D.W., Lopaticki, S., Schmidt, C.Q., Tetteh-Quarcoo, P.B., Barlow, P.N., Richard, D., Corbin, J.E., Beeson, J.G., and Cowman, A.F. (2010). Complement receptor 1 is the host erythrocyte receptor for Plasmodium falciparum PfRh4 invasion ligand. Proc. Natl. Acad. Sci. U. S. A. *107*, 17327–17332.

Thathy, V., Fujioka, H., Gantt, S., Nussenzweig, R., Nussenzweig, V., and Ménard, R. (2002). Levels of circumsporozoite protein in the Plasmodium oocyst determine sporozoite morphology. EMBO J. *21*, 1586–1596.

Thera, M.A., and Plowe, C. V (2012). Vaccines for malaria: how close are we? Annu. Rev. Med. *63*, 345–357.

Thera, M.A., Doumbo, O.K., Coulibaly, D., Laurens, M.B., Ouattara, A., Kone, A.K., Guindo, A.B., Traore, K., Traore, I., Kouriba, B., et al. (2011). A field trial to assess a blood-stage malaria vaccine. N. Engl. J. Med. *365*, 1004–1013.

Thomas, M.K., Francis, S.H., and Corbin, J.D. (1990). Characterization of a purified bovine lung cGMP-binding cGMP phosphodiesterase. J. Biol. Chem. *265*, 14964–14970.

Thomé, R., Lopes, S.C.P., Costa, F.T.M., and Verinaud, L. (2013). Chloroquine: modes of action of an undervalued drug. Immunol. Lett. *153*, 50–57.

Tibúrcio, M., Silvestrini, F., Bertuccini, L., Sander, A.F., Turner, L., Lavstsen, T., and Alano, P. (2012). Early gametocytes of the malaria parasite Plasmodium falciparum specifically remodel the adhesive properties of infected erythrocyte surface. Cell. Microbiol.

Trager, W., and Gill, G.S. (1989). Plasmodium falciparum gametocyte formation in vitro: its stimulation by phorbol diesters and by 8-bromo cyclic adenosine monophosphate. J. Protozool. *36*, 451–454.

Trager, W., and Jensen, J.B. (1977). Cultivation of erythrocytic stages. Bull. World Health Organ. *55*, 363–365.

Trivedi, A.K., and Kumar, V. (2014). Melatonin: an internal signal for daily and seasonal timing. Indian J. Exp. Biol. *52*, 425–437.

Turko, I. V, Francis, S.H., and Corbin, J.D. (1998). Potential roles of conserved amino acids in the catalytic domain of the cGMP-binding cGMP-specific phosphodiesterase. J. Biol. Chem. *273*, 6460–6466.

Tuteja, R. (2007). Malaria - an overview. FEBS J. *274*, 4670–4679.

Vaid, A., Thomas, D.C., and Sharma, P. (2008). Role of Ca2+/calmodulin-PfPKB signaling pathway in erythrocyte invasion by Plasmodium falciparum. J. Biol. Chem. *283*, 5589–5597.

Vaidya, A.B., and Mather, M.W. (2009). Mitochondrial evolution and functions in malaria parasites. Annu. Rev. Microbiol. *63*, 249–267.

Vanderberg, J.P. (1974). Studies on the motility of Plasmodium sporozoites. J. Protozool. *21*, 527–537.

Vanderberg, J.P., and Frevert, U. (2004). Intravital microscopy demonstrating antibody-mediated immobilisation of Plasmodium berghei sporozoites injected into skin by mosquitoes. Int. J. Parasitol. *34*, 991–996.

Vanhauwe, J.F., Thomas, T.O., Minshall, R.D., Tiruppathi, C., Li, A., Gilchrist, A., Yoon, E., Malik, A.B., and Hamm, H.E. (2002). Thrombin receptors activate G(o) proteins in endothelial cells to regulate intracellular calcium and cell shape changes. J. Biol. Chem. *277*, 34143–34149.

Verkhratsky, A., and Parpura, V. (2013). Calcium signalling and calcium channels: Evolution and general principles. Eur. J. Pharmacol. *739C*, 1–3.

Vlachou, D., Zimmermann, T., Cantera, R., Janse, C.J., Waters, A.P., and Kafatos, F.C. (2004). Real-time, in vivo analysis of malaria ookinete locomotion and mosquito midgut invasion. Cell. Microbiol. *6*, 671–685.

Wang, H., Liu, Y., Chen, Y., Robinson, H., and Ke, H. (2005). Multiple elements jointly determine inhibitor selectivity of cyclic nucleotide phosphodiesterases 4 and 7. J. Biol. Chem. *280*, 30949–30955.

Warsame, M., Olumese, P., and Mendis, K. (2010). Role of medicines in malaria control and elimination. Drug Dev. Res. n/a – n/a.

Wasserman, M., Alarcon, C., and Mendoza, P.M. (1982). Effects of CA++ depletion on the asexual cell cycle of Plasmodium falciparum. Am. J. Trop. Med. Hyg. *31*, 711–717.

Weishaar, R.E., Cain, M.H., and Bristol, J.A. (1985). A new generation of phosphodiesterase inhibitors: multiple molecular forms of phosphodiesterase and the potential for drug selectivity. J. Med. Chem. *28*, 537–545.

Wells, T.N.C., Burrows, J.N., and Baird, J.K. (2010). Targeting the hypnozoite reservoir of Plasmodium vivax: the hidden obstacle to malaria elimination. Trends Parasitol. *26*, 145–151.

Wentzinger, L., Bopp, S., Tenor, H., Klar, J., Brun, R., Beck, H.P., and Seebeck, T. (2008). Cyclic nucleotide-specific phosphodiesterases of Plasmodium falciparum: PfPDEalpha, a non-essential cGMP-specific PDE that is an integral membrane protein. Int. J. Parasitol. *38*, 1625–1637.

Wernet, W., Flockerzi, V., and Hofmann, F. (1989). The cDNA of the two isoforms of bovine cGMP-dependent protein kinase. FEBS Lett. *251*, 191–196.

WHO WHO | WHO Pesticide Evaluation Scheme: "WHOPES."

WHO (2013). World Malaria Report 2013 (Geneva).

Wickham, M.E., Culvenor, J.G., and Cowman, A.F. (2003). Selective inhibition of a two-step egress of malaria parasites from the host erythrocyte. J. Biol. Chem. *278*, 37658–37663.

Wickstead, B., Ersfeld, K., and Gull, K. (2003). Repetitive Elements in Genomes of Parasitic Protozoa. Microbiol. Mol. Biol. Rev. *67*, 360–375.

Wilson, D.W., Crabb, B.S., and Beeson, J.G. (2010). Development of fluorescent Plasmodium falciparum for in vitro growth inhibition assays. Malar. J. *9*, 152.

Wilson, D.W., Langer, C., Goodman, C.D., McFadden, G.I., and Beeson, J.G. (2013). Defining the timing of action of antimalarial drugs against Plasmodium falciparum. Antimicrob. Agents Chemother. *57*, 1455–1467.

Wirth, C.C., and Pradel, G. (2012). Molecular mechanisms of host cell egress by malaria parasites. Int. J. Med. Microbiol. *302*, 172–178.

Wong, W., and Scott, J.D. (2004). AKAP signalling complexes: focal points in space and time. Nat. Rev. Mol. Cell Biol. *5*, 959–970.

Wright, G.J., and Rayner, J.C. (2014). Plasmodium falciparum erythrocyte invasion: combining function with immune evasion. PLoS Pathog. *10*, e1003943.

Wu, Y., Sifri, C.D., Lei, H.H., Su, X.Z., and Wellems, T.E. (1995). Transfection of Plasmodium falciparum within human red blood cells. Proc. Natl. Acad. Sci. U. S. A. *92*, 973–977.

Wurtz, N., Chapus, C., Desplans, J., and Parzy, D. (2011). cAMP-dependent protein kinase from Plasmodium falciparum: an update. Parasitology *138*, 1–25.

Xu, R.X., Hassell, A.M., Vanderwall, D., Lambert, M.H., Holmes, W.D., Luther, M.A., Rocque, W.J., Milburn, M. V, Zhao, Y., Ke, H., et al. (2000). Atomic structure of PDE4: insights into phosphodiesterase mechanism and specificity. Science *288*, 1822–1825.

Xu, Y., Kong, J., and Kong, W. (2013). Improved membrane protein expression in Lactococcus lactis by fusion to Mistic. Microbiology *159*, 1002–1009.

Yap, A., Azevedo, M.F., Gilson, P.R., Weiss, G.E., O Neill, M.T., Wilson, D.W., Crabb, B.S., and Cowman, A.F. (2014). Conditional expression of apical membrane antigen 1 in Plasmodium falciparum shows it is required for erythrocyte invasion by merozoites. Cell. Microbiol.

Yeoh, S., O'Donnell, R.A., Koussis, K., Dluzewski, A.R., Ansell, K.H., Osborne, S.A., Hackett, F., Withers-Martinez, C., Mitchell, G.H., Bannister, L.H., et al. (2007). Subcellular discharge of a serine protease mediates release of invasive malaria parasites from host erythrocytes. Cell *131*, 1072–1083.

Yuasa, K., Mi-Ichi, F., Kobayashi, T., Yamanouchi, M., Kotera, J., Kita, K., and Omori, K. (2005). PfPDE1, a novel cGMP-specific phosphodiesterase from the human malaria parasite Plasmodium falciparum. Biochem. J. *392*, 221–229.

Zenonos, Z.A., Rayner, J.C., and Wright, G.J. (2014). Towards a comprehensive Plasmodium falciparum merozoite cell surface and secreted recombinant protein library. Malar. J. *13*, 93.

Zhang, K.Y.J., Card, G.L., Suzuki, Y., Artis, D.R., Fong, D., Gillette, S., Hsieh, D., Neiman, J., West, B.L., Zhang, C., et al. (2004). A glutamine switch mechanism for nucleotide selectivity by phosphodiesterases. Mol. Cell *15*, 279–286.

Zhao, Y., Chapman, D.A.G., and Jones, I.M. (2003). Improving baculovirus recombination. Nucleic Acids Res. *31*, E6–6.

Zhihui, Q. (2013). Modulating nitric oxide signaling in the CNS for Alzheimer's disease therapy. Future Med. Chem. *5*, 1451–1468.

Zuccala, E.S., and Baum, J. (2011). Cytoskeletal and membrane remodelling during malaria parasite invasion of the human erythrocyte. Br. J. Haematol.

(2014). Efficacy and Safety of the RTS,S/AS01 Malaria Vaccine during 18 Months after Vaccination: A Phase 3 Randomized, Controlled Trial in Children and Young Infants at 11 African Sites. PLoS Med. *11*, e1001685.

Appendices

Appendix 1: List of primers used in this study

	Name	Sequence
PfPDEα-DD cloning and sequencing	PDEα Forward 1	*AGCGCGGCCGC TAA* CGATAGATAATACTATACCTACATCGCC
	PDEα Forward 2	CTATGAATAAATTAGCTCTCTCACAAATCG
	PDEα Reverse 1	*TAGCTCGAG* TTCAAATTTGATGAGCTCAAGTTTGCTTAG
	PDEα Reverse 2	CGATTTAGTTTCTTCTTGATTTAATGGG
PfPDEβ-DD cloning and sequencing	PDEβ Forward 1	*AGCGCGGCCGC TAA* GATTGTATAAGTACTGACAAAGTGGATTTAGA
	PDEβ Forward 2	GTTGTCATGCCGTTATTTGAGG
	PDEβ Reverse 1	*TAGCTCGAG* ATCGGAAACATTcTTTATgAAAAATAGAGTTAAATCAATATAAC
	PDEβ Reverse 2	GATAAGGAACATTATTGTACTGCTTTTCAAC
	PDEβ Forward 3	CAACTAAACCAATGTAATATTTT
PfPDE-DD System Integration PCR	DD Backbone F	GTTGGACTCAAGACGATAGTTACCG
	gPDEα F	CCATTGGATAATTTCTTCTTTCCC
	gPDEβ F	GGAATTAGAGAACGAGACGGATAC
	DD Tag R	CTTTCCATCTTCAAGCATCCC
	gPDEα 3'UTR R	ACATGTTTTATGCAGTAATATAGGAGTGC
	gPDEβ 3'UTR R	GCCAAGTCGAATGGAAAGATATTG
PfPDE-DiCre System Integration PCR	Episomal F	GCATACATTATACGAAGTTATCAGG
	PDEβ Insert R	CGGGATCATAAACCTCGATTG
	Genomic PDEβ F	GTTGAAAAGCAGTACAATAATGTTCCTTATC
	PbDT3 R	CGAACATTAAGCTGCCATATCC
PvPDEβ protein expression sequencing	PvPDEβR1	GAGGTGGACCAGTGGATGGAG
	PvPDEβF1	GGAAGAGGACGACACCAAGATG
	PvPDEβF2	GAACCAGTCTAACGACAACGAGC
	PvPDEβF3	GTGATCGCTTACACCACCC
	PvPDEβF4	GCCTGAACTACTTCGAGAACAGC
	PvPDEβF5	CGAGGACTTCGACTACGTGAA
	PvPDEβF2.1	TCAAGTCCAACTTCACCG
	PvPDEβF3.1	TCATCGTCCTGAACTCCA
	PvPDEβF4.1	ATCAAGAAGTTCCTGAAGG
pRN16	pHFor	ACCATCTCGCAAATAAATAAG
	pHRev	GATTTACAGACAATTGTTGT
pMistic	Hmistic PvPDEβ F	GAAAACTTGTACTTTCAA GGATCC ATGGAAAACCCCGACAAGTCC
	Hmistic PvPDEβ R	ATAAATGTACTAATAACC GGATCC TTACTCGGAGATGTTCTTGATGAAG
	KpnI Mistic Primer F	CATCACCATCATCACCATGGTACCATGTTTTGTACATTTTTTGAAAAACATCACC

Appendix 2: Antipeptide antibodies

PDEα

MMDTKVDQTIQPKFYVDKKLSKSFDNKLDEDIFNYPFKKESFLKSEKFSFEHTKDSLWKCIKEK
AKKKSDMEYFNCVNNLCCKFICTIRKYVKYFLYLKDSSYEIYNINLYNNNNMNIINNKNITNNK
NITNNINNSFSNDYINYNHNYNHLNNSSSSKHNNYNVNNIDEKNIKNDYNTYHNIYEQIFFKYN
PSFYEYLMFTLMKKLIHYKNYIFNKTKKINNSYNNNDIKNIDGFLIFQNINFEEIFLNTFYSSF
PFKLFLHSLYMIFICFIYFVVLYFMLLKKIYTHPFIFHLSVLKFLFDIIFFLSFILYPLFLRLK
RIDKIIYSSYISSYIFVCVTFLYSFIIFKCSSYSVKMNSNTYQNNFVFQNMLFLLINIIYICIF
CFLKNYMILYSFLYNCRFSIFCILFIFLYYYLFFSLDFYRIIHLPLDNFFFPFLCFLFFSFLFI
FKIIMSLYYEYVYEKKYRILFVKKNNLIEKRITKRKNTNINNAYFTKYFSIDNTIPTSPIEDIL
NNFKHILETINIIEENPNHNLTTNIMKIKEKIKNCDNILRTKNINQVQIGKYRKFEKVYNIWCL
DKMYLNYPLNQEETKSFLSNSLNRISFNSFSNMHSLLSSKFQEHYNDIYDWNGNIENIYKANTF
ISIGYKLLYPLGVLEANFDKEKLKKFLFRICSYYNDIPYHTSLHAAQVAHFSKSMLFMLDMNHK
ISAIDEFCLHISSLCHDTGHPGLNNYFLINSENNLALTYNDNSVLENYHCSLLFKTLKNPNYNI
FEHYPYHIFISCKKNIIKAILSTDMKNHFEYISDFRTSKEFIDYDNLSNDQIWQIFCLILKASD
IGHSTLEWNKHLEWTLKINEEFYLQGLLEKSLNIQNSFLCDINTMNKLALSQIDFLKHLCIPLF
NELNYICKNNDVYTHCIQPIENNIERWESHKNDNQNLGLHEKYKEENLLSKLELIKFE

Sequence Length: 954 amino acids

| Peptide Sequence	Sample Number	
CGGSDFRTSKEFIDYDNLSND	4608	4609
CGGESHKNDNQNLGLHEKYKEENLLSK	4668	4669

PDEβ

MGKVEDFEEHNKNSNQDIEKNVGNRRRSNSNTINDQNENINKNKAIVTKKSFIMNLLRNKEKTK
VEQNDDNIVENMNERKNSLKDMSLISDNVEKDNKVKKKNSYLKNLNILGKTKSIEFSFPSNILN
NARKNIQEIDEESPLTSNSLRTYKEGISEDNRQNQRNADNNSLNWSTSNINTECNSEFSNIEVK
VLKTEKSNSVKLKDNIIDIPNDKNKKELQEINIKNTNKDSYKNLYLKVRNSISFNDNIKIDDEN
KNDKNNIIDNYNNYDDINSSNEITIDGLNHDDNIKKIDNINNFDNKHDDNLQDHHQNHVHHTFR
SSRKSLGNIKSNNTNIKLNNDKNFDTNINKRSILEKYFYDIWKRNITIKKEIYSLSSKNPPNPL
KSTFADACQNESSEKELLKKIPLKFNDDSIESLYVLNLNNWISSRMIIIGIVMLILSFIIWPLT
TWSLKTSTWGRETYIIILFHTLMAINTLILIFFIIIGSTELCKYSECMSYVLFSLMVALWGLWN
IAIGLTLEYNPNLSEMPTTTYELEMIYVLTYIYGFLPLVIIDIFFPSRTKYNWIIHLIFIFLNS
SSIILVGSAKPDFVPEIYVVFRILAYTTLCIFLYIGSYTSELQIRYVFYNLLVAGYKLDKIESD
MKNKTSNKKISTGIEDLINMLKECTKVILELENETDTNFNVHTKTSYCSNILEQCLSTLTKSDN
LYNIDYNVLENPENKKFIEAYVSKSKSNFAGEEVPKGVDFKLNKSFSNNDCISTDKVDLDKKQI
KKFLKQINISQLTKMIQFIDNKLLSDWDFNCLTYFDESEYPFFDINLSLICTIDHNIPINIIIN
FLCFVEKQYNNVPYHNTIHATMVTQKFFCLAKKLGIYDDLEYKIKLVMFISGICHDIGHPGYNN
LFFVNSLHPLSIIYNDISVLENYHASITFKILQLNQCNILKNFSEKDFRMMRSYIIELILSTDM
KHHFEIISKFRIRRENEDFDYIKNSDDLLILTKMIIKSADISHGSVSWSEHYCWCQRVLSEFYT
QGDEELKNKMPLSPLCDRTKHNEVCKSQITFLKFVVMPLFEELSHIDNNKFIKSFCLKRLNSNC
IMWDTLMKEEKTIEVYDPAAVKLKDKKKKKVDKKKKSYIDLTLFFIKNVSD

Sequence Length: 1139 amino acids

Peptide Sequence	Sample Number	
CGGRIRRENEDFDYIKNS	4608	4609

Appendix 3: Negative control IFAs
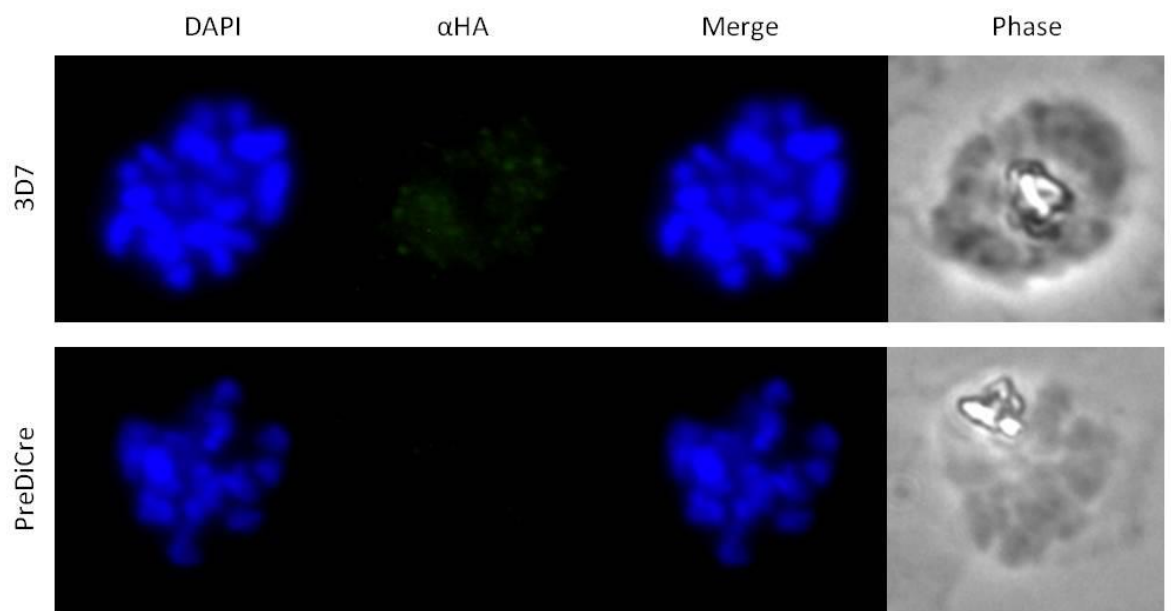
Appendix 4: Results of the 48 hour hypoxanthine incorporation assays

Compound	Average IC50			SE EC50	95% Confidence intervals		
	M	µM	nM				
PF-05257670	3.2E-07	0.32	319.70	1.17	233.40	to	437.90
PF-04290541	5.64E-05	56.41	56410.00	1.15	42530.00	to	74810.00
PF-03201245		>100					
PF-03455711	1.55E-05	15.53	15530.00	1.15	11770	to	20470
SC-58236		>100					
PF-03204683	1.58E-05	15.78	15780.00	1.13	12340.00	to	20190.00
PF-03120399		>100					
PF-03455723	8.56E-05	85.58	85580.00	1.19	60410.00	to	121200.00
PF-01273175	9.36E-07	0.94	935.80	1.16	695.7	to	1259
PF-05184913	6.34E-07	0.63	634.40	1.11	511.3	to	787
PF-05225388	1.3E-07	0.13	130.40	1.09	109.90	to	154.80
PF-00394183	5.47E-07	0.55	547.40	1.15	411.10	to	728.80
PF-05197824	8.5E-06	8.50	8501.00	1.62	3275.00	to	22070.00
PF-00388991	1.03E-06	1.03	1027.00	1.44	495.20	to	2128.00
Zaprinast		>100					
CP 80633	8.32E-05	83.22	83220.00	2.00	20890.00	to	331500.00
Dipyridamole	5.84E-06	5.84	5839.00	1.63	2224.00	to	15330.00
IBMX		>100					
EHNA Hydrochloride	4.58E-05	45.78	45780.00	1.39	23790.00	to	88100.00
BRL 50481		>100					
T 0156 Hydrochloride	7.05E-05	70.50	70500.00	1.21	48040.00	to	103400.00
Vinpocetine		>100					
Artemisinin	4.74E-08	0.05	47.39	1.15	36.01	to	62.36
Chloroquine	1.29E-08	0.01	12.88	1.54	5.459	to	30.39

Appendix 5: Sequence of the Mistic-tag

A 5.1 DNA sequence of the 10x His-tag followed by the Mistic-tag and a glycine serine linker with a TEV cleavage site

ATGCACCACCATCATCATCACCATCATCACCATGGTACCATGTTTTGTACATTTTTTGAAAAAC
ATCACCGGAAGTGGGACATACTGTTAGAAAAAAGCACGGGTGTGATGGAAGCTATGAAAGTGAC
GAGTGAGGAAAAGGAACAGCTGAGCACAGCAATCGACCGAATGAATGAAGGACTGGACGCGTTT
ATCCAGCTGTATAATGAATCGGAAATTGATGAACCGCTTATTCAGCTTGATGATGATACAGCCG
AGTTAATGAAGCAGGCCCGAGATATGTACGGCCAGGAAAAGCTAAATGAGAAATTAAATACAAT
TATTAAACAGATTTTATCCATCTCAGTATCTGAAGAAGGAGAAAAAGAAGGTAC<u>CGGCGGAGGC</u>
<u>TCGGGCGGCGGCTCAGAAAACTTGTACTTTCAAG</u>GATCC

A 5.2 Amino acid sequence of the 10x His-tag followed by the Mistic-tag and a glycine serine linker with a TEV cleavage site

MHHHHHHHHHHGTMFCTFFEKHHRKWDILLEKSTGVMEAMKVTSEEKEQLSTAIDRMNEGLDAF
IQLYNESEIDEPLIQLDDDTAELMKQARDMYGQEKLNEKLNTIIKQILSISVSEEGEKEGT<u>GGG</u>
<u>SGGGSENLYFQGS</u>

10x His-tag – shown in bold

Mistic-tag – shown highlighted

<u>Glycine serine linker – shown underlined</u>

Theoretical pI/Mw: 5.26 / 16.1KDa